UNIVERSITÀ DEGLI STUDI DI MILANO

PhD Course in Molecular and Cellular Biology

XXXI Cycle

Pleiotropic phenotype of *Pseudomonas aeruginosa* mutants defective in glucose uptake

Matteo Raneri

PhD Thesis

Scientific tutor: Prof. Federica Briani

Academic year: 2017-2018

SSD: BIO/11, BIO/18, BIO/19

Thesis performed at the Dipartimento di Bioscienze, Università degli Studi di Milano

Table of contents

SOMMARIO

Pseudomonas aeruginosa è un patogeno opportunista che provoca una vasta gamma di infezioni nell'uomo. È noto che l'incidenza delle infezioni da *P. aeruginosa* è maggiore in persone che presentano elevati livelli di glucosio nel sangue, a causa della capacità del batterio di utilizzare il glucosio in eccesso come nutriente per la crescita. Pertanto, bloccare l'attività di proteine coinvolte nel trasporto o nell'utilizzazione del glucosio da parte del batterio potrebbe essere una buona strategia per lo sviluppo di farmaci anti-pseudomonas.

Per valutare questa ipotesi, abbiamo costruito una serie di mutanti singoli e multipli difettivi nel trasporto del glucosio nel ceppo PAO1 di *P. aeruginosa* e li abbiamo analizzati per fenotipi correlati alla virulenza in saggi *in vitro* e *in vivo*, in due differenti modelli di infezione. In particolare, sono stati deleti i geni codificanti per i trasportatori della membrana interna Glt, GntP e Kgut, che mediano l'ingresso del glucosio e dei suoi derivati ossidati gluconato e 2-ketogluconato. Un triplo mutante privo dei suddetti trasportatori si è rivelato incapace di crescere su glucosio come unica fonte di carbonio (mutante GUN, Glucose Uptake Null).

Più di 500 geni, che controllano sia funzioni metaboliche che la virulenza, sono espressi in modo differenziale nel mutante GUN rispetto al ceppo parentale. Coerentemente con i dati dell'analisi trascrittomica, i saggi di virulenza *in vitro* hanno mostrato che il mutante GUN si comporta diversamente dal ceppo parentale, avendo una ridotta capacità di formare biofilm e una maggiore secrezione di proteasi, piocianina e pioverdina. Inoltre, questo mutante ha una produzione alterata delle molecole segnale che attivano il sistema del quorum sensing. È interessante notare che il profilo trascrizionale e la maggior parte dei tratti fenotipici analizzati differiscono tra il mutante GUN e il ceppo parentale

indipendentemente dalla presenza del glucosio, suggerendo che uno (o più) dei trasportatori deleti abbia una funzione addizionale non correlata al trasporto del glucosio.

Infine, alcuni mutanti hanno mostrato un diverso grado di virulenza in saggi di infezione negli ospiti modello *Caenorhabditis elegans* e *Galleria mellonella*. In particolare, mentre in *C. elegans* la virulenza dei mutanti è risultata simile a quella del ceppo parentale PAO1, i mutanti deleti del gene *kguT*, che codifica per il trasportatore del 2-ketogluconato, sono meno virulenti di PAO1 in *G. mellonella*. L'attenuazione è particolarmente significativa per il doppio mutante Δ*gntP* Δ*kguT* e per il mutante GUN. Questo risultato suggerisce che l'efficacia antibatterica di composti che bloccano l'utilizzo del glucosio da parte di *P. aeruginosa* potrebbe presumibilmente variare a seconda della capacità del patogeno di adattarsi allo specifico contesto nutrizionale dell'ospite infettato. Una maggiore conoscenza delle interazioni metaboliche che avvengono tra patogeno ed ospite nel sito d'infezione diventa quindi sempre più necessaria per poter sviluppare terapie antibatteriche efficaci.

ABSTRACT

Pseudomonas aeruginosa is an opportunistic pathogen causing a wide range of infections in humans. Pathologies leading to hyperglycaemia have been associated with augmented risk of developing serious *P. aeruginosa* infections due to the ability of the bacterium to utilize glucose as carbon source for the growth. Therefore, preventing the import of glucose might be a good strategy to develop anti-pseudomonas drugs.

To address this hypothesis, a collection of single and multiple glucose uptake defective mutants was generated in *P. aeruginosa* PAO1 and tested for virulence-related phenotypes in *in vitro* assays and *in vivo*, in two different infection models. In particular, we engineered mutants in genes encoding inner membrane (IM) proteins involved in the internalization of glucose and its oxidized derivatives gluconate and 2-ketogluconate, i.e. the Glt, GntP and KguT transporters. A triple mutant lacking these transporters was demonstrated to be completely unable to grow on glucose as sole carbon source (Glucose Uptake Null mutant, GUN).

The transcriptomic analysis revealed a strong divergence in the GUN transcriptional profile relative to the parental strain, with more than 500 differentially expressed genes, controlling both metabolic functions and virulence traits. Consistent with the transcriptomic data, the GUN mutant showed a pleiotropic phenotype in the *in vitro* assays, with a reduction in biofilm formation and an increased secretion of proteases, pyocyanin and pyoverdine. Furthermore, the production of quorum sensing signal molecules was altered in this mutant. Interestingly, the gene expression profile and most phenotypic traits differ between GUN and the parental strain irrespective of the presence of glucose, suggesting a possible additional role for the deleted transporter(s).

Finally, the *in vivo* assays demonstrated that while the virulence of all mutants in the *Caenorhabditis elegans* infection model was essentially comparable to that of the wild type strain, all mutants lacking *kguT* (i.e. the 2-ketogluconate transporter gene) and especially the double Δ*gntP* Δ*kguT* and GUN mutants, were attenuated in the *Galleria mellonella* model. This suggests that targeting glucose metabolism with specific drugs may alter *P. aeruginosa* pathogenicity depending on the ability of this pathogen to adapt to the specific nutritional context encountered at the site of infection. Therefore, a deeper knowledge of host-pathogen metabolic transactions is pivotal to develop effective antibacterial strategies based on hampering bacterial metabolic functions.

AIM OF THE THESIS

The aim of this thesis is to assess whether affecting the import of glucose may influence the expression of virulence traits in *P. aeruginosa*, thus validating glucose uptake pathway as a possible new target for anti-pseudomonas therapies.

Metabolic genes have been repeatedly identified among those contributing to the *in vivo* virulence of the opportunistic pathogen *P. aeruginosa* and are considered interesting targets for novel anti-pseudomonas drugs. In this regard, genes involved in glucose uptake deserve consideration. Indeed, pathologies leading to hyperglycaemia have been demonstrated to promote bacterial infections by stimulating the growth of human pathogens such as *P. aeruginosa*. This bacterium can utilize glucose as unique carbon source for the growth by importing it through either a phosphorylative route or a periplasmic oxidative pathway generating gluconate and 2-ketogluconate (2-KG). Different works have shown that the regulation of glucose catabolic genes, and in particular of 2-KG import, is tightly linked to that of *toxA*, the gene encoding the key virulence factor exotoxin A, establishing a connection between glucose and virulence.

The above general goal has been pursued through the fulfilment of the following **specific objectives**:

1. Generation of single and multiple *P. aeruginosa* PAO1 mutants in genes encoding outer membrane (OM) and inner membrane (IM) glucose transporters. Specific aims: i) to obtain mutant strains with specific defects in glucose transport for the phenotypic characterization; ii) to assess whether other unknown glucose transporters may supply the absence of the known ones.

2. Gene expression profiling of a *P. aeruginosa* mutant lacking all glucose transporters in comparison with the parental PAO1 strain and validation by RT-qPCR and *in vitro* phenotypic assays of transcriptomic data in presence/absence of glucose. Specific aims: i) identification of genes/pathways responding to glucose in *P. aeruginosa*; ii) identification of genes, if any, specifically responding to the lack of glucose transporters.

3. Evaluation of mutants' virulence in the *Caenorhabditis elegans* nematode and the *Galleria mellonella* insect infection models. Specific aims: to assess whether the lack of glucose transporter(s) affects virulence in different infection models. Besides being a prerequisite for validating glucose uptake pathway as a possible new target for anti-pseudomonas therapies, this analysis would contribute to shed light on *P. aeruginosa* metabolic state during the infection of these widely used non-mammalian models.

PART I

STATE OF THE ART

1. Pseudomonas *aeruginosa*: a versatile opportunistic pathogen

The genus *Pseudomonas* represents a large group belonging to the γ-proteobacteria class comprising more than 200 species isolated from various environmental sources. Indeed, members of this genus inhabit soil and aqueous environments, associate with plants in the rhizosphere as commensal but can also behave as pathogens of mammals, insects and plants (Singh et al. 2016). *Pseudomonas aeruginosa* is a prototypical *Pseudomonas* species considering its impressive ability to colonize the most disparate environments and hosts as different as plants, nematodes, insects and mammals. It is considered one of the major opportunistic pathogen for humans, as it can cause severe infections in subjects in which the physiological barriers against infection have been compromised. Indeed, *P. aeruginosa* is one of the most prevalent nosocomial pathogens and its infections are more prevalent among people with compromised host defences such as AIDS patients or neutropenic patients undergoing chemotherapy, but also patients with cystic fibrosis (CF) or severe burns (Lyczak et al. 2000; Gellatly & Hancock 2013). *P. aeruginosa* infections are linked to remarkable morbidity and mortality due to the ability of the bacterium to adapt to environmental changes and nutritional sources, to produce a wide range of virulence factors and to develop antibiotic resistance. Indeed, *P. aeruginosa* has been enclosed among "superbugs", namely bacteria endowed with intrinsic resistance to a variety of antibiotics, like aminoglycosides, fluoroquinolones and β-lactams (Poole 2011). The intrinsic mechanisms of *P. aeruginosa* resistance are largely due to the low permeability of its outer membrane and the presence of multiple efflux pumps (Breidenstein et al. 2011). Moreover, other mechanisms exploited by *P. aeruginosa* to increase the resistance rate are: i) the acquisition

of inheritable traits by horizontal genetic transfer; ii) adaptive resistance induced by sub-inhibitory concentrations of antibiotics or altered metabolic states, conditions commonly encountered in *P. aeruginosa* biofilms during chronic infections (Fernández et al. 2011).

The genome of *P. aeruginosa* PAO1 reference strain was the first to be sequenced among those of pseudomonads. With a size of 6.3 Mb, the PAO1 genome was the largest of the sequenced bacterial genomes at that time (Stover et al. 2000). Consistent with the capability of *P. aeruginosa* to exploit a variety of nutrients in disparate environmental niches, functional assignments of the predicted ORF revealed that 10% of the *P. aeruginosa* PAO1 genome (i.e. about 500 genes) encodes for proteins involved in the transport of nutrients. In particular, *P. aeruginosa* has a broad array of transporters for mono-, di-, and tricarboxylic acids, whereas the sugar transporters are quite scarce (Stover et al. 2000).

1.1. The arsenal of P. aeruginosa virulence factors

The remarkable ability of *P. aeruginosa* to invade and colonize the human host is owed to the high number of virulence factors it synthesizes. This pathogen produces both cell-associated (pili, flagella, lectins, glycocalyx, lipopolysaccharide and biofilm) and extracellular (proteases, haemolysins, pyocyanin, siderophores, exotoxin A, T3SS effectors) virulence factors that participate in the three stages of the infection: i) bacterial adhesion and colonization; ii) tissue invasion; iii) systemic dissemination (Strateva & Mitov 2011). A summary of the main *P. aeruginosa* virulence factors and their contribution to the pathogenesis is listed in **Table 1**.

Table 1. *P. aeruginosa* virulence factors and respective role in the pathogenesis

Pathogenetic function	Cell-associated factors	Extracellular factors
Adhesion	Type IV pili	
	Carbohydrate-binding proteins (lectins)	
	Glycocalix	
	Alginate slime (biofilm)	
Adhesion facilitation		Neuraminidase (sialidase)
Motility/chemotaxis	Flagella (swimming motility)	
	Retractile pili (twitching motility)	
Invasion		Elastases (LasB and LasA)
		Alkaline protease
		Haemolysins (phospholipases and rhamnolipid)
		Cytotoxin (leukocidin)
		Pyocyanin pigment
		Siderophores and siderophore uptake systems
Toxinogenesis	Lipopolysaccharide (endotoxin)	Exotoxin A
	LecA and LecB lectins	Type III effector cytotoxins – ExoS, ExoU, ExoT, ExoY
		Enterotoxin
Dissemination		
Antiphagocytic surface properties	Slime layers	
	Glycocalix	
	Lipopolysaccharide	
Defense against serum bactericidal reaction	Slime layers	Protease enzymes
	Glycocalix	
	Lipopolysaccharide	
Defense against immune responses	Slime layers	Protease enzymes
	Glycocalix	

From Strateva & Mitov 2011.

The adhesion and colonization phase requires a break in first-line physical and immunological barriers and is mostly dependent on cell-associated virulence factors, such as:

- Type IV pili and flagella: cell surface appendages mediating bacterial colonization thanks to their ability to adhere to epithelial cells (Farinha et al.

1994; Feldman et al. 1998). Type IV pili are pilin protein fibres that, besides binding to specific galactose, mannose and sialic acid-containing receptors on epithelial cells, are required for cell-to-cell interactions in biofilm microcolonies and twitching motility (O'Toole & Kolter 1998; Skariyachan et al. 2018). Twitching is a propulsion mechanism that *P. aeruginosa* exerts to reach and colonize the surface of abiotic substrates, like catheters. Flagella are complex organelles, composed of flagellin subunits, necessary for chemotaxis and motility. They mediate both single-cell swimming motility and swarming, a multicellular coordinated movement of a bacterial population across a semisolid surface contributing to early stages of *P. aeruginosa* biofilm (Shrout et al. 2006).

- Lectins: sugar-binding proteins interacting with carbohydrates located on host cell surfaces. *P. aeruginosa* produces two soluble lectins, LecA and LecB, which specifically bind to galactose and fucose, respectively. Besides their role in adhesion, lectins have a cytotoxic effect in lung epithelial cells and contribute to biofilm development (Chemani et al. 2009; Grishin et al. 2015). *P. aeruginosa* strains with mutations in *lecA* and *lecB* form thinner and less structured biofilms (Grishin et al. 2015). However, the specific function of lectins on the formation of a correct biofilm architecture remains unclear.

- Glycocalyx: extracellular polysaccharidic matrix, composed of uronic acids and carbohydrates, protecting *P. aeruginosa* from phagocytosis and acting as a barrier against cationic antibiotics, such as aminoglycosides, due to its polyanionic nature (Nikaido 1994).

- Lipopolysaccharide (LPS): carbohydrate-lipid complex forming the outer leaflet of gram-negative bacteria. In gram-negative bacteria, the LPS is composed of the lipid A, a polysaccharide core region and the O-antigen. The

major contribution to *P. aeruginosa* pathogenicity is exerted by lipid A and O-antigen. Lipid A is composed of a di-glucosamine biphosphate backbone anchored to the outer membrane by six or seven fatty acyl chains. It elicits the production of pro-inflammatory mediators by interaction with Toll-like receptor 4 (TLR 4) on the surface of immune cells (Akira et al. 2006). Linked to the lipid A moiety by the LPS core, the O-antigen is a variable repeating polysaccharidic region that shows immunogenicity. *P. aeruginosa* produces two different forms of O-antigen: A-band, a homopolymer of D-rhamnose triggering a weak antibody response, and B-band, a heteropolymer eliciting a strong antibody response that is the basis for serogroup specificity (King et al. 2009).

- Biofilm: complex of bacterial microcolonies embedded in a matrix named Extracellular Polymeric Substance (EPS) comprising three major exopolysaccharides (alginate, Pel and Psl), extracellular DNA (eDNA) and proteins (type IV pili and flagella). The physical structure and chemical properties of *P. aeruginosa* biofilm determine its protective role from the entry of antibiotics and the attack by immune cells (Skariyachan et al. 2018). Alginate, an exopolysaccharide composed of mannuronic and glucuronic acid repeats, enhances *P. aeruginosa* surface adhesion and promotes the conversion from non-mucoid to mucoid phenotype (Hay et al. 2009). Pel, a glucose-rich polysaccharide, and Psl, pentasaccharide consisting of D-glucose, D-mannose and L-rhamnose repeats, function as structural scaffolds to maintain biofilm integrity (Colvin et al. 2012). Extracellular DNA increases aminoglycosides resistance and acts as a nutrient source during starvation and as a "skeleton" by interacting with Psl to form Psl-eDNA fibres that allow bacterial adherence and growth (Chiang et al. 2013; Wang et al. 2015).

P. aeruginosa invasion of host tissues depends upon the secretion of extracellular enzymes and toxins interfering with host physical barriers, immune defences or cellular functions. The main secreted virulence factors are:

- Proteases: *P. aeruginosa* produces several extracellular proteases, such as elastases (LasA and LasB), alkaline protease and protease IV. The two elastases work synergistically to destroy elastin-containing human lung tissues (Van Delden & Iglewski 1998). LasB is a zinc metalloprotease able to degrade not only actin but also fibrin, fibronectin and collagen. LasA is a serine protease that enhances LasB activity by cleaving glycine-glycine bonds within elastin. Alkaline protease is a zinc metalloprotease degrading fibronectin and several components of host immune system (Laarman et al. 2012). Protease IV is a serine protease that can cleave complement proteins, immunoglobulins, fibrinogen and degrade the corneal epithelium (Engel et al. 1998).

- Haemolysins: two haemolysins are produced by *P. aeruginosa*, rhamnolipids and phospholipase C (PLC). Rhamnolipids are amphipathic molecules, composed of L-rhamnose containing glycolipids, promoting swarming motility and the maintenance of biofilm architecture (Caiazza et al. 2005; Davey et al. 2003). It was observed that rhamnolipids contribute to create interior cavities in the biofilm structure to permit the flow of water and nutrients (Chrzanowski et al. 2012). This haemolysin was also identified in the sputum of cystic fibrosis patients and can block the ciliary activity of human lung epithelium (Read et al. 1992). PLC especially hydrolyses phospholipids containing quaternary ammonium groups (e.g., phosphatidylcoline), which are major components of eukaryotic membranes but rarely found in prokaryotes (Berka & Vasil 1982).

- Pyocyanin (PYO): a blue pigment, belonging to the phenazine family, produced by *P. aeruginosa* secondary metabolism. It is a redox active compound that can serve as mobile electron carrier to modulate the intracellular redox state in conditions of electron acceptors restriction, such as oxygen limitation during stationary phase (Price-Whelan et al. 2007). PYO is essential for full virulence in different infection models, ranging from insects and nematodes to mammals (Lau et al. 2004). The presence of PYO in the lung epithelium strongly contributes to the severity of *P. aeruginosa* respiratory infections in CF patients by exposing epithelial cells to oxidative stress and stimulating the production of proinflammatory mediators. (Rada & Leto 2013). *P. aeruginosa* possesses two redundant operons, *phz1* and *phz2*, implicated in PYO biosynthesis (Mavrodi et al. 2001). These two operons share 99% identity but have distinct promoter regions. The transcription of *phz1* is induced by LasR, RhlR and PqsR, whereas only PqsR has a positive role in *phz2* expression (Whiteley et al. 1999; Déziel et al. 2004; Recinos et al. 2012).

- Pyoverdine (PVD): major siderophore of *P. aeruginosa* synthesized under conditions of iron starvation to sequester ferric iron from the environment for bacterial growth. PVD induces the production of virulence factors, such as exotoxin A, protease IV and PVD itself, and is important for biofilm development *in vitro* (Lamont et al. 2002; Visca et al. 2007). Moreover, the expression of PVD synthetic genes was demonstrated to be high during lung systemic infections and in the sputum of CF patients (Handfield et al. 2000; Haas et al. 1991).

- Exotoxin A (ETA): enzyme transferring the ADP-ribose moiety of NAD to the eukaryotic elongation factor 2 (eEF-2), leading to cessation of protein synthesis and cell death. *P. aeruginosa* isolates from different sites of

infection produced ETA (Hamood, Griswold, et al. 1996). ETA synthesis by *P. aeruginosa* is fine-tuned by positive and negative effectors and environmental conditions (Hamood et al. 2004). The expression of the *toxA* gene for ETA is induced by the iron starvation sigma factor PvdS and repressed by Fe^{2+} and the ferric-uptake regulator Fur (Hamood et al. 2004). Moreover, *toxA* expression is controlled by a pair of effectors, namely PtxR and PtxS, involved in the regulation of ketogluconate metabolism (see details in Section 4.4; Daddaoua et al. 2012).

- T3SS effectors: four exoenzymes (ExoS, ExoU, ExoT, ExoY) are secreted by the type III secretion system (T3SS), which is responsible for the direct injection of *P. aeruginosa* toxins into the host cell (Hauser 2009). ExoS and ExoU are the most potent exotoxins, whereas ExoT and ExoY have minor roles in cytotoxicity. ExoS is a bifunctional toxin with GTPase activating protein and ADP-rybosiltransferase activities that interferes with actin cytoskeletal organization and eukaryotic DNA synthesis, causing cell death (Pederson & Barbieri 1998). ExoU is a phospholipase causing rapid death of eukaryotic cells due to disruption of plasma membrane integrity. ExoT has the same function as ExoU, but only the 0.2% of ExoU activity. ExoY is an adenylate cyclase with uncertain significance in infection.

The systemic dissemination is a poorly characterized stage of *P. aeruginosa* pathogenesis supposed to be mediated by the same cell-associated and secreted virulence factors implicated in the localized infection (Strateva & Mitov 2011).

1.2. The P. aeruginosa quorum sensing network

The expression of most *P. aeruginosa* virulence factors is modulated by a cell-to-cell communication system known as Quorum Sensing (QS). This system is common in both gram-positive and gram-negative bacteria and is based on the production of small diffusible molecules called autoinducers. The level of these signal molecules rises along with the increase of bacterial population until it reaches a threshold concentration (the "quorum") that permits the interaction of these molecules with their cognate transcriptional regulator. In this way, the regulators can activate or repress the expression of their target genes.

P. aeruginosa possesses a sophisticated QS network, consisting of four systems (*las, rhl, pqs,* and *iqs*) and depending on the interaction of different regulators with distinct classes of autoinducers (**Fig. 1**; Lee & Zhang 2015).

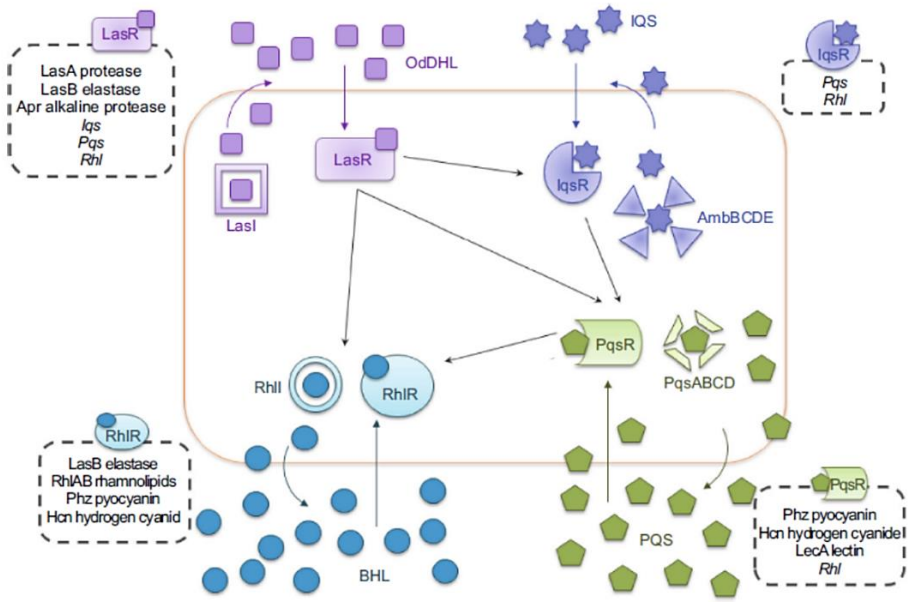

Fig. 1. The *P. aeruginosa* quorum sensing network. The four QS systems, with their respective autoinducers and transcriptional regulators, are represented with different colours. The main targets controlled by each regulator are indicated in dashed squares. Arrows, positive regulation. Modified from Lee & Zhang 2015.

The production of *N*-3-oxododecanoyl-homoserine lactone (OdDHL), by the autoinducer synthase LasI, mediates the activation of the *las* system. The interaction of OdDHL with its cognate regulator LasR induces the expression of virulence genes and *lasI*, thus creating a positive feedback loop (Seed et al. 1995). LasR positively regulates the expression of LasA and LasB elastases, alkaline protease and exotoxin A (Smith & Iglewski 2003). It was demonstrated that the OdDHL signal is necessary for normal biofilm differentiation (Davies et al. 1998).

As for the *las* system, the autoinducer of the *rhl* system is also an homoserine lactone, namely the *N*-butanoyl-homoserine lactone (BHL), synthetized by RhlI. The BHL signal molecule binds to its cognate regulator RhlR to activate the expression of *rhlAB*, *phz* and *lecAB* genes for the synthesis of rhamnolipids, pyocyanin and lectins, respectively (Brint & Ohman 1995). In addition, the RhlR-BHL complex is required for the full activation of the *lasB* promoter and induces the expression of *rhlI*, forming a second positive feedback loop (Brint & Ohman 1995; Ochsner & Reiser 1995).

P. aeruginosa expresses a third QS system, termed *pqs*, responding to a signal molecule chemically different from those of *las* and *rhl* systems. This molecule is termed Pseudomonas Quinolone Signal (PQS) and is structurally defined as 2-heptyl-3-hydroxy-4-quinolone. The PQS cognate regulator is PqsR, that positively regulates the expression of the *pqsABCDE* operon, for the production of the PQS precursor HHQ (4-hydroxy-2-heptyl-quinoline), and the *pqsH* gene for the conversion of HHQ to PQS (Cao et al. 2001). Mutants with a defective *pqs* system show a decreased production of virulence factors such as pyocyanin, elastases, lectins and rhamnolipids (Cao et al. 2001).

The autoinducer of the fourth QS system is IQS (Integrated QS signal), structurally identified as 2-2-hydroxyphenyl-thiazole-4-carbaldehyde. This

system is relevant under phosphate starvation and its disruption was demonstrated to cause a decrease in the production of BHL, PQS and virulence factors such as pyocyanin, rhamnolipids and elastases (Lee et al. 2013).

The four QS circuits are interconnected and hierarchically organized. The *las* system resides at the top of the signalling cascade, with the LasR-odDHL complex positively regulating the expression of *rhlR*, *rhlI*, *pqsR* and *pqsH* (Pesci et al. 1997; Deziel et al. 2004). Also the *iqs* system was demonstrated to be regulated by *las* when bacteria grow in rich medium (Lee et al. 2013). The *pqs* system indirectly enhances the expression of *rhl*-related virulence traits by inducing *rhlI* expression, forming a bridge between *las* and *rhl* circuits (McKnight et al. 2000). However, exceptions in this hierarchy occur. It was found that RhlR can induce the synthesis of *las*-controlled virulence factors and PQS in a Δ*lasR* mutant, indicating that a compensatory activation of the *rhl* system can override the QS hierarchy to maintain the expression of virulence genes when the *las* circuit is affected (Dekimpe & Deziel 2009). This is the situation often encountered during chronic infections of the CF lung, with *P. aeruginosa* isolates that may lose the *las* system but keep the RhlR-dependent regulation of QS virulence factors (Bjarnsholt et al. 2010). Furthermore, the timing in the expression of *las* and *rhl* systems was demonstrated to depend on the growth medium, with *rhl* activated earlier than *las* under certain conditions (Duan & Surette 2007). This suggests that the QS regulatory systems have a dynamic hierarchy to allow a precise and prompt expression of *P. aeruginosa* virulence genes in response to environmental changes.

1.3. Regulation of quorum sensing by environmental cues

The *P. aeruginosa* quorum sensing (QS) network is well integrated into global regulatory circuits, so that signals additional to cell density can be sensed by this

pathogen to regulate the production of virulence effectors. Indeed, the expression of QS systems in *P. aeruginosa* is influenced by a variety of metabolic and environmental signals, as well as by human host factors (**Fig. 2**; Venturi 2006; Lee & Zhang 2015).

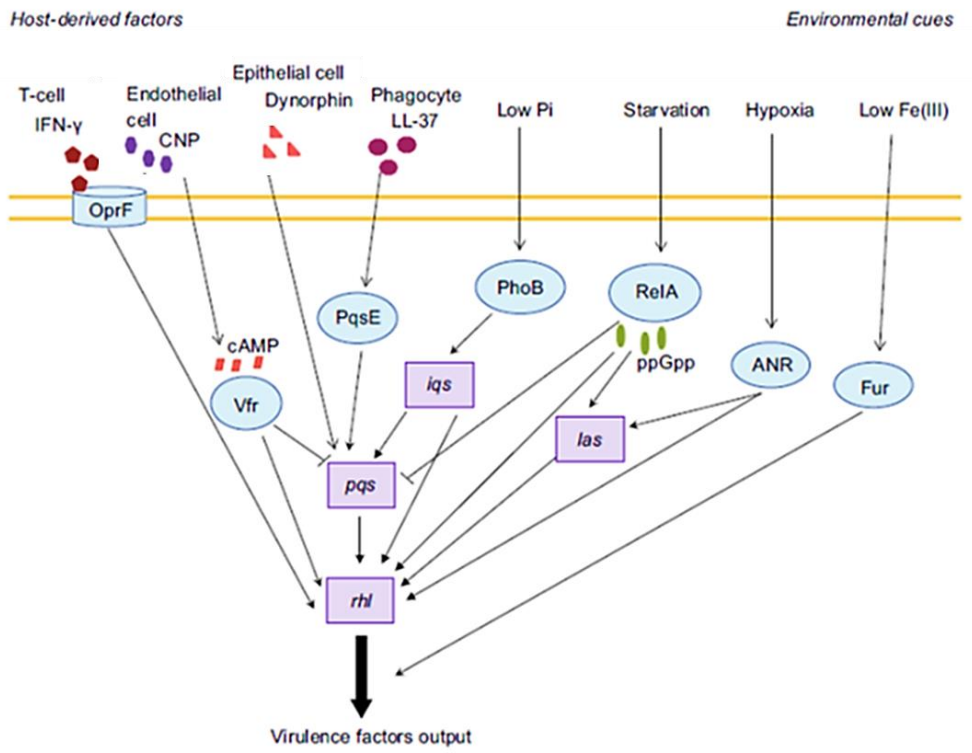

Fig. 2. Regulation of *P. aeruginosa* quorum sensing network by environmental cues and host factors. The four QS systems are represented in violet rectangles. Light blue circles highlight the factors mediating QS network regulation in response to extracellular signal, indicated in the upper part of the figure. Arrows, positive regulation. Perpendicular lines, negative regulation.
The regulation mechanisms are elucidated in the text. Modified from Lee & Zhang 2015.

Regulators of the stringent response, a conserved regulatory mechanism coordinating bacterial adaptation to nutrient starvation, differently affect the induction of QS systems. The overproduction of DksA, a regulator that increases the activity of the stringent response signal (p)ppGpp (penta- and tetra-phosphorylated guanosine), inhibits the *rhlI* expression and the translation of

LasB elastase and rhamnolipids encoding genes (Branny et al. 2001; Jude et al. 2003). On the contrary, the overproduction of the (p)ppGpp synthesizing protein RelA promotes a cell-density independent and premature transcription of *lasR* and *rhlR*, as well as elastase activity (van Delden et al. 2001). Accordingly, a (p)ppGpp deficient strain shows a significant downregulation of *las* and *rhl* systems, in line with a decrease in elastase and rhamnolipids production (Schafhauser et al. 2014).

The RpoS starvation sigma factor is also involved in the regulation of QS genes. RpoS represses *rhlI* transcription in early log phase, with a concomitant reduction in BHL levels and in the expression of the *rhl*-dependent *phz* and *hcn* operons for the biosynthesis of pyocyanin and hydrogen cyanide, respectively (Whiteley et al. 2000). Transcriptomic analysis revealed that RpoS influences the expression of many QS-controlled genes, suggesting that this sigma factor may act as a global regulator of QS network at the onset of stationary phase (Schuster et al. 2004). Some QS-dependent genes are induced by RpoS (*lecA*, *coxAB*), whereas others are repressed (*aprA*, *phz* and *hcn* operons).

Another alternative sigma factor, RpoN, involved in nitrogen metabolism and assimilation under nitrogen limiting conditions, negatively regulates *lasRI* and *rhlRI* expression in a nutrient-rich medium (Heurlier et al. 2003). On the other hand, this sigma factor act as a positive regulator of *rhlI* transcription when *P. aeruginosa* was grown in minimal medium supplemented with glucose (Thompson et al. 2003).

Phosphate deprivation stimulates the expression of the *pqs* system, promoting the formation of PQS-Fe^{3+} toxic complexes that elicit a rapid mortality in *C. elegans* (Zaborin et al. 2009). Moreover, the *iqs* system can partly take over the activity of *las* under phosphate-limiting conditions by inducing *rhl* and *pqs* systems (Lee et al. 2013). The PhoB/PhoR two-component system, which activates the cell

response to phosphate starvation, was found to mediate this induction (Zaborin et al. 2009; Lee et al. 2013).

Although the expression of QS-related virulence factors (proteases, exotoxin A) is triggered in iron-limiting environments, a direct connection between iron deprivation and the expression of QS genes has not been found so far. However, iron starvation indirectly increases PQS levels by triggering the Fur-dependent de-repression of PrrF1 and PrrF2, two small RNAs inhibiting the degradation of the PQS precursor anthranilate (Oglesby et al. 2008). PQS molecules can function as iron trap at the *P. aeruginosa* cell surface to facilitate the siderophore-dependent iron uptake (Diggle et al. 2007).

Oxygen limitation stimulates the synthesis of hydrogen cyanide (HCN), a potent inhibitor of the aerobic respiratory chain in many organisms. It was found that LasR and RhlR cooperate with ANR, a global regulator of the anaerobic response in *P. aeruginosa*, to induce the expression of the *hcnABC* cyanide biosynthetic operon (Pessi & Haas 2000).

The expression of QS-dependent genes changes also in response to human factors. As an example, the bind of interferon-γ cytokine to OprF, the major *P. aeruginosa* outer membrane protein, activates *rhlI* expression and the production of PA-I lectin and pyocyanin (Wu et al. 2005). This could be a strategy adopted by *P. aeruginosa* to counteract the activation of host immune response upon pathogen recognition. Different human peptides may also impact on *P. aeruginosa* QS. For instance, the opioid peptide dynorphin, normally found at high concentrations in intestinal tissues upon stress, is able to penetrate *P. aeruginosa* cells in a mouse model of infection (Zaborina et al. 2007). The recognition of dynorphin by *P. aeruginosa* was found to induce the expression of the *pqs* system and pyocyanin synthetic genes (Zaborina et al. 2007). Moreover, the C-type natriuretic peptide (CNP), produced by endothelial cells to

regulate body fluid homeostasis and blood pressure, triggers the cAMP-dependent activation of Vfr, a *P. aeruginosa* transcriptional factor positively regulating *lasR* transcription and the expression of a variety of virulence determinants, including exotoxin A (Blier et al. 2011). Finally, it was proved that the phagocytic antimicrobial peptide LL-37 promotes the synthesis of PQS and QS-related virulence factors, such as phenazines, hydrogen cyanide, elastase and rhamnolipids (Strempel et al. 2013).

2. *Caenorhabditis elegans* and *Galleria mellonella* as model hosts to study *P. aeruginosa* infections

Invertebrates can be used as model hosts to investigate bacterial pathogenesis and have several advantages over mammalian models (Glavis-Bloom et al. 2012). Indeed, invertebrates are much cheaper and easier to maintain, as they do not require special lab equipment, and no ethical approval is necessary for their use. Additionally, the small size and short lifespan make them ideal for high-throughput studies. Despite not presenting an adaptive immune system, invertebrates have a relatively advanced innate immune response sharing many similarities to that of mammals. A certain conservation was especially observed in the innate immune mechanisms of insects and mammals (Ganz & Lehrer 1994; Hoffmann 1995; Kopp & Medzhitov 1999).

The recognition of a pathogen by the host innate immune system is mediated by a set of proteins, termed pattern-recognition receptors (PRRs), which can directly identify invariant molecule structures shared by most of bacteria (pathogen-associated molecular patterns or PAMPs). Interestingly, it was observed that the Toll family of PRRs are crucial for the activation of innate host defence in both mammals and insects (Kopp & Medzhitov 1999). These receptors induce a signal-transduction pathway to activate the expression of defence-related genes

that is well conserved from insects to mammals (Kopp & Medzhitov 1999). A certain similarity was also found in the type of defence effectors produced to kill pathogens. For example, the antimicrobial peptides class of defensins is shared between insects and mammals (Ganz & Lehrer 1994).

As already mentioned in Section 1, *P. aeruginosa* is not only an opportunistic pathogen for mammals but it can also naturally infect invertebrates such as insects and nematodes. The relevance of using invertebrates as *P. aeruginosa* infection model arises from the possibility to screen libraries of mutants and, consequently, to study the contribution to pathogenesis of essentially all *P. aeruginosa* genes. Therefore, invertebrates might function as preliminary *in vivo* virulence screening systems to restrict the number of *P. aeruginosa* mutants to be tested in mammals.

In the next two sections, I provide a brief introduction to the invertebrate models I used for the *P. aeruginosa* infection assays: the *Caenorhabditis elegans* nematode and the *Galleria mellonella* insect larvae.

2.1. The Caenorhabditis elegans model

The *C. elegans* soil-living nematode is well suited for experimental studies, considering its small size (adults are ~1 mm), rapid life cycle (~3.5 days at 20 °C), short lifespan (~ 2 weeks) and transparent body. In addition, its genome was fully sequenced and it is possible to generate mutant strains (Waterston et al. 1993). Moreover, RNA interference was established to be a powerful system of genetic silencing in *C. elegans*, thanks to the possibility to deliver double-stranded interfering RNA to the nematode by feeding (Fire et al. 1998). *C. elegans* is particularly suitable to study bacterial infections because it naturally feeds on microorganisms and is susceptible to a variety of bacteria that are pathogenic also for mammals (Tan & Ausubel 2000).

P. aeruginosa was demonstrated to kill this nematode by two distinct modes according to the growth conditions. In low salt media, the highly virulent *P. aeruginosa* PA14 strain is able to colonize and accumulate in the nematode intestine, causing the death over 2-3 days ("slow killing"; Tan et al. 1999). The infectious process entails: i) severe distension of the intestinal lumen, with a consequent reduction in the volume of intestinal epithelial cells; ii) accumulation of an unidentified extracellular matrix in the intestinal lumen; iii) synthesis of outer membrane vesicles by *P. aeruginosa*; iv) abnormal autophagy in the intestinal cells (Irazoqui et al. 2010). By contrast, when grown in high salt media, *P. aeruginosa* PA14 kills the nematodes within 4-24 hours by the production of diffusible toxins, such as phenazines ("fast killing"; Mahajan-Miklos et al. 1999). It was demonstrated that phenazines exert their toxic activity through the *in vivo* generation of oxidative stress (Mahajan-Miklos et al. 1999).

A transposon mutant library generated in PA14 strain was screened for attenuation of virulence in *C. elegans* to gain insights into the genetic basis underlying the pathogenesis of this bacterium (Feinbaum et al. 2012). The screen revealed that the major contributors to virulence appear to be genes implicated in the regulation of virulence effectors expression (*lasR, rhlR, gacA, gacS*) and nutrient assimilation (*aru, glnK*). Curiously, only a small subset of the virulence genes identified in the screening contribute to the infection also in mammalian hosts. This is probably due to discrepancies in both physico-chemical characteristics (temperature, pH, nutrient availability) and components participating in the immune response.

The defence mechanisms that *C. elegans* induces upon pathogen recognition have not been completely understood. Although a Toll-receptor homolog, *tol-1*, is present in *C. elegans* genome, the genes encoding crucial components of the Toll signalling pathway of mammalian innate immunity seem to be absent.

Nevertheless, the expression of many immune response genes was found to be controlled by the PMK-1 p38 mitogen-activated protein kinase (MAPK), the terminal MAPK of the defence activating cascade that is present also in mammals (Troemel et al. 2006). The immune effectors induced by PMK-1 include defensin-like antimicrobial peptides, lysozyme and C-type lectins, proteins that bind sugar moieties on the surface of pathogens and stimulate phagocytosis.

2.2. The Galleria mellonella model

G. mellonella, or greater wax moth, is an insect of the *Pyralidae* family increasingly proposed as a new model to study bacterial infections. It is the larval stage of the wax moth that is used as animal model and the last instar larvae before pupation are those specifically employed for the infection assays. Like *C. elegans*, *G. mellonella* larvae are inexpensive, easy to be stored and have the advantage that they survive at 37 °C, allowing the investigation of temperature-dependent microbial virulence factors, whereas *C. elegans* cultivation temperature spans from 15 to 25 °C. Larvae infection is performed by intrahemocoelic injection in one of the pseudopods. While this infection mode is too labour-intensive to allow the utilization of *Galleria* in high throughput screenings, it has the advantage that a controlled number of bacteria can be inoculated in each larva; this gives the opportunity to estimate the half-maximum lethal dose (LD_{50}), a parameter commonly used to evaluate bacterial virulence (Ramarao et al. 2012). On the other hand, substantial limitations to this model are that its genome has not yet been sequenced and strategies to generate mutants have not been developed. Another problem is that the larvae are usually purchased from independent breeders who sell them as pet food. This implies that breeding conditions and larvae maintenance can influence the susceptibility to infections.

G. mellonella is sensitive to a wide range of gram-positive and gram-negative pathogens, such as *P. aeruginosa* (Tsai et al. 2016). Notably, the susceptibility of these larvae to *P. aeruginosa* infections is particularly high, with an LD_{50} of fewer than 10 bacteria observed for the PA14 strain (Jander et al. 2000; Miyata et al. 2003). The infectious process entails the bacterial dissemination into the larvae hemolymph, typically causing death by septicemia in less than 24 h.

The possibility to perform the infection assays at 37°C led to investigate whether the *P. aeruginosa* virulence factors implicated in *G. mellonella* killing were also relevant in mammalian infections. Nevertheless, ambiguous results have been reported so far. A significant positive correlation between the virulence of PA14 mutants in *G. mellonella* and in a burn mouse model was observed (Jander et al. 2000). In contrast, the pathogenic capacity of *P. aeruginosa* strains, isolated from either diseased patients or the environment, resulted highly variable between *G. mellonella* and a murine airway model (Hilker et al. 2015). Interestingly, the *G. mellonella* model was found to be convenient to study the involvement of type III secretion system (T3SS) in *P. aeruginosa* pathogenesis (Miyata et al. 2003). The *in vivo* virulence of PA14 mutants in genes encoding T3SS effectors indicated that none of them is essential for *G. mellonella* killing, but the simultaneous inactivation of ExoT and ExoU is necessary to obtain a highly attenuated killing phenotype. A high level of correlation was observed between the results obtained in *Galleria* and those found in cytopathology assays performed with a mammalian tissue culture system.

G. mellonella larvae appear to be also useful as animal model to test the *in vivo* efficacy of novel antimicrobial agents. As an example, this model was successfully exploited to demonstrate the efficacy of double and triple antibiotic combination therapies against a multidrug-resistant strain of *P. aeruginosa* (Krezdorn et al. 2014). A pre-screening with *G. mellonella* would reduce the

number of antibacterial candidates to be tested in mammalian models, with a significant reduction of times, costs and ethical issues.

Compared to other invertebrates, insects have an advanced innate immune system similar to that of mammals and consisting of both a cellular and a humoral response. The cellular response is mediated by phagocytic cells, termed hemocytes, located within the hemolymph. *G. mellonella* has 6 different types of hemocytes involved in bacterial encapsulation and phagocytosis (**Table 2**; Tsai et al. 2016).

Table 2. Elements of cellular and humoral immune responses in *G. mellonella*

	a) cellular response
hemocytes	prohemocytes
	plasmatocytes
	granular cells
	coagulocytes
	spherulocytes
	oenocytoids
	b) humoral response
opsonins	apolipophorin-III (apoL-III)
	peptidoglycan recognition proteins (PGRPs)
	cationic protein 8 (GmCP8)
	hemolin
antimicrobial peptides (AMPs)	lysozyme
	cecropin
	moricin-like peptides
	gloverin
	galiomycin
	gallerimycin
	Galleria defensin
	Gm proline-rich peptides 1 and 2
	Gm anionic peptide 1 and 2
	inducible serine protease inhibitor 2
	heliocin-like peptide
	x-tox
	Gm apolipophoricin
melanization	phenoloxidase pathway

Modified from Tsai et al. 2016.

The humoral response depends on the activity of soluble effector molecules that recognize, immobilize and kill pathogens. In *G. mellonella*, the humoral response relies on the production of opsonins and antimicrobial peptides, and on melanization (**Table 2**; Tsai et al. 2016). As mammalian pattern recognition receptors, opsonins recognize and bind to conserved bacterial structures, making them visible to the immune system. Apolipophorin-III (apoLp-III), the major opsonin of *Galleria*, specifically binds the bacterial lipopolysaccharide and lipoteichoic acid, stimulating the hemolymph antimicrobial activity (Niere et al. 1999). Another recognized bacterial component is peptidoglycan, which is bound by peptidoglycan recognition proteins (PGRPs) through a conserved domain homologous to T4 phage lysozyme.

G. mellonella produces 18 known or putative antimicrobial peptides (AMPs), including lysozyme, cecropins, moricins and defensins. Lysozyme disrupts cell wall peptidoglycan by cleaving the β-1, 4 bond between N-acetylglucosamine and N-acetylmuramic acid. Cecropins and moricins are amphipathic peptides able to create pores in the cytoplasmic membrane of both gram-positive and gram-negative bacteria, resulting in ion leakage. Defensins are cationic peptides causing the formation of voltage-dependent ion channels in the cytoplasmic membrane and triggering ion leakage and cell lysis.

Melanization represents the synthesis and deposition of melanin around invading pathogens to promote their encapsulation and opsonisation. This process starts with the formation of black dots on the larvae surface and leads to complete browning before larvae death (**Fig. 3**).

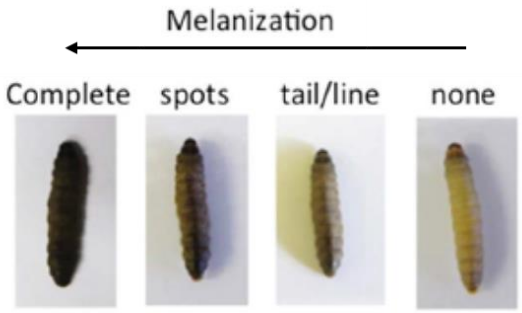

Fig. 3. The stages of *G. mellonella* melanisation upon bacterial infection. Modified from Tsai et al. 2016.

Melanin formation depends on the activity of phenoloxidase (PO), that is produced as the inactive form pro-phenoloxidase (Pro-PO) in hemocytes. The activation of Pro-PO to PO by cleavage occurs upon pathogen recognition and catalyses the conversion of phenols to quinines, which non-enzymatically polymerize to form melanin at the site of infection.

3. Glucose homeostasis and bacterial infections

Hyperglycaemia is a pathological disruption of glycaemic control systems causing an abnormal increase in glucose blood concentration. Indeed, hyperglycaemia was defined as a blood glucose concentration ≥ 7 mM, compared to 4-5.5 mM of healthy individuals (Baker et al. 2006). Pathologies leading to hyperglycaemia, such as diabetes mellitus (DM), are associated with an increased probability to develop serious bacterial infections and, indeed, patients with diabetes have a 4.4 higher risk of bloodstream infection than non-diabetics (Stoeckle et al. 2008). This enhanced susceptibility to bacterial infections is related with both immunity dysfunction due to hyperglycaemia and the glucose-stimulating effect on the growth of bacterial pathogens such as *P. aeruginosa* and *S. aureus* (Baker et al. 2006).

Hyperglycaemia can impair the innate immune system by interfering with the activity of polymorphonuclear neutrophils (PMNs) (Geerlings & Hoepelman 1999; Peleg et al. 2007). All the steps of PMNs functioning, i.e. adherence to the site of infection, transmigration through the vessels, phagocytosis and microbial killing, are affected in diabetic patients (Delamaire et al. 1997; Geerlings & Hoepelman 1999). In particular, it was demonstrated that superoxide production by PMNs is reduced in diabetics, due to the diversion of NADPH into the polyol pathway, a process converting the excess of glucose into sorbitol (Mazade & Edwards 2001). Moreover, a consequence of hyperglycaemia is the formation of excessive advanced glycation end products (AGEs), a group non-enzymatically and irreversibly glycated macromolecules interfering with neutrophil functions. Indeed, AGE albumin was able to inhibit neutrophils trans-endothelial migration and *S. aureus*-mediated production of reactive oxygen species (Collison et al. 2002).

On the other hand, infections are a major cause of stress-induced hyperglycaemia. The release of cytokines during the inflammatory process caused by infection results in failure of insulin to repress hepatic gluconeogenesis, thus increasing blood glucose levels (McCowen et al. 2001). In this way, a vicious circle between inflammation and hyperglycaemia is established.

3.1. Common infections in hyperglycaemic subjects

The most recurring bacterial infections in diabetic patients are in order: urinary tract infections (UTIs), respiratory infections, soft tissue infections and bacteraemia (Peleg et al. 2007; Burekovic et al. 2014).

The most common bacterial pathogens isolated in the urine of diabetic subjects with UTI are *E. coli* and other Enterobacteriaceae (*Klebsiella* spp, *Proteus* spp and *Enterobacter* spp) and Enterococci (Peleg et al. 2007). Moreover, this

patients are more prone to have resistant pathogens as cause of their UTI, due to the frequent antibiotic treatments to which they are subjected and the increased incidence of hospital-acquired UTIs (Nitzan et al. 2015).

Hyperglycaemia is associated with augmented risk of contracting community acquired pneumonia (CAP; Baker et al. 2006). There is a wide spectrum of bacteria implicated in CAP, with an over-representation of *S. aureus* and gram-negative pathogens (Baker et al. 2006). Patients with chronic obstructive pulmonary disease (COPD) have increased presence of gram-negative pathogens in their sputum when blood glucose levels raise (Loukides & Polyzogopoulos 1996). Together with *S. aureus*, *P. aeruginosa* is the major responsible for lung infections in hyperglycaemic subjects, thanks to its ability to use the excess of glucose in airway secretions for the growth (see details in Section 3.2).

Diabetic foot ulcer and necrotizing fasciitis are the most frequent soft-tissue infections in diabetics. Aerobic gram-positive cocci (especially *S. aureus*) are the predominant microorganisms in diabetic foot infections, but patients with chronic wounds may be also infected by gram-negative rods like *P. aeruginosa* (Lipsky et al. 2006). Both polymicrobial and monomicrobial infections are related to necrotizing fasciitis, with gram-positive (*Streptococcus*, *Staphylococcus*, *Clostridium*) and gram-negative (*Vibrio*) species involved (Iacopi et al. 2015).

Community-acquired bacteraemia caused by *E. coli* and other enterobacteria has higher incidence and poorer outcome in diabetic patients, when compared with non-diabetic individuals (Thomsen et al. 2005). Diabetes is also a major risk for community-acquired pneumococcal bacteraemia (Thomsen et al. 2004).

3.2. Hyperglycaemia exacerbates P. aeruginosa lung infections

The apical surface of airway epithelia is covered by a layer of fluid, the Airway Surface Liquid (ASL), that is normally maintained sterile thanks to the activity of antimicrobials and innate immune components, and to mucociliary clearance (Bartlett et al. 2008). The ASL contains also factors necessary for bacterial growth, such as proteins, lipids and sugars, that are cleared from this layer when in excess. In particular, it was observed that glucose deprivation from the ASL is pivotal to safeguard the sterility of the airways (Pezzulo et al. 2011). Indeed, glucose levels in the ASL of healthy subjects are maintained very low (~ 0.4 mM; 12 times lower than glucose blood concentration), in spite of a big trans-epithelial gradient for the passive transport of glucose from blood to ASL (Baker et al. 2007). The restriction of ASL glucose concentration is mediated by: i) the epithelial tight junctions, which are poorly permeable to glucose; ii) glucose metabolism in the epithelial cells; iii) the presence of apical and basolateral facilitative glucose transporters (GLUTs) permitting the passive movement of glucose across cell membranes to maintain glucose homeostasis (**Fig. 4A**; Baker & Baines 2018).

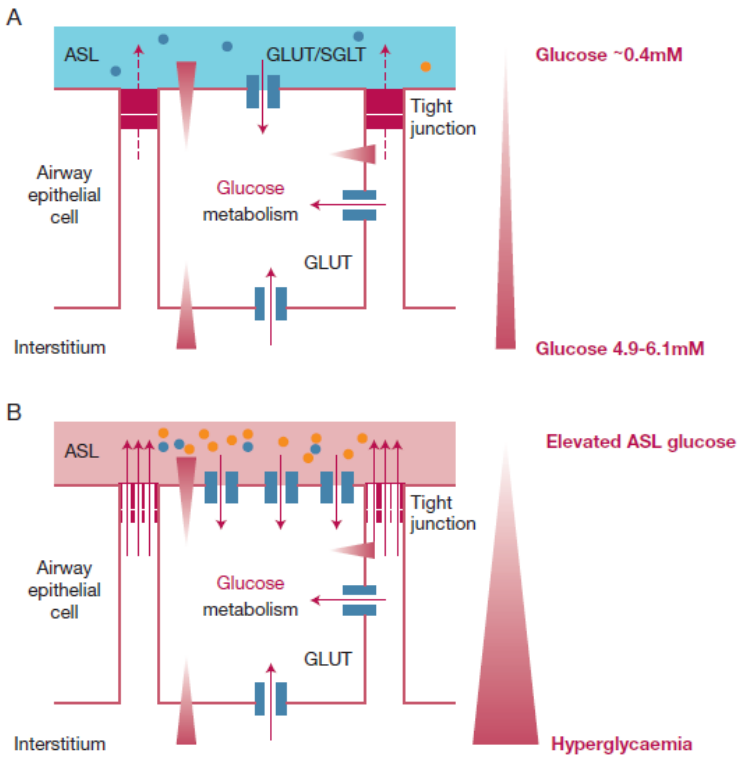

Fig. 4. Glucose homeostasis is essential for airways sterility. A. In healthy subjects, ASL glucose levels are very low (~ 0,4 mM) thanks to functional epithelial tight junctions, epithelial glucose metabolism and glucose transporters (GLUTs). This limits the growth of bacteria in the ASL (orange and blue circles). B. Airway glucose homeostasis can be disrupted by hyperglycaemia, which increases the glucose gradient towards ASL, and inflammation, which enhances the permeability of tight junctions. The resulting higher glucose levels in the ASL stimulates the growth of bacteria able to use glucose as carbon source (orange circles). From Baker & Baines 2018.

Both hyperglycaemia and airway inflammation promote the disruption of airway glucose homeostasis, increasing the levels of glucose in the ASL (**Fig. 4B**). Diabetes elevates the glucose trans-epithelial gradient in the airways, leading to an ASL glucose concentration of about 1.2 mM (Baker et al. 2007). In cystic fibrosis (CF) patients, who have chronic lung inflammation, glucose in the ASL reaches a concentration of 2 mM (Baker et al. 2007). The reason for this phenomenon is the increase in paracellular glucose diffusion across the airway epithelium into ASL, due to the altered expression of epithelial tight junction

proteins (Garnett et al. 2013). The high ASL glucose concentration was demonstrated to stimulate the growth of respiratory pathogens, such as *P. aeruginosa*, able to use glucose as carbon source for growth (Garnett et al. 2013). *P. aeruginosa* proliferation triggers the production of virulence factors that can damage the airway epithelium, thus enhancing the inflammatory response and the paracellular glucose movement into the ASL (Garnett et al. 2013). In this way, a vicious circle among bacterial proliferation, inflammation and glucose flux into the ASL is established.

P. aeruginosa pulmonary infections are particularly severe in people that are subjected to both airway inflammation and hyperglycaemia. This is the case of cystic fibrosis related diabetes (CFRD) patients. CFRD is the most common comorbidity in CF subjects, with an incidence 20% in adolescents and 40-50% in adults (Moran et al. 2009). Survival is significantly affected in people with CFRD, with fewer than 25% surviving to an age of 30, compared to 60% of non-diabetic CF patients (Finkelstein et al. 1988). One of the main reasons for the greater mortality of CFRD subjects is the accelerated decline in lung function (Koch et al. 2001). It was proved that ASL glucose levels are further elevated to 4 mM in people with CFRD (Baker et al. 2007). This additional perturbation in airway glucose homeostasis exacerbates the aforementioned vicious circle in CRFD airways, contributing to the worse outcome of bacterial lung infections observed in these patients.

The glucose-dependent stimulation of *P. aeruginosa* lung proliferation was also shown in murine models of hyperglycaemia, CF and CFRD (Gill et al. 2016; Hunt et al. 2014). *P. aeruginosa* burden is clearly higher in the lungs of hyperglycaemic mice, which have significantly greater airway glucose, and in non-diabetic CF mice (**Fig. 5**; Hunt et al. 2014). Diabetic CF mice showed a minor bacterial clearance from their lung compared to both hyperglycaemic and

CF mice, leading to a further increase in *P. aeruginosa* load (**Fig. 5**; Hunt et al. 2014).

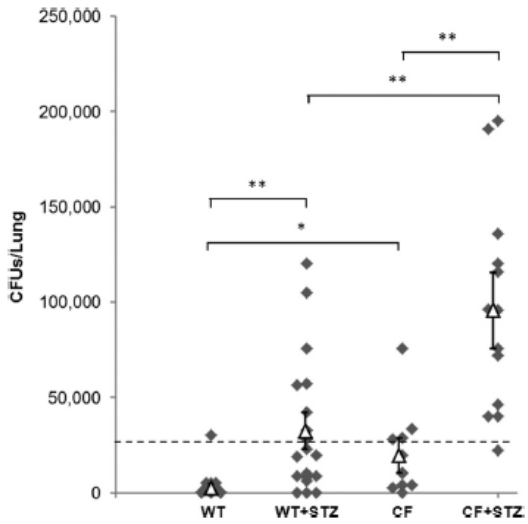

Fig. 5. *P. aeruginosa* clearance from mice lungs. Lung homogenate colony-forming units (CFUs) recovered 18 h after *P. aeruginosa* PAO1 infection of wt mice, hyperglycaemic mice (wt+stz), cystic fibrosis mice (cf) and diabetic CF mice (cf+stz). The dashed line indicates the clearance threshold, based on 3-times the standard deviation above the mean value obtained in wt mice.
*P < 0.05, **P < 0.01. From Hunt et al. 2014.

The increased proliferation of *P. aeruginosa* in the lungs of diabetic mice is a direct consequence of its ability to metabolize the excessive ASL glucose, since it was not observed in some mutant strains in which glucose uptake and utilization genes were deleted (see Section 4.4; Pezzulo et al. 2011; Gill et al. 2016).

4. *P. aeruginosa* glucose metabolism

4.1. Metabolic versatility and hierarchical management of carbon sources in P. aeruginosa

Pseudomonas spp. usually inhabit environmental niches characterized by a restricted presence of sugars. This is probably the reason why the bacteria of this genus can metabolize a very limited number of sugars (glucose, glycerol, mannitol and fructose), despite their huge metabolic versatility, which allows them to use many different compounds as carbon and energy sources. However, metabolic versatility must be fine-tuned to guarantee a rapid adaptation to the frequently changed environmental conditions and optimize the ecological fitness. In this respect, bacteria adopt a regulatory process, named Carbon Catabolite Repression (CCR), to preferentially use the carbon source providing the most efficient growth and to concurrently inhibit the uptake and catabolism of all the other exploitable compounds. Therefore, CCR leads to a hierarchy in the consumption of the different carbon sources.

The regulatory factor operating CCR in *P. aeruginosa* is the Crc protein. Crc is an RNA-binding protein that inhibits the expression of genes for the uptake and catabolism of the non-preferred carbon sources by associating to their mRNAs and preventing the formation of a productive translation initiation complex (Rojo 2010; **Fig. 6a**). The CrcZ small RNA regulates Crc availability. Indeed, this sRNA contains five Crc binding sites and is able to sequester the regulator in conditions that produce low or no CCR (Rojo 2010; **Fig. 6b**).

crcZ expression is directly activated by the CbrA/CbrB two-component system (TCS) and the RpoN sigma factor (Sonnleitner et al. 2009). The CbrA/B TCS is required for the expression of genes involved in the utilization of several carbon and nitrogen sources, including mannitol, glucose, arginine, histidine and proline

(Nishijyo et al. 2001). It was suggested that this TCS works co-ordinately with the NtrB-NtrC TCS, which regulates amino acids catabolism, to balance the carbon-nitrogen ratio in the cell (Nishijyo et al. 2001; Li & Lu 2007). However, the specific signals inducing the autophosphorylation of the CbrA sensor are currently unknown.

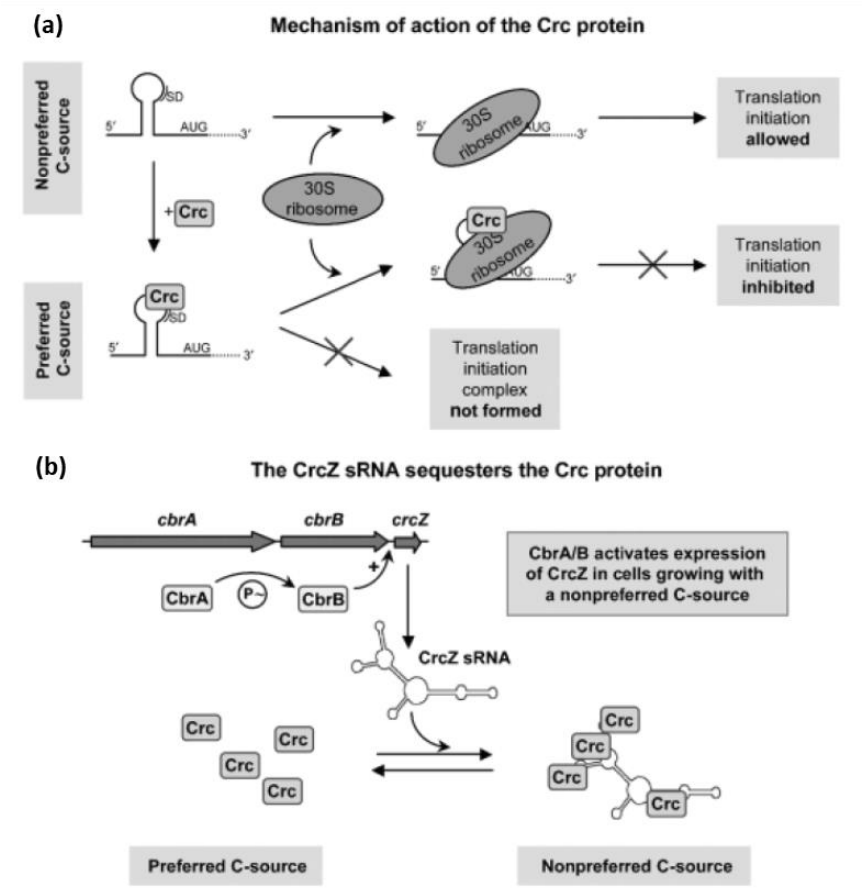

Fig. 6. Regulation of CCR in *P. aeruginosa.* (a) Activity of the Crc protein. Crc binds at specific sites of target mRNAs close to the AUG translation start site, interfering with the formation of a productive translation initiation complex. (b) Crc regulation by the CrcZ sRNA. CrcZ contains five Crc-binding sites in its structure and can sequester Crc under conditions that generate low or no CCR. CrcZ levels depend on the CbrA/B two-component system, according to the carbon sources present in the medium. From Rojo 2010.

CrcZ sRNA was exploited as a bioindicator of CCR. A chromosomal *crcZ-gfp* fusion was created to monitor the contribution of different carbon sources to CCR (**Fig 7**; Valentini et al. 2014). The stronger is the activation of CCR, the lower is the expression of *crcZ* and thus fluorescence. As expected, C_4 dicarboxylates (fumarate, malate and succinate), the preferred carbon source for *P. aeruginosa*, are the stronger inducer of CCR. In contrast, glucose causes an intermediate induction of CCR, being used less efficiently than C_4 dicarboxylates, but more efficiently than other sugars (mannitol) and amino acids.

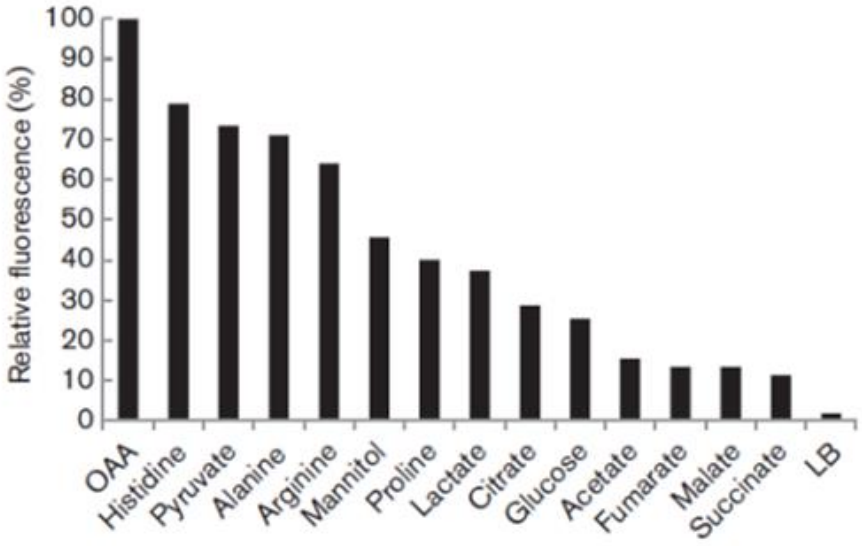

Fig. 7. Carbon source dependent activation of *crcZ* in *P. aeruginosa*. The expression of the *crcZ-gfp* fusion was monitored in *P. aeruginosa* PAO1 grown to mid-log phase in minimal medium, supplemented with the indicated carbon sources, or in LB medium. Fluorescence values are relative to *crcZ-gfp* expression in the presence of oxaloacetate (OAA). From Valentini et al. 2014.

4.2. Glucose metabolism in P. aeruginosa

Glucose metabolism was first clarified in *P. putida* as a three-pronged metabolic process converting glucose to 6-phosphogluconate (6-PG; del Castillo et al. 2007). All the key enzymes for the synthesis of 6-PG from glucose are also present in *P. aeruginosa*, with a very high sequence conservation ranging from 70% to 95% similarity (del Castillo et al. 2007). A schematic representation of glucose metabolism in *Pseudomonas* spp. is depicted in **Fig. 8**.

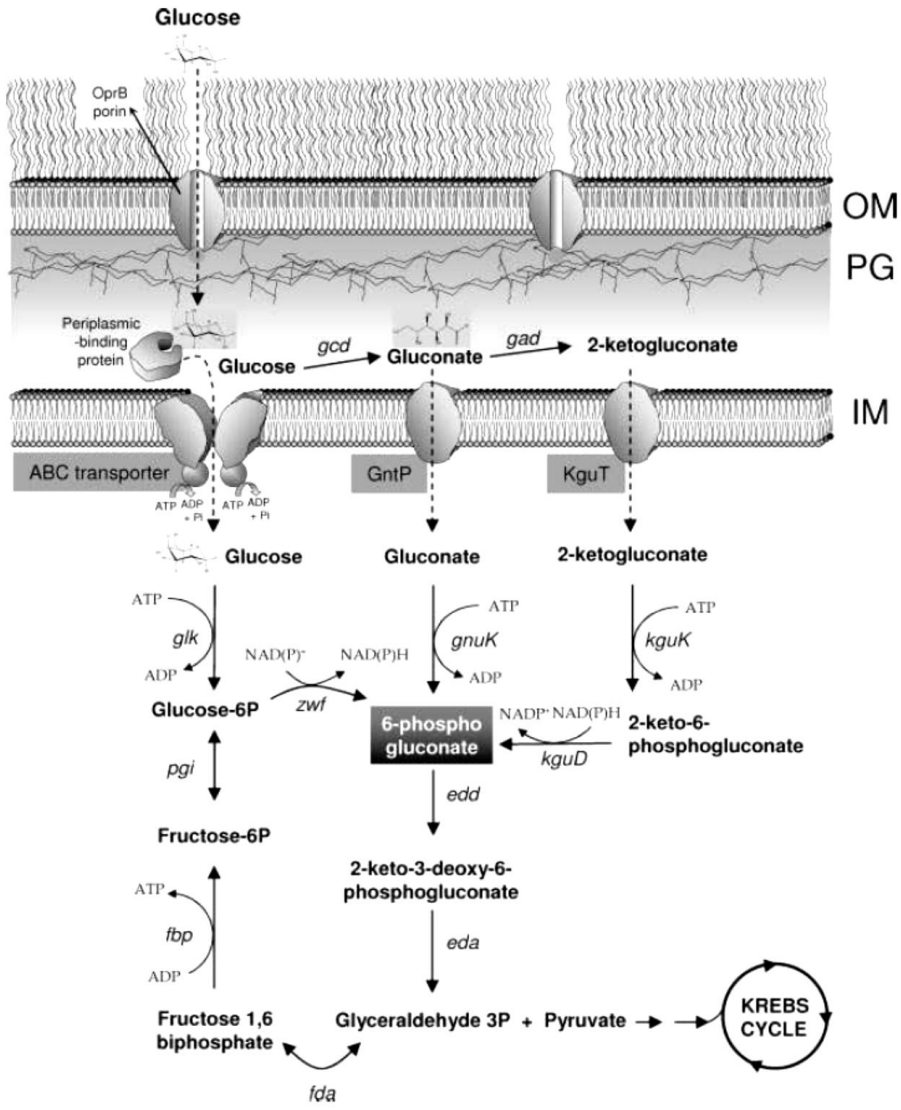

Fig. 8. Glucose metabolism in *Pseudomonas* spp. The genes for glucose uptake and catabolism, indicated in italics, are: *gcd*, glucose dehydrogenase; *gad*, gluconate dehydrogenase; *gntP*, gluconate permease; *kguT*, 2-ketogluconate transporter; *glk*, glucokinase; *gnuK*, gluconokinase; *kguK*, 2-ketogluconate kinase; *zwf*, glucose-6-P-dehydrogenase; *kguD*, 2-ketogluconate reductase; *pgi*, glucose-6-P-isomerase; *fbp*, fructose diphosphatase; *fda*, fructose diphosphate aldolase; *edd*, phosphogluconate dehydratase; *eda*, 2-keto-3-deoxy gluconate aldolase.
OM, outer membrane; IM, inner membrane; PG, periplasmic space. From del Castillo et al. 2007.

Glucose can cross the outer membrane (OM) barrier through the OprB and OprB2 selective porins. OprB does not strictly function as a glucose-selective porin, but

has a broad specificity, facilitating the diffusion of several carbohydrates, including mannitol, glycerol and fructose (Wylie & Worobec 1995). Even though at a quite reduced rate, OprB null-mutants still retain the capability to transport glucose, suggesting that glucose can non-specifically diffuse across the OM through other porins (Wylie & Worobec 1995). A second porin, OprB2, appears to be implicated in glucose transport across the OM. This porin has the same size and is 95% identical to OprB (Chevalier et al. 2017).

Unlike most bacteria, the intake of glucose in *Pseudomonas* spp. is not dependent on the phosphotransferase system, a multiprotein phosphorelay coupling the transport of carbohydrates across the inner membrane (IM) with their concomitant phosphorylation. Instead, once crossed the OM, periplasmic glucose can be internalized into the cytoplasm and metabolized to 6-phosphogluconate by two distinct pathways: the phosphorylative and oxidative routes of glucose uptake (**Fig. 8**; Udaondo et al. 2018).

In the phosphorylative pathway, glucose is directly transported as free sugar across the IM by Glt, an ABC transporter consisting of three components: the permease, encoded by *gltF* and *gltG*, the ATP-binding protein, encoded by *gltK*, and the periplasmic binding protein, encoded by *gltB* (Adewoye & Worobec 2000). Once reached the cytoplasm, glucose is phosphorylated by glucokinase (GlK) to give glucose-6-phosphate (G6P). Next, the NADP-dependent glucose-6-phosphate dehydrogenase (Zwf) converts G6P to 6-phosphogluconolactone, which is then transformed to 6-phosphogluconate by the 6-phosphogluconolactonase (Pgl) (Ma et al. 1998; Hager et al. 2000).

On the other hand, in the oxidative pathway, periplasmic glucose is oxidized to gluconate by the membrane-bound glucose dehydrogenase (Gcd), which uses pyrroloquinoline quinone (PQQ) as cofactor (Midgley & Dawes 1973). At this stage, gluconate can be transported into the cytoplasm or further oxidized in the

periplasm to 2-ketogluconate (2-KG). Gluconate internalization is mediated by the GntP gluconate permease, a predicted gluconate:H^+ symporter, whereas its oxidation to 2-KG depends on the activity of the Gad gluconate dehydrogenase, a membrane-bound enzyme supposed to use FAD as cofactor (Roberts et al. 1973). In turn, 2-KG can enter the cytoplasm through the KguT ketogluconate transporter, a putative anion:cation symporter (Swanson et al. 2000). Once in the cytoplasm, gluconate and 2-KG are respectively phosphorylated to 6-phosphogluconate and 2-keto-6-phosphogluconate by gluconate kinase (GnuK) and 2-ketogluconate kinase (KguK) (Swanson et al. 2000). Finally, 2-keto-6-phosphogluconate is reduced by the NADP-dependent KguD reductase to give 6-phosphogluconate (Swanson et al. 2000).

Then, the convergent product of glucose metabolism, 6-phospogluconate (6-PG), enters the Entner-Doudoroff (ED) pathway, a series of reactions alternate to glycolysis (Lessie & Phibbs 1984). Indeed, *P. aeruginosa* lacks the glycolytic phosphofructokinase and thus exploits the ED route to obtain glyceraldehyde-3-phosphate (G3P) and pyruvate from 6-PG by a two-step reaction. At first, the 6-phosphogluconate dehydratase (Edd) transforms 6-PG to 2-keto-3-deoxy-6-phosphogluconate (KDPG), which is then hydrolysed to produce G3P and pyruvate by the KDPG aldolase (Eda). While pyruvate is decarboxylated to acetyl-CoA and enters the Krebs cycle, G3P may be converted to pyruvate, by lower glycolytic pathway, or recycled to 6-PG via gluconeogenic enzymes (Fda fructose diphosphate aldolase, Fbp fructose diphosphatase and Pgi phosphoglucoisomerase). This cyclic ED pathway helps in the generation of more reducing power in terms of NADPH cofactor.

Metabolic flux analysis in *P. aeruginosa* under high glucose concentrations revealed that the carbon flow through the oxidative route is 10-fold higher that that entering by the Glt uptake system (Midgley & Dawes 1973).

4.3. Genetic organization and transcriptional regulation of glucose metabolic genes in P. aeruginosa

P. aeruginosa glucose metabolism genes are highly organized, with the genes belonging to the distinct catabolic segments arranged in operons under the control of different regulators, namely HexR, PtxS, GntR, and the GltR/GtrS two-component system (**Fig. 9**; Udaondo et al. 2018).

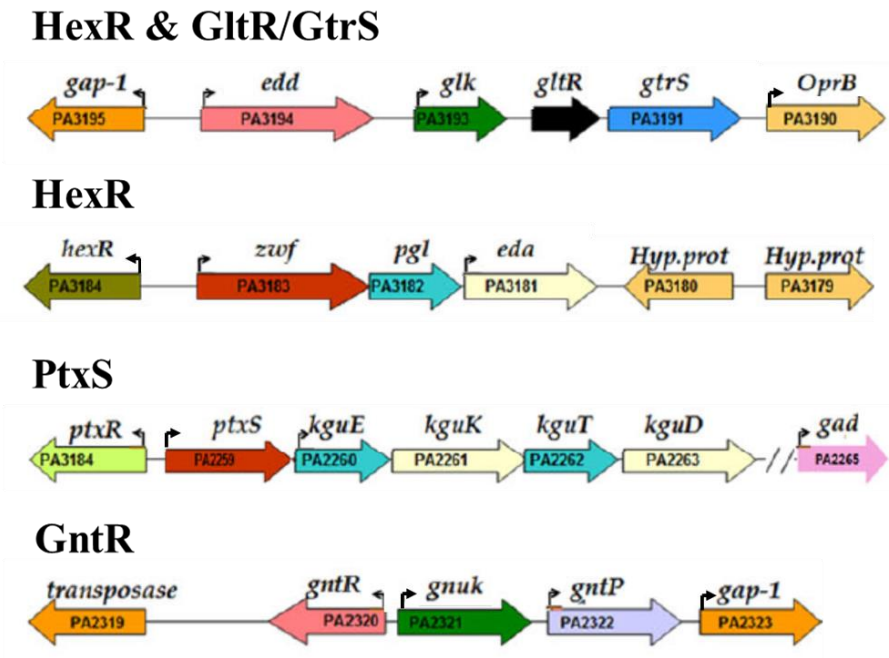

Fig. 9. Genetic organization of glucose metabolic genes in *P. aeruginosa*. Glucose metabolic genes are divided in four blocks according to their respective regulators, indicated above each block. The black arrows on genes represent the promoter. Only the promoters relevant for the thesis are reported. The regulation of each block is detailed in the text. Modified from Udaondo et al. 2018.

Concerning the genomic organization of glucose uptake and catabolic genes, it can be observed that:

- The *kgu* genes for 2-ketogluconate uptake and catabolism are organized in an operon immediately downstream *ptxS*, the gene coding for the transcriptional

regulator of this metabolic branch (Swanson et al. 2000; Daddaoua et al. 2012). The other operon regulated by PtxS is *gad*, encoding gluconate dehydrogenase and located next to the *kgu* genes (Daddaoua et al. 2012). The expression of *kgu* and *gad* is also controlled by another transcriptional regulator, *ptxR*, located next to and transcribed divergently from *ptxS* (Hamood et al. 1996).

- The *gntR* gene, coding for the transcriptional regulator of gluconate metabolic branch, is divergently transcribed from gluconokinase *gnuK*, which is located adjacent to gluconate permease *gntP* (Daddaoua et al. 2017). The three genes are transcribed as monocistronic units.

- The Entner-Doudoroff genes *edd* and *eda* do not belong to the same operon. Indeed, *edd* is located between glyceraldehyde 3-phosphate dehydrogenase *gap-1* and the *glk* operon, comprising glucokinase *glk*, and the genes for the GltR/GtrS TCS. The *gtrS* gene precedes the *oprB* operon, encompassing the genes for the OprB porin and the Glt transporter. The *eda* gene is part of an operon also including glucose-6-phosphate dehydrogenase *zwf* and 6-phosphogluconolactonase *pgl*. The gene for the HexR regulator is immediately upstream this operon and transcribed in opposite direction.

Besides being highly organized, glucose catabolic segments are also tightly regulated by the concerted action of HexR, PtxS, GntR and the GltR/GtrS two-component system (TCS), which guarantee a simultaneous induction of all glucose metabolic routes. Interestingly, glucose is not the effector molecule of any of these systems, which differentially respond to distinct pathway intermediates. Thus, the activation of glucose metabolism requires the initial degradation of glucose.

A comprehensive scheme of glucose metabolism regulators, with an indication of their effectors and target genes, is depicted in **Fig. 10**.

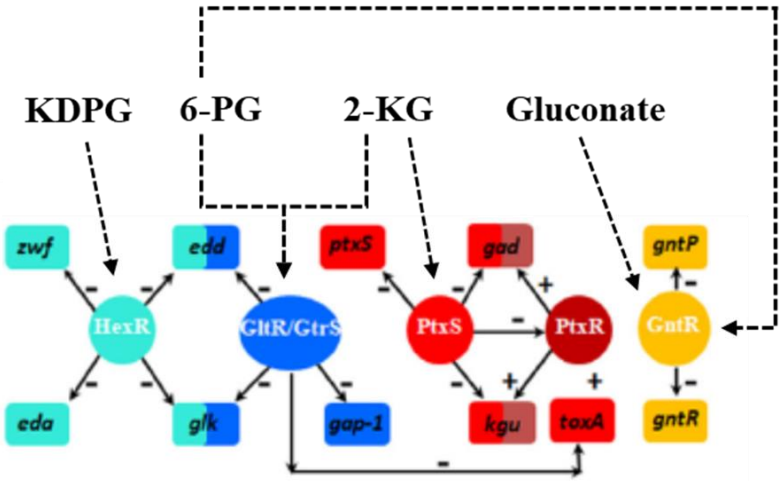

Fig. 10. The regulatory network of *P. aeruginosa* glucose metabolism. The regulators involved in glucose metabolism are indicated in the circles with different colours. The respective target genes are represented in the rectangles with the same colour code. The – and + symbols indicate repression or activation of gene expression respectively. The effector molecules are placed above the regulatory network, with the dashed arrows pointing the regulator(s) they bind.
KDPG, 2-keto-3-deoxy-6-phosphogluconate; 6-PG, 6-phosphogluconate; 2-KG, 2-ketogluconate.
Modified from Udaondo et al. 2018.

The HexR regulator belongs to the RpiR family and was demonstrated to negatively regulate the expression of *zwf/pgl/eda* and *edd/glk/gltR/gtrS* operons, as well as of *gap-1* gene, in *P. putida* (Daddaoua et al. 2009). The HexR-mediated regulatory mechanism seems to be highly conserved in pseudomonads, considering that the physical organization of these genes is maintained within *Pseudomonas* (del Castillo et al. 2007). HexR operator sites were identified in *zwf*, *edd* and *gap-1* promoters and led to the identification of the 5'-TTG-$N_{7/8}$-ACAA-3' consensus sequence (Daddaoua et al. 2009). Binding of the Entner-Doudoroff intermediate 2-keto-3-deoxy-6-phosphogluconate (KDPG) to DNA-bound HexR triggers the dissociation of the regulator, enabling transcriptional activation (Daddaoua et al. 2009).

PtxS is a repressor of the LacI family that binds to the palindromic sequence 5'-TGAAACCGGTTTCA-3' immediately downstream of the transcriptional start sites of *kgu* and *gad* operons in *P. aeruginosa* (Daddaoua et al. 2012). Besides controlling the expression these operons, PtxS was demonstrated to regulate its own expression in *P. putida* (Daddaoua et al. 2010). Interestingly, in *P. aeruginosa* PtxS post-transcriptionally regulates PtxR, a transcriptional activator of *kgu*/*gad* operons and *toxA*, the exotoxin A coding gene (Hamood et al. 1996; Daddaoua et al. 2012). It was proved that 2-ketogluconate is the effector molecule releasing PtxS-dependent repression (Daddaoua et al. 2012).

GntR is a transcriptional repressor of both its own and *gntP* expression (Daddaoua et al. 2017). This regulator binds directly to the consensus sequence 5'-AC-N-AAG-N-TAGCGCT-3' in *gntR* and *gntP* promoters. The release of promoter-bound GntR is induced by gluconate and 6-phosphogluconate, the allosteric inducers of this repressor. GntR was demonstrated to be a paralogous of PtxS, with 23% sequence identity (Daddaoua et al. 2017).

The GltR/GtrS TCS regulates the expression of several genes involved in glucose metabolism: *gap-1*, *edd* and those belonging to *oprB* and *glk* operons (Daddaoua et al. 2014). GtrS is the transmembrane sensor kinase, endowed with a periplasmic ligand binding domain specifically recognizing 2-ketogluconate and 6-phosphogluconate. The binding of these effector molecules to GtrS triggers its autophosphorylation and the transphosphorylation of GltR response regulator. GltR acts as a transcriptional repressor of the aforementioned genes, and it is released from DNA upon phopsphorylation. The analysis of GltR operator sites determined the consensus sequence as 5'-tgGTTTTTc-3' (Daddaoua et al. 2014). Most importantly, GltR was demonstrated to regulate also *toxA* expression (see details in Section 4.4).

An overview of this complex regulatory network suggests that there are two key metabolites implicated in the induction of glucose metabolism: 2-ketogluconate (effector of PtxS and GltR/GtrS) and 6-phosphogluconate (effector of GntR and GltR/GtrS). Moreover, the presence of the GltR/GtrS TCS among the regulators broadens the transcriptional response also to extracytosolic signals.

4.4. Involvement of glucose metabolic genes in P. aeruginosa virulence

As previously mentioned in Section 3.2, a link between glucose metabolism and colonization of the respiratory tract by *P. aeruginosa* has been established. Indeed, studies in hyperglycaemic mice revealed that deletions of glucose metabolic genes cause a clear reduction of *P. aeruginosa* lung proliferation. This decrease was observed for mutants defective in genes involved in glucose transport (*oprB* and *gltK*), catabolism (*glk*, *edd*) and belonging to its regulatory network (*gtrS*) (Pezzulo et al. 2011; Gill et al. 2016).

Besides their growth-promoting role, glucose metabolic genes were found to participate in the expression of *P. aeruginosa* virulence factors. For example, the GtrS sensor kinase was discovered to be relevant for *P. aeruginosa* dissemination in a mouse infection model by modulating the expression of type III secretion system (T3SS) in response to host cells (O'Callaghan et al. 2012). In particular, the GtrS/GltR-dependent induction of OprB leads to the production of pyruvate metabolic intermediates that activate the Anr-NarL anaerobic pathway; NarL, in turn, promotes the activation of ExsA, the positive transcriptional regulator of T3SS.

Furthermore, a direct connection between glucose assimilation and exotoxin A production was established. Indeed, both GltR/GtrS TCS and PtxS were shown to regulate *toxA* expression, albeit through different mechanisms. The GltR response regulator is able to bind P_{toxA} promoter in the proximity of the

transcriptional start site and probably inhibits *toxA* transcription by interfering with RNA polymerase recruitment (Daddaoua et al. 2014). In contrast, PtxS indirectly controls exotoxin A biosynthesis by affecting the activity of PtxR transcriptional activator. Interestingly, 2-ketogluconate is the allosteric inducer of both PtxS and GltR/GtrS TCS, supporting the relevance of this glucose metabolism intermediate in the expression of exotoxin A.

RESULTS AND DISCUSSION

5. Generation of *P. aeruginosa* mutants with deletions of glucose uptake genes

A panel of single and multiple mutants of *P. aeruginosa* PAO1 lacking genes implicated in glucose uptake were constructed by gene replacement (see ***Raneri et al.,* Supplementary Methods** for details). The single mutants carry the untagged deletion of the genes for the outer membrane (OM) OprB porin, its paralogue PA2291 (encoding the OprB2 porin), the inner membrane (IM) GntP gluconate permease and the KguT ketogluconate transporter (***Raneri et al.,* Fig. 1a and 1b**). These mutations were combined to create strains lacking the glucose porins (Δ*oprB* ΔPA2291) or the transporters involved in the oxidative route of glucose uptake (Δ*gntP* Δ*kguT*). Despite various attempts, it was impossible to obtain a mutant lacking *gltK*, the gene coding for the ATP-binding subunit of Glt IM glucose transporter, whereas we could obtain the deletion of a portion of *gltK* (234 out of the 386 codons) together with *gltG* and *gltF*, i.e. the permease subunits encoding genes (***Raneri et al.,* Fig. 1b**). The resulting Δ*glt* mutation was inserted in both PAO1 and the Δ*gntP* Δ*kguT* double mutant to generate a strain devoid of the GntP, KguT and Glt IM glucose transporters.

6. Growth of OM and IM mutants on different carbon sources

The mutants were analysed for the ability to grow in minimal medium in the presence of glucose or gluconate as sole carbon sources, in order to investigate whether the deleted transporters are essential for the transport of such molecules. As a control, growth in succinate was also analysed. Indeed, succinate internalization was demonstrated to specifically rely on the Dct dicarboxylates transport systems (Valentini et al. 2011). The optical density of PAO1 wild type

(PAO1) and mutant strains was monitored for 7 h, to analyse their growth curves, and after 24 h of incubation.

- OM mutants

We found that the deletion of either one or both OprB and OprB2 glucose porins did not affect growth on glucose, which was comparable to that of PAO1 (***Raneri et al.*, Fig. 2a and Supplementary Fig. S1**). These results indicate that other porins may facilitate glucose entry into the periplasm. In agreement with this observation, gluconate entry can be promoted by the OprD porin, which allows also the diffusion of basic amino acids and imipenem (Huang & Hancock 1993). Moreover, since the OprF non-specific porin has a predominant role in the internalization of sugar larger than disaccharides in *P. aeruginosa* (Bellido et al. 1992), it cannot be ruled out that it may also permit the passage of glucose in the absence of glucose-specific porins.

It has been recently published that the growth of a PAO1 Δ*oprB* mutant in minimal medium supplemented with glucose is limited when compared to that of the wild type strain (Gill et al. 2016). This discrepancy with our results can be ascribed to a differential expression of genes encoding alternate OM glucose transporters in different PAO1 sublines (Klockgether et al. 2010). Interestingly, a hotspot of mutation in PAO1 genomes is the *mexT* gene, which codes for a repressor of OprD expression (Ochs et al. 1999).

- IM mutants

Concerning the mutants lacking IM transporters, the Δ*gntP* and Δ*kguT* single mutants reached comparable optical density as PAO1 after 24 h of incubation in all tested media (***Raneri et al.*, Fig. 2b**), although the Δ*gntP* strain showed a longer lag phase in glucose and gluconate and slower growth rate in the latter medium (***Raneri et al.*, Table 1 and Supplementary Fig S1**). These two mutants were also evaluated for growth with 2- ketogluconate (2-KG) as unique carbon

source to discriminate the GntP and KguT roles in the uptake of gluconate and 2-KG. Unlike Δ*gntP*, the Δ*kguT* strain did not grow with 2-KG as sole carbon source (***Raneri et al.*, Fig. 2c**), confirming that 2-KG internalization is performed only by the KguT transporter (Swanson et al. 2000). The combination of Δ*gntP* and Δ*kguT* mutations resulted in a double mutant totally unable to use gluconate as unique carbon source (***Raneri et al.*, Fig. 2b and Supplementary Fig. S1**). The Δ*gntP* Δ*kguT* double mutant had also restricted growth on glucose, as Δ*gntP* Δ*kguT* cultures had a slower growth rate and reached the half of the optical density of PAO1 cultures grown in the same conditions for 24 h (***Raneri et al.*, Table 1**, **Fig. 2b and Supplementary Fig. S1**). In contrast, the Δ*glt* mutant was able to grow on glucose as PAO1 (***Raneri et al.*, Table1** and **Fig. 2b**). Finally, the deletion of the IM transporters in the Δ*glt* Δ*gntP* Δ*kguT* triple mutant completely prevents growth on glucose or gluconate as sole carbon source (***Raneri et al.*, Fig 2b and Supplementary Fig. S1**). Being this mutant unable to use glucose for growth, it was renamed GUN, i.e. Glucose Uptake-Null.

These data demonstrate that Glt, GntP and KguT are the unique transporters that can accomplish the passage of glucose across the IM in PAO1, with GntP and KguT specifically involved in the transport of gluconate and 2-ketogluconate (2-KG), respectively. In the conditions of temperature and aeration of our assay, the oxidative route can entirely overcome the inability to perform glucose uptake by the phosphorylative route. In contrast, glucose transport by Glt cannot offset the lack of both gluconate and 2-KG transporters. This could be due to periplasmic glucose oxidation, which would convert glucose in molecules (i.e. gluconate and 2-KG) that cannot be transported by Glt.

7. The lack of glucose transporters deeply impacts *P. aeruginosa* gene expression profile

The availability of the GUN mutant allowed to examine how preventing glucose uptake might affect *P. aeruginosa* physiology through the analysis of the global transcription profile of this mutant strain in comparison with PAO1.

RNASeq samples were collected 10 and 60 min after the supplementation of 0.4% glucose to PAO1 and GUN cultures grown up to mid-log phase (OD_{600} ~ 0.4) in M9 minimal medium supplemented with casamino acids (CAA), which can be used by *P. aeruginosa* as unique carbon source. It should be noted that casamino acids stock solution used for medium preparation is devoid of glucose (***Raneri et al.***, **Supplementary Fig. S2**). Moreover, the growth of PAO1 and GUN strains in M9-CAA supplemented with glucose and of PAO1 in either presence or absence of glucose is comparable for the timespan of the experiment, with the mutant having a slightly lower growth rate (***Raneri et al.*, Supplementary Fig. S3; Fig. 11**).

During my PhD training, I focused on the transcriptomic analysis of the 60 min condition, whose results were validated by RT-qPCR and phenotypic assays. The data are illustrated in the attached article and will be briefly presented and discussed in this section. The transcriptomic data of the 10 min condition will be illustrated in a separate section (Section 11).

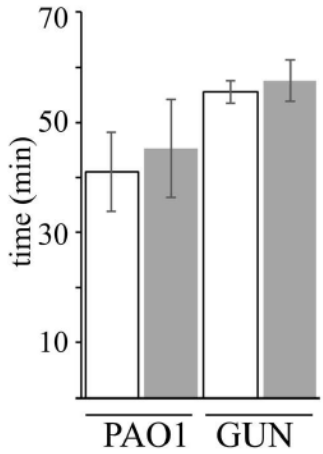

Fig. 11. Growth of PAO1 and GUN cultures in the RNASeq experiment. Generation time of PAO1 and GUN cultures in the 60 min of incubation with glucose 0.4% (w/v). Bars represent average (n=2) with SD. Empty bars, no glucose added; grey bars, culture supplemented with glucose.

We expected to identify as differentially expressed genes those responding to the presence of glucose, or its metabolites, and possibly other genes specifically responding to the lack of IM glucose transporters. The transcriptional analysis of PAO1 grown as described above (namely in M9 minimal medium supplemented with casamino acids) without glucose supplementation was included to discriminate between these two categories. Genes with at least two-fold differential expression (i.e. with a $\log_2$FC ≥ 1 or ≤ -1) and an adjusted P value ≥ 0.05 were considered as differentially expressed in the evaluation of RNASeq results. For a subset of differentially expressed genes, RT-qPCR was performed to validate transcriptomic data (***Raneri et al.***, **Fig. 3b**).

Only 28 genes were identified as differentially expressed (DEGs) in PAO1 60 min upon glucose addition (PAO1+ *vs*. PAO1; ***Raneri et al.***, **Fig. 3a**), with 24 up-regulated and 4 down-regulated genes. On the contrary, when the PAO1+ transcriptome was compared to that of the GUN mutant grown in the same conditions, we found 514 DEGs (GUN+ *vs*. PAO1+; ***Raneri et al.***, **Fig. 3a**), with 256 up-regulated and 258 down-regulated genes. Interestingly, a comparable and high number of DEGs (549) was identified in the comparison of GUN

transcriptional profile with that of PAO1 grown in absence of glucose (GUN+ vs. PAO1; ***Raneri et al.***, **Fig. 3a**).

As expected, glucose addition to PAO1 cultures increased the expression of genes implicated in glucose uptake and metabolism (***Raneri et al.***, **Supplementary Tables S2 and S3**). On the other hand, down-regulated DEGs included genes coding for components of amino acid or dipeptide ABC transporters (***Raneri et al.***, **Supplementary Table S3).**

Genes related to energy and carbon metabolism were enriched among those down-regulated in the GUN mutant relative to PAO1 grown in either presence or absence of glucose (***Raneri et al.,* Table 2**). In particular, the expression of genes implicated in oxidative phosphorylation was lower in the mutant, which appears to undergo a reorganization of the electron transport chain (***Raneri et al.***, **Supplementary Table S2**). In addition, genes encoding components of the denitrification process, i.e. the dissimilatory nitrate respiration performed by *P. aeruginosa* to grow under anaerobic conditions (Arai 2011), were also down-regulated in GUN (***Raneri et al.***, **Supplementary Tables S2**). The perturbation of energy metabolism affected also the production of NAD(H) cofactors. Indeed, genes for NAD biosynthesis and for NADH dehydrogenase, which regenerates NAD^+ in the electron transport chain, had lower expression in the mutant relative to PAO1 (***Raneri et al.***, **Supplementary Table S2**). To confirm this observation, total NAD(H) was measured in PAO1 and GUN mid-log cultures grown in minimal medium with casamino acids and with or without glucose (***Raneri et al.,* Fig. 3c**). In line with transcriptomic data, the NAD(H) cellular content was significantly reduced in the GUN mutant compared to PAO1 grown in absence of glucose, suggesting that the lack of glucose transporters may perturb the cellular redox balance. As for carbon metabolism, the mutant showed a decreased expression of genes required for the degradation of glucose and some amino acids

(***Raneri et al.***, **Supplementary Table S2**). Notably, genes for arginine and histidine utilization were significantly down-regulated in GUN (***Raneri et al.***, **Fig. 3b and Supplementary Tables S2**). The stress condition of the GUN mutant was also suggested by the lower expression of genes typically associated with growth like those coding for ribosomal proteins, for the enzymes required for purine biosynthesis and for RNA polymerase subunits (***Raneri et al.,*** **Supplementary Table S2**). Indeed, the genes coding for the housekeeping (*rpoD*) and starvation (*rpoS*) sigma factors were down- and up-regulated in the mutant, respectively (***Raneri et al.,*** **Table 3**). Interestingly, quorum sensing-dependent virulence genes involved in the synthesis of elastases, alkaline protease, rhamnolipids, pyocyanin and lectins were also up-regulated in the GUN mutant (***Raneri et al.,*** **Supplementary Table S2**). In addition, the mutant showed increased expression of genes coding for type I and type II secretion systems, respectively mediating the transport of alkaline protease and elastases outside the cell (Strateva & Mitov 2011), for multidrug efflux systems and for the synthesis and secretion of pyoverdine (***Raneri et al.,*** **Supplementary Table S2**).

Overall, PAO1 transcriptional response to glucose is consistent with the results of a transcriptomic analysis performed in *P. putida* grown on glucose, which showed an up-regulation of genes mediating glucose transport and catabolism and a down-regulation of few genes involved in the uptake and utilization of alternative carbon sources (del Castillo et al. 2007). Lower expression of genes related to amino acids uptake in the presence of glucose could be a result of catabolite repression, since *P. aeruginosa* was demonstrated to preferentially use glucose over amino acids as growth substrate (Section 4.1; Valentini et al. 2014). The comparison of PAO1 and GUN transcriptomes suggests that a nutritional dysregulation occurs in the mutant. While lower expression of glucose catabolic genes in the GUN mutant was predictable, the strong repression of genes for

arginine and histidine degradation is unexpected because it does not occur in PAO1 growing without glucose although both strains rely only on casamino acids for their growth. Since the GUN mutant can grow on both arginine and histidine as unique carbon source as the wild type strain (data not shown), it may be hypothesized that PAO1 and GUN use the amino acids in the medium in a different order and/or at a different rate, leading to their exhaustion in the culture medium, and thus to the shutoff of genes encoding functions involved in their metabolism, at different times. Repression of genes linked to energy metabolism most likely depends on the nutrient shortage experienced by the GUN mutant under the tested conditions. This was supported by the higher expression in the mutant of genes for the aa_3 terminal oxidase (*coxAB, coIII;* ***Raneri et al.,*** **Fig. 3b and Supplementary Table S2**), which is known to be induced upon carbon starvation (Kawakami et al. 2010). The mutant appeared also to have an altered redox state, reflected by lower NAD(H) pool. The over-expression in the mutant of *nap* genes (***Raneri et al.,*** **Fig. 3b and Supplementary Table S2**), encoding the periplasmic nitrate reductase, may be related to redox imbalance. Indeed, Nap reductase was found to mediate redox balancing of *Rhodobacter sphaeroides* by using nitrate as an ancillary oxidant to dissipate excess reductant (Gavira et al. 2002).

8. The GUN mutant has altered production of quorum sensing autoinducers and defective biofilm formation

Up-regulation of genes belonging to the quorum sensing (QS) regulatory network was observed in the GUN mutant relative to PAO1, regardless of the presence of glucose, in the RNASeq experiment. In particular, the expression of *lasR* and *rhlR* genes for QS regulators was found to be induced in the GUN strain, together with that of virulence genes controlled by LasR and RhlR (***Raneri et al.,*** **Fig. 3b**

and Supplementary Table S2). Nevertheless, the *lasI* and *rhlI* genes, implicated in the synthesis of *las* and *rhl* autoinducers, were not identified as differentially expressed in the transcriptomic analysis, although their expression is known to be positively regulated by LasR and RhlR, respectively (Seed et al. 1995; Ochsner & Reiser 1995).

To gain insight into the organization of QS network in the GUN mutant, the production of $3OC_{12}$-HSL and C_4-HSL (the signal molecules of *las* and *rhl* systems, respectively) was estimated in PAO1 and GUN cultures grown in minimal medium supplemented with casamino acids in presence or absence of glucose. Moreover, since biofilm formation depends on QS network (Gellatly & Hancock 2013; Skariyachan et al. 2018), we also measured the ability of the GUN strain to grow in a biofilm. These experiments were performed by our collaborators G. Rampioni and L. Leoni (Università degli Studi Roma Tre). We observed that the levels of $3OC_{12}$-HSL and C_4-HSL autoinducers were respectively increased and not significantly changed in GUN relative to PAO1, irrespective of glucose presence (***Raneri et al.*, Fig. 4a**).

Enhanced production of $3OC_{12}$-HSL in the GUN mutant is consistent with the higher expression of *lasR* and genes controlled by this QS regulator, such as *lasA*, *lasB* and *aprA* (***Raneri et al.*, Fig. 3b and Supplementary Table S2**). As indicated in Sections 1.2 and 1.3, both metabolic and environmental stress were found to modify the *P. aeruginosa* QS network, causing distortions in the hierarchical organization of QS systems and in the connection of *las* and *rhl* autoinducer synthases expression to that of their respective regulators (Duan & Surette 2007). Therefore, the metabolic dysregulation of the GUN mutant suggested by its transcription profile may explain its altered QS.

Biofilm formation in the GUN mutant was estimated by means of crystal violet assay in polystyrene 96-well microplates and by laser scanning confocal microscopy (LSCM) on glass slides. Both assays were conducted in minimal

medium supplemented with casamino acids, in either presence or absence of glucose, and revealed that biofilm formation was reduced in the GUN mutant relative to PAO1 (***Raneri et al.,* Fig. 4b**). As observed for QS perturbation, reduced biofilm formation by the GUN mutant did not depend on the mutant's inability to use glucose, as no reduction in biofilm formation was observed with PAO1 growing without glucose.

9. Analysis of virulence-related phenotypes in *P. aeruginosa* glucose uptake mutants

As mentioned in Section 7, transcriptomic analysis revealed the up-regulation of several genes coding for virulence determinants in the GUN mutant. To validate these data, *in vitro* assays for virulence-related phenotypic traits were applied to the glucose uptake defective mutants. In particular, we assessed: i) the production of pyocyanin, pyoverdine, rhamnolipids and extracellular proteases; ii) the ability to grow in microaerophilic and anaerobic conditions. Since their importance in *P. aeruginosa* pathogenicity (Kipnis et al. 2006), swimming and twitching motilities were also investigated, although genes involved in flagella and pili biosynthesis were not differentially expressed in the GUN mutant according to RNASeq data.

- Production of pyocyanin, pyoverdine and rhamnolipids

Pyocyanin (PYO), pyoverdine (PVD) and rhamnolipids secretion was estimated in cultures grown in LD broth up to the stationary phase because in our hands, in minimal medium, the production of these two molecules was low making unreliable the results of the assays. Glucose is present at low levels in LD medium, with a concentration ranging from 10 to 40 µM in different batches (***Raneri et al.,* Supplementary Fig. S2**). The production of PYO and, to a lesser extent, PVD was higher in all strains lacking the KguT ketogluconate transporter,

i.e. the Δ*kguT*, Δ*gntP* Δ*kguT* and GUN mutants (***Raneri et al.*, Fig. 5a and 5b**). We speculated that PYO and PVD synthesis might be promoted by the accumulation of 2-ketogluconate (2-KG) in the periplasm or by the absence of this molecule from the cytoplasm. However, the addition of 2-KG to the medium did not result in a further increase of PYO and PVD levels in any strain, rejecting the former hypothesis (**Fig. 12**). Since 2-KG is the allosteric inducer of PtxS repressor, we also hypothesized that this molecule could act as a signal to modulate the expression of genes involved in PYO and PVD production or secretion through a PtxS-dependent regulation. Nevertheless, PYO and PVD levels were unaffected between PAO1 and a Δ*ptxS* isogenic mutant (**Fig. 12**).

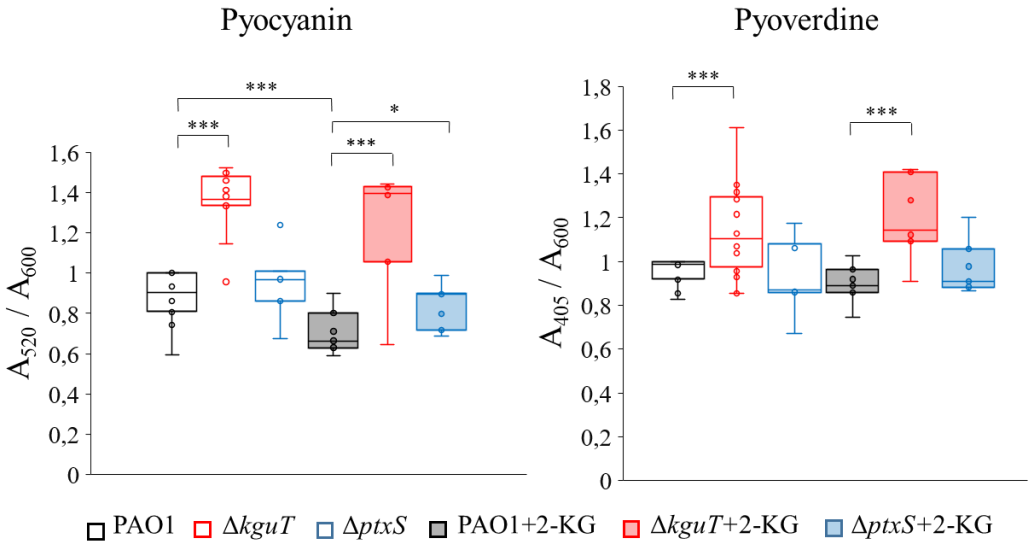

Fig. 12. Pyocyanin and pyoverdine secretion upon 2-ketogluconate addition. Pyocyanin (left panel) and pyoverdine (right panel) were measured in the supernatants of PAO1, Δ*kguT* and Δ*ptxS* cultures grown 24 h at 37° C in LD not supplemented (empty boxes) or supplemented with 1 mM 2-ketogluconate (2-KG; coloured boxes), as described in ***Raneri et al.*, Supplementary Methods**. Values are normalized for the A_{600} of the cultures and expressed relative to PAO1 without 2-KG. The median (line) is reported inside the boxes (n≥5). The whiskers represent the minimum and maximum value observed. Significance was estimated with one-way Anova and Tukey post-hoc analysis (*, P<0.05; ***, P<0.001).

PYO can be used as mobile electron carrier for *P. aeruginosa*, accepting or donating electrons to maintain redox homeostasis (Price-Whelan et al. 2006). Thus, it is possible that increased pyocyanin production may be linked to perturbed redox homeostasis, which was actually observed for the GUN mutant (see Section 7). On the other hand, the synthesis of pyoverdine siderophore may be linked to a dysregulated iron metabolism. This appears to occur in the GUN mutant due to a reorganization of the electron transport chain, which would entail the synthesis of heme-containing proteins leading to iron starvation. Accordingly, the expression of the *pvdS* iron starvation sigma factor was found to be increased in the GUN mutant (***Raneri et al.,* Table 3**).

Rhamnolipids secretion was detected on plates containing the cationic surfactant CTAB and methylene blue (MB) to allow their visualization. The ion-pairing of negatively charged rhamnolipids, whenever produced, with positively charged MB and CTAB leads to the formation of a dark blue halo surrounding the spotted colony due to methylene blue precipitation. The diameter of this halo, which reflects the amount of secreted rhamnolipids, was slightly increased in all strains lacking *kguT* and in Δ*gntP*, whereas the single deletion of *glt* had no impact on the synthesis of this virulence factor (***Raneri et al.,* Supplementary Fig. S4a**).

- Production of extracellular proteases

Proteases secretion was qualitatively estimated by performing a casein diffusion plate assay. In this experiment, the supernatants of cultures of PAO1 and mutant strains, grown in minimal medium supplemented with casamino acids in either absence or presence of glucose, were spotted onto casein-agar plates. The secretion of proteases is indicated by the formation of a white precipitate, as a result of the hydrolysis of soluble casein to the insoluble *para*-casein derivative (Lawrence & Creamer 1969). Since such precipitation can also spontaneously occur at acidic pH, we measured the pH of culture supernatants and we found

that it was around 6.5 for all strains irrespective on glucose presence or absence (data not shown). All strains produced a similar level of proteases when grown without glucose supplementation (a condition in which the growth of all cultures stopped approximately at OD_{600} 0.8), whereas glucose addition to the cultures inhibited proteases secretion in the single mutants, but not in the Δ*gntP* Δ*kguT* and GUN strains (***Raneri et al.,* Supplementary Fig. S4b**), suggesting that protease secretion may be a response to nutritional starvation.

- Growth in microaerophilic and anaerobic conditions

The growth in anaerobiosis was performed by spotting cultures on LD-agar plates supplemented with nitrate, which were incubated in both anaerobic and aerobic conditions. As for the microaerophilic growth, cultures were inoculated in LD rich medium or in minimal medium supplemented with casamino acids in 96-well microplates overlaid with paraffin oil, to prevent evaporation, and incubated without stirring to restrict oxygen influx. No difference between PAO1 and mutant strains was detected in either assays (***Raneri et al.,* Supplementary Fig. S4c and S4d**).

- Swimming and twitching motilities

Swimming and twitching motilities were analysed in minimal medium-agar plates supplemented with LD 5%, in the presence of glucose, gluconate or succinate. As for the twitching assay, cultures were spotted at the interface between the solidified nutrient medium and the petri dish bottom and their ability to spread across this interstitial space was monitored by measuring the diameter of growth halo. On the other hand, the growth halo deriving from dispersal of bacterial cultures inside semi-solid agar plates was evaluated in the swimming assay. A slightly reduced twitching zone was observed for the Δ*kguT* and Δ*gntP* Δ*kguT* mutants on gluconate and for GUN on both glucose and gluconate (**Fig. 13A**). Swimming was inhibited for Δ*gntP* Δ*kguT* on gluconate and for GUN on

both glucose and gluconate, a result due to poor growth of these strains in such conditions (**Fig. 13B**). Furthermore, in glucose and, to a minor extent, in gluconate swimming plates all strains showed autolysis, a phenotype which has been linked to membrane disruption due to oxidative stress (Hazan et al. 2016).

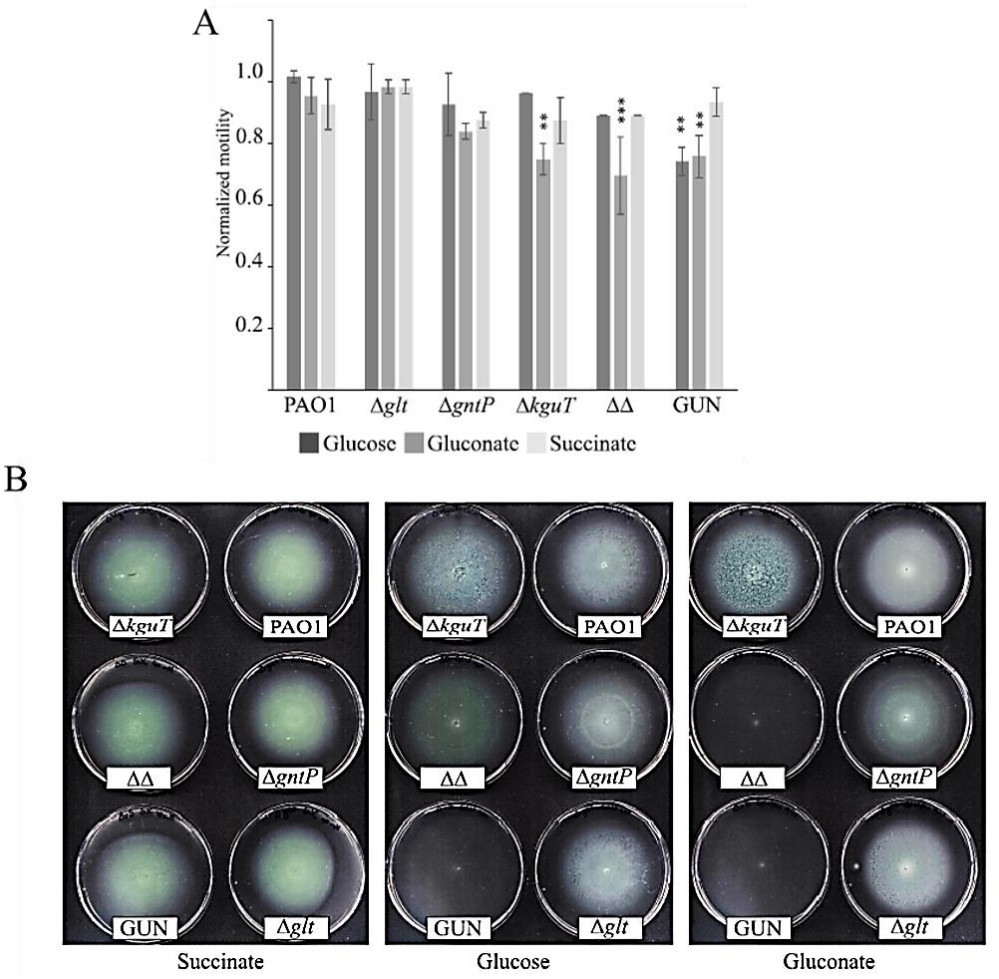

Fig. 13. Twitching and swimming motilities of glucose uptake defective mutants. A. Diameters of PAO1 and mutants' twitching zones (TZ) in the indicated carbon sources, normalized for the TZ diameter of PAO1 in glucose. Bars represent average (n=3) with standard deviation. Significance was estimated with one-way Anova and Tukey post-hoc analysis (**, P<0.01; ***, P<0.001).
B. Swimming motility of PAO1 and mutant strains with the indicated carbon sources. The experiment was performed three times in different days with similar results. In both panels, ΔΔ indicates the PAO1 Δ*gntP* Δ*kguT* strain.

10. Virulence degree of glucose uptake defective mutants in *Caenorhabditis elegans* and *Galleria mellonella*

We investigated the virulence of glucose uptake mutants in two host models largely used to study *P. aeruginosa* infections, i.e. the *Caenorhabditis elegans* nematode and the *Galleria mellonella* insect larvae.

- *Caenorhabditis elegans* infections

The experiments in *C. elegans* were performed by our collaborators I. Bianconi and O. Jousson (Università degli Studi di Trento), whereas I did the experiments with *G. mellonella*. In the *C. elegans* slow-killing assay, nematodes are fed on *P. aeruginosa* cells, which proliferate within an extracellular matrix in the nematode gut lumen, thus colonizing the intestinal tract and killing the nematodes over several days at 20 °C (Tan et al. 1999). The virulence of Δ*gntP*, Δ*glt* and GUN mutants was comparable to that of PAO1, whereas the Δ*kguT* and Δ*gntP* Δ*kguT* mutants were slightly, but significantly more virulent than PAO1 (***Raneri et al.*, Supplementary Fig. 5**). The higher virulence of Δ*kguT* and Δ*gntP* Δ*kguT* mutants in *C. elegans* may be related to enhanced pyocyanin secretion. As discussed in Section 9, the *in vitro* production of this virulence factor, which is relevant for *P. aeruginosa* pathogenicity in *C. elegans* (Mahajan-Miklos et al. 1999), is increased in all strains lacking *kguT*. Curiously, despite the GUN strain produces more pyocyanin and other virulence determinants *in vitro*, its pathogenic potential was comparable to that of PAO1 in *C. elegans*. This may be ascribed to a metabolic stress restricting the ability of this mutant to thrive in the nematode nutritional context. Indeed, also genes related to metabolic functions play a role in *C. elegans* infections by *P. aeruginosa* (Feinbaum et al. 2012).

- *Galleria mellonella* infections

As *G. mellonella* normally feed on honey, high levels of sugars are generally present in larvae. Indeed, it was estimated that the total amount of free glucose, fructose and sucrose ranges from 0.05 to 0.4 mg/ml in *G. mellonella* hemolymph (Wyatt et al. 1956). A preliminary estimation of glucose concentration in the hemolymph was therefore necessary to properly evaluate the results of the infection assays. Interestingly, glucose levels in *G. mellonella* larvae were significantly lower than the previous estimation (mean value 11.2 µM, corresponding to 2.0 µg/ml; ***Raneri et al.,* Supplementary Fig. S2**), probably because the larvae were starved for 24/48 h before being infected by *P. aeruginosa*. In the *G. mellonella* infection assay, *P. aeruginosa* is directly injected in larvae hemolymph and systemically disseminates *via* circulation, causing an acute infection that kills the larvae in 18-42 h at 37 °C (Ramarao et al. 2012). The Δ*gntP* Δ*kguT* and GUN mutants resulted significantly less virulent that PAO1 and the other mutants (***Raneri et al.,* Fig. 6a**). Indeed, the mortality rate of larvae injected with Δ*gntP* Δ*kguT* and GUN strains was clearly lower than those observed for PAO1 and the other mutants at 24 h post infection (h.p.i; less than 40% for the two attenuated mutants, *vs.* > 70% for the other strains). Moreover, a slight but significant decrease in the virulence was also observed for Δ*kguT* up to 22 h.p.i. To assess whether virulence decrease in *G. mellonella* was due to *in larva* growth defects, we titred hemolymph bacteria at 16 h.p.i. Indeed, the hemolymph bacterial burden was significantly reduced for all the tested mutants compared to PAO1 (***Raneri et al.,* Fig. 6b**). In addition, parental PAO1 and all mutants lacking *kguT* were investigated for their ability to induce the innate immune response of *G. mellonella*. To this end, phenoloxidase (PO) activity in the hemolymph of larvae infected with a lethal dose of PAO1 and mutant strains was measured (***Raneri et al.,* Fig. 6c**). PO production was significantly induced upon infection of the larvae with all the bacterial strains

compared to those mock-infected (i.e. injected with sterile physiological solution). Moreover, PO levels were significantly lower in larvae infected with the Δ*gntP* Δ*kguT* or GUN mutants relative to those infected with PAO1 or the Δ*kguT* strains.

Differential adaptation of *P. aeruginosa* to the specific nutritional context of the two different hosts may explain the divergent effect exerted by the mutations in glucose uptake genes (and in particular by *kguT* deletion) on the pathogenicity. It is likely that *C. elegans* localized gut infection and *G. mellonella* systemic one pose two distinct nutritional contexts to infecting bacteria, with the latter having greater amount of sugars and amino acids (McGhee 2007; Wyatt et al. 1956). The contribution of metabolic functions to the infection process of *P. aeruginosa* and other pathogens is very relevant (de Lorenzo 2014 and 2015). For example, the Entner-Doudoroff pathway for sugar consumption contributes to the pathogenicity of *L. pneumophila* and *V. cholerae* under oxidative stress conditions (Harada et al. 2010; Patra et al. 2012). Moreover, the inactivation of NAD biosynthesis regulation affects *P. aeruginosa* metabolism and pathogenicity (Okon et al. 2017). Interestingly, a whole-genome screening for multi-host *P. aeruginosa* virulence genes identified a mutant lacking the *crc* gene, encoding the global regulator of catabolite repression, as one of the few attenuated in both non-mammalian systems and in a murine model of pneumonia (Dubern et al. 2015).

11. Preliminary analysis of PAO1 and GUN transcriptional profiles in early exponential cultures

As mentioned in Section 7, samples for RNASeq were collected also at an early time point (10 min) after the supplementation with 0.4% glucose to PAO1 and GUN cultures at OD_{600} ~ 0.4. Also in this case, a multiple comparison between

the transcriptomes of PAO1 growing with and without glucose and of GUN growing with glucose was performed. 78 DEGs were identified in PAO1 upon glucose addition (PAO1+ *vs.* PAO1; **Fig. 14**), with 44 up-regulated and 43 down-regulated genes. As for GUN transcription profile, we found 483 DEGs (243 and 240 genes up- and down-regulated, respectively) compared to PAO1 with glucose (GUN+ *vs.* PAO1+; **Fig. 14**) and 1022 DEGs (521 and 501 up- and down-regulated, respectively) with respect to PAO1 without glucose supplementation (GUN+ vs. PAO1; **Fig 14**).

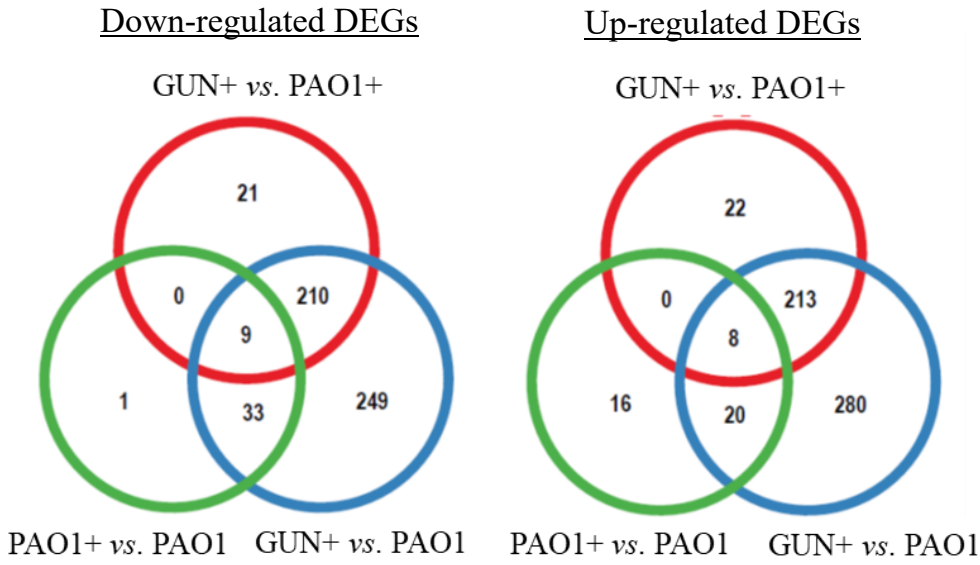

Fig. 14. Venn-diagrams of differentially expressed genes (DEGs). The diagrams represent the number of under- (left panel) and over- (right panel) expressed genes between GUN+ and PAO1+, GUN+ and PAO1, PAO1+ and PAO1, as indicated. +, RNA extracted from cultures supplemented with glucose.

DEGs were analysed to identify enriched functional categories. As expected, glucose addition to PAO1 cultures resulted in an increased expression of genes involved in glucose uptake and metabolism (**Supplementary Table S6**). Up-regulated DEGs included also genes related to virulence such as *mexA* and *oprM*, two components of the MexAB-OprM antibiotic efflux system (Li et al. 1995),

and *suhB*, a regulator of multiple virulence factors playing an essential role in *P. aeruginosa* pathogenesis (Li et al. 2013) (**Supplementary Table S6**). On the contrary, genes involved in amino acids uptake (*aat*) and metabolism (*dad*) were identified among those less expressed in PAO1 upon glucose addition (**Supplementary Table S6**). In addition, genes coding for the ATP-dependent protease AsrA and heat-shock proteins induced by this protease (*ibpA*, *clpB*, *dnaK*, *grpE* and *hslVU*) were identified among those down-regulated in PAO1 with glucose (**Supplementary Table S6**). AsrA-dependent activation of the heat shock response was found to occur in response to lethal tobramycin concentrations in *P. aeruginosa* (Kindrachuk et al. 2011).

Differentially expressed genes (DEGs) identified in the GUN mutant relative to PAO1 belong to several functional categories (**Table 3**).

Table 3. Enriched functional categories among DEGs

GUN+ vs. PAO1+	GUN+ vs. PAO1
Down-regulated DEGs[1]	
Polyamine catabolism (16)	Polyamine catabolism (19)
Propanoate metabolism (5)	Propanoate metabolism (9)
Ala, Asp, Glu[2] metabolism (4)	Val, Leu, Ile[2] degradation (9)
Val, Leu, Ile[2] degradation (7)	Butanoate metabolism (10)
Carbon metabolism (16)	Carbon metabolism (19)
Geraniol degradation (6)	Dycarboxylate metabolism (9)
Aromatic compounds catabolism (5)	ABC transporters (33)
Butanoate metabolism (6)	Ala, Asp, Glu[2] metabolism (3)
ABC transporters (22)	Geraniol degradation (6)
Arginine and proline metabolism (8)	Aromatic compounds catabolism (6)
Metabolic pathways (70)	Triptophan metabolism (3)
	Arginine and proline metabolism (10)
Up-regulated DEGs[1]	
Ribosome (23)	Ribosome (40)
Oxidative phosphorylation (22)	Oxidative phosphorylation (23)
Phenazine biosynthesis (7)	Fatty acid biosynthesis (12)
Fatty acid biosynthesis (8)	

[1]Categories are ordered according to increased adjusted probability value. The number of DEGs belonging to each category is indicated in brackets.
[2]Ala, alanine; Asp, aspartic acid; Glu, glutamic acid; Val, valine; Leu, leucine; Ile, isoleucine.

The expression of genes implicated in the metabolism of glucose, amino acids, polyamines, short-chain fatty acids (propanoate and butanoate), acyclic terpenes (geraniol) and aromatic compounds was decreased in the GUN mutant compared to PAO1, irrespective glucose presence or absence (**Supplementary Table S5**).

Down-regulation in the mutant of genes coding for ABC transporters and transcriptional factors mediating the uptake and utilization of amino acids and polyamines was also found (**Supplementary Tables S5 and S7**). Up-regulated DEGs in GUN relative to PAO1 were enriched in genes involved in oxidative phosphorylation, such as the *atp* operon for the ATP synthase complex and the genes encoding the cbb_3-1 (*cco1*), cbb_3-2 (*cco2*) and bo_3 (*cyoAB*) terminal oxidases of the electron transport chain (**Supplementary Table S5**). In addition, genes coding for ribosomal proteins, RNA polymerase subunits and required for fatty acid biosynthesis were over-expressed in the mutant (**Supplementary Table S5**). Finally, the GUN mutant showed an increased expression of several genes encoding QS-dependent virulence factors, such as elastases (*lasAB*), rhamnolipids (*rhlAB*), lectins (*lecAB*), phenazines (*phz*), and hydrogen cyanide (*hcn*) (**Supplementary Table S5**), a result somewhat unexpected given the low cell density of the cultures at the early time point, but in line with the altered QS network observed in the mutant at 60 min.

Albeit still preliminary and requiring validation, we can make some preliminary considerations about the GUN and PAO1 global transcription profiles at the early time point after glucose addition (10 min), also in the light of the previously presented results about the transcriptomes of the two strains at a later time point (60 min after glucose addition).

At both time points, glucose effect on PAO1 transcriptional profile is limited and shows the up-regulation of glucose metabolic genes and down-regulation of genes required for the utilization of amino acids. As mentioned in Section 7, glucose may repress the expression of genes involved in amino acids metabolism as a result of catabolite repression, considering that *P. aeruginosa* preferentially uses glucose over amino acids as carbon source for growth (Section 4.1; Valentini et al. 2014).

In contrast, the differential expression of both virulence-related genes (*mexA*, *oprM* and *suhB*) and AsrA-dependent genes in PAO1 with glucose is transient, as it was no longer observed 60 min after glucose addition. However, the latter genes have a decreased expression in the GUN mutant with respect to PAO1 at both time points, suggesting that the lack of glucose uptake systems may interfere with AsrA regulatory network.

About 400 genes are differentially expressed between GUN and PAO1 at both time points irrespective of glucose. 117 of these genes are conserved between 10 and 60 min conditions but only 45 share the same regulation at the two time points, a third of which encodes for virulence-related traits. On the other hand, a large fraction of the genes showing opposite regulation between 10 and 60 min codes for ribosomal proteins and components of the electron transport chain. Therefore, we can conclude that the lack of glucose transporters deeply affects *P. aeruginosa* gene expression at both 10 and 60 min after glucose addition, albeit with significant differences between the two time points that probably depend on the metabolic state of the GUN mutant.

On the contrary, only 43 DEGs were exclusively identified in the GUN strain when compared to PAO1 with glucose, whereas 529 genes resulted differentially expressed only in the comparison between GUN and PAO1 without glucose. This difference was not observed at 60 min, as in that case a similar number of genes (121 and 144 genes, respectively) was found in the two comparisons.

It is tempting to speculate that the accumulation of a great amount of glucose (and/or its derivatives gluconate and 2-KG) in the periplasm of the GUN mutant may be sensed as a signal to activate energy metabolism and, more in general, functions related with fast growth. In fact, significantly higher expression of genes implicated in oxidative phosphorylation and coding for ribosomal proteins is observed in the GUN mutant.

CONCLUSIONS AND FUTURE PERSPECTIVES

In this Ph.D. thesis I describe the generation and characterization of a panel of single and multiple *P. aeruginosa* PAO1 mutants carrying untagged deletions of genes coding for IM proteins implicated in the uptake of glucose and its oxidative derivatives gluconate and 2-ketogluconate (2-KG). On the whole, my results show that Glt, GntP and KguT transporters are the only involved in the internalization of glucose, with GntP and KguT specifically required for the transport of gluconate and 2-KG, respectively.

The analysis of wild type PAO1 and GUN transcriptomes 60 min upon glucose addition revealed that PAO1 transcriptional response to glucose is limited, whereas the mutant has a deeply altered gene expression relative to PAO1, with a high number of differentially expressed genes belonging to various pathways. Functional classification of differentially expresses genes (DEGs) indicated that the GUN mutant undergoes a complex metabolic dysregulation leading to nutritional disorders and interfering with energy metabolism and quorum sensing. Furthermore, the expression of several virulence genes is increased in this strain compared to parental PAO1. Interestingly, most of DEGs showed altered expression in the mutant even with respect to PAO1 grown in the absence of glucose, a result that was validated by RT-qPCR experiments.

Phenotypic assays confirmed the transcriptomic data and depicted a pleiotropic phenotype for the GUN mutant, with lower NAD(H) content, altered quorum sensing, decreased biofilm formation and enhanced secretion of virulence factors such as pyocyanin, pyoverdine and extracellular proteases. Interestingly, also in this case, most of the tested phenotypic traits differs in the GUN mutant relative to PAO1 regardless of the presence of glucose, suggesting that Glt, GntP and/or KguT may contribute to an accessory function not related to glucose transport.

It is tempting to speculate that one or more of the deleted transporters may be involved in the regulation of cell metabolism, possibly by modulating the activity of histidine kinases (HK) of two-component systems. It has been shown, for example, that the *E. coli* dicarboxylic acid (C_4-diC) transporter DauA activates the expression of DctA, the main C_4-diC transporter at neutral pH, by regulating the activity of the HK DcuS (Karinou et al. 2017). This has been proposed as a strategy adopted by *E. coli* to maximize C_4-diC utilization. KguT may be eligible for such an additional function. Indeed, this transporter plays a prominent role in *in vitro* virulence-related phenotypes and is relevant for the *in vivo* virulence of *P. aeruginosa* in *C. elegans* and *G. mellonella*, with all mutants lacking KguT attenuated in *G. mellonella*, whereas the single Δ*kguT* and the double Δ*gntP* Δ*kguT* mutants were slightly more virulent than PAO1 in *C. elegans*.

To investigate the putative accessory function of Glt, GntP and/or KguT, we plan to implement two-hybrid systems and co-purification assays using the transporters (with proper tags) as baits. This will allow to identify their interactors and will shed light on their putative additional role.

We also plan to carry out the analysis of the transcription profile of PAO1 and the GUN mutant at the early time upon glucose addition, with the relevant aspects that will be validated by RT-qPCR. In particular, the transient over-expression of genes implicated in oxidative phosphorylation in the GUN mutant deserves consideration. The expression of these genes will be assessed in PAO1 and in the single and multiple mutants to assess whether the lack of a specific glucose transporter and/or the presence of glucose (or its gluconate and 2-KG derivatives) in the periplasm may specifically affect the expression of genes encoding functions of the electron transport chain.

Different virulence degree of our mutants in *C. elegans* and *G. mellonella* suggests that the ability to import glucose and/or the accessory function of

glucose transporters may differently impact *P. aeruginosa* adaptation to the nutritional context posed by the infection in either animal. In order to understand whether one or more proteins involved in glucose uptake may be a good target to develop novel drugs to tackle *P. aeruginosa* infections, it will be interesting to evaluate the pathogenic potential of our mutants in both acute and chronic murine models of infections and in hyperglycaemic mice.

MATERIALS AND METHODS

Bacterial strains, plasmids and oligonucleotides used in this this study are listed in ***Raneri et al.,* Supplementary Table S1**. The experimental procedures are described in ***Raneri et al.,* Methods and Supplementary Methods**. The procedures of the experiments not included in the attached article are reported in this section.

Swimming and twitching motilities

Stationary bacterial cultures were washed in 1x PBS and inoculated as 2 µl spots onto swimming and twitching plates. Swimming plates were prepared with M9 minimal medium supplemented with 5% (v/v) LD in the presence of 0.4% (w/v) glucose, 0.4% (w/v) gluconate or 1% (w/v) succinate and 0.3% (w/v) BactoAgar (Difco). Bacterial cultures were inoculated at the centre of the plates, which were incubated at 37 °C for 24 h. The size of the swimming halo, originating from bacterial diffusion inside the semi-solid plates, was then evaluated. Twitching plates were made with M9 minimal medium supplemented with 5% (v/v) LD in the presence of 0.4% (w/v) glucose, 0.4% (w/v) gluconate or 0.5% (w/v) succinate and 1% (w/v) BactoAgar (Difco). 3 mm-thick plates were used for the twitching assay. Bacterial cultures were inoculated to the bottom of the Petri dish and the plates were incubated at 37 °C for 20 h. The diameter of the twitching zone (i.e. the halo resulting from bacterial movement at the agar/Petri dish interface) was then measured.

REFERENCES

Adewoye, L.O. & Worobec, E.A., 2000. Identification and characterization of the *gltK* gene encoding a membrane-associated glucose transport protein of *Pseudomonas aeruginosa*. *Gene*, 253(2), pp.323–330.

Akira, S., Uematsu, S. & Takeuchi, O., 2006. Pathogen recognition and innate immunity. *Cell*, 124(4), pp.783–801.

Arai, H., 2011. Regulation and Function of Versatile Aerobic and Anaerobic Respiratory Metabolism in *Pseudomonas aeruginosa*. *Frontiers in Microbiology*, 2:103.

Baker, E.H. & Baines, D.L., 2018. Airway Glucose Homeostasis. *Chest*, 153(2), pp.507–514.

Baker, E.H. et al., 2007. Hyperglycemia and cystic fibrosis alter respiratory fluid glucose concentrations estimated by breath condensate analysis. *Journal of Applied Physiology*, 102(5), pp.1969–1975.

Baker, E.H. et al., 2006. Hyperglycaemia and pulmonary infection. *Proceedings of the Nutrition Society*, 65(03), pp.227–235.

Bartlett, J.A., Fischer, A.J. & McCray, P.B.J., 2008. Innate Immune Functions of the Airway Epithelium. In *Trends in Innate Immunity*. 15, pp. 147–163.

Bellido, F. et al., 1992. Reevaluation, Using Intact Cells, of the Exclusion Limit and Role of Porin OprF in *Pseudomonas aeruginosa* Outer Membrane Permeability. *Journal of bacteriology*, 174(16), pp.5196-5203.

Berka, R.M. & Vasil, M.L., 1982. Phospholipase C (heat-labile hemolysin) of *Pseudomonas aeruginosa*: purification and preliminary characterization. *Journal of bacteriology*, 152(1), pp.239–45.

Bjarnsholt, T. et al., 2010. Quorum Sensing and Virulence of *Pseudomonas aeruginosa* during Lung Infection of Cystic Fibrosis Patients. *PLoS ONE*, 5(4), e10115.

Blier, A. S. et al., 2011. C-type natriuretic peptide modulates quorum sensing molecule and toxin production in *Pseudomonas aeruginosa*. *Microbiology*, 157(7), pp.1929–1944.

Branny, P. et al., 2001. Inhibition of Quorum Sensing by a *Pseudomonas aeruginosa dksA* Homologue. *Journal of Bacteriology*, 183(5), pp.1531–1539.

Breidenstein, E.B.M., de la Fuente-Núñez, C. & Hancock, R.E.W., 2011. *Pseudomonas aeruginosa*: all roads lead to resistance. *Trends in Microbiology*, 19(8), pp.419–426.

Brint, J.M. & Ohman, D.E., 1995. Synthesis of multiple exoproducts in *Pseudomonas aeruginosa* is under the control of RhlR-RhlI, another set of regulators in strain PAO1 with homology to the autoinducer-responsive LuxR-LuxI family. *Journal of bacteriology*, 177(24), pp.7155–63.

Burekovic, A., Dizdarevic-Bostandzic, A. & Godinjak, A., 2014. Poorly Regulated Blood Glucose in Diabetic Patients-predictor of Acute Infections. *Medical Archives*, 68(3), p.163-6.

Caiazza, N.C., Shanks, R.M.Q. & O'Toole, G.A., 2005. Rhamnolipids Modulate Swarming Motility Patterns of *Pseudomonas aeruginosa*. *Journal of Bacteriology*, 187(21), pp.7351–7361.

Cao, H. et al., 2001. A quorum sensing-associated virulence gene of *Pseudomonas aeruginosa* encodes a LysR-like transcription regulator with a unique self-regulatory mechanism. *Proceedings of the National Academy of Sciences*, 98(25), pp.14613–14618.

Chemani, C. et al., 2009. Role of LecA and LecB lectins in *Pseudomonas aeruginosa*-induced lung injury and effect of carbohydrate ligands. *Infection and immunity*, 77(5), pp.2065–75.

Chevalier, S. et al., 2017. Structure, function and regulation of *Pseudomonas aeruginosa* porins. *FEMS Microbiology Reviews*, 41(5), pp.698–722.

Chiang, W.C. et al., 2013. Extracellular DNA Shields against Aminoglycosides in *Pseudomonas aeruginosa* Biofilms. *Antimicrobial Agents and Chemotherapy*, 57(5), pp.2352–2361.

Chrzanowski, L., Lawniczak, L. & Czaczyk, K., 2012. Why do microorganisms produce rhamnolipids? *World Journal of Microbiology and Biotechnology*, 28(2), pp.401–419.

Collison, K.S. et al., 2002. RAGE-mediated neutrophil dysfunction is evoked by advanced glycation end products (AGEs). *Journal of leukocyte biology*, 71(3), pp.433–44.

Colvin, K.M. et al., 2012. The Pel and Psl polysaccharides provide *Pseudomonas aeruginosa* structural redundancy within the biofilm matrix. *Environmental microbiology*, 14(8), pp.1913–28.

Daddaoua, A., Krell, T. & Ramos, J.L., 2009. Regulation of Glucose Metabolism in *Pseudomonas*. *Journal of Biological Chemistry*, 284(32), pp.21360–21368.

Daddaoua, A. et al., 2010. Compartmentalized Glucose Metabolism in *Pseudomonas putida* Is Controlled by the PtxS Repressor. *Journal of Bacteriology*, 192(17), pp.4357–4366.

Daddaoua, A. et al., 2012. Genes for Carbon Metabolism and the ToxA Virulence Factor in *Pseudomonas aeruginosa* Are Regulated through Molecular Interactions of PtxR and PtxS. *PLoS ONE*, 7(7), e39390.

Daddaoua, A. et al., 2014. GtrS and GltR form a two-component system: the central role of 2-ketogluconate in the expression of exotoxin A and glucose catabolic enzymes in *Pseudomonas aeruginosa*. *Nucleic Acids Research*, 42(12), pp.7654–7665.

Daddaoua, A. et al., 2017. Identification of GntR as regulator of the glucose metabolism in *Pseudomonas aeruginosa*. *Environmental Microbiology*, 19(9), pp.3721–3733.

Davey, M.E., Caiazza, N.C. & O'Toole, G.A., 2003. Rhamnolipid surfactant production affects biofilm architecture in *Pseudomonas aeruginosa* PAO1. *Journal of bacteriology*, 185(3), pp.1027–36.

Davies, D.G. et al., 1998. The involvement of cell-to-cell signals in the development of a bacterial biofilm. *Science*, 280(5361), pp.295–8.

de Lorenzo, V., 2014. From the selfish gene to selfish metabolism: Revisiting the central dogma. *BioEssays*, 36(3), pp.226–235.

de Lorenzo, V., 2015. *Pseudomonas aeruginosa*: the making of a pathogen. *Environmental Microbiology*, 17(1), pp.1–3.

Dekimpe, V. & Deziel, E., 2009. Revisiting the quorum-sensing hierarchy in *Pseudomonas aeruginosa*: the transcriptional regulator RhlR regulates LasR-specific factors. *Microbiology*, 155(3), pp.712–723.

del Castillo, T. et al., 2007. Convergent Peripheral Pathways Catalyze Initial Glucose Catabolism in *Pseudomonas putida*: Genomic and Flux Analysis. *Journal of Bacteriology*, 189(14), pp.5142–5152.

Delamaire, M. et al., 1997. Impaired Leucocyte Functions in Diabetic Patients. *Diabetic Medicine*, 14(1), pp.29–34.

Déziel, E. et al., 2004. Analysis of *Pseudomonas aeruginosa* 4-hydroxy-2-alkylquinolines (HAQs) reveals a role for 4-hydroxy-2-heptylquinoline in cell-to-cell communication. *Proceedings of the National Academy of Sciences*, 101(5), pp.1339–1344.

Déziel, E. et al., 2004. The contribution of MvfR to *Pseudomonas aeruginosa* pathogenesis and quorum sensing circuitry regulation: multiple quorum sensing-regulated genes are modulated without affecting *lasRI*, *rhlRI* or the production of N-acyl- l-homoserine lactones. *Molecular Microbiology*, 55(4), pp.998–1014.

Diggle, S.P. et al., 2007. The *Pseudomonas aeruginosa* 4-Quinolone Signal Molecules HHQ and PQS Play Multifunctional Roles in Quorum Sensing and Iron Entrapment. *Chemistry & Biology*, 14(1), pp.87–96.

Duan, K. & Surette, M.G., 2007. Environmental Regulation of *Pseudomonas aeruginosa* PAO1 Las and Rhl Quorum-Sensing Systems. *Journal of Bacteriology*, 189(13), pp.4827–4836.

Dubern, J.F. et al., 2015. Integrated whole-genome screening for *Pseudomonas aeruginosa* virulence genes using multiple disease models reveals that pathogenicity is host specific. *Environmental Microbiology*, 17(11), pp.4379–4393.

Engel, L.S. et al., 1998. *Pseudomonas aeruginosa* protease IV produces corneal damage and contributes to bacterial virulence. *Investigative ophthalmology & visual science*, 39(3), pp.662–5.

Farinha, M.A. et al., 1994. Alteration of the pilin adhesin of *Pseudomonas aeruginosa* PAO1 results in normal pilus biogenesis but a loss of adherence to human pneumocyte cells and decreased virulence in mice. *Infection and immunity*, 62(10), pp.4118–23.

Feinbaum, R.L. et al., 2012. Genome-Wide Identification of *Pseudomonas aeruginosa* Virulence-Related Genes Using a *Caenorhabditis elegans* Infection Model. *PLoS Pathogens*, 8(7), e1002813.

Feldman, M. et al., 1998. Role of flagella in pathogenesis of *Pseudomonas aeruginosa* pulmonary infection. *Infection and immunity*, 66(1), pp.43–51.

Fernández, L., Breidenstein, E.B.M. & Hancock, R.E.W., 2011. Creeping baselines and adaptive resistance to antibiotics. *Drug Resistance Updates*, 14(1), pp.1–21.

Finkelstein, S.M. et al., 1988. Diabetes mellitus associated with cystic fibrosis. *The Journal of pediatrics*, 112(3), pp.373–7.

Fire, A. et al., 1998. Potent and specific genetic interference by double-stranded RNA in *Caenorhabditis elegans*. *Nature*, 391(6669), pp.806–811.

Ganz, T. & Lehrer, R.I., 1994. Defensins. *Current opinion in immunology*, 6(4), pp.584–9.

Garnett, J.P. et al., 2013. Elevated Paracellular Glucose Flux across Cystic Fibrosis Airway Epithelial Monolayers Is an Important Factor for *Pseudomonas aeruginosa* Growth. *PLoS ONE*, 8(10), e76283.

Gavira, M. et al., 2002. Regulation of nap gene expression and periplasmic nitrate reductase activity in the phototrophic bacterium *Rhodobacter sphaeroides* DSM158. *Journal of Bacteriology*, 184(6), pp.1693–1702.

Geerlings, S.E. & Hoepelman, A.I., 1999. Immune dysfunction in patients with diabetes mellitus (DM). *FEMS Immunology & Medical Microbiology*, 26(3–4), pp.259–265.

Gellatly, S.L. & Hancock, R.E.W., 2013. *Pseudomonas aeruginosa*: new insights into pathogenesis and host defenses. *Pathogens and Disease*, 67(3), pp.159–173.

Gill, S.K. et al., 2016. Increased airway glucose increases airway bacterial load in hyperglycaemia. *Scientific Reports*, 6, 27636.

Glavis-Bloom, J., Muhammed, M. & Mylonakis, E., 2012. Of Model Hosts and Man: Using *Caenorhabditis elegans*, *Drosophila melanogaster* and *Galleria mellonella* as Model Hosts for Infectious Disease Research. In *Advances in experimental medicine and biology*. 710, pp. 11–17.

Grishin, A. V et al., 2015. *Pseudomonas Aeruginosa* Lectins As Targets for Novel Antibacterials. *Acta naturae*, 7(2), pp.29–41.

Haas, B. et al., 1991. Siderophore presence in sputa of cystic fibrosis patients. *Infection and immunity*, 59(11), pp.3997–4000.

Hager, P.W., Calfee, M.W. & Phibbs, P. V, 2000. The Pseudomonas aeruginosa devB/SOL homolog, *pgl*, is a member of the hex regulon and encodes 6-phosphogluconolactonase. *Journal of bacteriology*, 182(14), pp.3934–41.

Hamood, A.N. et al., 1996. Isolation and characterization of a *Pseudomonas aeruginosa* gene, *ptxR*, which positively regulates exotoxin A production. *Molecular Microbiology*, 21(1), pp.97–110.

Hamood, A.N., Griswold, J.A. & Duhan, C.M., 1996. Production of Extracellular Virulence Factors by *Pseudomonas aeruginosa* Isolates obtained from Tracheal, Urinary Tract, and Wound Infections. *Journal of Surgical Research*, 61(2), pp.425–432.

Hamood, A.N., Colmer-Hamood, J.A. & Carty, N.L., 2004. Regulation of *Pseudomonas aeruginosa* Exotoxin A Synthesis. In *Pseudomonas, Volume 2*, pp. 389–423.

Handfield, M. et al., 2000. *In vivo*-Induced Genes in *Pseudomonas aeruginosa*. *Infection and Immunity*, 68(4), pp.2359–2362.

Harada, E. et al., 2010. Glucose metabolism in *Legionella pneumophila*: dependence on the Entner-Doudoroff pathway and connection with intracellular bacterial growth. *Journal of bacteriology*, 192(11), pp.2892–9.

Hauser, A.R., 2009. The type III secretion system of *Pseudomonas aeruginosa*: infection by injection. *Nature reviews. Microbiology*, 7(9), pp.654–65.

Hay, I.D., Remminghorst, U. & Rehm, B.H.A., 2009. MucR, a novel membrane-associated regulator of alginate biosynthesis in *Pseudomonas aeruginosa*. *Applied and environmental microbiology*, 75(4), pp.1110–20.

Hazan, R. et al., 2016. Auto Poisoning of the Respiratory Chain by a Quorum-Sensing-Regulated Molecule Favors Biofilm Formation and Antibiotic Tolerance. *Current biology*, 26(2), pp.195–206.

Heurlier, K. et al., 2003. Negative control of quorum sensing by RpoN (sigma54) in *Pseudomonas aeruginosa* PAO1. *Journal of bacteriology*, 185(7), pp.2227–35.

Hilker, R. et al., 2015. Interclonal gradient of virulence in the *Pseudomonas aeruginosa* pangenome from disease and environment. *Environmental Microbiology*, 17(1), pp.29–46.

Hoffmann, J.A., 1995. Innate immunity of insects. *Current opinion in immunology*, 7(1), pp.4–10.

Huang, H. & Hancock, R.E., 1993. Genetic definition of the substrate selectivity of outer membrane porin protein OprD of *Pseudomonas aeruginosa*. *Journal of bacteriology*, 175(24), pp.7793–800.

Hunt, W.R. et al., 2014. Hyperglycemia impedes lung bacterial clearance in a murine model of cystic fibrosis-related diabetes. *American Journal of Physiology. Lung Cellular and Molecular Physiology*, 306(1), pp.L43–L49.

Iacopi, E. et al., 2015. Necrotizing Fasciitis and The Diabetic Foot. *The International Journal of Lower Extremity Wounds*, 14(4), pp.316–327.

Irazoqui, J.E. et al., 2010. Distinct Pathogenesis and Host Responses during Infection of *C. elegans* by *P. aeruginosa* and *S. aureus*. *PLoS Pathogens*, 6(7), e1000982.

Jander, G., Rahme, L.G. & Ausubel, F.M., 2000. Positive correlation between virulence of *Pseudomonas aeruginosa* mutants in mice and insects. *Journal of bacteriology*, 182(13), pp.3843–5.

Jeffrey B. Lyczak, Carolyn L. Cannon, G.B.P., 2000. Establishment of *Pseudomonas aeruginosa* infection: lessons from a versatile opportunistic pathogen. *Microbes and Infection*, 2, pp.1051–1060.

Jude, F. et al., 2003. Posttranscriptional control of quorum-sensing-dependent virulence genes by DksA in *Pseudomonas aeruginosa*. *Journal of bacteriology*, 185(12), pp.3558–66.

Karinou, E. et al., 2017. The *E. coli* dicarboxylic acid transporters DauA act as a signal transducer by interacting with the DctA uptake system. *Scientific Reports*, 7(1), 16331.

Kawakami, T. et al., 2010. Differential expression of multiple terminal oxidases for aerobic respiration in *Pseudomonas aeruginosa*. *Environmental Microbiology*, 12(6), pp.1399–1412.

Kindrachuk, K.N. et al., 2011. Involvement of an ATP-Dependent Protease, PA0779/AsrA, in Inducing Heat Shock in Response to Tobramycin in

Pseudomonas aeruginosa. *Antimicrobial Agents and Chemotherapy*, 55(5), pp.1874–1882.

King, J.D. et al., 2009. Review: Lipopolysaccharide biosynthesis in *Pseudomonas aeruginosa*. *Innate Immunity*, 15(5), pp.261–312.

Kipnis, E., Sawa, T. & Wiener-Kronish, J., 2006. Targeting mechanisms of *Pseudomonas aeruginosa* pathogenesis. *Medecine et Maladies Infectieuses*, 36(2), pp.78–91.

Klockgether, J. et al., 2010. Genome diversity of *Pseudomonas aeruginosa* PAO1 laboratory strains. *Journal of bacteriology*, 192(4), pp.1113–21.

Koch, C. et al., 2001. Presence of cystic fibrosis-related diabetes mellitus is tightly linked to poor lung function in patients with cystic fibrosis: data from the European Epidemiologic Registry of Cystic Fibrosis. *Pediatric pulmonology*, 32(5), pp.343–50.

Kopp, E.B. & Medzhitov, R., 1999. The Toll-receptor family and control of innate immunity. *Current Opinion in Immunology*, 11(1), pp.13–18.

Krezdorn, J., Adams, S. & Coote, P.J., 2014. A *Galleria mellonella* infection model reveals double and triple antibiotic combination therapies with enhanced efficacy versus a multidrug-resistant strain of *Pseudomonas aeruginosa*. *Journal of Medical Microbiology*, 63(7), pp.945–955.

Laarman, A.J. et al., 2012. *Pseudomonas aeruginosa* Alkaline Protease Blocks Complement Activation via the Classical and Lectin Pathways. *The Journal of Immunology*, 188(1), pp.386–393.

Lamont, I.L. et al., 2002. Siderophore-mediated signalling regulates virulence factor production in *Pseudomonas aeruginosa*. *Proceedings of the National Academy of Sciences*, 99(10), pp.7072–7077.

Lau, G.W. et al., 2004. The role of pyocyanin in *Pseudomonas aeruginosa* infection. *Trends in Molecular Medicine*, 10(12), pp.599–606.

Lawrence, R.C. & Creamer, L.K., 1969. The action of calf rennet and other proteolytic enzymes on κ-casein. *Journal of Dairy Research*, 36(1), pp.11–20.

Lee, J. et al., 2013. A cell-cell communication signal integrates quorum sensing and stress response. *Nature Chemical Biology*, 9(5), pp.339–343.

Lee, J. & Zhang, L., 2015. The hierarchy quorum sensing network in *Pseudomonas aeruginosa*. *Protein & Cell*, 6(1), pp.26–41.

Lessie, T.G. & Phibbs, P. V, 1984. Alternative Pathways of Carbohydrate Utilization in Pseudomonads. *Annual Review of Microbiology*, 38(1), pp.359–388.

Li, K. et al., 2013. SuhB is a regulator of multiple virulence genes and essential for pathogenesis of *Pseudomonas aeruginosa*. *mBio*, 4(6), e00419-13.

Li, W. & Lu, C.D., 2007. Regulation of Carbon and Nitrogen Utilization by CbrAB and NtrBC Two-Component Systems in *Pseudomonas aeruginosa*. *Journal of Bacteriology*, 189(15), pp.5413–5420.

Li, X.Z., Nikaido, H. & Poole, K., 1995. Role of *mexA-mexB-oprM* in antibiotic efflux in *Pseudomonas aeruginosa*. *Antimicrobial agents and chemotherapy*, 39(9), pp.1948–53.

Lipsky, B.A. et al., 2006. Diagnosis and Treatment of Diabetic Foot Infections. *Plastic and Reconstructive Surgery*, 117(7 Suppl), pp.212S–238S.

Loukides, S. & Polyzogopoulos, D., 1996. The Effect of Diabetes mellitus on the Outcome of Patients with Chronic Obstructive Pulmonary Disease Exacerbated due to Respiratory Infections. *Respiration*, 63(3), pp.170–173.

Ma, J.F. et al., 1998. Cloning and characterization of the *Pseudomonas aeruginosa zwf* gene encoding glucose-6-phosphate dehydrogenase, an enzyme important in resistance to methyl viologen (paraquat). *Journal of bacteriology*, 180(7), pp.1741–9.

Mahajan-Miklos, S. et al., 1999. Molecular Mechanisms of Bacterial Virulence Elucidated Using a *Pseudomonas aeruginosa – Caenorhabditis elegans* Pathogenesis Model. *Cell*, 96(1), pp.47–56.

Masuda, N. et al., 2000. Contribution of the MexX-MexY-OprM efflux system to intrinsic resistance in *Pseudomonas aeruginosa*. *Antimicrobial agents and chemotherapy*, 44(9), pp.2242–6.

Mavrodi, D.V. et al., 2001. Functional Analysis of Genes for Biosynthesis of Pyocyanin and Phenazine-1-Carboxamide from *Pseudomonas aeruginosa* PAO1. *Journal of Bacteriology*, 183(21), pp.6454–6465.

Mazade, M.A. & Edwards, M.S., 2001. Impairment of Type III Group B Streptococcus-Stimulated Superoxide Production and Opsonophagocytosis by Neutrophils in Diabetes. *Molecular Genetics and Metabolism*, 73(3), pp.259–267.

McCowen, K.C., Malhotra, A. & Bistrian, B.R., 2001. Stress-Induced Hyperglycemia. *Critical Care Clinics*, 17(1), pp.107–124.

McGhee, J., 2007. The *C. elegans* intestine. In *WormBook: The Online Review of C. elegans Biology*.

McKnight, S.L., Iglewski, B.H. & Pesci, E.C., 2000. The Pseudomonas quinolone signal regulates *rhl* quorum sensing in *Pseudomonas aeruginosa*. *Journal of bacteriology*, 182(10), pp.2702–8.

Midgley, M. & Dawes, E.A., 1973. The Regulation of Transport of Glucose and Methyl α-Glucoside in *Pseudomonas aeruginosa*. *Biochemical Journal*, 132(2), pp.141-154.

Miyata, S. et al., 2003. Use of the *Galleria mellonella* Caterpillar as a Model Host To Study the Role of the Type III Secretion System in *Pseudomonas aeruginosa* Pathogenesis. *Infection and Immunity*, 71(5), pp.2404–2413.

Moran, A. et al., 2009. Cystic Fibrosis-Related Diabetes: Current Trends in Prevalence, Incidence, and Mortality. *Diabetes Care*, 32(9), pp.1626–1631.

Niere, M. et al., 1999. Insect immune activation by recombinant *Galleria mellonella* apolipophorin III (1). *Biochimica et biophysica acta*, 1433(1–2), pp.16–26.

Nikaido, H., 1994. Prevention of drug access to bacterial targets: permeability barriers and active efflux. *Science*, 264(5157), pp.382–8.

Nishijyo, T., Haas, D. & Itoh, Y., 2001. The CbrA-CbrB two-component regulatory system controls the utilization of multiple carbon and nitrogen sources in *Pseudomonas aeruginosa*. *Molecular Microbiology*, 40(4), pp.917–931.

Nitzan, O. et al., 2015. Urinary tract infections in patients with type 2 diabetes mellitus: review of prevalence, diagnosis, and management. *Diabetes, Metabolic Syndrome and Obesity: Targets and Therapy*, 8, pp.129–136.

O'Callaghan, J. et al., 2012. A novel host-responsive sensor mediates virulence and type III secretion during *Pseudomonas aeruginosa*-host cell interactions. *Microbiology*, 158(4), pp.1057–1070.

Ochs, M.M. et al., 1999. Negative regulation of the *Pseudomonas aeruginosa* outer membrane porin OprD selective for imipenem and basic amino acids. *Antimicrobial agents and chemotherapy*, 43(5), pp.1085–90.

Ochsner, U.A. & Reiser, J., 1995. Autoinducer-mediated regulation of rhamnolipid biosurfactant synthesis in *Pseudomonas aeruginosa*. *Proceedings of the National Academy of Sciences of the United States of America*, 92(14), pp.6424–8.

Oglesby, A.G. et al., 2008. The Influence of Iron on *Pseudomonas aeruginosa* Physiology. *Journal of Biological Chemistry*, 283(23), pp.15558–15567.

Okon, E. et al., 2017. Key role of an ADP - ribose - dependent transcriptional regulator of NAD metabolism for fitness and virulence of *Pseudomonas aeruginosa*. *International Journal of Medical Microbiology*, 307(1), pp.83–94.

O'Toole, G.A. & Kolter, R., 1998. Flagellar and twitching motility are necessary for *Pseudomonas aeruginosa* biofilm development. *Molecular Microbiology*, 30(2), pp.295–304.

Patkee, W.R.A. et al., 2016. Metformin prevents the effects of *Pseudomonas aeruginosa* on airway epithelial tight junctions and restricts hyperglycaemia-

induced bacterial growth. *Journal of Cellular and Molecular Medicine*, 20(4), pp.758–764.

Patra, T. et al., 2012. The Entner-Doudoroff pathway is obligatory for gluconate utilization and contributes to the pathogenicity of *Vibrio cholerae*. *Journal of bacteriology*, 194(13), pp.3377–85.

Pederson, K.J. & Barbieri, J.T., 1998. Intracellular expression of the ADP-ribosyltransferase domain of *Pseudomonas* exoenzyme S is cytotoxic to eukaryotic cells. *Molecular microbiology*, 30(4), pp.751–9.

Peleg, A.Y. et al., 2007. Common infections in diabetes: pathogenesis, management and relationship to glycaemic control. *Diabetes/Metabolism Research and Reviews*, 23(1), pp.3–13.

Pesci, E.C. et al., 1997. Regulation of *las* and *rhl* quorum sensing in *Pseudomonas aeruginosa*. *Journal of bacteriology*, 179(10), pp.3127–32.

Pessi, G. & Haas, D., 2000. Transcriptional control of the hydrogen cyanide biosynthetic genes *hcnABC* by the anaerobic regulator ANR and the quorum-sensing regulators LasR and RhlR in *Pseudomonas aeruginosa*. *Journal of bacteriology*, 182(24), pp.6940–9.

Pezzulo, A.A. et al., 2011. Glucose Depletion in the Airway Surface Liquid Is Essential for Sterility of the Airways. *PLoS ONE*, 6(1), e16166.

Poole, K., 2011. *Pseudomonas aeruginosa*: resistance to the max. *Frontiers in microbiology*, 2:65.

Price-Whelan, A., Dietrich, L.E.P. & Newman, D.K., 2006. Rethinking "secondary" metabolism: physiological roles for phenazine antibiotics. *Nature Chemical Biology*, 2(2), pp.71–78.

Price-Whelan, A., Dietrich, L.E.P. & Newman, D.K., 2007. Pyocyanin Alters Redox Homeostasis and Carbon Flux through Central Metabolic Pathways in *Pseudomonas aeruginosa* PA14. *Journal of Bacteriology*, 189(17), pp.6372–6381.

Rada, B. & Leto, T.L., 2013. Pyocyanin effects on respiratory epithelium: relevance in *Pseudomonas aeruginosa* airway infections. *Trends in Microbiology*, 21(2), pp.73–81.

Ramarao, N., Nielsen-Leroux, C. & Lereclus, D., 2012. The Insect *Galleria mellonella* as a Powerful Infection Model to Investigate Bacterial Pathogenesis. *Journal of Visualized Experiments*, (70), e4392.

Read, R.C. et al., 1992. Effect of *Pseudomonas aeruginosa* rhamnolipids on mucociliary transport and ciliary beating. *Journal of Applied Physiology*, 72(6), pp.2271–2277.

Recinos, D.A. et al., 2012. Redundant phenazine operons in *Pseudomonas aeruginosa* exhibit environment-dependent expression and differential roles in pathogenicity. *Proceedings of the National Academy of Sciences*, 109(47), pp.19420–19425.

Roberts, B.K., Midgley, M. & Dawes, E.A., 1973. The Metabolism of 2-Oxogluconate by *Pseudomonas aeruginosa*. *Journal of General Microbiology*, 78(2), pp.319–329.

Rojo, F., 2010. Carbon catabolite repression in *Pseudomonas*: optimizing metabolic versatility and interactions with the environment. *FEMS Microbiology Reviews*, 34(5), pp.658–684.

Schafhauser, J. et al., 2014. The stringent response modulates 4-hydroxy-2-alkylquinoline biosynthesis and quorum-sensing hierarchy in *Pseudomonas aeruginosa*. *Journal of bacteriology*, 196(9), pp.1641–50.

Schuster, M. et al., 2004. The *Pseudomonas aeruginosa* RpoS regulon and its relationship to quorum sensing. *Molecular microbiology*, 51(4), pp.973–85.

Seed, P.C., Passador, L. & Iglewski, B.H., 1995. Activation of the *Pseudomonas aeruginosa lasI* gene by LasR and the *Pseudomonas autoinducer* PAI: an autoinduction regulatory hierarchy. *Journal of bacteriology*, 177(3), pp.654–9.

Shrout, J.D. et al., 2006. The impact of quorum sensing and swarming motility on *Pseudomonas aeruginosa* biofilm formation is nutritionally conditional. *Molecular Microbiology*, 62(5), pp.1264–1277.

Singh, P.B., Saini, H.S. & Kahlon, R.S., 2016. *Pseudomonas*: The Versatile and Adaptive Metabolic Network. In *Pseudomonas: Molecular and Applied Biology*, pp. 81–126.

Skariyachan, S. et al., 2018. Recent perspectives on the molecular basis of biofilm formation by *Pseudomonas aeruginosa* and approaches for treatment and biofilm dispersal. *Folia Microbiologica*, 63(4), pp.413–432.

Smith, R.S. & Iglewski, B.H., 2003. *P. aeruginosa* quorum-sensing systems and virulence. *Current opinion in microbiology*, 6(1), pp.56–60.

Sonnleitner, E., Abdou, L. & Haas, D., 2009. Small RNA as global regulator of carbon catabolite repression in *Pseudomonas aeruginosa*. *Proceedings of the National Academy of Sciences*, 106(51), pp.21866–21871.

Stoeckle, M. et al., 2008. The role of diabetes mellitus in patients with bloodstream infections. *Swiss medical weekly*, 138(35–36), pp.512–9.

Stover, C.K. et al., 2000. Complete genome sequence of *Pseudomonas aeruginosa* PAO1, an opportunistic pathogen. *Nature*, 406(6799), pp.959–964.

Strateva, T. & Mitov, I., 2011. Contribution of an arsenal of virulence factors to pathogenesis of *Pseudomonas aeruginosa* infections. *Annals of Microbiology*, 61(4), pp.717–732.

Strempel, N. et al., 2013. Human Host Defense Peptide LL-37 Stimulates Virulence Factor Production and Adaptive Resistance in *Pseudomonas aeruginosa*. *PLoS ONE*, 8(12), e82240.

Tan, M.W., Mahajan-Miklos, S. & Ausubel, F.M., 1999. Killing of *Caenorhabditis elegans* by *Pseudomonas aeruginosa* used to model mammalian bacterial pathogenesis. *Proceedings of the National Academy of Sciences*, 96(2), pp.715–720.

Tan, M. & Ausubel, F.M., 2000. *Caenorhabditis elegans*: a model genetic host to study *Pseudomonas aeruginosa* pathogenesis. *Current Opinion in Microbiology*, 3(1), pp.29–34.

Thompson, L.S. et al., 2003. The alternative sigma factor RpoN regulates the quorum sensing gene *rhlI* in *Pseudomonas aeruginosa*. *FEMS microbiology letters*, 220(2), pp.187–95.

Thomsen, R.W. et al., 2004. Risk of Community-Acquired Pneumococcal Bacteremia in Patients With Diabetes: A population-based case-control study. *Diabetes Care*, 27(5), pp.1143-7.

Thomsen, R.W. et al., 2005. Diabetes Mellitus as a Risk and Prognostic Factor for Community-Acquired Bacteremia Due to Enterobacteria: A 10-Year, Population-Based Study among Adults. *Clinical Infectious Diseases*, 40(4), pp.628–631.

Troemel, E.R. et al., 2006. p38 MAPK regulates expression of immune response genes and contributes to longevity in *C. elegans*. *PLoS Genetics*, 2(11), e183.

Tsai, C.J.-Y., Loh, J.M.S. & Proft, T., 2016. *Galleria mellonella* infection models for the study of bacterial diseases and for antimicrobial drug testing. *Virulence*, 7(3), pp.214–229.

Udaondo, Z. et al., 2018. Regulation of carbohydrate degradation pathways in *Pseudomonas* involves a versatile set of transcriptional regulators. *Microbial Biotechnology*, 11(3), pp.442–454.

Valentini, M., Storelli, N. & Lapouge, K., 2011. Identification of C4-Dicarboxylate Transport Systems in *Pseudomonas aeruginosa* PAO1. *Journal of Bacteriology*, 193(17), pp.4307–4316.

Valentini, M. et al., 2014. Hierarchical management of carbon sources is regulated similarly by the CbrA/B systems in *Pseudomonas aeruginosa* and *Pseudomonas putida*. *Microbiology*, 160(Pt 10), pp.2243-52.

Van Delden, C. & Iglewski, B.H., 1998. Cell-to-cell signalling and *Pseudomonas aeruginosa* infections. *Emerging Infectious Diseases*, 4(4), pp.551–560.

Van Delden, C., Comte, R. & Bally, A.M., 2001. Stringent response activates quorum sensing and modulates cell density-dependent gene expression in *Pseudomonas aeruginosa*. *Journal of bacteriology*, 183(18), pp.5376–84.

Venturi, V., 2006. Regulation of quorum sensing in *Pseudomonas*. *FEMS Microbiology Reviews*, 30(2), pp.274–291.

Visca, P., Imperi, F. & Lamont, I.L., 2007. Pyoverdine siderophores: from biogenesis to biosignificance. *Trends in Microbiology*, 15(1), pp.22–30.

Wang, S. et al., 2015. The exopolysaccharide Psl-eDNA interaction enables the formation of a biofilm skeleton in *Pseudomonas aeruginosa*. *Environmental microbiology reports*, 7(2), pp.330–40.

Waterston, R. et al., 1993. The genome of the nematode *Caenorhabditis elegans*. *Cold Spring Harbor symposia on quantitative biology*, 58, pp.367–76.

Whiteley, M., Lee, K.M. & Greenberg, E.P., 1999. Identification of genes controlled by quorum sensing in *Pseudomonas aeruginosa*. *Proceedings of the National Academy of Sciences of the United States of America*, 96(24), pp.13904–9.

Whiteley, M., Parsek, M.R. & Greenberg, E.P., 2000. Regulation of quorum sensing by RpoS in *Pseudomonas aeruginosa*. *Journal of bacteriology*, 182(15), pp.4356–60.

Wu, L. et al., 2005. Recognition of host immune activation by *Pseudomonas aeruginosa*. *Science*, 309(5735), pp.774–7.

Wyatt, R., Loughheed, T.C. & Wyatt, S.S., 1956. The chemistry of insect hemolymph; organic components of the hemolymph of the silkworm, *Bombyx mori*, and two other species. *The Journal of general physiology*, 39(6), pp.853–68.

Wylie, J.L. & Worobec, E.A., 1995. The OprB porin plays a central role in carbohydrate uptake in *Pseudomonas aeruginosa*. *Journal of bacteriology*, 177(11), pp.3021–6.

Zaborin, A. et al., 2009. Red death in *Caenorhabditis elegans* caused by *Pseudomonas aeruginosa* PAO1. *Proceedings of the National Academy of Sciences*, 106(15), pp.6327–6332.

Zaborina, O. et al., 2007. Dynorphin activates quorum sensing quinolone signalling in *Pseudomonas aeruginosa*. *PLoS pathogens*, 3(3), e35.

PART II

Content

- Research article:

  Raneri, M., Pinatel, E., Peano, C., Rampioni, G., Leoni, L., Bianconi, I., Jousson, Olivier., Dalmasio, C., Ferrante, P. & Briani, F. (2018). *Pseudomonas aeruginosa* mutants defective in glucose uptake have pleiotropic phenotype and altered virulence in non-mammal infection models. *Scientific Reports*, 8(1), p.16912.

- Article supplementary materials:

  Supplementary Results and Methods

  Supplementary Tables S1, S2, S3 and S4

  Supplementary Figures S1, S2, S3, S4, S5 and S6

- Thesis appendices:

  Supplementary Tables S5, S6 and S7

Contribution to the study

I performed most experiments described in this thesis and in the attached article, namely the generation of the glucose uptake defective mutants, the preparation of RNA samples for the RNASeq analysis, the experiments in *G. mellonella* and all the *in vitro* phenotypic assays except for quorum sensing molecules and biofilm production, which were assayed by G. Rampioni and L. Leoni (Università degli Studi Roma Tre). The RNASeq analysis was performed by E. Pinatel and C. Peano (Istituto di Tecnologie Biomediche-CNR), whereas the experiments in *C. elegans* were carried out by I. Bianconi and O. Jousson (Università degli Studi di Trento).

In addition, I have contributed to design the experiments and analyse RNASeq data and the other results.

SCIENTIFIC REPORTS

OPEN

Pseudomonas aeruginosa mutants defective in glucose uptake have pleiotropic phenotype and altered virulence in non-mammal infection models

Received: 9 August 2018
Accepted: 30 October 2018
Published online: 15 November 2018

Matteo Raneri[1], Eva Pinatel[2], Clelia Peano[2,5], Giordano Rampioni[3], Livia Leoni[3], Irene Bianconi[4], Olivier Jousson[4], Chiara Dalmasio[1], Palma Ferrante[1] & Federica Briani[1]

Pseudomonas **spp. are endowed with a complex pathway for glucose uptake that relies on multiple transporters. In this work we report the construction and characterization of** ***Pseudomonas aeruginosa*** **single and multiple mutants with unmarked deletions of genes encoding outer membrane (OM) and inner membrane (IM) proteins involved in glucose uptake. We found that a triple Δ*gltKGF* Δ*gntP* Δ*kguT* mutant lacking all known IM transporters (named GUN for Glucose Uptake Null) is unable to grow on glucose as unique carbon source. More than 500 genes controlling both metabolic functions and virulence traits show differential expression in GUN relative to the parental strain. Consistent with transcriptomic data, the GUN mutant displays a pleiotropic phenotype. Notably, the genome-wide transcriptional profile and most phenotypic traits differ between the GUN mutant and the wild type strain irrespective of the presence of glucose, suggesting that the investigated genes may have additional roles besides glucose transport. Finally, mutants carrying single or multiple deletions in the glucose uptake genes showed attenuated virulence relative to the wild type strain in** ***Galleria mellonella*****, but not in** ***Caenorhabditis elegans*** **infection model, supporting the notion that metabolic functions may deeply impact** ***P. aeruginosa*** **adaptation to specific environments found inside the host.**

Pseudomonas aeruginosa is a Gram-negative ubiquitous bacterium with high metabolic versatility, able to thrive in disparate environments and to infect hosts as different as plants, insects and mammals. However, the number of sugars that *P. aeruginosa* (and other species belonging to the *Pseudomonas* genus) can exploit as carbon and energy sources is relatively low and substantially limited to glucose, glucuronic acid and fructose[1].

Pseudomonas glucose uptake pathway was first clarified in *P. putida*[2,3]. Homologues of *P. putida* transporters were identified in *P. aeruginosa* and in some cases, shown to be *bona fide* orthologues (i.e. endowed with the same function) of *P. putida* proteins. Once crossed the outer membrane through the OprB porin, glucose can either cross the inner membrane thanks to the ABC transporter Glt or enter a periplasmic oxidative pathway producing gluconate and 2-ketogluconate (2-KG)[4,5]. Gluconate and 2-KG are internalized into the cytoplasm by the specific transporters GntP and KguT, respectively (Fig. 1a). In the cytoplasm, the two import pathways converge on the synthesis of 6-phosphogluconate, which enters the Entner-Doudoroff pathway[3]. The two alternate pathways (i.e. the Glt- dependent phosphorylative pathway and the GntP and KguT-dependent oxidative one) are regulated by glucose availability, with the oxidative route being preferentially used under high glucose[1,6,7]. Different regulators modulate the expression of the operons encoding Glt, GntP and KguT (Fig. 1b). The *gntP* gene and the *kgu* operon are negatively regulated by the GntR and PtxS repressors, respectively, whereas *glt-oprB* transcription is negatively modulated by the GltR response regulator, whose activity is controlled by the histidine kinase GtrS[8]. In the presence of glucose, repression by all these regulators is relieved (Fig. 1b)[1,5,8–11]. Interestingly, GtrS and PtxS

[1]Dipartimento di Bioscienze, Università degli Studi di Milano, Milano, Italy. [2]Istituto di Tecnologie Biomediche-CNR, Segrate, Italy. [3]Dipartimento di Scienze, Università degli Studi Roma Tre, Roma, Italy. [4]Centre for Integrative Biology, Università degli Studi di Trento, Trento, Italy. [5]Present address: Istituto Clinico Humanitas-CNR, Rozzano, Italy. Correspondence and requests for materials should be addressed to F.B. (email: federica.briani@unimi.it)

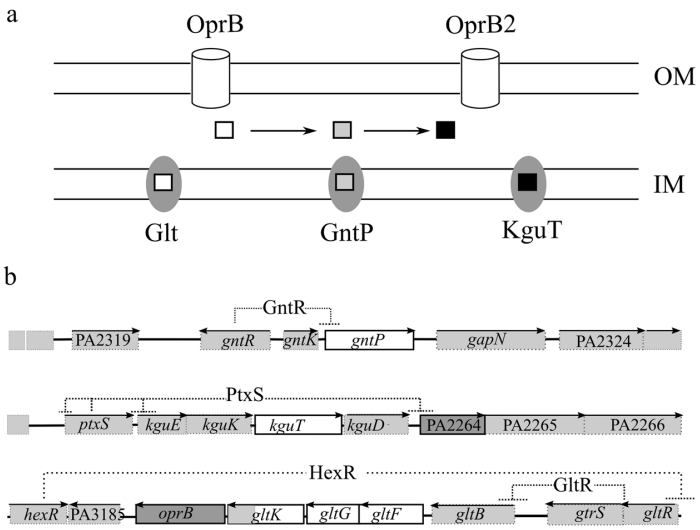

Figure 1. Glucose uptake pathways and organization of glucose uptake genes on *P. aeruginosa* genome. (**a**) Different porins allow glucose (empty square) entry into the periplasm. Once in the periplasm, glucose can be transported into the cytoplasm by Glt or oxidized to gluconate (grey square) and 2-KG (black square). Gluconate and 2-KG enter the cytoplasm thanks to GntP and KguT. Cylinders, outer membrane (OM) porins implicated in glucose uptake; ovals, inner membrane (IM) transporters. (**b**) Organization and regulation of glucose uptake genes in *P. aeruginosa* PAO1. 10 kbp long genomic regions encompassing the deleted loci encoding IM and OM proteins (represented as empty and dark boxes, respectively) are schematized. Boxes, ORFs; lines, intergenic regions; arrows on top of boxes indicate the transcription direction. Dashed lines connect genes encoding negative regulators with their target promoter(s).

regulate also transcription of *toxA*, the gene encoding the key virulence factor exotoxin A, thus establishing a link between glucose metabolism and virulence[8–10,12].

Metabolic genes have been repeatedly identified in *in vivo* screenings for *P. aeruginosa* functions contributing to virulence[13,14], suggesting that the inhibition of metabolic pathways may represent a sound strategy for the development of antibacterial therapies. In this respect, factors involved in glucose transport and utilization deserve consideration. In fact, pathologies leading to increased glucose concentration in the host fluids, from blood to liquid covering the respiratory mucosae, determine an augmented risk of developing serious bacterial infections not only for the immunity dysfunction due to hyperglycemia, but also because of glucose-dependent stimulation of bacterial growth[15–18]. Interfering with the ability of pathogenic bacteria to import or use glucose could thus represent a promising antibacterial strategy[19].

In this work, we report the generation of a collection of *P. aeruginosa* mutants with unmarked deletions in genes encoding the outer membrane (OM) OprB and PA2291 porins or the inner membrane (IM) Glt, GntP and KguT transporters. Deletions of the genes for porins and for the IM oxidative route transporters were combined in the double Δ*oprB* ΔPA2291 and Δ*gntP* Δ*kguT* mutants, respectively. A triple Δ*glt* Δ*gntP* Δ*kguT* mutant lacking all IM transporters was also generated and characterized. The mutants were assayed for phenotypes linked to *P. aeruginosa* virulence[20]. Interestingly, mutants lacking the oxidative route of glucose import showed altered virulence in the *Caenorhabditis elegans* and *Galleria mellonella* infection models.

Results

Generation of *P. aeruginosa* mutants defective in glucose uptake. We constructed single mutants of *P. aeruginosa* PAO1 lacking the genes for the OM porin OprB, its paralogue PA2291 (encoding OprB2, a porin 95% identical to OprB)[21], the IM putative gluconate permease GntP or the 2-KG transporter KguT. Single mutations were combined in order to generate strains defective for both *oprB* and PA2291, or both *gntP* and *kguT* genes of the oxidative route of glucose transport. We also inserted a Δ*gltKGF* mutation, eliminating *gltG*, *gltF* and part of *gltK*, both in PAO1 and in the double mutant Δ*gntP* Δ*kguT*, obtaining *P. aeruginosa* strains devoid of Glt only or lacking all the Glt, GntP and KguT IM transporters (Fig. 1b; Supplementary Table S1).

The growth curves and optical density reached by the mutants after 24 hours of incubation in minimal medium supplemented with glucose or gluconate were analysed. As a control, growth in succinate was monitored, since succinate uptake depends on other transporters[22]. Both single and double mutants lacking the OM OprB and/or OprB2 did not show any growth difference with respect to PAO1 (Supplementary Fig. S1) and in the optical density reached after 24 h of growth (Fig. 2a) in the tested media. These results indicate that the OprB and OprB2 porins are dispensable for glucose utilization, and that glucose can likely pass the OM through other porins. Therefore, we did not further characterize the mutants lacking OprB or/and OprB2, and we focused our analyses on mutants lacking IM transporters.

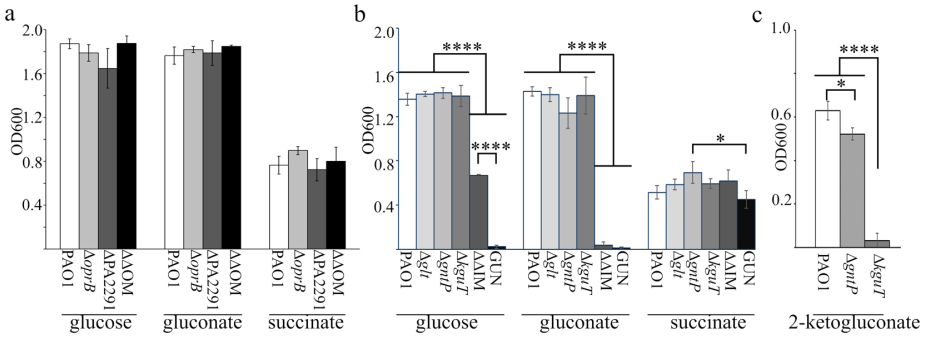

Figure 2. Growth of glucose uptake mutants with different carbon sources. PAO1 and mutant strains were inoculated at the same OD_{600} in M9-Triton X-100 supplemented with either 0.4% glucose, 0.4% gluconate, 0.1% 2-ketogluconate or 0.5% succinate, as indicated below the bars. Bacterial cell density (OD_{600}) was measured after aerate incubation for 24 h at 37 °C. The bars represent average (n = 3) with standard deviation (SD). (**a**) OM mutants. ΔΔOM, Δ*oprB* ΔPA2291 mutant. (**b**). IM mutants. ΔΔIM, Δ*gntP* Δ*kguT* mutant. (**c**). Growth in 0.1% 2-ketogluconate of the indicated mutants. (**a**,**b**) Significance was evaluated with One-way Anova and Tukey post-hoc test. (**a**) According to one-way Anova analysis, growth differences were not statistically significant at 0.05 level. (**b**,**c**). *P < 0.5; ****P < 0.0001. All comparisons for which P is not shown were not significant at 0.05 level.

Strain[b]	Generation time (min)[a]		
	Glucose[c]	Gluconate[c]	Succinate
PAO1	$36.7 \pm 2.8^{(a)}$	$34.1 \pm 3.6^{(a)}$	$36.4 \pm 3.9^{(ab)}$
Δ*glt*	$39.5 \pm 1.6^{(a)}$	$36.1 \pm 2.2^{(a)}$	$39.9 \pm 1.9^{(ab)}$
Δ*gntP*	$40.5 \pm 1.1^{(a)}$	$53.4 \pm 7.2^{(b)}$	$32.6 \pm 2.4^{(b)}$
Δ*kguT*	$38.6 \pm 5.7^{(a)}$	$39.3 \pm 3.1^{(a)}$	$43.5 \pm 3.7^{(ab)}$
Δ*gntP* Δ*kguT*	$64.2 \pm 11.6^{(b)}$	na	$48.3 \pm 4.6^{(a)}$
GUN	na	na	$48.8 \pm 8.6^{(a)}$

Table 1. Generation time of glucose uptake mutants. [a]Mean values (n = 3) with SD of generation time in exponential growth phase. Cultures were grown as described in Supplementary Fig. S1 legend. The differences between means reported in the same column and sharing at least one letter (in brackets) were not statistically significant according to One-way ANOVA and Tukey post-hoc test. [b]PAO1 single and double mutants are indicated by their cognate mutation(s). [c]na, not applicable. No OD_{600} increase detectable in the timespan of the experiments (7 h).

Single IM mutants and PAO1 reached comparable optical density after 24 h incubation in the tested media (Fig. 2b). However, the Δ*gntP* mutant had a longer lag phase in glucose and gluconate and lower growth rate in the latter medium (Table 1; Supplementary Fig. S1). To discriminate the roles of GntP and KguT in the transport of gluconate and 2-KG, the growth of the Δ*gntP* and Δ*kguT* mutants in minimal medium supplemented with 2-KG was analysed. The Δ*gntP* mutant was able to grow on 2-KG as sole carbon source, whereas Δ*kguT* was not (Fig. 2c), thus confirming that 2-KG enters the cytoplasm only through the KguT transporter[5].

As expected, the multiple mutants exhibited stronger growth defect in glucose/gluconate media. In fact, the Δ*gntP* Δ*kguT* double mutant showed reduced growth in glucose and did not grow in gluconate. Finally, the Δ*glt* Δ*gntP* Δ*kguT* strain was unable to grow in either glucose or gluconate, showing that no transporters other than Glt, GntP and KguT operate glucose uptake in *P. aeruginosa* (Table 1; Fig. 2b). Because of its inability to grow with glucose as sole carbon source, the Δ*glt* Δ*gntP* Δ*kguT* mutant was named GUN (i.e. Glucose Uptake Null).

Lack of glucose uptake systems deeply affects *P. aeruginosa* transcription profile. To assess how the lack of glucose uptake systems may impact *P. aeruginosa* physiology, we analysed the global transcription profile of the GUN mutant by RNASeq in comparison with that of PAO1. RNA was extracted from GUN and PAO1 cultures grown in minimal medium with casamino acids as carbon source (a medium in which glucose is virtually absent, see Supplementary Fig. S2) up to mid log phase, and then incubated 60 min with 0.4% glucose. In these conditions, genes responding to the presence of glucose and its metabolism and possibly other genes not related to glucose metabolism, but responding to the lack of Glt, GntP and KguT, could be differentially expressed in GUN relative to PAO1. To discriminate between these two categories and identify glucose responsive genes in *P. aeruginosa*, RNASeq was performed also on RNA extracted from a culture of PAO1 grown in the same conditions as above, but without glucose addition, and the transcriptomes of PAO1 grown in the presence or absence

of glucose were compared. Moreover, we compared the transcriptome of the GUN mutant grown in the presence of glucose with that of PAO1 grown either in the presence or in the absence of glucose. Notably, for the timespan of the experiment, PAO1 generation time did not significantly change upon glucose addition with respect to the culture without glucose (Supplementary Fig. S3), indicating that glucose is not required to sustain growth. Only 24 and 4 genes were up- and down-regulated (e.g. with a $\log_2FC \geq 1$ or ≤ -1 and Padj < 0.05), respectively, upon glucose addition to PAO1 cultures (Fig. 3a). Down-regulated genes encoded components of amino acid or dipeptide ABC transporters, whereas the 24 up-regulated genes encoded functions mostly related to glucose catabolism (Fig. 3a and Supplementary Tables S2 and S3). Only 5 up-regulated genes were not directly related to glucose metabolism, namely *fruIKA*, encoding the phosphotransferase system for fructose transport, *gdhA* and *phuR*, coding for the glutamate dehydrogenase and the OM receptor of heme uptake, respectively. The *gntR* and *gltR* genes, encoding the GntR and GltR repressors of *gntP* and *glt-oprB* operons, respectively, were identified among the genes induced by glucose in PAO1. Conversely, the *ptxS* gene, which was previously demonstrated to be induced by glucose[5], was not enclosed among differentially expressed genes because of its adjusted P value, which was slightly higher than the selected threshold (i. e. $\log_2FC = 1.55$; Padj $= 0.08$). However, RT-qPCR analysis of *ptxS* mRNA demonstrated that *ptxS* is actually up-regulated by glucose (Fig. 3b). On the whole, glucose effect on PAO1 transcriptome is similar to that observed in *P. putida*[2], as in both cases, glucose addition results in the up-regulation of genes mainly implicated in glucose uptake and utilization and down-regulation of few genes controlling the transport and utilization of alternative carbon sources.

Although in our experimental settings glucose limitedly affected gene expression of PAO1 parental strain, the lack of glucose transporters in the GUN mutant had a striking impact on the transcriptome of the mutant relative to that of the wild type. 514 genes were differentially regulated at least two-fold in the GUN mutant with respect to PAO1 when both strains were grown in the presence of glucose. In detail, 258 and 256 genes were down- or up-regulated in the GUN mutant, respectively.

Genes coding for ribosomal proteins, for enzymes required for purine biosynthesis, for the RNA polymerase subunits (*rpoA*, *rpoB* and *rpoC*), and genes involved in energy metabolism like the NAD biosynthetic genes *nadD* and *nadE*, the *nuo* operon for NADH dehydrogenase and genes encoding cbb_3−1 (*cco-1*), cbb_3−2 (*cco2*) and cyo (*cyoAB*) terminal oxidases of the electron transport were enriched among genes down-regulated in the GUN mutant (Table 2; Supplementary Table S2). Conversely, genes for the subunits of aa_3 terminal oxidase (i.e. *coxAB* and *coIII*), whose expression is induced upon nutrient starvation[23], were up-regulated in the GUN mutant. Likewise, a subset of quorum sensing-dependent genes, including those involved in pyocyanin biosynthesis and efflux (namely *phz* and *mexGHI* genes[24]), lectins (*lecA* and *lecB*) and extracellular proteases (*lasA* and *lasB*), were more expressed in the GUN mutant relative to PAO1. Genes encoding chemotactic functions, pyoverdine biosynthetic genes and those encoding factors of the Apr and Xcp secretion systems were also up-regulated in the GUN mutant. Finally, some genes coding for global regulators (i.e. *dnr*, *argR*, *rhlR*, *hfq*, *gbdR*) were differentially expressed. In particular, *rpoD* and *rpoS*, encoding sigma factors σ^D and σ^S, were down- and up-regulated in GUN, respectively (Table 3; Supplementary Tables S2 and S4). Interestingly, most of the above mentioned genes showed differential expression in the GUN mutant grown with glucose compared with PAO1 grown both with or without glucose (Table 3 and Supplementary Table S2).

The RNASeq data for a subset of differentially expressed genes (Table 3) were validated by RT-qPCR and/or phenotypic assays. As for the RT-qPCR analyses, the RNA was extracted from PAO1 and GUN cultures grown in the same conditions as the cultures for RNASeq. The RNA of the GUN mutant grown in the absence of glucose was also enclosed in the analysis. We tested genes with different expression patterns, namely PA2264, which was found by RNASeq to be up-regulated in PAO1 upon glucose addition, PA5348, *lasB*, *coxB* and *napA*, all up-regulated in GUN with respect to PAO1, and the two genes *aruC* and *hutU*, which are down-regulated in the GUN mutant. Since *lasB* gene is positively regulated by LasR[25], we also analysed the transcription of *lasR*, which was not included among differentially expressed genes because its $\log_2FC$ was slightly below the selected threshold ($\log_2FC = 0.9$).

Overall, the RT-qPCR results (Fig. 3b) were consistent with those of the RNASeq experiment (Table 3). For most genes, the transcription profile of the GUN mutant was not affected by glucose. The only exceptions were *coxB* and *napA* (coding for subunits of the aa_3 terminal oxidase and of the periplasmic nitrate reductase, respectively), whose expression, although remaining much higher than in PAO1, was reduced in the GUN mutant upon glucose addition. The RT-qPCR results confirmed the strong repression of *hutU* and *aruC* genes of the assimilative pathways of histidine and arginine in the GUN mutant in comparison to PAO1 without glucose. This observation was unexpected because both PAO1 and the GUN mutant can rely only on casamino acids as carbon source in the absence of glucose. Thus, in principle, they should have a similar expression profile of genes involved in amino acids transport and metabolism. Indeed, both genes were expressed in all tested strains/conditions in cultures at an early time point (10 min after the addition of glucose; Fig. 3b).

Finally, since *nadD* and *nadE* were down-regulated in the GUN mutant with respect to PAO1 (Table 3), we measured total NAD(H) in PAO1 and GUN. In agreement with transcriptomic data, we found that in the GUN mutant growing with or without glucose, NAD(H) cellular content was significantly reduced in comparison to PAO1 growing in the absence of glucose (Fig. 3c), whereas the difference was not significant with respect to PAO1 growing with glucose.

Overall, these results show that the inactivation of glucose uptake systems largely affects *P. aeruginosa* gene expression regardless of the presence of glucose.

Quorum sensing signal molecules and biofilm formation are altered in the GUN mutant. Transcriptomic analysis and/or RT-qPCR showed a significant up-regulation of QS-dependent genes in the GUN mutant. Accordingly, the QS receptor genes *lasR* and *rhlR*, responding to *N*−3-oxododecanoyl-homoserine lactone ($3OC_{12}$-HSL) and *N*-butanoyl-homoserine lactone (C_4-HSL) signal molecules, respectively, were also

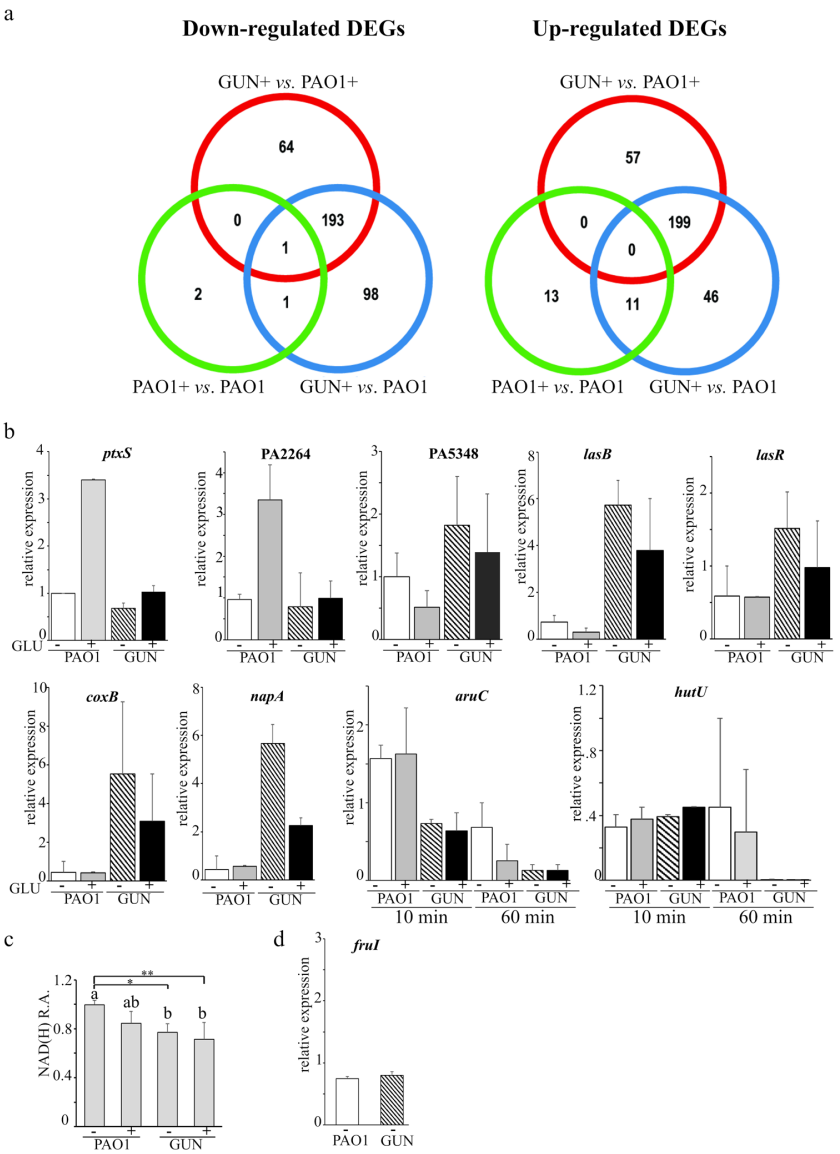

Figure 3. Transcriptome analysis results and differential gene expression validation. (**a**) Venn-diagrams of differentially expressed genes (DEGs). Venn diagrams representing the number of under- (left panel) and over-(right panel) expressed genes between GUN + and PAO1 +, GUN + and PAO1 and PAO1 and PAO1 +, as indicated. +, RNA extracted from cultures supplemented with glucose. (**b**,**d**). RT-qPCR mRNA analyses of differentially expressed genes. RNA was extracted from cultures of PAO1 or GUN mutant grown in M9-CAA up to $OD_{600} = 0.4$ and further incubated 60 min with (+GLU) or without (- GLU) 0.4% (w/v) glucose and analysed by RT-qPCR with proper oligonucleotides. For *aruC* and *hutU* gene expression, RNA extracted 10 min after the addition of glucose was also analysed as indicated below the histograms. The bars represent relative expression with respect to the reference condition (i.e. PAO1 incubated 60 min without glucose; the replicate with lower expression was used for normalization). The lowest values obtained in two independent experiments, each performed on two technical replicates, are reported. The error bars represent the replicate range. (**c**). NAD(H) relative amount (R.A.). NAD(H) was extracted from cultures grown as described above and quantified as detailed in Supplementary Methods. Values were normalized for the lowest value obtained for PAO1 grown without glucose. Bars represent average (n = 4) with SD. Significance was evaluated with one-way Anova and Tukey post hoc test. *$P < 0.05$; **$P < 0.01$. Differences between means that share a letter (on top of the columns) are not statistically significant at 0.05 level.

GUN + *vs.* PAO1+	GUN + *vs.* PAO1
Down-regulated DEGs[a]	
Ribosome (45)	Ribosome (39)
Purine metabolism (19)	Oxidative phosphorylation (20)
Carbon metabolism (24)	Purine metabolism (18)
RNA degradation (7)	Metabolic pathways (90)
Denitrification (7)	Arginine and proline metabolism (13)
Penthose phosphate cycle (8)	RNA degradation (6)
Up-regulated DEGs[a]	
Quorum sensing (21)	Quorum sensing (16)
Phenazine biosynthesis (7)	Pyoverdine synthesis (6)
Xcp type II secretion system (5)	Apr type I secretion system (4)
Apr type I secretion system (5)	Phenazine biosynthesis (6)
Pyoverdine synthesis (6)	Xcp type II secretion system (5)
Bacterial chemotaxis (10)	Nitrogen metabolism (9)
AMB[b] biosynthesis (3)	Bacterial chemotaxis (8)

Table 2. Enriched functional categories among DEGs. [a]Categories are ordered according to increased adjusted probability values. The number of DEGs belonging to each category is indicated in brackets. [b]AMB, L-2-amino-4-methoxy-trans-3-butenoic acid.

up-regulated in the GUN mutant (Table 3). To test whether the *las* and *rhl* QS circuits were actually altered in the GUN mutant, the levels of $3OC_{12}$-HSL and C_4-HSL signals were measured in PAO1 and GUN cultures grown in minimal medium supplemented with casamino acids, with or without glucose. As shown in Fig. 4a, maximal $3OC_{12}$-HSL production was significantly increased in the GUN mutant relative to PAO1. This effect did not depend on the differential ability of the two strains to import glucose, since it occurred also in the absence of glucose. Conversely, C_4-HSL levels were not significantly affected in all the tested conditions.

Biofilm formation in *P. aeruginosa* is a pleiotropic phenotype depending also upon QS and involving lectins and rhamnolipids, which expression was up-regulated in the GUN mutant (i.e. *lecA*, *lecB* and *rhlAB* genes; Table 3). Hence the biofilm forming ability of the GUN mutant was investigated by means of both standard crystal violet assay in polystyrene 96-well microtiter and laser scanning confocal microscopy (LSCM) on glass slides (Fig. 4b,c). These experiments revealed that biofilm formation was reduced in the GUN mutant relative to PAO1 irrespective of glucose presence in the medium.

Virulence-related traits of *P. aeruginosa* mutants defective in glucose uptake. The glucose uptake defective mutants were assayed for selected virulence traits, according to the results of GUN transcriptomic analysis and/or to literature data linking glucose and *P. aeruginosa* pathogenic potential[20,26–28]. In particular, we investigated the production of: extracellular proteases; pyocyanin, a blue redox-active molecule inducing oxidative stress in host cells; pyoverdine, a siderophore allowing iron acquisition and bacterial growth within the host; rhamnolipids, biosurfactants playing a role in biofilm formation and chronic infection; growth in microaerophilic and in anaerobic environments. We found that all strains carrying the *kguT* deletion produced more pyocyanin, pyoverdine and rhamnolipids than PAO1, whereas the *glt* deletion had no effect on their production. Single *gntP* deletion slightly increased and reduced rhamnolipids and pyoverdine production, respectively, and had no effect on pyocyanin (Fig. 5 and Supplementary Fig. S4). It should be noted that, albeit statistically significant, the differences between the mutants and PAO1 in the production of both pyoverdine and rhamnolipids were small and thus their biological meaning uncertain. As for extracellular proteases, they were comparably produced by all strains in the absence of glucose. Glucose supplementation repressed protease production by PAO1 and by the single mutants, whereas it did not affect production by the Δ*gntP* Δ*kguT* and GUN mutants. Finally, none of the tested mutations affected the growth in microaerophilic or anaerobic conditions (Supplementary Fig. S4).

Interfering with oxidative route of glucose import has different outcomes on the virulence in *Caenorhabditis elegans* and *Galleria mellonella* infection models. The virulence of the glucose uptake defective mutants was assayed in two *P. aeruginosa* infection models, i.e. the nematode *Caenorhabditis elegans* and the *Galleria mellonella* insect larvae. It should be noted that the paths of *P. aeruginosa* invasion, and presumably the physiology of bacterial cells in the two systems, are largely different. In particular, while in *G. mellonella* infections bacteria are injected in the insect hemolymph, thus causing an acute infection that kills the larvae within 18–40 h at 37 °C, in *C. elegans* slow-killing assay worms are fed on *P. aeruginosa* cells, which colonize the intestine while staying embedded in an extracellular matrix and kill the worms over the course of several days at 20 °C[29–32].

In *C. elegans* slow-killing assay (Supplementary Fig. S5), lethality was visible 7–8 days post-infection with PAO1. The Δ*kguT* and the Δ*gntP* Δ*kguT* mutants were slightly but significantly more virulent than PAO1, whereas Δ*gntP*, Δ*glt* and GUN mutants did not show significant differences in virulence relative to the wild type.

Preliminarily to *G. mellonella* infection with *P. aeruginosa*, we measured the concentration of glucose in the larvae hemolymph. We observed that glucose was relatively scarce (mean value 11.2 μM, corresponding to 2.0 μg/ml; Supplementary Fig. S2) with respect to a previous estimation[33], probably because the larvae were starved for 24h-48h before starting the experiment. In the larva infection model, the Δ*kguT* mutant was less virulent than

Locus[a]	Name	Fold Change			Description
		PAO1 + *vs.* PAO1 −	GUN + *vs.* PAO1 +	GUN + *vs.* PAO1 −	
Genes up-regulated in GUN mutant[b]					
PA0105	*coxB*	0.8	8.2	6.5	cytochrome C oxidase subunit
PA1174	*napA*	0.8	4.8	3.6	nitrate reductase subunit
PA1430	*lasR*	1.0	1.7	1.8	transcriptional regulator LasR
PA2426	*pvdS*	2.5	1.9	4.8	sigma factor PvdS
PA2570	*lecA*	0.7	4.7	3.1	LecA lectin
PA3361	*lecB*	0.6	5.2	2.9	fucose-binding lectin PA-IIL
PA3477	*rhlR*	0.8	2.4	1.9	transcriptional regulator RhlR
PA3478	*rhlB*	0.8	3.0	2.3	rhamnosyltransferase subunit B
PA3479	*rhlA*	0.7	3.3	2.5	rhamnosyltransferase subunit A
PA3622	*rpoS*	0.9	2.6	2.4	sigma factor σ^S
PA3724	*lasB*	0.5	7.8	3.5	elastase LasB
PA4210	*phzA1*	0.4	6.2	2.7	phenazine biosynthesis protein
PA4211	*phzB1*	0.5	7.2	3.2	phenazine biosynthesis protein
PA5348	PA5348	0.8	3.0	2.4	probable DNA-binding protein
Genes down-regulated in the GUN mutant[b]					
PA0576	*rpoD*	1.1	0.4	0.5	sigma factor σ^D
PA0893	*argR*	0.6	0.6	0.4	transcriptional regulator ArgR
PA0895	*aruC*	0.5	0.3	0.2	acetylornithine aminotransferase
PA2259	*ptxS*	2.9	0.5	1.4	transcriptional regulator PtxS
PA2264	PA2264	3.4	0.5	1.5	conserved hypothetical protein[c]
PA2320	*gntR*	3.7	0.3	1.1	GntR transcriptional regulator
PA4006	*nadD*	0.9	0.5	0.5	NAM adenylyltransferase
PA4920	*nadE*	1.5	0.5	0.8	NAD synthetase
PA5100	*hutU*	0.8	0.0	0.0	urocanate hydratase
PA5105	*hutC*	0.8	0.2	0.1	Transcriptional regulator HutC
Genes for glucose IM transporters deleted in this work					
PA2262	*kguT*	1.3	0.3	0.4	2-ketogluconate transporter
PA2322	*gntP*	35.5	0.0	0.6	gluconate permease
PA3187	*gltK*	52.0	0.1	6.7	ABC transporter ATP-binding protein
PA3188	*gltG*	31.6	0.0	0.4	sugar ABC transporter permease
PA3189	*gltF*	3.5	0.3	0.9	probable permease of ABC sugar transporter

Table 3. Differential expression of selected *P. aeruginosa* genes. [a]Boldface characters, genes analysed by RT-qPCR. [b]Genes up- and down-regulated in GUN mutant with respect to PAO1 (with and/or without glucose). [c]The protein contains a domain belonging to the Gluconate 2-dehydrogenase subunit 3 family (InterPro IPR027056).

PAO1, and significant attenuation was shown by the Δ*gntT* Δ*kguT* and GUN multiple mutants. Indeed, 24 h post-infection (h.p.i.) the mortality of larvae injected with either Δ*gntT* Δ*kguT* or GUN was lower than 40%, while the mortality rate of larvae challenged with wild type PAO1 exceeded 75% (Fig. 6a). To test whether attenuation of strains lacking the *kguT* gene was due to slower growth of the mutants *in vivo*, the hemolymph of larvae infected with a comparable number (between 20 and 30) of PAO1, Δ*kguT*, Δ*gntT* Δ*kguT* or GUN cells was recovered 16 h.p.i. and bacteria were titrated. As shown in Fig. 6b, the *in larva* bacterial load was significantly lower for all tested mutants compared to PAO1, whereas no significant difference was detectable among the mutants.

We also evaluated the stimulation of the larvae immune system by measuring the activation of prophenoloxidase cascade in the hemolymph[34] after larvae infection with a lethal dose of PAO1 or of single and multiple mutants lacking *kguT* (Fig. 6c). As expected, we observed an increase in the phenoloxidase production in larvae infected with either PAO1 or any of the mutants with respect to larvae injected with sterile physiological solution. Phenoloxidase was significantly less abundant in larvae infected with the Δ*gntT* Δ*kguT* or GUN mutants with respect to those infected with PAO1 or the Δ*kguT* single mutant.

Discussion

In this work we describe the generation and characterization of a collection of single and multiple mutants of *P. aeruginosa* PAO1 with unmarked, non-polar deletions (see Supplementary results and Supplementary Fig. S6 for the analysis of mutation polarity) of genes encoding IM proteins involved in glucose transport. The inability of the GUN mutant to grow on glucose as unique carbon source confirms that *P. aeruginosa* does not have any

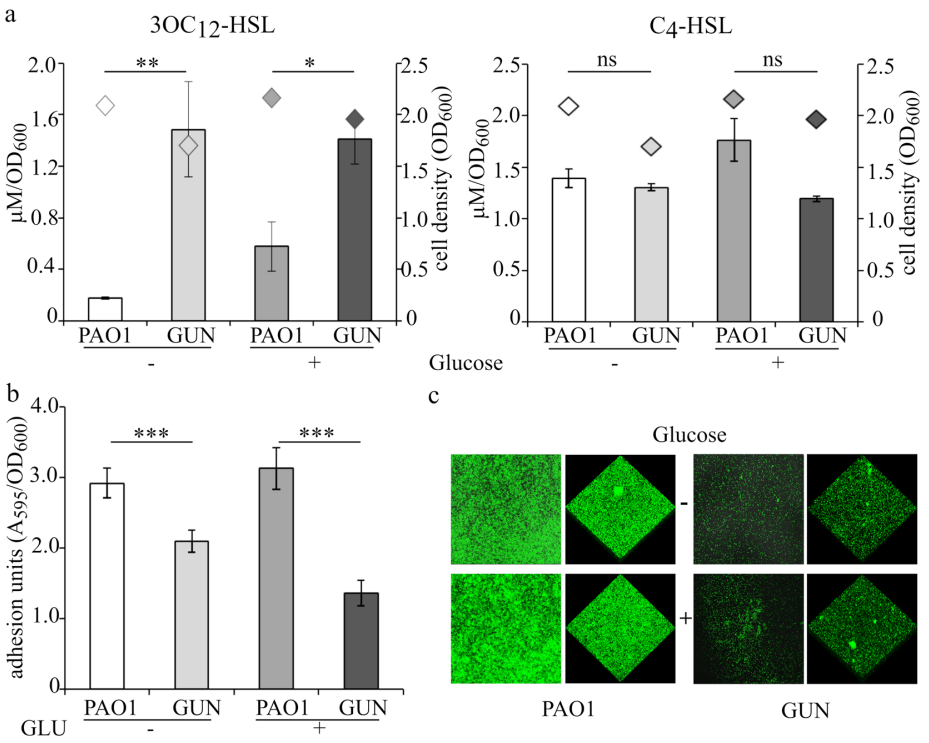

Figure 4. Autoinducers production and adhesion assays. (**a**) Histograms reporting the maximal production of QS signal molecules $3OC_{12}$-HSL and C_4-HSL normalized to the cell density of the culture in the indicated strains grown in M9-CAA in the absence (−) or in the presence (+) of 0.4% (w/v) glucose; diamonds indicate the corresponding cell density (OD_{600}). Median values of three independent experiments are reported with SD (*$P < 0.05$; **$P < 0.01$; ns, not statistically significant). (**b**) Adhesion units determined as A_{595} of the crystal violet stained solubilized biofilms formed by the indicated strains in M9-CAA in the absence (−) or in the presence (+) of 0.4% (w/v) glucose, normalized to the cell density (OD_{600}) of the corresponding planktonic cultures. Median values of three independent experiments, each performed on 6 technical replicates, are reported with SD (***$P < 0.001$). (**c**) Representative LSCM images of biofilms formed by the indicated strains constitutively expressing GFP grown in M9-CAA in the absence (−) or in the presence (+) of 0.4% (w/v) glucose.

other IM transporter for this sugar besides Glt, GntP and KguT. Similarly, the failure of the double mutant Δ*gntP* Δ*kguT* and of the single mutant Δ*kguT* to grow on gluconate and on 2-KG, respectively, confirms that GntP and KguT are the only transporters involved in the uptake of intermediates of the oxidative branch of glucose utilization, with the latter being specifically required for 2-KG uptake. Conversely, the lack of any apparent growth defect on minimal medium supplemented with glucose (or gluconate) of strains defective for the glucose-specific OprB porin and for its paralogue OprB2, whose expression is also regulated by glucose, shows that glucose and gluconate can cross the OM through other porins. Indeed, the amino acid- and imipenem- specific OprD porin has been shown to facilitate gluconate entry in *P. aeruginosa*[35]. Gill *et al.*[36] observed slower growth in minimal medium supplemented with glucose by a PAO1 Δ*oprB* mutant. This discrepancy with respect to our results could be explained by the known heterogeneity of PAO1 sublines[37] used in different laboratories, and may be due to differential expression of genes encoding facilitators of glucose entry in the various PAO1 sublines.

The transcription profile of genes involved in glucose, gluconate and 2-KG transport was coherent with their expected regulation by GltR, GntR and PtxS, respectively[1]. Repression by GntR and PtxS is relieved only if their cognate effectors (i.e. gluconate/6-phosphogluconate for GntR and 2-KG for PtxS) are present within the cell cytoplasm. Conversely, phosphorylation of the response regulator GltR, which determines its detachment from DNA, is triggered by 2-KG interaction with the histidine kinase GtrS in the periplasm[1]. Consistently, in the presence of glucose, the GltR-regulated *glt-oprB* operon was highly and comparably expressed in PAO1 and in the GUN mutant, whereas the expression of the *gntP* and *kgu* operons was lower in the mutant and similar to that observed in PAO1 grown in the absence of glucose. The same expression pattern was shown by other genes connected with glucose catabolism and regulated by HexR, whose effector is synthesized only upon glucose entry into the cell[1].

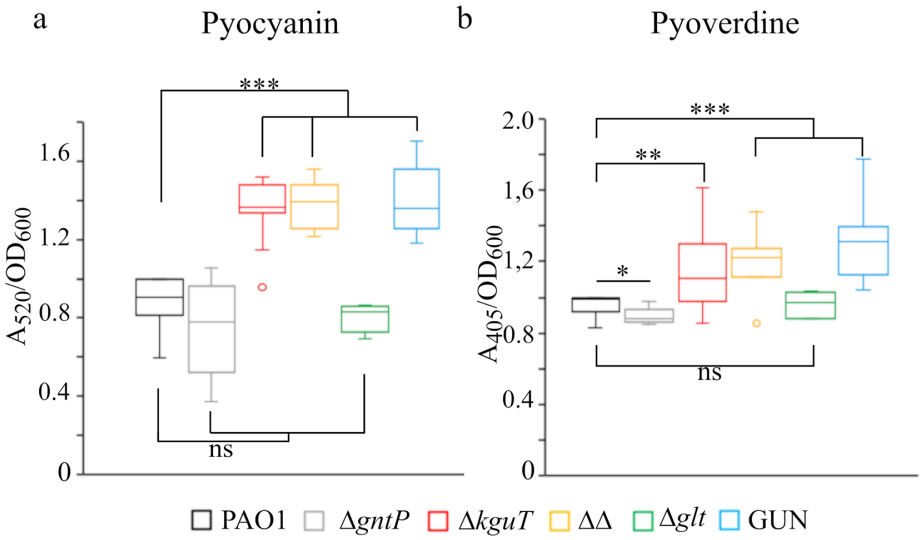

Figure 5. Pyocyanin and pyoverdine production by glucose uptake mutants. Cultures of the strains listed above the panels were grown 24 h at 37 °C in LD. ΔΔ indicates PAO1 Δ*gntP* Δ*kguT* strain. Pyocyanin (**a**) and pyoverdine (**b**) were measured as described in Supplementary Experimental procedures. The median (line) is reported inside the boxes ($n \geq 5$). The whiskers represent the minimum and maximum values observed. Significance was estimated with one-way Anova and Tukey post-hoc analysis (ns, not significant; *$P < 0.05$; **$P < 0.01$; ***$P < 0.001$), only the results relative to PAO1 are reported.

We observed enhanced transcription of both the *gntR*, *gltR* and *ptxS* repressor genes and their *gntP*, *glt-oprB* and *kgu* target operons upon glucose addition to PAO1 cultures. This result can be explained considering that i) transcription of *gntR*, *gltR* and *ptxS* genes is subject to negative auto-regulation and, limitedly to *gltR*, also to repression by HexR; and ii) increased intracellular concentration of GntR, GltR and PtxS should not result in repression of their target operons as long as glucose is present because of the allosteric induction of GntR and PtxS and the GltS-dependent phosphorylation of GltR triggered by glucose derivatives[1]. We speculate that increasing the GntR, GltR and PtxS amount as part of the response to glucose may contribute to quickly switch off the transcription of the operons regulated by such repressors upon glucose exhaustion.

The effect of glucose addition on PAO1 transcriptome was limited to the induction of 24 genes, mostly involved in glucose transport and catabolism, and to the down-regulation of few genes mainly belonging to ArgR regulon connected with the transport and utilization of arginine[38], which is likely used by PAO1 as carbon source when growing in minimal medium with casamino acids. Glucose-dependent induction of *fruIKA* in PAO1 and in the GUN mutant (Supplementary Table S2 and Fig. 3d) was likely due to contaminating fructose originated by spontaneous glucose isomerization to fructose[39].

The lack of glucose transporters deeply impacts *P. aeruginosa* transcriptome, with a large numbers of genes belonging to various pathways differentially regulated in the GUN mutant with respect to PAO1. The results of RT-qPCR and phenotypic assays were consistent with those of the RNASeq analysis and showed that the GUN mutant is endowed with a complex phenotype having decreased NAD(H) content, dysregulated quorum sensing, reduced biofilm formation and virulence attenuation in *G. mellonella* in spite of enhanced production of virulence factors like pyocyanin, pyoverdine and extracellular proteases. The panorama of genes differentially expressed in GUN provides some hints on the physiology of this mutant strain. Downregulation of genes typically expressed in the exponential phase and connected with growth, like those encoding ribosomal proteins or the RNA polymerase subunits, together with the up-regulation of *rpoS*, encoding the alternative sigma factor σ^S, testifies the stress condition of the GUN strain. Moreover, *aru* and *hut* genes for arginine and histidine utilization are equally expressed in PAO1 and GUN mutant in cultures in mid exponential phase (i.e. 10 min after glucose addition to cultures at $OD_{600} = 0.4$), whereas they are down-regulated in the GUN mutant relative to PAO1 at a later time point, suggesting that PAO1 and the GUN mutant could use the amino acids in the medium in a different order and/or at a different rate. *aru* and *hut* operons are regulated by ArgR and HutC, whose genes are down-regulated in the GUN mutant (Table 3), and by the CbrA/CbrB response regulator, which activates transcription of the arginine and histidine utilization operons in response to an unknown signal[40].

The iron starvation sigma factor *pvdS*, a major global regulator of iron uptake systems and virulence[41], is up-regulated in the GUN mutant. The consequent up-regulation of PvdS target genes (e.g. *pvd* pyoverdine biosynthetic genes) and the enhanced pyoverdine production may be linked to a dysregulated iron metabolism. Indeed, transcriptomic data suggest that in the GUN mutant a complex reorganization of the electron transport chain may take place, and this would require the synthesis of heme- (and thus iron-) containing proteins, possibly enhancing the iron demand of the mutant. However, a regulatory link coordinating iron supply and carbon

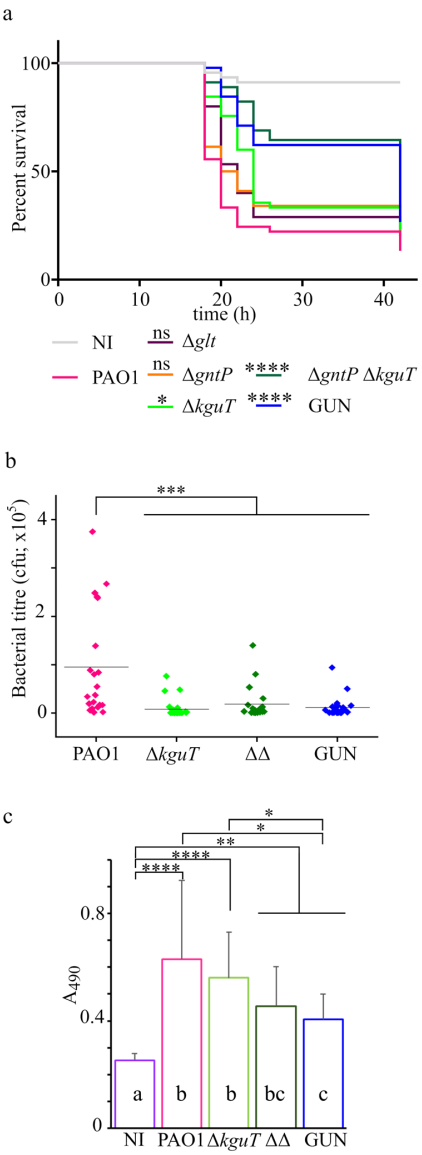

Figure 6. *G. mellonella* infection assay. (**a**) Survival curves of *G. mellonella* larvae infected with glucose uptake mutants. Kaplan-Meyer curves represent results deriving from three independent experiments in which groups of 15 larvae were injected with the indicated strains. The average number of *P. aeruginosa* cells injected was 26 ± 5 (PAO1), 31 ± 6 (Δ*glt*), 30 ± 5 (Δ*gntP*), 28 ± 8 (Δ*kguT*), 27 ± 6 (Δ*gntP* Δ*kguT*), 34 ± 6 (GUN). h, hours post-infection. NI (not infected), larvae injected with sterile physiological solution. Significance was estimated with log-rank test; only the results relative to PAO1 are reported (*$P < 0.05$; ****$P < 0.0001$; ns, not significant). (**b**) The dots represent bacterial titre 16 h post-infection in the hemolymph of larvae ($n = 24 \pm 4$) infected with 10 µl of physiological solution containing the following number of bacterial cells: 33 ± 8 (PAO1), 37 ± 5 (Δ*kguT*), 34 ± 8 (ΔΔ, Δ*gntP* Δ*kguT*), 34 ± 9 (GUN). The results were plotted with OriginPro (OriginLab). The line represents the mean value. Significance was estimated with one-way Anova and Tukey post-hoc analysis (***$P < 0.001$). Differences among the Δ*kguT*, Δ*gntP* Δ*kguT* and GUN mutants were not significant at 0.05 level. (**c**) Phenoloxidase activity assay. Hemolymph was collected 4 h post-infection with 20000 cfu of the bacterial strains listed in the panel. The hemolymph samples deriving from groups of ten larvae infected with the same strain were pooled and phenoloxidase activity at 30 min was estimated as described in Methods. The results of four experiments done in different days ($n = 12$) are shown. Bars represent average with SD. Significance was estimated with one-way Anova and Tukey post-hoc analysis (****$P < 0.0001$; **$P < 0.01$; P*$P < 0.05$). Differences between means that share a letter (on the columns) are not statistically significant at 0.05 level.

metabolism has been recently established in pseudomonads[42,43], opening the possibility that *pvdS* up-regulation may be actually part of a stress response elicited by carbon metabolism defects of the GUN mutant.

It is likely that the altered QS cascade and biofilm formation observed in in the GUN mutant may also be related to its complex metabolic dysregulation. We observed increased production of the $3OC_{12}$-HSL signal molecule in the GUN mutant relative to PAO1, in line with increased RNA level of the *lasR* gene and with the enhanced production of LasR-controlled virulence factors, like pyocyanin and proteases. The *las* QS system usually exerts a positive regulatory role on the C_4- HSL-dependent *rhl* QS circuit. Indeed, the *rhlR* gene and the RhlR-dependent *rhlAB* genes for rhamnolipids production were up-regulated, but unexpectedly production of the C_4-HSL signal molecule was unaffected. QS circuits in *P. aeruginosa* not only respond to cell density, since their activation is finely modulated by a plethora of environmental and metabolic stimuli[44,45]. Moreover, hierarchical organization of the QS cascade in *P. aeruginosa*, with the *las* system being required for full activation of the *rhl* QS circuit, has been mainly described in rich media, while this connection is possibly missing or altered in other growth conditions[46,47]. Altered QS cascade may in turn interfere with biofilm formation, as it is known that a large number of factors controlled by QS may impact biofilm formation[48]. However, biofilm formation is a pleiotropic phenotype affected by multiple environmental and metabolic stimuli whose signalling pathways are altered in the GUN mutant, including QS, iron uptake systems, and arginine metabolism[49,50]. Hence, while altered biofilm formation in the GUN mutant relative to PAO1 is not surprising, defining the specific impact of GUN-controlled phenotypes on biofilm formation is a puzzling issue that will deserve further investigation.

Interestingly, the global transcription profile and most of the assayed phenotypic traits differ between the GUN mutant and PAO1 irrespective of the presence of glucose. In particular, the GUN mutant seems to perceive nutrient starvation in conditions in which PAO1 does not. As an example, in the GUN mutant, a strong up-regulation of *cox* genes encoding the aa3 terminal oxidase, which is expressed in nutrient starvation conditions[23], is observed (Table 3 and Fig. 3b). This suggests that the investigated glucose uptake systems may have other functions independent of glucose transport. It is tempting to speculate that one or more of the proteins missing in the GUN mutant may participate in the regulation of cell metabolism, for instance by modulating the activity of sensor histidine kinases (HK) of two-component systems as it has been found for the *E. coli* dicarboxylic acid transporters DauA, which regulates the HK DcuS[51]. KguT could be a good candidate for such an accessory function as it plays a major role in determining relevant phenotypes *in vitro* and *in vivo*. Indeed, we observed enhanced *in vitro* secretion of the virulence factors pyocyanin and pyoverdine by all mutants lacking the KguT transporter. On the other hand, such mutants showed attenuated virulence in *G. mellonella*, suggesting that pyocyanin and pyoverdine increased production, if occurring also *in vivo*, is either scarcely relevant or counteracted by other mutants' features detrimental to the *in larva* growth.

Larvae infected with the GUN mutant showed lower phenoloxidase production than those infected with PAO1 or the Δ*kguT* single mutant. Pro-phenoloxidase cascade is triggered not only by the lipopolysaccharide of the bacterial OM, but also by specific bacterial proteins like thermolysin[52]. Further analyses will be required to assess whether factors stimulating pro-phenoloxidase cascade are differentially produced by the GUN mutant with respect to PAO1 and the Δ*kguT* strain.

The single Δ*kguT* and the double Δ*gntP* Δ*kguT* mutants were slightly more virulent than PAO1 in *C. elegans*. Thus, the bacterial ability to import (and use) glucose, as well as the accessory function of the glucose uptake transporters in the regulation of cell metabolism highlighted in this study, may have a different relevance in different infection models. In agreement with this observation, PAO1 mutants defective in glucose metabolism genes (i.e. Δ*oprB*, Δ*gltK*, Δ*gtrS* and Δ*glk* mutants) were shown to cause a reduced bacterial load with respect to wild type PAO1 in the airways of hyperglycaemic mice, but not in those of normal ones[36]. This suggests that targeting glucose metabolism with specific drugs may differentially impact the outcome of chronic and acute human infections caused by *P. aeruginosa*, depending on the particular nutritional milieu at the site of infection and on the specific strategy adopted by *P. aeruginosa* to thrive within the host in each case. A deeper knowledge of bacterial physiological state in the different human infections together with the availability of proper preclinical infection models recapitulating them are needed to develop effective therapeutic strategies based on the inhibition of bacterial metabolic functions.

Methods

Bacteria, plasmids and oligonucleotides. Bacterial strains, plasmids and oligonucleotides used in this study are listed in Supplementary Table S1. *P. aeruginosa* genome coordinates throughout this work refer to PAO1 strain, Genbank Accession Number NC_002516.2. Construction of PAO1 deletion mutants in glucose uptake genes by gene replacement[53] and *kguT* cloning in pGM2071 plasmid are detailed in Supplementary Methods. Bacterial cultures were grown in LD broth or M8 and M9 minimal media[54,55]. M9-CAA is M9 supplemented with 0.2% (w/v) casamino acids (i.e. Casein Hydrolysate, Sigma-Aldrich). When needed, media were supplemented as follows: 100 µg/ml ampicillin, 150–300 µg/ml carbenicillin, 10 µg/ml nalidixic acid, 0.4% (w/v) glucose, 0.4% (w/v) gluconate, 0.1% (w/v) 2-ketogluconate, 0.5–1% (w/v) succinate, 0.02% (w/v) arabinose, 10% (w/v) sucrose and 0.05% (v/v) Triton X-100. To prevent calcium precipitation, a calcium free solution of 2-ketogluconate was prepared as previously indicated[5].

RNA extraction for RNA-Seq. Total RNA was extracted as previously described[56] from *P. aeruginosa* cultures grown in M9-CAA at 37 °C up to $OD_{600} = 0.4$ and further incubated 60 min with or without 0.4% (w/v) glucose; biological duplicates of the experiments were performed. Ribosomal RNA was depleted from 1 µg of total RNA with the RiboZero Gram positive kit (Illumina) according to the manufacturer's instructions. Strand specific RNA-Seq libraries were prepared with the ScriptSeqTM v2 RNAseq library preparation kit (Illumina) from 50 ng of rRNA-depleted RNA. The libraries were sequenced on a MiSeq Illumina sequencer; 75 bp Single End reads were produced.

RNA-Seq data analysis and PAO1 genome annotation. The strategy that we followed to obtain a comprehensive annotation of PAO1 genome is detailed in Supplementary Methods. Bowtie 2 (v2.2.6)[57] was used to align raw reads to *P. aeruginosa* PAO1 genome (GCF_000006765.1) and only high quality reads (MAPQ > 30) were considered for the subsequent step of the analysis. The R[58] package DESeq. 2 (v1.14.1)[59] was used to normalize the counts and to produce the differentially expressed gene lists, setting independent filtering to FALSE. The enrichment of functional categories was calculated using Fisher test and Benjamini Hochberg correction for multiple testing. The categories with an adjusted P value (Padj) ≤ 0.05 were considered significantly enriched.

RT-qPCR mRNA analysis. RT-qPCR (Reverse Transcription-quantitative PCR) was performed on 1 µg of RNA extracted from two independent cultures for each strain grown as for the RNASeq. Technical details and the list of primers specific for each analysed gene is provided in Supplementary Methods and Table S1. Two technical duplicates were performed for each biological replicate. 16 S rRNA was used as reference gene.

***In vitro* phenotypic assays.** Anaerobic and microaerophilic growth condition and a detailed description of the *in vitro* phenotypic assays applied in this work are provided in Supplementary Methods. In brief, NAD(H) content in samples of PAO1 and GUN cultures grown as for the RNASeq was quantified by a cyclic assay[60]. Pyocyanin, pyoverdine and rhamnolipids production was estimated as described[54,61,62] on stationary cultures grown in LD at 37 °C. Extracellular proteases were tested by spotting supernatants of cultures grown 17 h at 37 °C in M9-CAA with or without 0.4% glucose onto casein-agar plates. Levels of QS signal molecules in *P. aeruginosa* PAO1 wild type and GUN mutant culture supernatants were determined at different times during bacterial growth in M9-CAA with or without 0.4% (w/v) glucose as described[63]. Maximal QS signal molecule concentration determined during bacterial growth is reported in Fig. 4a. Biofilm formation by PAO1 wild type GUN mutant grown in M9-CAA with or without 0.4% (w/v) glucose for overnight (i.e. 16 h) was assessed using the microtiter plate biofilm assay[64]. For microscopic visualization of biofilm, *P. aeruginosa* PAO1 wild type and GUN mutant constitutively expressing GFP *via* the pMRP9–1 plasmid[65] were grown in an 8-well chamber slide, as previously described[66], in M9-CAA in the absence or in the presence of 0.4% (w/v) glucose. Biofilms formation was examined after 3 days incubation by using the Leica TCS SP5 confocal microscope. For QS signal molecules and CV biofilm quantification statistical analyses were performed by using the GraphPad Prism software (San Diego, CA, USA), with a Tuckey test of the One-way ANOVA tool.

***C. elegans* slow killing assay.** 50 worms synchronised at the L4 stage[67,68] (see Supplementary Methods) were individually transferred from a Nematode Growth Medium (NGM) plate (US Biological) onto an NGM plate supplemented with 5-Fluoro-2′-deoxyuridine thymidylate synthase inhibitor (FUDR, Sigma-Aldrich), an inhibitor of DNA synthesis preventing *C. elegans* reproduction, without interfering with nematodes development and ageing[69]. Each plate was seeded with one bacterial strain using a sterilized platinum wire with the aid of a stereomicroscope. As negative control, 50 synchronized worms were transferred to an NGM plus FUDR plate seeded with *E. coli* OP50. Plates were incubated at 20 °C and the number of live nematodes was counted every day over a period of 21 days. A worm was considered dead when it no longer responded to touch. The experiment was repeated at least three times for each strains. The software GraphPad Prism (GraphPad Software, San Diego, CA, USA) was used to plot charts and perform statistical analyses.

***G. mellonella* infection experiments.** *P. aeruginosa* cultures for *G. mellonella* infections were grown to mid-log phase in LD medium, washed, re-suspended to $OD_{600} = 1$ and diluted in physiological solution (0.9% (w/v) NaCl) accordingly to the required inoculum size. *G. mellonella* caterpillars in the final instar larval stage were purchased from the Allevamento Cirà, Como, Italy, and starved 24–48 h before starting the experiments. The larvae were infected by injection in the last proleg of bacterial cells resuspended in 10 µl of physiological solution. Infected and mock-infected (i.e. with sterile physiological solution) larvae were incubated at 37 °C in Petri dishes and survival monitored for 42 h. Larvae were considered dead when they did not respond to gentle prodding. Statistical analyses were carried out using GraphPad Prism (GraphPad Software, San Diego, CA, USA). Survival curves were plotted using the Kaplan-Meier method, and differences in survival were calculated using the log-rank test for multiple comparisons. For measuring the bacterial titre in the hemolymph, larvae infected as described above, were sacrificed after 16 h incubation at 37 °C. The hemolymph was collected by puncturing with a needle cold-anesthetized larvae, diluted in physiological solution and plated on LD-ampicillin. Prophenoloxidase cascade activation in the hemolymph was measured as described[70] on samples collected as described above from larvae infected with 10 µl of physiological solution containing about 2×10^4 CFU or mock-infected. The larvae were sacrificed after 4 h incubation at 37 °C. Hemolymph samples obtained from 5 individuals per condition (15 µl/larva) were mixed and centrifuged at 1500 g for 10 min at 4 °C for removing hemocytes. Immediately after centrifugation, samples were diluted tenfold in TBS (50 mM Tris–HCl pH 6.8, 1 mM NaCl). 2 µl were added to 18 µl of TBS additionated with 5 mM $CaCl_2$ in polystyrene 96-well microplates and incubated 20 min at room temperature. 180 µl of 2 mM dopamine in 50 mM sodium phosphate (pH 6.5) were added. Melanin formation was estimated by measuring absorbance at 490 nm over 45 min at 15-min intervals using an Ensight (PerkinElmer) microplate reader.

Glucose quantification in growth media and *G. mellonella* hemolymph. Glucose concentration in growth media (LD and 2% casamino acids stock solution) and *Galleria mellonella* hemolymph was measured with the Glucose (HK) Assay Kit (Sigma-Aldrich) as detailed in Supplementary Methods.

Data Availability

Raw sequencing data are publicly available at Sequence Reads Archive under accession number PRJNA479815. Bacterial strains and other datasets presented in this study are available from the corresponding author.

References

1. Udaondo, Z., Ramos, J.-L., Segura, A., Krell, T. & Daddaoua, A. Regulation of carbohydrate degradation pathways in *Pseudomonas* involves a versatile set of transcriptional regulators. *Microb. Biotechnol.* **11**, 442–454 (2018).
2. del Castillo, T. *et al*. Convergent peripheral pathways catalyze initial glucose catabolism in *Pseudomonas putida*: genomic and flux analysis. *J. Bacteriol.* **189**, 5142–5152 (2007).
3. Lessie, T. G. & Phibbs, P. V. Alternative pathways of carbohydrate utilization in pseudomonads. *Annu. Rev. Microbiol.* **38**, 359–388 (1984).
4. Adewoye, L. O. & Worobec, E. A. Identification and characterization of the *gltK* gene encoding a membrane-associated glucose transport protein of *Pseudomonas aeruginosa*. *Gene* **253**, 323–330 (2000).
5. Swanson, B. L. *et al*. Characterization of the 2-ketogluconate utilization operon in *Pseudomonas aeruginosa* PAO1. *Mol. Microbiol.* **37**, 561–573 (2000).
6. Whiting, P. H., Midgley, M. & Dawes, E. A. The regulation of transport of glucose, gluconate and 2-oxogluconate and of glucose catabolism in *Pseudomonas aeruginosa*. *Biochem J* **154**, 659–668 (1976).
7. Whiting, P. H., Midgley, M. & Dawes, E. A. The role of glucose limitation in the regulation of the transport of glucose, gluconate and 2-oxogluconate, and of glucose metabolism in *Pseudomonas aeruginosa*. *J. Gen. Microbiol.* **92**, 304–310 (1976).
8. Daddaoua, A., Molina-Santiago, C., de la Torre, J., Krell, T. & Ramos, J.-L. GtrS and GltR form a two-component system: the central role of 2-ketogluconate in the expression of exotoxin A and glucose catabolic enzymes in *Pseudomonas aeruginosa*. *Nucleic Acids Res.* **42**, 7654–7663 (2014).
9. Colmer, J. A. & Hamood, A. N. Characterization of *ptxS*, a *Pseudomonas aeruginosa* gene which interferes with the effect of the exotoxin A positive regulatory gene, *ptxR*. *Mol. Gen. Genet.* **258**, 250–259 (1998).
10. Swanson, B. L., Colmer, J. A. & Hamood, A. N. The *Pseudomonas aeruginosa* exotoxin A regulatory gene, *ptxS*: evidence for negative autoregulation. *J. Bacteriol.* **181**, 4890–4895 (1999).
11. del Castillo, T., Duque, E. & Ramos, J. L. A set of activators and repressors control peripheral glucose pathways in *Pseudomonas putida* to yield a common central intermediate. *J. Bacteriol.* **190**, 2331–2339 (2008).
12. O'Callaghan, J. *et al*. A novel host-responsive sensor mediates virulence and type III secretion during *Pseudomonas aeruginosa*-host cell interactions. *Microbiology* **158**, 1057–1070 (2012).
13. Handfield, M. *et al*. *In vivo*-induced genes in *Pseudomonas aeruginosa*. *Infect. Immun.* **68**, 2359–2362 (2000).
14. Dubern, J.-F. *et al*. Integrated whole-genome screening for *Pseudomonas aeruginosa* virulence genes using multiple disease models reveals that pathogenicity is host specific. *Environ. Microbiol.* **17**, 4379–4393 (2015).
15. Rayfield, E. J. *et al*. Infection and diabetes: The case for glucose control. *The American Journal of Medicine* **72**, 439–450 (1982).
16. Burekovic, A., DizdarevicBostandzic, A. & Godinjak, A. Poorly Regulated Blood Glucose in Diabetic Patients-predictor of Acute Infections. *Med. Arch.* **68**, 163 (2014).
17. Baker, E. H. *et al*. Hyperglycaemia and pulmonary infection. *Proc. Nutr. Soc.* **65**, 227–235 (2006).
18. Geerlings, S. E. & Hoepelman, A. I. Immune dysfunction in patients with diabetes mellitus (DM). *FEMS Immunol. Med. Microbiol.* **26**, 259–265 (1999).
19. Baker, E. H. & Baines, D. L. Airway glucose homeostasis: a new target in the prevention and treatment of pulmonary infection. *Chest*, https://doi.org/10.1016/j.chest.2017.05.031 (2017).
20. Strateva, T. & Mitov, I. Contribution of an arsenal of virulence factors to pathogenesis of *Pseudomonas aeruginosa* infections. *Ann. Microbiol.* **61**, 717–732 (2011).
21. Chevalier, S. *et al*. Structure, function and regulation of *Pseudomonas aeruginosa* porins. *FEMS Microbiology Reviews* **41**, 698–722 (2017).
22. Valentini, M., Storelli, N. & Lapouge, K. Identification of C(4)-dicarboxylate transport systems in *Pseudomonas aeruginosa* PAO1. *J. Bacteriol.* **193**, 4307–4316 (2011).
23. Kawakami, T., Kuroki, M., Ishii, M., Igarashi, Y. & Arai, H. Differential expression of multiple terminal oxidases for aerobic respiration in *Pseudomonas aeruginosa*. *Environ. Microbiol.* **12**, 1399–1412 (2010).
24. Wolloscheck, D., Krishnamoorthy, G., Nguyen, J. & Zgurskaya, H. I. Kinetic Control of Quorum Sensing in *Pseudomonas aeruginosa* by Multidrug Efflux Pumps. *ACS Infect. Dis.* **4**, 185–195 (2018).
25. Passador, L., Cook, J. M., Gambello, M. J., Rust, L. & Iglewski, B. H. Expression of *Pseudomonas aeruginosa* virulence genes requires cell-to-cell communication. *Science* **260**, 1127–1130 (1993).
26. Driscoll, J. A., Brody, S. L. & Kollef, M. H. The epidemiology, pathogenesis and treatment of *Pseudomonas aeruginosa* infections. *Drugs* **67**, 351–368 (2007).
27. Alhede, M., Bjarnsholt, T., Givskov, M. & Alhede, M. *Pseudomonas aeruginosa* biofilms. Mechanisms of immune evasion. *Adv. Appl. Microbiol.* **86**, 1–40 (2014).
28. Schobert, M. & Jahn, D. Anaerobic physiology of *Pseudomonas aeruginosa* in the cystic fibrosis lung. *International Journal of Medical Microbiology* **300**, 549–556 (2010).
29. Glavis-Bloom, J., Muhammed, M. & Mylonakis, E. Of model hosts and man: Using *Caenorhabditis elegans*, *Drosophila melanogaster* and *Galleria mellonella* as model hosts for infectious disease research. *Adv. Exp. Med. Biol.* **710**, 11–17 (2012).
30. Jia, C., Tsai, -Yun Mei, J., Loh, S. & Proft, T. *Galleria mellonella* infection models for the study of bacterial diseases and for antimicrobial drug testing. *Virulence* **7**, 214–229 (2016).
31. Tan, M.-W., Rahme, L. G., Sternberg, J. A., Tompkins, R. G. & Ausubel, F. M. *Pseudomonas aeruginosa* killing of *Caenorhabditis elegans* used to identify *P. aeruginosa* virulence factors. *Proc. Natl. Acad. Sci.* **96**, 2408–2413 (1999).
32. Ramarao, N., Nielsen-Leroux, C. & Lereclus, D. The insect *Galleria mellonella* as a powerful infection model to investigate bacterial pathogenesis. *J. Vis. Exp.* e4392, https://doi.org/10.3791/4392 (2012).
33. Wyatt, G. R., Loughheed, T. C. & Wyatt, S. S. The chemistry of insect hemolymph; organic components of the hemolymph of the silkworm, *Bombyx mori*, and two other species. *J. Gen. Physiol.* **39**, 853–868 (1956).
34. Andrejko, M., Zdybicka-Barabas, A. & Cytryńska, M. Diverse effects of *Galleria mellonella* infection with entomopathogenic and clinical strains of *Pseudomonas aeruginosa*. *J. Invertebr. Pathol.* **115**, 14–25 (2014).
35. Huang, H. & Hancock, R. E. Genetic definition of the substrate selectivity of outer membrane porin protein OprD of *Pseudomonas aeruginosa*. *J. Bacteriol.* **175**, 7793–7800 (1993).
36. Gill, S. K. *et al*. Increased airway glucose increases airway bacterial load in hyperglycaemia. *Sci. Rep.* **6**, 27636 (2016).
37. Klockgether, J. *et al*. Genome diversity of *Pseudomonas aeruginosa* PAO1 laboratory strains. *J. Bacteriol.* **192**, 1113–1121 (2010).
38. Lu, C. D., Yang, Z. & Li, W. Transcriptome analysis of the ArgR regulon in *Pseudomonas aeruginosa*. *J. Bacteriol.* **186**, 3855–3861 (2004).
39. Chavarría, M. *et al*. Fructose 1-phosphate is the one and only physiological effector of the Cra (FruR) regulator of *Pseudomonas putida*. *FEBS Open Bio* **4**, 377–386 (2014).

40. Nishijyo, T., Haas, D. & Itoh, Y. The CbrA-CbrB two-component regulatory system controls the utilization of multiple carbon and nitrogen sources in *Pseudomonas aeruginosa*. *Mol. Microbiol.* **40**, 917–931 (2001).
41. Visca, P., Leoni, L., Wilson, M. J. & Lamont, I. L. Iron transport and regulation, cell signalling and genomics: Lessons from *Escherichia coli* and *Pseudomonas*. *Molecular Microbiology* **45**, 1177–1190 (2002).
42. Sonnleitner, E., Prindl, K. & Bläsi, U. The *Pseudomonas aeruginosa* CrcZ RNA interferes with Hfq-mediated riboregulation. *PLoS One* **12**, e0180887 (2017).
43. Sánchez-Hevia, D. L., Yuste, L., Moreno, R. & Rojo, F. Influence of the Hfq and Crc global regulators on the control of iron homeostasis in *Pseudomonas putida*. *Environ. Microbiol.*, https://doi.org/10.1111/1462-2920.14263 (2018).
44. Venturi, V. Regulation of quorum sensing in *Pseudomonas*. *FEMS Microbiology Reviews* **30**, 274–291 (2006).
45. Lee, J. & Zhang, L. The hierarchy quorum sensing network in *Pseudomonas aeruginosa*. *Protein Cell* **6**, 26–41 (2014).
46. Cornforth, D. M. *et al*. *Pseudomonas aeruginosa* transcriptome during human infection. *Proc. Natl. Acad. Sci. USA* **115**, E5125–E5134 (2018).
47. Duan, K. & Surette, M. G. Environmental regulation of *Pseudomonas aeruginosa* PAO1 Las and Rhl quorum-sensing systems. *J. Bacteriol.* **189**, 4827–4836 (2007).
48. Passos da Silva, D., Schofield, M., Parsek, M. & Tseng, B. An Update on the Sociomicrobiology of Quorum Sensing in Gram-Negative Biofilm Development. *Pathogens* **6**, E51 (2017).
49. Chang, C.-Y. Surface Sensing for Biofilm Formation in *Pseudomonas aeruginosa*. *Front. Microbiol.* **8**, 2671 (2018).
50. Rossi, E., Paroni, M. & Landini, P. Biofilm and motility in response to environmental and host-related signals in Gram negative opportunistic pathogens. *J. Appl. Microbiol.*, https://doi.org/10.1111/jam.14089 (2018).
51. Karinou, E., Hoskisson, P. A., Strecker, A., Unden, G. & Javelle, A. The *E. coli* dicarboxylic acid transporters DauA act as a signal transducer by interacting with the DctA uptake system. *Sci. Rep.* **7**, 16331 (2017).
52. Altincicek, B., Linder, M., Linder, D., Preissner, K. T. & Vilcinskas, A. Microbial metalloproteinases mediate sensing of invading pathogens and activate innate immune responses in the lepidopteran model host *Galleria mellonella*. *Infect. Immun.* **75**, 175–183 (2007).
53. Kaniga, K., Delor, I. & Cornelis, G. R. A wide-host-range suicide vector for improving reverse genetics in Gram-negative bacteria: inactivation of the *blaA* gene of *Yersinia enterocolitica*. *Gene* **109**, 137–141 (1991).
54. Kohler, T., Curty, L. K., Barja, F., Van Delden, C. & Pechere, J. C. Swarming of *Pseudomonas aeruginosa* is dependent on cell-to-cell signaling and requires flagella and pili. *J. Bacteriol.* **182**, 5990–5996 (2000).
55. Raneri, M., Sciandrone, B. & Briani, F. A whole-cell assay for specific inhibitors of translation initiation in bacteria. *J. Biomol. Screen.* **20**, 627–633 (2015).
56. Dehò, G., Zangrossi, S., Sabbattini, P., Sironi, G. & Ghisotti, D. Bacteriophage P4 immunity controlled by small RNAs via transcription termination. *Mol. Microbiol.* **6**, 3415–3425 (1992).
57. Langmead, B. & Salzberg, S. L. Fast gapped-read alignment with Bowtie 2. *Nat. Methods* **9**, 357–359 (2012).
58. R Development Core Team. R: A language and environment for statistical computing. R Foundation for Statistical Computing, Vienna, Austria. ISBN 3-900051-07-0, http://www.R-project.org/. *R Found. Stat. Comput. Vienna, Austria.* (2012).
59. Love, M. I., Anders, S. & Huber, W. *Differential analysis of count data - the DESeq. 2 package. Genome Biology* **15** (2014).
60. Price-Whelan, A., Dietrich, L. E. P. & Newman, D. K. Pyocyanin alters redox homeostasis and carbon flux through central metabolic pathways in *Pseudomonas aeruginosa* PA14. *J. Bacteriol.* **189**, 6372–6381 (2007).
61. Essar, D. W., Eberly, L., Hadero, A. & Crawford, I. P. Identification and characterization of genes for a second anthranilate synthase in *Pseudomonas aeruginosa*: interchangeability of the two anthranilate synthases and evolutionary implications. *J. Bacteriol.* **172**, 884–900 (1990).
62. Imperi, F., Tiburzi, F. & Visca, P. Molecular basis of pyoverdine siderophore recycling in *Pseudomonas aeruginosa*. *Proc. Natl. Acad. Sci.* **106**, 20440–20445 (2009).
63. Imperi, F. *et al.* New life for an old Drug: The anthelmintic drug niclosamide inhibits *Pseudomonas aeruginosa* quorum sensing. *Antimicrob. Agents Chemother.* **57**, 996–1005 (2013).
64. Merritt, J. H., Kadouri, D. E. & O'Toole, G. A. Growing and analyzing static biofilms. *Curr. Protoc. Microbiol.* https://doi.org/10.1002/9780471729259.mc01b01s22 (2011).
65. Davies, D. G. *et al*. The involvement of cell-to-cell signals in the development of a bacterial biofilm. *Science.* **280**, 295–298 (1998).
66. Jurcisek, J. A., Dickson, A. C., Bruggeman, M. E. & Bakaletz, L. O. *In vitro* Biofilm Formation in an 8-well Chamber Slide. *J. Vis. Exp.* https://doi.org/10.3791/2481 (2011).
67. Stiernagle, T. Maintenance of *C. elegans*. *WormBook* 1–11 https://doi.org/10.1895/wormbook.1.101.1 (2006).
68. Porta-de-la-Riva, M., Fontrodona, L., Villanueva, A. & Cerón, J. Basic *Caenorhabditis elegans*methods: synchronization and observation. *J. Vis. Exp.* e4019 https://doi.org/10.3791/4019 (2012).
69. Mitchell, D. H., Stiles, J. W., Santelli, J. & Rao Sanadi, D. Synchronous growth and aging of *Caenorhabditis elegans* in the presence of fluorodeoxyuridine. *Journals Gerontol.* **34**, 28–36 (1979).
70. Andrejko, M., Zdybicka-Barabas, A., Wawrzoszek, M. & Cytryńska, M. Diverse susceptibility of *Galleria mellonella* humoral immune response factors to the exoproteinase activity of entomopathogenic and clinical strains of *Pseudomonas aeruginosa*. *Zoolog. Sci.* **30**, 345–351 (2013).

Acknowledgements

We thank Karl Perron (University of Geneva) for helpful discussions. This work was supported by grants from Università degli Studi di Milano, Piano di Sviluppo di Ateneo 2015–2016 and 2016–2017 to FB. The Grant of Excellence Departments, MIUR-Italy is also acknowledged. MR was a recipient of a PhD fellowship of the Università degli Studi di Milano (UNIMI), PhD program in Molecular and Cell Biology.

Author Contributions

F.B. conceived the project and wrote the paper, M.R., E.P., C.P., G.R., L.L., I.B., O.J. and F.B. designed the experiments and analysed the results, M.R., E.P., C.P., G.R., I.B., C.D. and P.F. performed the experiments. All authors revised the manuscript.

Additional Information

Supplementary information accompanies this paper at https://doi.org/10.1038/s41598-018-35087-y.

Competing Interests: The authors declare no competing interests.

Publisher's note: Springer Nature remains neutral with regard to jurisdictional claims in published maps and institutional affiliations.

Matteo Raneri[1], Eva Pinatel[2], Clelia Peano[2,5], Giordano Rampioni[3], Livia Leoni[3], Irene Bianconi[4], Olivier Jousson[4], Chiara Dalmasio[1], Palma Ferrante[1] and Federica Briani[1,*]

Pseudomonas aeruginosa mutants defective in glucose uptake have pleiotropic phenotype and altered virulence in non-mammal infection models

[1]Dipartimento di Bioscienze, Università degli Studi di Milano, Italy

[2]Istituto di Tecnologie Biomediche-CNR, Segrate, Italy

[3]Dipartimento di Scienze, Università degli Studi Roma Tre, Italy

[4]Centre for Integrative Biology, Università degli Studi di Trento, Italy

This file contains (in the stated order):

SUPPLEMENTARY RESULTS

***glt, gntP* and *kguT* deletions have not polar effect on the transcription of downstream genes**

We analysed the transcription profile in the GUN mutant of *oprB, gapN* and *kguD* genes, which are located downstream of *gltK*, *gntP* and *kguT*, respectively, to verify whether the Δ*glt,* Δ*gntP* and Δ*kguT* deletions may have polar effect. We observed that the transcription pattern of *gapN* and *oprB* was very similar in the GUN mutant and in the wild type PAO1 (regardless of the presence of glucose; Supplementary Fig. S6). However, the analysis of transcription profile did not allow to draw any conclusion about the expression of *kguD*, the gene downstream of *kguT*, because the *kgu* operon was poorly transcribed in the tested strains. We thus expressed *in trans* the *kguT* gene in the Δ*kguT* mutant *via* an arabinose-inducible expression vector, and tested the ability of this strain to growth on 2-KG as sole carbon source. As shown in Supplementary Figure S6, plasmid-driven expression of *kguT* restored growth to wild type levels in the Δ*kguT* mutant in this medium. Since the *kguT* downstream gene *kguD* should be required for *P. aeruginosa* growth on 2-KG[1], this result suggests that the Δ*kguT* mutation has no polar effect on the expression of *kguD*.

SUPPLEMENTARY METHODS

Bacterial strains and plasmid construction

PAO1 deletion mutants of glucose uptake genes were constructed by gene replacement[2]. 500 bp long amplicons corresponding to the regions flanking the section to be deleted were obtained by PCR with proper oligonucleotides (i.e. *oprB*, 3287-3288 and 3289-3290; PA2291, 3291-3292 and 3304-3294; *kguT*, 3338-3339 and 3340-3341; *gntP*, 3343-3344 and 3345-3346; *gltKGF*, 3287-3367 and 3368-3369; Supplementary Table S1) and fused by overlapping PCR into a unique 1kb-long fragment, which was cloned into the BamHI-SpeI restriction sites of the suicide vector pKNG101. The recombinant plasmids (Supplementary Table S1) were constructed in *E. coli* CC118λpir and mobilized into *P. aeruginosa* by triparental conjugation[3]. Clones bearing the plasmids integrated into the chromosome were selected on streptomycin plates. The deletion mutants were selected on LD plates containing 10% sucrose as previously described[2]. Gene deletion was confirmed by PCR with proper oligonucleotides.

pGM2071 plasmid was constructed as follows. A PCR product covering the 2490689-2492060 region (i.e. the *kguT* open reading frame with the 50 bp upstream) was amplified using oligonucleotides 3401 and 3402. The product was digested with KpnI and ligated into pGM931

downstream of the *araBp* promoter, obtaining pGM2071. The plasmid was constructed in *E. coli* DH10B and transferred into PAMO108 (namely PAO1 Δ*kguT*) by transformation.

PAO1 genome annotation and RNA-Seq data analysis

To obtain a comprehensive annotation of PAO1 genome, we merged the annotations provided by the *Pseudomonas* Genome Database www.Pseudomonas.com[4] and RefSeq in the versions available on Dec 2017. The *Pseudomonas* Genome Database was selected as main reference and records present only in RefSeq annotation were manually integrated. Few genes showed the same Locus_Tag but different start and/or end among the two annotations; in such case, we choose to consider the largest gene unless if it included other annotated features. To functionally annotate the genome, we integrated KEGG and pseudoCAP information in the version provided by the *Pseudomonas* Genome Database and we merged the corresponding functional categories showing slightly different names among the two (see Supplementary Table S2).

BEDTools (v2.24.0)[5] and SAMtools (v0.1.19)[6] were adopted to verify library preparation and sequencing performances (see sequencing statistics sheet in Supplementary Table S2). A minimum of 2.8 M of reads was produced for each sample and biological replica and, on average, more than 90% of the reads resulted of high quality. Less than 1% of the mapped reads mapped on ribosomal RNAs; reads strand specificity, calculated on annotated CDS, was higher than 90% in every sample and the CDS coverage was enough for the gene expression analysis (i.e. 90% of the genes were covered by a minimum of 4 strand specific reads). To avoid double counting of reads mapping across two genes, only strand specific reads covering a CDS for at least 50% of their length were considered for gene read counts.

RT-qPCR mRNA analysis

The RNA was reverse-transcribed with the Takara PrimeScript™ RT kit (Perfect Real Time) and cDNA was used for Real-Time PCR with SYBR® Premix Ex Taq™ (Takara) and primers specific for each gene (3478-3479, *lasR*; 3480-3481, *ptxS*; 3482-3483, PA2264; 3492-3493, *fruI*; 3494-3495, *lasB*; 3511-3512, *coxB*; 3513-3514, *napA*; 3522-3523, *aruC*; 3524-3525, *hutU*; 3526-3527, PA5348; see Supplementary Table S1). 16S rRNA was used as reference gene (primers 3398-3399) to normalize Real Time PCR results and to calculate the relative fold change in gene expression with the $2^{-\Delta\Delta Ct}$ method[7].

NAD(H) quantification

Cells were harvested by centrifugation from 40 ml cultures of PAO1 and GUN strains grown as for the RNASeq. Cells were resuspended in 1 ml of cold physiological solution, split in two 1.5 ml tubes and immediately centrifuged at 16000xg for 1 min. 100 µl of either 0.2 M NAOH (for NAD^+ extraction) or 0.2 M HCl (for NADH extraction) were added to the cell pellets. Samples were incubated 10 min at 50 °C and then on ice for 10 min. 100 µl of either 0.1 M HCl (for NAD^+ extraction) or 0.1 M NaOH (for NADH extraction) were added dropwise while agitating the samples, which were then centrifuged 10 min at 16000xg. The supernatants containing NAD dinucleotide were transferred to fresh tubes. NADH and NAD^+ were immediately quantified by a cyclic assay as previously described[8]. 90-µl aliquots of a mix prepared with 1 vol of Bicine buffer (2.0 M, pH 8.0), 8 vol water, 1 vol 80 mM EDTA, 2 vol 100% ethanol, 2 vol 4.2 mM thiazolyl blue and 4 vol 16.6 mM phenazine ethosulfate were dispensed into the wells of a 96-well microtiter plate. Five microliters of either NAD^+ (Sigma) and NADH (Sigma) standard solutions or sample were added to each well and the reaction was started by the addition of 5 µl of alcohol dehydrogenase (Sigma) at 347 units/ml in 0.1 M Bicine (pH 8.0). Absorbance at 570 nm was read every 60 seconds by means an Ensight (PerkinElmer) microplate reader. Slopes of the absorbance curves over time of NADH and NAD^+ solutions were used to generate standard curves, which were used to calculate NAD concentrations (in µM) in the samples. Values were normalized for the optical density of the original cell culture sample and for NAD concentration in reference condition (i.e. PAO1 without glucose).

Secretion of pyocyanin, pyoverdine, proteases and rhamnolipids

Bacterial cultures for pyocyanin and pyoverdine extraction were grown at 37°C for 24 h in LD. Pyocyanin was extracted from the supernatant with chloroform and HCl as described[9]. The relative concentration of pyocyanin was determined as the ratio between the A_{520} of the resulting solution and the OD_{600} of the culture. Relative pyoverdine concentration[10] was determined as the ratio between the A_{405} of the culture supernatant mixed with an equal volume of 200 mM Tris-HCl (pH 8) and the OD_{600} of the culture. Extracellular proteases were tested by spotting onto casein-agar plates (1% agar supplemented with 1% casein and 150 µg/ml carbenicillin, to prevent cell growth) 2 µl of supernatants of cultures grown as described in Supplementary Fig. S4 legend and properly diluted to the same OD_{600} before cells removal by centrifugation and plating. For detection of rhamnolipids[11], overnight cultures in LD were washed in 1x PBS and resuspended in the same solution at OD_{600}= 4. 5 µl were spotted onto 1.6% M8-BactoAgar (Difco) medium supplemented with 2 mM $MgSO_4$, 0.05% (w/v) glutamic acid, 2% (v/v) glycerol, 0.5% (w/v) succinate, 0.02%

(w/v) cetyltrimethylammonium bromide (CTAB), and 0.0005% (w/v) methylene blue. Plates were incubated at 37°C for 24 h, then at room temperature for 4 days, and finally at 4°C for 24 h. The dark blue halo surrounding the cell spot due to the precipitation of CTAB and methylene blue was measured as an indication of rhamnolipid secretion.

Growth in anaerobiosis and microaerophilic conditions

A single colony was resuspended in 100 µl of 1x PBS in 96-well polystyrene microplates. Serial ten-fold dilutions were replicated on plates of LD/Agar supplemented with 100 mM KNO_3. The plates were incubated at 37°C for 16 h in aerobic conditions or for 48 h inside an anaerobic jar AnaeroJar (Oxoid) containing an AnaeroGen sachet (Oxoid). For microaerophilic growth, bacterial cultures were inoculated at OD_{600}= 0.1 in 100 µl of LD or M9-CAA in 96-well polystyrene microplates and overlaid with 50 µl of paraffin oil to prevent evaporation. The microplates were incubated static for 16 h at 37°C and the OD_{600} was measured by means of an Ensight (PerkinElmer) microplate reader.

Quantification of QS signal molecules

Levels of QS signal molecules in *P. aeruginosa* PAO1 wild type and GUN mutant culture supernatants were determined at different times during bacterial growth as previously described[12]. Briefly, the strains were grown at 37°C in shaking (200 rpm) in M9-CAA in the absence or in the presence of 0.4 % (w/v) glucose. Ten-µl of culture supernatants (or appropriate dilutions) were added to 190 µl of LB inoculated with reporter strains specific for $3OC_{12}$-HSL[13], or C_4-HSL[14] to a final OD_{600} of 0.045 in black clear-bottom 96-well microtiter plates. Microtiter plates were incubated at 37°C with gentle shaking, and the OD_{600} and relative light units (RLU) were measured after 4 h of growth for the $3OC_{12}$-HSL biosensor or 7 h of growth for the C_4-HSL biosensor. Dedicated calibration curves were generated by growing each reporter strain in the presence of increasing concentrations of the corresponding synthetic signal molecule, and these curves were used to calculate the concentration of the different QS signal molecules in each culture supernatant. Maximal QS signal molecule concentration determined during bacterial growth is reported in Fig. 4a.

Biofilm formation

Biofilm formation was assessed using the microtiter plate biofilm assay[15]. Briefly, *P. aeruginosa* PAO1 wild type an GUN mutant were grown in M9-CAA at 37°C in shaking (200 rpm) in M9-CAA in the absence or in the presence of 0.4 % (w/v) glucose for overnight (i.e. 16 h). Overnight

cultures were diluted to an OD_{600} of 0.05 in the corresponding medium, and 100 µl aliquots were transferred to a sterile 96-well polystyrene microtiter plate (6 wells per sample) and incubated at 30°C for 8 h. Planktonic cells were transferred to a sterile microtiter plate for OD_{600} measurements in a TECAN Spark 10M multilabel plate reader, while the attached cells were stained with 1% (w/v) crystal violet. After washing the wells five times with distilled water, the surface-associated dye was solubilized with 200 µl of ethanol. The A_{595} of the dye solution was measured in a TECAN Spark 10M multilabel plate reader. Adhesion units were determined as A_{595} normalized to OD_{600}.

For microscopic visualization of biofilm, *P. aeruginosa* PAO1 wild type and GUN mutant constitutively expressing GFP *via* the pMRP9-1 plasmid[16] were grown in an 8-well chamber slide, as previously described[17], with minor modifications. Briefly, bacterial cells were inoculated at an OD_{600} of 0.02 in 700 µL of M9-CAA in the absence or in the presence of 0.4 % (w/v) glucose. Cultures were incubated at 30°C for 24 h to allow the adhesion of the bacterial cells on the glass surface. To maintain bacterial viability, the medium was changed every 24 h. Biofilms formation was examined after 3 days incubation by using the Leica TCS SP5 confocal microscope. Ten random fields were examined for each sample, and representative images are reported in Fig. 4c.

Synchronization of *C. elegans*

The bleaching technique was used to synchronise *C. elegans* at the first larval stage (L1)[18], with minor modifications. Adult worms are sensitive to bleach (5% solution of sodium hypochlorite, NaClO) and die quickly, while the embryos are protected by the eggshell. *C. elegans* NGM plates were washed twice with 7 ml of M9 medium (Sigma-Aldrich). The supernatant containing the worms was transfer in a centrifuge tube and the worms pelleted for 1 min centrifugation at 1500xg. Worms' pellet was washed with until the liquid was clear. 3.5 ml of M9, 500 µl of 5 M NaOH and 1 ml of bleach were then added to the pellet. To not damage embryos, bleach-induced death was observed by using a stereomicroscope to verify the dissolution of adult worms that typically occurs within 4 minutes. Bleach was inactivated by adding M9 to a final volume of 15 ml, and the tubes centrifuged 2 minutes at 1500xg. Eggs' pellet was then washed five times with 15 ml of M9. 6 ml of M9 were then added and the tubes were placed in a dark environment at room temperature and slow agitation for two days. Synchronized worms were then gently transferred to NGM plates seeded with *E. coli* OP50 and maintained at 20° C for two days.

Glucose quantification in growth media and *G. mellonella* hemolymph

Glucose concentration in growth media (LD and 2% casamino acids stock solution) and *Galleria mellonella* hemolymph was measured with the Glucose (HK) Assay Kit (Sigma-Aldrich) following

the recommendations of the provider. Hemolymph samples obtained from 5 larvae (30 µl/larva) were mixed and centrifuged at 1500xg for 10 min at 4°C for hemocytes removal. 40 µl samples were combined with 200 µl of either Glucose Assay Reagent or 50mM Tris-HCl pH 7.5 (blank samples) and incubated 15 min at room temperature before reading the absorbance at 340 nm by means of an Ensight (PerkinElmer) microplate reader. Glucose concentration was determined by comparison with a glucose standard curve obtained by testing known dilutions of Glucose Standard Solution (Sigma-Aldrich).

SUPPLEMENTARY REFERENCES

1. del Castillo, T. *et al.* Convergent peripheral pathways catalyze initial glucose catabolism in *Pseudomonas putida*: genomic and flux analysis. *J. Bacteriol.* **189,** 5142–52 (2007).
2. Kaniga, K., Delor, I. & Cornelis, G. R. A wide-host-range suicide vector for improving reverse genetics in Gram-negative bacteria: inactivation of the *blaA* gene of *Yersinia enterocolitica*. *Gene* **109,** 137–141 (1991).
3. Goldberg, J. B. & Ohman, D. E. Cloning and expression in *Pseudomonas aeruginosa* of a gene involved in the production of alginate. *J. Bacteriol.* **158,** 1115–1121 (1984).
4. Winsor, G. L. *et al.* Enhanced annotations and features for comparing thousands of *Pseudomonas* genomes in the *Pseudomonas* genome database. *Nucleic Acids Res.* **44,** D646–D653 (2016).
5. Quinlan, A. R. & Hall, I. M. BEDTools: A flexible suite of utilities for comparing genomic features. *Bioinformatics* **26,** 841–842 (2010).
6. Li, H. *et al.* The Sequence Alignment/Map format and SAMtools. *Bioinformatics* **25,** 2078–2079 (2009).
7. Livak, K. J. & Schmittgen, T. D. Analysis of relative gene expression data using real-time quantitative PCR and the $2^{-\Delta\Delta C}{}_T$ Method. *Methods* **25,** 402–408 (2001).
8. Price-Whelan, A., Dietrich, L. E. P. & Newman, D. K. Pyocyanin alters redox homeostasis and carbon flux through central metabolic pathways in *Pseudomonas aeruginosa* PA14. *J. Bacteriol.* **189,** 6372–6381 (2007).
9. Essar, D. W., Eberly, L., Hadero, A. & Crawford, I. P. Identification and characterization of genes for a second anthranilate synthase in *Pseudomonas aeruginosa*: interchangeability of the two anthranilate synthases and evolutionary implications. *J. Bacteriol.* **172,** 884–900 (1990).
10. Imperi, F., Tiburzi, F. & Visca, P. Molecular basis of pyoverdine siderophore recycling in *Pseudomonas aeruginosa*. *Proc. Natl. Acad. Sci.* **106,** 20440–20445 (2009).
11. Kohler, T., Curty, L. K., Barja, F., Van Delden, C. & Pechere, J. C. Swarming of *Pseudomonas aeruginosa* is dependent on cell-to-cell signaling and requires flagella and pili. *J. Bacteriol.* **182,** 5990–5996 (2000).
12. Imperi, F. *et al.* New life for an old Drug: The anthelmintic drug niclosamide inhibits *Pseudomonas aeruginosa* quorum sensing. *Antimicrob. Agents Chemother.* **57,** 996–1005 (2013).
13. Massai, F. *et al.* A multitask biosensor for micro-volumetric detection of N-3-oxo-dodecanoyl-homoserine lactone quorum sensing signal. *Biosens. Bioelectron.* **26,** 3444–3449 (2011).
14. Duan, K. & Surette, M. G. Environmental regulation of *Pseudomonas aeruginosa* PAO1 Las and Rhl quorum-sensing systems. *J. Bacteriol.* **189,** 4827–4836 (2007).

15. Merritt, J. H., Kadouri, D. E. & O'Toole, G. A. Growing and analyzing static biofilms. *Curr. Protoc. Microbiol.* (2011). doi:10.1002/9780471729259.mc01b01s22
16. Davies, D. G. *et al.* The involvement of cell-to-cell signals in the development of a bacterial biofilm. *Science (80-.).* **280,** 295–298 (1998).
17. Jurcisek, J. A., Dickson, A. C., Bruggeman, M. E. & Bakaletz, L. O. *In vitro* Biofilm Formation in an 8-well Chamber Slide. *J. Vis. Exp.* (2011). doi:10.3791/2481
18. Porta-de-la-Riva, M., Fontrodona, L., Villanueva, A. & Cerón, J. Basic *Caenorhabditis elegans* methods: synchronization and observation. *J. Vis. Exp.* e4019 (2012). doi:10.3791/4019
19. Holloway, B. W. Genetic Recombination in *Pseudomonas aeruginosa*. *J Gen Microbiol* (1955). doi:10.1099/00221287-13-3-572
20. Herrero, M., De Lorenzo, V. & Timmis, K. N. Transposon vectors containing non-antibiotic resistance selection markers for cloning and stable chromosomal insertion of foreign genes in gram-negative bacteria. *J. Bacteriol.* **172,** 6557–6567 (1990).
21. Grant, S. G. N., Jessee, J., Bloom, F. R. & Hanahan, D. Differential plasmid rescue from transgenic mouse DNAs into *Escherichia coli* methylation-restriction mutants. *Proc. Natl. Acad. Sci. U. S. A.* **87,** 4645–4649 (1990).
22. Boyer, H. W. & Roulland-dussoix, D. A complementation analysis of the restriction and modification of DNA in *Escherichia coli*. *J. Mol. Biol.* **41,** 459–472 (1969).
23. Figurski, D. H., Meyer, R. J. & Helinski, D. R. Suppression of colE1 replication properties by the Inc P-1 plasmid RK2 in hybrid plasmids constructed *in vitro*. *J. Mol. Biol.* **133,** 295–318 (1979).
24. Delvillani, F. *et al.* Tet-Trap, a genetic approach to the identification of bacterial RNA thermometers: application to *Pseudomonas aeruginosa*. *RNA* **20,** 1963–1976 (2014).
25. Lu, C. D., Yang, Z. & Li, W. Transcriptome analysis of the ArgR regulon in *Pseudomonas aeruginosa*. *J. Bacteriol.* **186,** 3855–3861 (2004).
26. Udaondo, Z., Ramos, J.-L., Segura, A., Krell, T. & Daddaoua, A. Regulation of carbohydrate degradation pathways in *Pseudomonas* involves a versatile set of transcriptional regulators. *Microb. Biotechnol.* **11,** 442–454 (2018).
27. Chavarría, M. *et al.* Fructose 1-phosphate is the one and only physiological effector of the Cra (FruR) regulator of *Pseudomonas putida*. *FEBS Open Bio* **4,** 377–386 (2014).
28. Ochsner, U. A., Johnson, Z. & Vasil, M. L. Genetics and regulation of two distinct haem-uptake systems, *phu* and *has*, in *Pseudomonas aeruginosa*. *Microbiology* **146,** 185–198 (2000).

Supplementary Table S1. Bacterial strains, oligonucleotides and plasmids

Bacteria

Strain	Mutation	Deletion[a]	Reference
P. aeruginosa			
PAO1	na	none	19
PAMO104	Δ*oprB*	Δ1 (3575912-3577276)	this work
PAMO105	ΔPA2291	Δ2 (2521224-2522643)	this work
PAMO106	Δ*oprB* ΔPA2291	Δ1 and Δ2	this work
PAMO107	Δ*gntP*	Δ3 (2560762-2562114)	this work
PAMO108	Δ*kguT*	Δ4 (2490738-2492045)	this work
PAMO109	Δ*gntP* Δ*kguT*	Δ3 and Δ4	this work
PAMO110	Δ*gltKGF* Δ*gntP* Δ*kguT*	Δ3, Δ4 and Δ5	this work
PAMO111	Δ*gltKGF*	Δ5 (3577778-3580283)	this work
E. coli			
CC118λpir			20
DH10B			21
HB101			22

Oligonucleotides

Name	5'→3' Sequence[b]	Coordinates[a]
3287	GGGGGATCCTCATCGGTTCGCCGCCGA	3577777 - 3577760
3288	TTCCAGCGTCCTCGTGGTTG	3577277 - 3577296
3289	CACGAGGACGCTGGAATCGTCGCGTTGCCTGCTC	3577292 - 3577277
		3575911 - 3575894
3290	GGGACTAGTGCGGCCATTCGCTGCCG	3575412 - 3575428
3291	GGGGGATCCGCAATGCCGGGCGCAGC	2523117 - 2523101

3292	GCGAACGCTTCCTCGTTGC	2522617 - 2522635
3294	GGGACTAGTGTCGGCCAGCAGCGGGC	2520757 - 2520773
3304	GATCCAGACGGTGTTCTAGGC	2521276 - 2521256
3316	CGGGGTCGACGAGGTCGACAACGCG	2521318 - 2521294
3317	CTGGTGGCGGGGATCAAGATCCAGACGGTG	2521293 - 2521264
3338	GGGGGATCCCATGATCGCCGAGATCAACGC	2490261 - 2490281
3339	GGTCGGGTATCTCCTGAGC	2490737 - 2490719
3340	GCTCAGGAGATACCCGACCCCGACTCCGGAGCATCCG	2490719 - 2490737
		2492046 - 2492063
3341	GGGACTAGTCCCATGCCGACGATACCGAG	2492521 -2492502
3342	CAACCCGCACGCCGACAAGCGCG	2491967 - 2491989
3343	GGGGGATCCACATCCGCAAGATGAGCGCC	2560274 - 2560293
3344	GGAGGGCTCTCCTTTTGTCG	2560761 - 2560742
3345	CGACAAAAGGAGAGCCCTCCGCACCAGCCCGACCGGA	2560742 - 2560761
		2562115 - 2562131
3346	GGGACTAGTCGAGGAATACCGGGCTGCGT	2562609 - 2562590
3347	GACCGCGATGGAGACCATCCTCTCCG	2562045 - 2562070
3354	TCGCTGTGGCCCAGCGAGCGCCG	2490238 - 2490260
3355	CGGGCCAGGGCCTCGCCGATGC	2492524 - 2492545
3367	GGGACTAGTTGGTCTAGGCAGTACGAAAGGAT	3577297 - 3577319
3368	TCGGCGGCGAACCGATGAGCGTTTTCTCGCGTGCGAAG	3577760 - 3577777
		3580284 - 3580303
3369	GGGGTCGACAGCAACGCGGAGAACCGCAA	3580722 - 3580703
3370	ACTCGCTGGTGATGTTCAAGCT	3580745 - 3580724
3371	TATTCCGAACTGCGAGGCAAGC	3579383 - 3579362
3372	TTGTGCAGGTTGCGCAGTTCG	3578449 - 3578469
3401	GGGGGTACCATGCTCCGGAGTCGGTCAG	2492060 - 2492042
3402	GGGGGTACCGCGGCACCTGTTGCGACAA	2490689 - 2490707

3478	AGCACGAGTTCTTCGAGGAAG	1558463 - 1558483
3479	GTTTTCCGCTTCCACGCTGA	1558578 - 1558559
3480	AACACGGCTACAGCCTGGTG	2488148 - 2488167
3481	ACGATCAGTCCTTCGACGTTGTA	2488250 - 2488228
3482	CATCGACCGACAGATGGAAAC	2493478 - 2493498
3483	GTGGCACCAGCTTCAACTGAT	2493590 - 2493570
3492	ACCGAACAGTTGCAGCAGGC	3992539 - 3992520
3493	AGGTTGGCGCAGACTTCCAC	3992412 - 3992431
3494	AAGACCGGCGAAGTGCTCGA	4169934 - 4169915
3495	TAGTCGCTACCGTAGGTGTACTT	4169831 - 4169853
3511	GAGAGCACCACGGTGGAAAT	127618 - 127637
3512	GGAAGTGTCGTAGATGTGGATC	127722 - 127701
3513	ACATCAAGGCCGAGGTCAAC	1275599 - 1275580
3514	AACTTGCCGTCCTTCATGCG	1275482 - 1275501
3522	AACTGATCGATTTCGCCGGC	978037 - 978056
3523	GACGTTGGAAACGTGCCAGAT	978149 - 978129
3524	GCATGCTGATGAACAACCTCG	5744659 - 5744639
3525	TGTCGTAGCACTCCCAGTTG	5744555 - 5744574
3526	AAGGCCGATCTCACCAAGGAA	6017386 - 6017366
3527	GTTGCAGGAAGGTGCCGAAA	6017266 - 6017285

Plasmids

Name	**Relevant characteristics**[c]	**Reference**
pRK2013	ColE1 *ori tra*$^{+}$ *mob*$^{+}$ Km^{r}	23
pKNG101	Suicide vector in *P. aeruginosa sacB* Sm^{r}	2
pGM931	pHERD20T derivative carrying *araBp*-tΩ region	24
pGM2050	pKNG101 derivative, carries *oprB* US (3577277-3577777) and DS (3575412-3575911) fragments	this work

pGM2051	pKNG101 derivative, carries PA2291 US (2522617- - 2523117) and DS (2520757-2521257) fragments	this work
pGM2059	pKNG101 derivative, carries *gntP* US (2560274-2560761) and DS (2562115-2562609) fragments	this work
pGM2060	pKNG101 derivative, carries *kguT* US (2490261-2490737) and DS (2492046-2492545) fragments	this work
pGM2066	pKNG101 derivative, carries *gltF* US (3580284-3580722) and *gltK* (3577297-3577777) fragments	this work
pGM2071	pGM931 derivative, carries *kguT* (2490689-2492060) under *araBp* control	this work
pMRP9-1		16

[a]Coordinates refer to *P. aeruginosa* PAO1 NCBI Reference Sequence: NC_002516.2.
[b]Underlined characters, restriction sites.
[c]US, upstream; DS, downstream

Supplementary Table S2. List of differentially expressed genes and general statistics

Locus[2]	Log2 Fold Change[1]			Name	Description
	GUN+ *vs.* PAO1+	GUN+ *vs.* PAO1	PAO1+ *vs.* PAO1		
PA0009	-0,94	**-1,05**	-0,11	glyQ	glycyl-tRNA synthetase alpha chain
PA0039	**1,17**	**1,39**	0,22	NA	hypothetical protein
PA0045	**-1,62**	**-1,93**	-0,31	NA	hypothetical protein
PA0046	**-1,97**	**-2,00**	-0,04	NA	hypothetical protein
PA0047	-1,20	**-1,29**	-0,09	NA	hypothetical protein
PA0049	**-3,54**	**-4,25**	-0,71	NA	hypothetical protein
PA0052	**1,67**	0,95	-0,72	NA	hypothetical protein
PA0059	**1,37**	**1,93**	0,56	osmC	osmotically inducible protein OsmC
PA0082	-0,73	**-1,38**	-0,65	tssA1	TssA1
PA0083	-0,75	**-1,28**	-0,53	tssB1	TssB1
PA0084	-0,79	**-1,22**	-0,42	tssC1	TssC1
PA0090	-0,76	**-1,19**	-0,43	clpV1	ClpV1
PA0105	**3,03**	**2,69**	-0,33	coxB	cytochrome c oxidase, subunit II
PA0106	**3,06**	**2,94**	-0,12	coxA	cytochrome c oxidase, subunit I
PA0107	**2,40**	**2,60**	0,19	NA	conserved hypothetical protein
PA0108	**2,38**	**2,19**	-0,19	coIII	cytochrome c oxidase, subunit III
PA0110	**2,85**	**2,11**	-0,75	NA	hypothetical protein
PA0111	**2,44**	**1,97**	-0,47	NA	hypothetical protein
PA0112	**1,91**	**1,48**	-0,43	NA	hypothetical protein
PA0113	**2,14**	**1,36**	-0,78	NA	probable cytochrome c oxidase assembly factor
PA0122	**2,61**	**1,91**	-0,70	rahU	rahU
PA0128	**-1,21**	**-1,27**	-0,06	phnA	conserved hypothetical protein
PA0141	**-2,05**	**-1,50**	0,55	NA	conserved hypothetical protein
PA0176	**1,64**	**1,55**	-0,09	aer2	aerotaxis transducer Aer2
PA0177	**1,57**	**1,50**	-0,07	NA	probable purine-binding chemotaxis protein
PA0178	**1,81**	**1,26**	-0,55	NA	probable two-component sensor
PA0179	**1,44**	**1,10**	-0,34	NA	probable two-component response regulator
PA0180	**1,30**	1,02	-0,27	cttP	chemotactic transducer for trichloroethylene [positive chemotaxis], CttP
PA0208	**3,19**	**2,22**	-0,97	mdcA	malonate decarboxylase alpha subunit
PA0209	**2,63**	**2,39**	-0,24	mdcB	conserved hypothetical protein
PA0210	**1,67**	1,63	-0,04	mdcC	malonate decarboxylase delta subunit
PA0211	**1,99**	**1,88**	-0,11	mdcD	malonate decarboxylase beta subunit
PA0212	**2,05**	**1,74**	-0,31	mdcE	malonate decarboxylase gamma subunit
PA0213	**1,95**	**1,50**	-0,44	mdcG	hypothetical protein

PA0214	**2,55**	**2,03**	-0,52	mdcH	probable acyl transferase
PA0215	**1,60**	**1,59**	0,00	madL	malonate transporter MadL
PA0216	**1,58**	1,07	-0,51	madM	malonate transporter MadM
PA0256	**1,03**	0,80	-0,23	NA	hypothetical protein
PA0277	**-1,37**	**-1,52**	-0,15	NA	conserved hypothetical protein
PA0285	-0,76	**-1,07**	-0,31	NA	conserved hypothetical protein
PA0316	**-1,08**	-0,84	0,24	serA	D-3-phosphoglycerate dehydrogenase
PA0329	**1,17**	**1,67**	0,50	NA	conserved hypothetical protein
PA0355	**2,02**	**2,43**	0,41	pfpI	protease PfpI
PA0365	**1,17**	0,64	-0,53	NA	hypothetical protein
PA0394	-0,83	**-1,19**	-0,37	yggS	conserved hypothetical protein
PA0447	**-1,21**	-0,73	0,48	gcdH	glutaryl-CoA dehydrogenase
PA0459	0,93	**1,16**	0,22	clpC	probable ClpA/B protease ATP binding subunit
PA0484	**1,62**	**1,26**	-0,36	NA	conserved hypothetical protein
PA0510	**-2,01**	**-1,75**	0,25	nirE	NirE
PA0511	**-2,14**	**-1,77**	0,37	nirJ	heme d1 biosynthesis protein NirJ
PA0512	**-1,80**	**-1,58**	0,22	nirH	NirH
PA0513	**-1,33**	**-1,39**	-0,06	nirG	NirG
PA0517	**-1,35**	-0,91	0,44	nirC	probable c-type cytochrome precursor
PA0519	**-1,58**	**-1,18**	0,40	nirS	nitrite reductase precursor
PA0527	**-1,46**	-0,64	0,82	dnr	transcriptional regulator Dnr
PA0546	**1,09**	**1,16**	0,08	metK	methionine adenosyltransferase
PA0547	**1,23**	**1,04**	-0,19	NA	probable transcriptional regulator
PA0551	-0,52	**-1,19**	-0,66	epd	D-erythrose 4-phosphate dehydrogenase
PA0563	-0,68	**-1,05**	-0,37	NA	conserved hypothetical protein
PA0575	**1,34**	1,10	-0,24	NA	conserved hypothetical protein
PA0576	**-1,21**	**-1,12**	0,09	rpoD	sigma factor RpoD
PA0577	**-1,09**	**-1,23**	-0,13	dnaG	DNA primase
PA0579	-1,04	**-1,15**	-0,11	rpsU	30S ribosomal protein S21
PA0586	**2,09**	**1,87**	-0,22	ycgB	conserved hypothetical protein
PA0587	**2,29**	**1,90**	-0,39	yeaH	conserved hypothetical protein
PA0588	**2,27**	**2,02**	-0,26	yeaG	conserved hypothetical protein
PA0654	**-2,26**	**-2,24**	0,02	speD	S-adenosylmethionine decarboxylase proenzyme
PA0663	-0,72	**-1,05**	-0,33	NA	hypothetical protein
PA0708	**1,90**	**1,65**	-0,25	NA	probable transcriptional regulator
PA0709	**-1,07**	**-1,11**	-0,04	NA	hypothetical protein
PA0710	**-1,75**	**-1,94**	-0,19	gloA2	lactoylglutathione lyase
PA0713	**-1,93**	**-1,97**	-0,04	NA	hypothetical protein
PA0714	**-1,70**	**-1,36**	0,34	NA	hypothetical protein
PA0730	-0,87	**-1,05**	-0,17	NA	probable transferase
PA0745	**1,02**	0,80	-0,22	NA	probable enoyl-CoA hydratase/isomerase
PA0779	**-1,50**	**-1,45**	0,05	asrA	AsrA

PA0783	**-1,08**	-0,85	0,24	putP	sodium/proline symporter PutP
PA0789	**-1,59**	**-2,08**	-0,48	NA	probable amino acid permease
PA0792	**1,40**	**1,55**	0,16	prpD	propionate catabolic protein PrpD
PA0798	**1,82**	**1,22**	-0,61	pmtA	phospholipid methyltransferase
PA0852	**1,42**	**1,02**	-0,39	cbpD	chitin-binding protein CbpD precursor
PA0852.1	**1,37**	1,00	-0,37	NA	Uncharacterized protein
PA0866	**1,85**	**1,16**	-0,69	aroP2	aromatic amino acid transport protein AroP2
PA0888	**-1,49**	**-2,80**	**-1,31**	aotJ	arginine/ornithine binding protein AotJ
PA0889	-1,09	**-2,04**	-0,94	aotQ	arginine/ornithine transport protein AotQ
PA0890	-1,25	**-1,80**	-0,55	aotM	arginine/ornithine transport protein AotM
PA0891	**-1,54**	**-2,61**	-1,06	aotO	hypothetical protein
PA0892	**-1,31**	**-1,68**	-0,37	aotP	arginine/ornithine transport protein AotP
PA0893	-0,69	**-1,39**	-0,69	argR	transcriptional regulator ArgR
PA0895	**-1,56**	**-2,63**	-1,06	aruC	N2-Succinylornithine 5-aminotransferase (SOAT) = N2-acetylornithine 5-aminotransferase (ACOAT)
PA0896	-1,04	**-2,23**	-1,19	aruF	subunit I of arginine N2-succinyltransferase = ornithine N2-succinyltransferase
PA0897	**-1,69**	**-2,91**	-1,22	aruG	subunit II of arginine N2-succinyltransferase = ornithine N2-succinyltransferase
PA0898	**-1,45**	**-2,34**	-0,89	aruD	N-Succinylglutamate 5-semialdehyde dehydrogenase
PA0899	-1,13	**-1,82**	-0,69	aruB	N2-Succinylarginine dihydrolase
PA0901	-0,89	**-1,15**	-0,26	aruE	N-Succinylglutamate desuccinylase
PA0916	-0,93	**-1,50**	-0,56	yliG	conserved hypothetical protein
PA0945	**-1,08**	**-1,09**	-0,01	purM	phosphoribosylaminoimidazole synthetase
PA0956	-0,89	**-1,11**	-0,22	proS	prolyl-tRNA synthetase
PA0969	**-1,13**	-0,80	0,33	tolQ	TolQ protein
PA1011	-0,91	**-1,12**	-0,21	NA	hypothetical protein
PA1041	**2,94**	**2,39**	-0,55	NA	probable outer membrane protein precursor
PA1070	-0,58	**-1,15**	-0,57	braG	branched-chain amino acid transport protein BraG
PA1071	-0,56	**-1,24**	-0,68	braF	branched-chain amino acid transport protein BraF
PA1123	-1,22	**-1,33**	-0,11	NA	hypothetical protein
PA1130	**2,15**	**1,40**	-0,75	rhlC	rhamnosyltransferase 2
PA1135	1,02	**1,29**	0,27	yedU	conserved hypothetical protein
PA1155	**-1,13**	-0,88	0,24	nrdB	NrdB, tyrosyl radical-harboring component of class Ia ribonucleotide reductase
PA1156	**-1,05**	-0,99	0,06	nrdA	NrdA, catalytic component of class Ia ribonucleotide reductase

PA1166	**1,58**	**1,59**	0,02	NA	hypothetical protein
PA1168	**1,97**	**1,88**	-0,10	NA	hypothetical protein
PA1169	**1,73**	**1,51**	-0,22	NA	probable lipoxygenase
PA1172	**1,79**	**2,06**	0,27	napC	cytochrome c-type protein NapC
PA1173	**1,59**	**1,63**	0,04	napB	cytochrome c-type protein NapB precursor
PA1174	**2,26**	**1,86**	-0,40	napA	periplasmic nitrate reductase protein NapA
PA1175	**2,12**	**1,74**	-0,39	napD	NapD protein of periplasmic nitrate reductase
PA1176	**2,31**	**1,89**	-0,43	napF	ferredoxin protein NapF
PA1177	**1,50**	**1,70**	0,20	napE	periplasmic nitrate reductase protein NapE
PA1190	**2,08**	**2,11**	0,02	yohC	conserved hypothetical protein
PA1196	**-1,46**	-0,61	0,86	ddaR	transcriptional regulator DdaR
PA1211	1,63	**1,82**	0,19	NA	hypothetical protein
PA1212	**2,29**	**2,50**	0,20	NA	probable major facilitator superfamily (MFS) transporter
PA1213	**3,77**	**2,90**	-0,87	NA	hypothetical protein
PA1214	**3,31**	**2,88**	-0,42	NA	hypothetical protein
PA1215	**3,15**	**1,94**	-1,20	NA	hypothetical protein
PA1216	**3,56**	**2,91**	-0,66	NA	hypothetical protein
PA1217	**3,21**	**2,62**	-0,58	NA	probable 2-isopropylmalate synthase
PA1218	**3,13**	**2,36**	-0,78	NA	hypothetical protein
PA1219	**1,96**	**1,75**	-0,20	NA	hypothetical protein
PA1220	**3,09**	**2,68**	-0,41	NA	hypothetical protein
PA1221	**2,98**	**2,46**	-0,52	NA	hypothetical protein
PA1228	**-1,81**	**-1,59**	0,22	NA	hypothetical protein
PA1245	**1,25**	**1,28**	0,04	aprX	AprX
PA1246	**1,69**	**1,51**	-0,17	aprD	alkaline protease secretion protein AprD
PA1247	**1,35**	**1,16**	-0,19	aprE	alkaline protease secretion protein AprE
PA1248	**1,22**	0,82	-0,41	aprF	Alkaline protease secretion outer membrane protein AprF precursor
PA1249	**2,41**	**1,80**	-0,61	aprA	alkaline metalloproteinase precursor
PA1250	**1,23**	**1,11**	-0,12	aprI	alkaline proteinase inhibitor AprI
PA1256	**1,62**	0,97	-0,65	lhpO	ABC transporter ATP-binding protein, LhpO
PA1317	-1,00	**-1,19**	-0,19	cyoA	cytochrome o ubiquinol oxidase subunit II
PA1318	-1,01	**-1,12**	-0,11	cyoB	cytochrome o ubiquinol oxidase subunit I
PA1323	**2,13**	**2,63**	0,50	NA	hypothetical protein
PA1324	**2,22**	**2,55**	0,33	NA	hypothetical protein
PA1353	**2,07**	**2,31**	0,24	NA	hypothetical protein
PA1361	-0,73	**-1,26**	-0,54	norM	NorM
PA1404	**2,00**	**1,80**	-0,19	NA	hypothetical protein
PA1471	0,95	**1,33**	0,38	NA	hypothetical protein

PA1546	**-1,16**	-0,33	0,82	hemN	oxygen-independent coproporphyrinogen III oxidase
PA1549	-0,81	**-1,21**	-0,40	fixI	probable cation-transporting P-type ATPase
PA1551	-0,93	**-1,23**	-0,30	fixG	probable ferredoxin
PA1552	-0,82	**-1,04**	-0,22	ccoP1	Cytochrome c oxidase, cbb3-type, CcoP subunit
PA1554	-0,86	**-1,19**	-0,33	ccoN1	Cytochrome c oxidase, cbb3-type, CcoN subunit
PA1555	**-2,37**	**-1,93**	0,43	ccoP2	Cytochrome c oxidase, cbb3-type, CcoP subunit
PA1555.1	**-2,24**	**-2,21**	0,03	ccoQ2	Cytochrome c oxidase, cbb3-type, CcoQ subunit
PA1556	**-2,10**	**-1,44**	0,66	ccoO2	Cytochrome c oxidase, cbb3-type, CcoO subunit
PA1557	**-2,03**	**-1,35**	0,68	ccoN2	Cytochrome c oxidase, cbb3-type, CcoN subunit
PA1562	0,98	**1,02**	0,04	acnA	aconitate hydratase 1
PA1582	-0,65	**-1,07**	-0,43	sdhD	succinate dehydrogenase (D subunit)
PA1583	-0,86	**-1,27**	-0,41	sdhA	succinate dehydrogenase (A subunit)
PA1584	-0,81	**-1,20**	-0,38	sdhB	succinate dehydrogenase (B subunit)
PA1592	**1,12**	**1,71**	0,59	NA	hypothetical protein
PA1596	**-1,80**	**-1,62**	0,18	htpG	heat shock protein HtpG
PA1617	**1,13**	**1,10**	-0,03	NA	probable AMP-binding enzyme
PA1643a	**1,50**	1,15	-0,35	NA	NA
PA1673	**-1,73**	**-1,29**	0,43	NA	hypothetical protein
PA1687	**-1,13**	-0,80	0,33	speE	spermidine synthase
PA1732	**1,40**	0,82	-0,58	NA	conserved hypothetical protein
PA1745	**1,70**	1,27	-0,44	NA	hypothetical protein
PA1750	-0,96	**-1,14**	-0,17	NA	phospho-2-dehydro-3-deoxyheptonate aldolase
PA1761	**1,62**	**1,21**	-0,40	NA	hypothetical protein
PA1784	**2,16**	**1,61**	-0,55	NA	hypothetical protein
PA1791	**-1,22**	**-1,49**	-0,27	NA	hypothetical protein
PA1805	-0,96	**-1,11**	-0,15	ppiD	peptidyl-prolyl cis-trans isomerase D
PA1818	-0,66	**-1,86**	-1,20	ldcA,cadA	lysine decarboxylase
PA1830	0,59	**1,20**	0,61	NA	hypothetical protein
PA1837a	**1,58**	1,06	-0,51	NA	NA
PA1838	**-1,07**	-0,42	0,64	cysI	sulfite reductase
PA1839	-0,88	**-1,34**	-0,46	NA	hypothetical protein
PA1869	**1,46**	0,77	-0,69	NA	probable acyl carrier protein
PA1871	**2,45**	**1,75**	-0,70	lasA	LasA protease precursor
PA1874	**1,46**	1,03	-0,43	NA	hypothetical protein
PA1880	**1,56**	**1,21**	-0,35	NA	probable oxidoreductase
PA1881	**1,30**	**1,07**	-0,23	NA	probable oxidoreductase
PA1887	**1,79**	**2,26**	0,47	NA	hypothetical protein
PA1888	**2,46**	**2,62**	0,16	NA	hypothetical protein
PA1894	**1,15**	0,71	-0,44	NA	hypothetical protein

PA1895	**1,12**	0,55	-0,57	NA	hypothetical protein
PA1897	**1,42**	0,93	-0,49	NA	hypothetical protein
PA1899	**4,48**	**3,32**	-1,16	phzA2	probable phenazine biosynthesis protein
PA1900	**4,30**	**3,01**	-1,28	phzB2	probable phenazine biosynthesis protein
PA1927	**1,80**	**1,38**	-0,42	metE	5-methyltetrahydropteroyltriglutamate-homocysteine S-methyltransferase
PA1930	**1,82**	**2,10**	0,28	NA	probable chemotaxis transducer
PA1946	**1,17**	**1,08**	-0,09	rbsB	binding protein component precursor of ABC ribose transporter
PA1951	**2,00**	**1,56**	-0,44	fapF	FapF
PA1964	**-1,20**	-1,06	0,14	ybiT	probable ATP-binding component of ABC transporter
PA2018	**1,50**	**1,41**	-0,08	mexY	Resistance-Nodulation-Cell Division (RND) multidrug efflux transporter MexY
PA2042	-0,78	**-1,71**	-0,93	ygjU	probable transporter (membrane subunit)
PA2066	**2,32**	**1,99**	-0,33	NA	hypothetical protein
PA2068	**2,61**	**2,33**	-0,28	NA	probable major facilitator superfamily (MFS) transporter
PA2069	**3,92**	**2,50**	-1,42	NA	probable carbamoyl transferase
PA2071	**1,29**	**1,22**	-0,07	fusA2	elongation factor G
PA2072	**2,00**	**1,72**	-0,27	NA	conserved hypothetical protein
PA2109	**-2,42**	**-2,46**	-0,04	NA	hypothetical protein
PA2111	**-3,35**	**-3,42**	-0,08	NA	hypothetical protein
PA2112	**-1,93**	**-2,07**	-0,14	NA	conserved hypothetical protein
PA2113	-1,57	**-2,23**	-0,66	opdO	pyroglutamate porin OpdO
PA2142a	1,62	**2,05**	0,43	NA	NA
PA2164	**1,58**	1,29	-0,29	NA	probable glycosyl hydrolase
PA2167	**1,47**	**1,51**	0,04	NA	hypothetical protein
PA2171	**1,52**	**2,18**	0,66	NA	hypothetical protein
PA2177	1,07	**1,42**	0,35	NA	probable sensor/response regulator hybrid
PA2262	**-1,86**	-1,42	0,43	kguT	probable 2-ketogluconate transporter
PA2264	-1,13	0,62	**1,75**	NA	conserved hypothetical protein
PA2265	-0,84	0,93	**1,77**	gad	gluconate dehydrogenase
PA2290	-0,48	**1,20**	**1,68**	gcd	glucose dehydrogenase
PA2291	-0,09	**1,79**	**1,88**	oprB2; opbA	probable glucose-sensitive porin
PA2300	**1,96**	**1,28**	-0,68	chiC	chitinase
PA2302	**1,41**	**1,28**	-0,13	ambE	AmbE
PA2303	**1,17**	0,96	-0,20	ambD	AmbD
PA2304	**1,18**	**1,22**	0,04	ambC	AmbC
PA2320	**-1,67**	0,20	**1,88**	gntR	transcriptional regulator GntR
PA2321	**-5,62**	-0,34	**5,28**	gntV; gntK; gnuK	gluconokinase
PA2322	**-5,87**	-0,72	**5,15**	gntP	gluconate permease

PA2323	**-1,62**	**3,09**	**4,71**	gapN; gapB	probable glyceraldehyde-3-phosphate dehydrogenase
PA2329	1,13	**1,29**	0,15	NA	probable ATP-binding component of ABC transporter
PA2331	**1,67**	**1,47**	-0,20	NA	hypothetical protein
PA2363	**1,44**	1,14	-0,30	hsiJ3	HsiJ3
PA2365	**2,55**	**2,00**	-0,55	hsiB3	HsiB3
PA2366	**2,79**	**2,10**	-0,69	hsiC3	HsiC3
PA2367	**2,66**	**2,11**	-0,55	hcp3	Hcp3
PA2369	**2,48**	**2,03**	-0,45	hsiG3	HsiG3
PA2371	**2,04**	**1,32**	-0,73	clpV3	ClpV3
PA2372	**2,25**	**1,74**	-0,52	NA	hypothetical protein
PA2373	**1,58**	**1,10**	-0,48	vgrG3	VgrG3
PA2375	1,29	**1,62**	0,33	NA	hypothetical protein
PA2385	**1,33**	**1,83**	0,50	pvdQ	3-oxo-C12-homoserine lactone acylase PvdQ
PA2386	**1,49**	**2,40**	0,91	pvdA	L-ornithine N5-oxygenase
PA2392	**1,19**	**1,57**	0,38	pvdP	PvdP
PA2393	**1,50**	**2,10**	0,59	NA	putative dipeptidase
PA2394	**1,22**	**2,00**	0,78	pvdN	PvdN
PA2396	**1,37**	**2,09**	0,72	pvdF	pyoverdine synthetase F
PA2397	**1,21**	**1,43**	0,22	pvdE	pyoverdine biosynthesis protein PvdE
PA2399	0,87	**1,31**	0,44	pvdD	pyoverdine synthetase D
PA2400	0,60	**1,02**	0,42	pvdJ	PvdJ
PA2402	**1,02**	**1,50**	0,48	NA	probable non-ribosomal peptide synthetase
PA2412	1,42	**2,21**	0,79	NA	conserved hypothetical protein
PA2413	**1,42**	**2,09**	0,68	pvdH	L-2,4-diaminobutyrate:2-ketoglutarate 4-aminotransferase, PvdH
PA2414	1,25	**1,53**	0,28	NA	L-sorbosone dehydrogenase
PA2424	**1,15**	**1,86**	0,71	pvdL	PvdL
PA2426	0,96	**2,27**	1,31	pvdS	sigma factor PvdS
PA2433	**2,07**	**2,59**	0,52	NA	hypothetical protein
PA2441	1,03	**1,66**	0,63	NA	hypothetical protein
PA2486	1,00	**1,23**	0,23	NA	hypothetical protein
PA2504	**1,49**	**1,83**	0,35	NA	hypothetical protein
PA2512	-0,75	**-1,46**	-0,71	antA	anthranilate dioxygenase large subunit
PA2513	-0,77	**-1,41**	-0,64	antB	anthranilate dioxygenase small subunit
PA2514	-1,05	**-1,73**	-0,67	antC	anthranilate dioxygenase reductase
PA2544	1,19	**1,39**	0,20	NA	hypothetical protein
PA2562	**1,27**	**1,49**	0,21	NA	hypothetical protein
PA2564	**1,60**	1,09	-0,50	tam	hypothetical protein
PA2566	**2,26**	**1,39**	-0,87	NA	conserved hypothetical protein
PA2570	**2,23**	**1,61**	-0,61	lecA	LecA
PA2571	**1,24**	1,00	-0,23	NA	probable two-component sensor
PA2572	**1,51**	**1,46**	-0,05	NA	probable two-component response

					regulator
PA2573	**2,36**	**1,87**	-0,49	NA	probable chemotaxis transducer
PA2579	-0,55	**-1,06**	-0,52	kynA	L-Tryptophan:oxygen 2,3-oxidoreductase (decyclizing) KynA
PA2584	-0,59	**-1,12**	-0,53	pgsA	CDP-diacylglycerol--glycerol-3-phosphate 3-phosphatidyltransferase
PA2622	**1,55**	**1,64**	0,09	cspD	cold-shock protein CspD
PA2624	**-1,49**	**-1,21**	0,29	idh	isocitrate dehydrogenase
PA2629	**-1,25**	**-1,35**	-0,10	purB	adenylosuccinate lyase
PA2630	**-1,49**	-1,03	0,46	ycfD	conserved hypothetical protein
PA2634	**1,01**	0,58	-0,43	aceA	isocitrate lyase AceA
PA2639	**-1,02**	**-1,04**	-0,01	nuoD	NADH dehydrogenase I chain C,D
PA2641	**-1,17**	**-1,26**	-0,09	nuoF	NADH dehydrogenase I chain F
PA2647	**-1,02**	-0,99	0,03	nuoL	NADH dehydrogenase I chain L
PA2722	**1,36**	1,22	-0,14	NA	hypothetical protein
PA2740	**-1,12**	-0,90	0,22	pheS	phenylalanyl-tRNA synthetase, alpha-subunit
PA2743	-0,87	**-1,19**	-0,32	infC	translation initiation factor IF-3
PA2747	**1,99**	**1,88**	-0,11	NA	hypothetical protein
PA2754	0,54	**1,70**	1,17	NA	conserved hypothetical protein
PA2760	-0,72	**-1,08**	-0,35	oprQ	OprQ
PA2765	-0,72	**-1,01**	-0,29	NA	hypothetical protein
PA2771	**1,97**	**1,62**	-0,35	NA	diguanylate cyclase with a self-blocked I-site, Dcsbis
PA2787	1,11	**1,73**	0,61	cpg2	carboxypeptidase G2 precursor
PA2815	**1,44**	**1,34**	-0,10	yafH	probable acyl-CoA dehydrogenase
PA2851	**-1,28**	**-1,20**	0,07	efp	translation elongation factor P
PA2853	0,45	**1,19**	0,74	oprI	Outer membrane lipoprotein OprI precursor
PA2862	**1,86**	**1,85**	-0,02	lipA	lactonizing lipase precursor
PA2863	**1,48**	**1,36**	-0,12	lipH	lipase modulator protein
PA2864	**1,53**	**1,48**	-0,05	NA	conserved hypothetical protein
PA2911	**-1,03**	**-1,02**	0,00	NA	probable TonB-dependent receptor
PA2937	**2,48**	**2,03**	-0,45	NA	hypothetical protein
PA2939	**3,88**	**3,23**	-0,66	pepB	probable aminopeptidase
PA2950	**-1,00**	**-1,03**	-0,03	pfm¦	proton motive force protein, PMF
PA2967	**-1,11**	**-1,33**	-0,22	fabG	3-oxoacyl-[acyl-carrier-protein] reductase
PA2968	**-1,01**	-0,97	0,04	fabD	malonyl-CoA-[acyl-carrier-protein] transacylase
PA2969	**-1,52**	**-1,68**	-0,16	plsX	fatty acid biosynthesis protein PlsX
PA2971	-0,82	**-1,30**	-0,48	yceD	conserved hypothetical protein
PA2976	**-1,05**	**-1,09**	-0,04	rne	ribonuclease E
PA2995	-0,80	**-1,09**	-0,30	nqrE	Na+-translocating NADH:quinone oxidoreductase subunit Nqr5
PA2997	**-1,04**	**-1,14**	-0,10	nqrC	Na+-translocating NADH:ubiquinone oxidoreductase subunit Nrq3

PA3019	-0,82	**-1,03**	-0,21	uup	probable ATP-binding component of ABC transporter
PA3023	1,27	**1,42**	0,15	yegS	conserved hypothetical protein
PA3032	**2,01**	**1,90**	-0,11	snr1	cytochrome c Snr1
PA3040	**1,50**	**1,62**	0,12	yqjD	conserved hypothetical protein
PA3042	0,99	**1,51**	0,52	NA	hypothetical protein
PA3049	**2,47**	**2,09**	-0,38	rmf	ribosome modulation factor
PA3089	1,00	**1,96**	0,96	NA	hypothetical protein
PA3162	**-1,56**	**-1,57**	-0,01	rpsA	30S ribosomal protein S1
PA3179	-0,72	**-1,14**	-0,42	yciL	conserved hypothetical protein
PA3181	**-3,77**	-0,99	**2,78**	edaA	2-keto-3-deoxy-6-phosphogluconate aldolase
PA3182	**-3,77**	-1,03	**2,74**	pgl	6-phosphogluconolactonase
PA3183	**-4,01**	**-1,09**	**2,92**	zwf	glucose-6-phosphate 1-dehydrogenase
PA3186	-0,15	**5,55**	**5,69**	oprB	Glucose/carbohydrate outer membrane porin OprB precursor
PA3187	**-2,96**	**2,74**	**5,70**	gltK	probable ATP-binding component of ABC transporter
PA3188	**-6,24**	-1,26	**4,98**	gltG	probable permease of ABC sugar transporter
PA3189	**-1,92**	-0,10	1,82	gltF	probable permease of ABC sugar transporter
PA3190	0,23	**5,83**	**5,60**	gltB	probable binding protein component of ABC sugar transporter
PA3191	**-1,32**	0,04	1,36	gtrS	glucose transport sensor, GtrS
PA3192	**-1,90**	-0,12	**1,78**	gltR	two-component response regulator GltR
PA3193	**-1,91**	-0,12	**1,79**	glk	glucokinase
PA3194	**-3,07**	-0,72	**2,35**	edd	phosphogluconate dehydratase
PA3195	**-3,04**	-0,58	**2,46**	gapA	glyceraldehyde 3-phosphate dehydrogenase
PA3229	**1,04**	**1,48**	0,45	NA	hypothetical protein
PA3236	**1,43**	1,11	-0,31	betX	BetX
PA3246	**-1,30**	**-1,27**	0,03	rluA	pseudouridine synthase RluA
PA3250	**1,78**	**1,47**	-0,31	NA	hypothetical protein
PA3251	0,92	**1,63**	0,71	NA	hypothetical protein
PA3263	**-1,14**	-0,78	0,37	yaiD	conserved hypothetical protein
PA3268	**-1,58**	-0,98	0,60	NA	probable TonB-dependent receptor
PA3274	1,63	**1,72**	0,08	NA	hypothetical protein
PA3308	-0,99	**-1,00**	-0,01	hepA	RNA helicase HepA
PA3309	**-1,20**	-0,41	0,79	uspK	conserved hypothetical protein
PA3311	**1,50**	**1,57**	0,07	nbdA	NbdA
PA3327	**1,34**	0,62	-0,72	NA	probable non-ribosomal peptide synthetase
PA3328	**1,61**	**1,13**	-0,47	NA	probable FAD-dependent monooxygenase
PA3329	**1,73**	**1,14**	-0,58	NA	hypothetical protein
PA3330	**1,67**	0,98	-0,70	NA	probable short chain dehydrogenase

PA3331	**1,80**	**1,20**	-0,60	NA	cytochrome P450
PA3332	**1,75**	**1,27**	-0,49	NA	conserved hypothetical protein
PA3333	**1,83**	**1,03**	-0,80	fabH2	3-oxoacyl-[acyl-carrier-protein] synthase III
PA3334	**2,19**	**1,32**	-0,87	NA	probable acyl carrier protein
PA3335	**1,70**	**1,13**	-0,57	NA	hypothetical protein
PA3336	**1,83**	1,04	-0,78	NA	probable major facilitator superfamily (MFS) transporter
PA3347	**1,15**	**1,17**	0,02	hsbA	HptB-dependent secretion and biofilm anti anti-sigma factor HsbA
PA3361	**2,37**	**1,56**	-0,81	lecB	fucose-binding lectin PA-IIL
PA3369	**1,57**	**1,49**	-0,08	NA	hypothetical protein
PA3415	**1,93**	1,53	-0,40	NA	probable dihydrolipoamide acetyltransferase
PA3416	**2,34**	**2,36**	0,02	NA	probable pyruvate dehydrogenase E1 component, beta chain
PA3417	**1,71**	**2,05**	0,33	NA	probable pyruvate dehydrogenase E1 component, alpha subunit
PA3418	**1,65**	**2,17**	0,52	ldh	leucine dehydrogenase
PA3432	**-1,67**	-0,73	0,94	NA	hypothetical protein
PA3451	**2,46**	**1,90**	-0,56	NA	hypothetical protein
PA3459	0,89	**1,23**	0,34	asnB	probable glutamine amidotransferase
PA3465	0,57	**1,35**	0,78	yfiS	conserved hypothetical protein
PA3477	**1,25**	0,89	-0,37	rhlR	transcriptional regulator RhlR
PA3478	**1,60**	**1,19**	-0,40	rhlB	rhamnosyltransferase chain B
PA3479	**1,74**	**1,31**	-0,43	rhlA	rhamnosyltransferase chain A
PA3484	-0,83	**-1,09**	-0,26	tse3	Tse3
PA3516	**1,21**	0,94	-0,27	NA	probable lyase
PA3519	**1,90**	**1,28**	-0,63	NA	hypothetical protein
PA3531	**-1,40**	**-1,36**	0,05	bfrB	bacterioferritin
PA3560	-0,39	**2,01**	**2,40**	fruA	phosphotransferase system transporter fructose-specific IIBC component, FruA
PA3561	0,16	**2,55**	**2,38**	fruK	1-phosphofructokinase
PA3562	-0,25	**2,53**	**2,78**	fruI	phosphotransferase system transporter enzyme I, FruI
PA3568	**1,93**	0,82	-1,11	ymmS	probable acetyl-coa synthetase
PA3569	**1,33**	0,42	-0,90	mmsB	3-hydroxyisobutyrate dehydrogenase
PA3570	**1,56**	0,87	-0,69	mmsA	methylmalonate-semialdehyde dehydrogenase
PA3621	**-1,27**	**-1,27**	0,00	fdxA	ferredoxin I
PA3622	**1,36**	**1,26**	-0,10	rpoS	sigma factor RpoS
PA3635	**-1,11**	**-1,13**	-0,02	eno	enolase
PA3640	-0,82	**-1,00**	-0,18	dnaE	DNA polymerase III, alpha chain
PA3641	**-1,78**	**-1,92**	-0,14	NA	probable amino acid permease
PA3645	-0,77	**-1,09**	-0,31	fabZ	(3R)-hydroxymyristoyl-[acyl carrier protein] dehydratase

PA3652	**-1,17**	**-1,23**	-0,06	uppS	undecaprenyl pyrophosphate synthetase
PA3653	**-1,05**	**-1,23**	-0,18	frr	ribosome recycling factor
PA3655	**-1,50**	**-1,41**	0,09	tsf	elongation factor Ts
PA3656	**-1,46**	**-1,52**	-0,06	rpsB	30S ribosomal protein S2
PA3675	**-1,09**	**-1,01**	0,08	NA	hypothetical protein
PA3688	1,06	**1,70**	0,63	NA	hypothetical protein
PA3691	**1,61**	**2,11**	0,50	NA	hypothetical protein
PA3692	**1,54**	**2,05**	0,50	lptF	Lipotoxon F, LptF
PA3700	**-1,40**	**-1,27**	0,13	lysS	lysyl-tRNA synthetase
PA3709	**1,46**	**1,51**	0,05	NA	probable major facilitator superfamily (MFS) transporter
PA3710	**1,36**	0,75	-0,62	NA	probable GMC-type oxidoreductase
PA3716	**-1,03**	**-1,04**	-0,01	NA	hypothetical protein
PA3723	**2,20**	**1,42**	-0,79	yqjM	probable FMN oxidoreductase
PA3724	**2,96**	**1,82**	-1,14	lasB	elastase LasB
PA3729	-0,99	**-1,21**	-0,22	NA	conserved hypothetical protein
PA3734	**1,65**	**1,64**	-0,01	NA	hypothetical protein
PA3742	**-1,53**	-1,05	0,48	rplS	50S ribosomal protein L19
PA3743	**-1,15**	**-1,35**	-0,20	trmD	tRNA (guanine-N1)-methyltransferase
PA3744	**-1,11**	**-1,32**	-0,22	rimM	16S rRNA processing protein
PA3745	**-1,35**	**-1,73**	-0,38	rpsP	30S ribosomal protein S16
PA3763	-0,99	**-1,04**	-0,05	purL	phosphoribosylformylglycinamidine synthase
PA3769	**-1,41**	**-1,27**	0,14	guaA	GMP synthase
PA3770	**-1,09**	**-1,17**	-0,08	guaB	inosine-5'-monophosphate dehydrogenase
PA3790	**-1,52**	**-1,68**	-0,16	oprC	Putative copper transport outer membrane porin OprC precursor
PA3795	0,93	**1,02**	0,08	NA	probable oxidoreductase
PA3807	**-1,02**	-0,76	0,26	ndk	nucleoside diphosphate kinase
PA3812	-0,78	**-1,17**	-0,39	iscA	probable iron-binding protein IscA
PA3818	**-1,06**	-0,89	0,17	suhB	extragenic suppressor protein SuhB
PA3821	**-1,58**	**-1,62**	-0,04	secD	secretion protein SecD
PA3822	-0,79	**-1,07**	-0,27	yajC	conserved hypothetical protein
PA3834	**-1,09**	-0,90	0,19	valS	valyl-tRNA synthetase
PA3858	**1,16**	0,86	-0,30	aapJ	probable amino acid-binding protein
PA3863	**-1,51**	-0,84	0,67	dauA	FAD-dependent catabolic D-arginine dehydrogenase, DauA
PA3890	0,95	**1,28**	0,33	opuCB	OpuC ABC transporter, permease protein, OpuCB
PA3891	0,91	**1,33**	0,42	opuCA	OpuC ABC transporter, ATP-binding protein, OpuCA
PA3892	-0,99	**-1,37**	-0,38	NA	conserved hypothetical protein
PA3919	**1,02**	**1,26**	0,23	ylaK	conserved hypothetical protein
PA3922	**2,37**	**1,95**	-0,42	NA	conserved hypothetical protein
PA3923	**2,11**	**1,53**	-0,58	NA	hypothetical protein

PA3924	**1,08**	0,90	-0,18	NA	probable medium-chain acyl-CoA ligase
PA3934	-0,55	**-1,51**	-0,96	NA	conserved hypothetical protein
PA3969a	-0,74	**-1,34**	-0,59	NA	NA
PA3980	-0,98	**-1,20**	-0,22	miaB; yleA	conserved hypothetical protein
PA3986	**1,50**	**1,58**	0,08	NA	hypothetical protein
PA4000	-0,63	**-1,07**	-0,44	rlpA	RlpA
PA4006	-0,87	**-1,07**	-0,20	nadD1,nadD	nicotinate mononucleotide adenylyltransferase NadD1
PA4015	**1,29**	**1,33**	0,04	NA	conserved hypothetical protein
PA4031	**-1,20**	**-1,16**	0,04	ppa	inorganic pyrophosphatase
PA4053	**-1,09**	**-1,34**	-0,25	ribE	6,7-dimethyl-8-ribityllumazine synthase
PA4061	**-1,03**	**-1,08**	-0,06	ybbN	probable thioredoxin
PA4067	**-1,43**	-0,75	0,69	oprG	Outer membrane protein OprG precursor
PA4078	**1,94**	**1,66**	-0,29	NA	probable nonribosomal peptide synthetase
PA4112	**1,56**	**1,37**	-0,19	NA	probable sensor/response regulator hybrid
PA4139	**2,23**	**1,83**	-0,40	NA	hypothetical protein
PA4140	**2,02**	**1,53**	-0,49	NA	hypothetical protein
PA4141	**2,00**	**1,69**	-0,31	NA	hypothetical protein
PA4142	**1,54**	1,17	-0,37	NA	probable secretion protein
PA4205	**1,69**	**1,90**	0,21	mexG	hypothetical protein
PA4206	**1,90**	**1,45**	-0,45	mexH	probable Resistance-Nodulation-Cell Division (RND) efflux membrane fusion protein precursor
PA4207	**1,59**	**1,24**	-0,34	mexI	probable Resistance-Nodulation-Cell Division (RND) efflux transporter
PA4209	**2,72**	**1,80**	-0,91	phzM	probable phenazine-specific methyltransferase
PA4210	**2,63**	**1,42**	-1,21	phzA1	probable phenazine biosynthesis protein
PA4211	**2,84**	**1,70**	-1,14	phzB1	probable phenazine biosynthesis protein
PA4212	**1,92**	0,96	-0,95	phzC1	phenazine biosynthesis protein PhzC
PA4217	**3,01**	**1,82**	-1,19	phzS	flavin-containing monooxygenase
PA4234	**-1,13**	-0,90	0,23	uvrA	excinuclease ABC subunit A
PA4237	**-1,08**	-0,57	0,51	rplQ	50S ribosomal protein L17
PA4238	**-1,43**	**-1,40**	0,03	rpoA	DNA-directed RNA polymerase alpha chain
PA4239	**-1,51**	**-1,62**	-0,11	rpsD	30S ribosomal protein S4
PA4240	**-1,20**	-0,92	0,28	rpsK	30S ribosomal protein S11
PA4241	**-1,40**	**-1,05**	0,36	rpsM	30S ribosomal protein S13
PA4242	**-1,32**	**-1,68**	-0,36	rpmJ	50S ribosomal protein L36
PA4243	**-1,62**	**-1,63**	0,00	secY	secretion protein SecY
PA4244	**-1,86**	**-1,96**	-0,10	rplO	50S ribosomal protein L15
PA4245	**-1,52**	**-1,59**	-0,08	rpmD	50S ribosomal protein L30
PA4246	**-1,68**	**-1,79**	-0,11	rpsE	30S ribosomal protein S5
PA4247	**-1,78**	**-1,68**	0,10	rplR	50S ribosomal protein L18

PA4248	**-1,84**	**-1,69**	0,16	rplF	50S ribosomal protein L6
PA4249	**-1,47**	**-1,36**	0,12	rpsH	30S ribosomal protein S8
PA4250	**-1,03**	-0,56	0,46	rpsN	30S ribosomal protein S14
PA4251	**-1,24**	**-1,09**	0,15	rplE	50S ribosomal protein L5
PA4252	**-1,46**	**-1,56**	-0,10	rplX	50S ribosomal protein L24
PA4253	**-1,12**	**-1,05**	0,07	rplN	50S ribosomal protein L14
PA4254	**-1,27**	**-1,10**	0,17	rpsQ	30S ribosomal protein S17
PA4255	**-1,47**	**-1,40**	0,07	rpmC	50S ribosomal protein L29
PA4256	**-1,36**	**-1,42**	-0,06	rplP	50S ribosomal protein L16
PA4257	**-1,49**	**-1,27**	0,22	rpsC	30S ribosomal protein S3
PA4258	**-1,65**	**-1,54**	0,11	rplV	50S ribosomal protein L22
PA4259	**-1,60**	**-1,75**	-0,14	rpsS	30S ribosomal protein S19
PA4260	**-1,78**	**-2,22**	-0,44	rplB	50S ribosomal protein L2
PA4261	**-2,01**	**-1,91**	0,10	rplW	50S ribosomal protein L23
PA4262	**-2,08**	**-2,16**	-0,08	rplD	50S ribosomal protein L4
PA4263	**-1,69**	**-1,55**	0,14	rplC	50S ribosomal protein L3
PA4264	**-1,77**	**-1,90**	-0,13	rpsJ	30S ribosomal protein S10
PA4265	**-1,45**	**-1,40**	0,04	tufA	elongation factor Tu
PA4266	**-1,47**	**-1,49**	-0,02	fusA1	elongation factor G
PA4267	**-1,35**	**-1,30**	0,06	rpsG	30S ribosomal protein S7
PA4268	**-1,56**	**-1,56**	0,00	rpsL	30S ribosomal protein S12
PA4269	**-1,27**	**-1,39**	-0,12	rpoC	DNA-directed RNA polymerase beta* chain
PA4270	**-1,12**	**-1,05**	0,07	rpoB	DNA-directed RNA polymerase beta chain
PA4271	**-1,64**	**-1,35**	0,30	rplL	50S ribosomal protein L7 / L12
PA4272	**-1,94**	**-2,03**	-0,09	rplJ	50S ribosomal protein L10
PA4273	**-1,72**	**-1,88**	-0,17	rplA	50S ribosomal protein L1
PA4274	**-1,62**	**-1,49**	0,13	rplK	50S ribosomal protein L11
PA4276	**-1,07**	**-1,36**	-0,29	secE	secretion protein SecE
PA4277	**-1,34**	**-1,35**	0,00	tufB	elongation factor Tu
PA4279	-0,96	**-1,09**	-0,13	NA	hypothetical protein
PA4280	-0,92	**-1,28**	-0,36	birA	BirA bifunctional protein
PA4292	**-1,25**	**-1,43**	-0,18	NA	probable phosphate transporter
PA4296	**1,88**	**1,31**	-0,57	pprB	two-component response regulator, PprB
PA4305	1,25	**1,56**	0,31	rcpC	RcpC
PA4311	**1,47**	**1,27**	-0,19	NA	conserved hypothetical protein
PA4333	**-1,12**	**-1,12**	0,00	fumA	probable fumarase
PA4362	**1,98**	**1,89**	-0,09	NA	hypothetical protein
PA4377	1,32	**1,56**	0,24	NA	hypothetical protein
PA4385	**-1,49**	**-1,39**	0,10	groEL	GroEL protein
PA4386	**-1,55**	**-1,51**	0,04	groES	GroES protein
PA4387	**-1,78**	**-2,11**	-0,33	fxsA	conserved hypothetical protein
PA4402	-0,98	**-1,36**	-0,39	argJ	glutamate N-acetyltransferase
PA4428	-1,13	**-1,19**	-0,06	sspA	stringent starvation protein A

PA4429	**-1,05**	**-1,02**	0,03	NA	probable cytochrome c1 precursor
PA4430	**-1,14**	**-1,15**	-0,01	NA	probable cytochrome b
PA4431	**-1,06**	**-1,01**	0,04	NA	probable iron-sulfur protein
PA4433	**-1,53**	**-1,53**	0,00	rplM	50S ribosomal protein L13
PA4438	**-1,03**	**-1,23**	-0,19	yhcM	conserved hypothetical protein
PA4443	**-1,15**	-0,67	0,48	cysD	ATP sulfurylase small subunit
PA4457	-0,73	**-1,04**	-0,31	kpsF; yrbH; kdsD	arabinose-5-phosphate isomerase KdsD
PA4458	-0,85	**-1,12**	-0,27	yrbI	conserved hypothetical protein
PA4463	0,69	**1,12**	0,43	yhbH	conserved hypothetical protein
PA4468	1,03	**1,76**	0,73	sodM	superoxide dismutase
PA4469	0,73	**1,53**	0,79	NA	hypothetical protein
PA4470	0,48	**1,61**	1,14	fumC1	fumarate hydratase
PA4471	**1,16**	**1,90**	0,73	fagA	hypothetical protein
PA4480	**-1,06**	**-1,13**	-0,06	mreC	rod shape-determining protein MreC
PA4481	-0,99	**-1,10**	-0,11	mreB	rod shape-determining protein MreB
PA4483	**-1,12**	**-1,14**	-0,01	gatA	Glu-tRNA(Gln) amidotransferase subunit A
PA4484	**-1,20**	**-1,20**	0,01	gatB	Glu-tRNA(Gln) amidotransferase subunit B
PA4496	**1,23**	-0,05	**-1,28**	dppA1	probable binding protein component of ABC transporter
PA4497	**1,43**	0,58	-0,84	dppA2	probable binding protein component of ABC transporter
PA4501	**1,48**	0,86	-0,62	opdD,opdP	Glycine-glutamate dipeptide porin OpdP
PA4542	**-1,68**	**-1,48**	0,20	clpB	ClpB protein
PA4566	**-1,02**	-1,00	0,03	obg	GTP-binding protein Obg
PA4568	**-1,53**	**-1,79**	-0,26	rplU	50S ribosomal protein L21
PA4572	**-1,20**	**-1,24**	-0,04	fklB	peptidyl-prolyl cis-trans isomerase FklB
PA4587	**-1,74**	**-1,59**	0,15	ccpR	cytochrome c551 peroxidase precursor
PA4588	0,36	**2,09**	**1,74**	gdhA	glutamate dehydrogenase
PA4590	**2,01**	**1,72**	-0,29	pra	protein activator
PA4602	**-1,10**	**-1,10**	0,00	glyA3	serine hydroxymethyltransferase
PA4607	**2,49**	**2,46**	-0,03	NA	hypothetical protein
PA4614	**1,23**	**1,85**	0,62	mscL	conductance mechanosensitive channel
PA4623	**1,20**	**1,28**	0,08	NA	hypothetical protein
PA4624	**1,04**	0,66	-0,37	cdrB	cyclic diguanylate-regulated TPS partner B, CdrB
PA4640	**-1,06**	**-1,28**	-0,22	mqoB	malate:quinone oxidoreductase
PA4645	-0,89	**-1,06**	-0,17	hpt; hprT	probable purine/pyrimidine phosphoribosyl transferase
PA4646	**-1,06**	**-1,21**	-0,15	upp	uracil phosphoribosyltransferase
PA4647	-0,81	**-1,06**	-0,25	uraA	uracil permease
PA4665	**-1,01**	**-1,03**	-0,02	prfA	peptide chain release factor 1
PA4670	**-1,13**	**-1,47**	-0,35	prs	ribose-phosphate pyrophosphokinase

PA4671	**-1,63**	**-1,60**	0,03	rplY	probable ribosomal protein L25
PA4672	-0,87	**-1,14**	-0,27	pth	peptidyl-tRNA hydrolase
PA4673	**-1,55**	**-1,21**	0,34	ychF	conserved hypothetical protein
PA4675	**-1,36**	-0,88	0,48	chtA	ChtA
PA4680	**1,69**	**1,78**	0,09	NA	hypothetical protein
PA4681	1,41	**1,52**	0,11	NA	hypothetical protein
PA4682	**1,39**	**1,23**	-0,16	NA	hypothetical protein
PA4684	-0,98	**-1,05**	-0,07	NA	hypothetical protein
PA4686	**-1,19**	-0,96	0,22	NA	hypothetical protein
PA4695	-0,85	**-1,03**	-0,18	ilvH	acetolactate synthase isozyme III small subunit
PA4709	0,06	**1,24**	1,18	phuS	PhuS
PA4710	-0,05	**1,26**	**1,31**	phuR	Heme/Hemoglobin uptake outer membrane receptor PhuR precursor
PA4720	**-1,56**	**-1,36**	0,20	trmA	tRNA (uracil-5-)-methyltransferase
PA4730	**-1,20**	**-1,09**	0,10	panC	pantoate--beta-alanine ligase
PA4738	**3,20**	**3,44**	0,24	yjbJ	conserved hypothetical protein
PA4739	**2,64**	**2,73**	0,09	NA	conserved hypothetical protein
PA4740	**-1,07**	**-1,02**	0,05	pnp	polyribonucleotide nucleotidyltransferase
PA4741	**-1,19**	-0,81	0,38	rpsO	30S ribosomal protein S15
PA4743	**-1,19**	-1,03	0,16	rbfA	ribosome-binding factor A
PA4744	**-1,51**	**-1,52**	-0,01	infB	translation initiation factor IF-2
PA4745	**-1,25**	**-1,33**	-0,08	nusA	N utilization substance protein A
PA4746	-0,69	**-1,21**	-0,52	yhbC	conserved hypothetical protein
PA4748	-0,54	**-1,00**	-0,47	tpiA	triosephosphate isomerase
PA4749	**-1,24**	**-1,24**	0,01	glmM	phosphoglucosamine mutase
PA4750	-1,01	**-1,23**	-0,21	folP	dihydropteroate synthase
PA4757	-0,87	**-1,00**	-0,13	yeaS	conserved hypothetical protein
PA4759	**-1,26**	**-1,21**	0,05	dapB	dihydrodipicolinate reductase
PA4760	**-1,57**	**-1,59**	-0,02	dnaJ	DnaJ protein
PA4761	**-2,02**	**-1,88**	0,14	dnaK	DnaK protein
PA4762	**-1,93**	**-1,86**	0,07	grpE	heat shock protein GrpE
PA4765	-0,91	**-1,20**	-0,29	omlA	Outer membrane lipoprotein OmlA precursor
PA4774	-0,94	**-1,08**	-0,13	NA	hypothetical protein
PA4781	**1,23**	1,03	-0,20	NA	cyclic di-GMP phosphodiesterase
PA4848	**-1,11**	-0,92	0,19	accC	biotin carboxylase
PA4852	**-1,13**	**-1,37**	-0,25	yhdG	conserved hypothetical protein
PA4854	**-1,39**	**-1,21**	0,18	purH	phosphoribosylaminoimidazolecarboxamide formyltransferase
PA4855	**-1,63**	**-1,23**	0,40	purD	phosphoribosylamine--glycine ligase
PA4876	**1,87**	**2,86**	0,99	osmE	osmotically inducible lipoprotein OsmE
PA4877	1,25	**1,71**	0,45	NA	hypothetical protein
PA4880	**1,20**	**1,23**	0,03	NA	probable bacterioferritin

PA4910	**1,52**	**1,54**	0,02	NA	branched chain amino acid ABC transporter ATP binding protein
PA4911	**1,61**	1,07	-0,54	NA	probable permease of ABC branched-chain amino acid transporter
PA4913	**1,96**	**1,40**	-0,56	NA	probable binding protein component of ABC transporter
PA4915	**1,56**	**1,17**	-0,40	NA	probable chemotaxis transducer
PA4918	**-1,92**	**-1,44**	0,48	pcnA	nicotinamidase, PcnA
PA4920	**-1,00**	-0,39	0,62	nadE	NH3-dependent NAD synthetase
PA4928	-0,79	**-1,04**	-0,25	ygiR; ygiQ	conserved hypothetical protein
PA4929	**1,56**	1,31	-0,25	NA	hypothetical protein
PA4932	**-1,34**	-0,92	0,42	rplI	50S ribosomal protein L9
PA4933	**-1,56**	**-1,44**	0,12	NA	hypothetical protein
PA4934	**-1,46**	**-1,07**	0,39	rpsR	30S ribosomal protein S18
PA4935	**-1,65**	**-1,77**	-0,12	rpsF	30S ribosomal protein S6
PA4943	**-1,08**	**-1,09**	-0,01	hflX	probable GTP-binding protein
PA4944	**-1,02**	-0,90	0,12	hfq	Hfq
PA5001	-0,98	**-1,02**	-0,04	ssg	cell surface-sugar biosynthetic glycosyltransferase, Ssg
PA5002	-0,77	**-1,06**	-0,29	dnpA	de-N-acetylase involved in persistence, DnpA
PA5009	-0,85	**-1,01**	-0,16	waaP	lipopolysaccharide kinase WaaP
PA5010	**-1,11**	**-1,19**	-0,08	waaG	UDP-glucose:(heptosyl) LPS alpha 1,3-glucosyltransferase WaaG
PA5015	**-1,46**	-0,98	0,47	aceE	pyruvate dehydrogenase
PA5016	**-1,55**	-0,99	0,56	aceF	dihydrolipoamide acetyltransferase
PA5036	0,11	**1,23**	1,12	gltB	glutamate synthase large chain precursor
PA5046	**-1,19**	**-1,19**	-0,01	NA	malic enzyme
PA5047	-0,89	**-1,03**	-0,15	NA	hypothetical protein
PA5049	**-1,44**	-0,86	0,58	rpmE	50S ribosomal protein L31
PA5052	**-1,41**	**-1,53**	-0,12	NA	hypothetical protein
PA5053	**-1,54**	**-1,64**	-0,10	hslV	heat shock protein HslV
PA5054	**-1,80**	**-1,54**	0,25	hslU	heat shock protein HslU
PA5058	**1,41**	**1,03**	-0,38	phaC2	poly(3-hydroxyalkanoic acid) synthase 2
PA5087	**-1,06**	**-1,44**	-0,38	NA	hypothetical protein
PA5088	**-1,57**	**-1,83**	-0,25	NA	hypothetical protein
PA5089	**-1,64**	**-2,11**	-0,47	pldB	PldB
PA5090	**-1,46**	**-1,92**	-0,46	vgrG5	VgrG5
PA5091	**-2,40**	**-2,65**	-0,25	hutG	N-formylglutamate amidohydrolase
PA5092	**-2,92**	**-3,18**	-0,27	hutI	imidazolone-5-propionate hydrolase HutI
PA5093	**-2,73**	**-3,06**	-0,33	NA	probable histidine/phenylalanine ammonia-lyase
PA5094	**-2,31**	**-2,60**	-0,29	NA	probable ATP-binding component of ABC transporter

PA5095	**-2,06**	**-2,44**	-0,38	NA	probable permease of ABC transporter
PA5096	**-1,81**	**-2,52**	-0,71	NA	probable binding protein component of ABC transporter
PA5097	**-2,06**	**-2,58**	-0,52	hutT	probable amino acid permease
PA5098	**-4,21**	**-4,74**	-0,54	hutH	histidine ammonia-lyase
PA5099	**-4,05**	**-4,73**	-0,68	NA	probable transporter
PA5100	**-5,11**	**-5,50**	-0,38	hutU	urocanase
PA5105	**-2,55**	**-2,79**	-0,24	hutC	histidine utilization repressor HutC
PA5106	**-3,54**	**-3,86**	-0,32	NA	conserved hypothetical protein
PA5117	**-1,34**	**-1,11**	0,23	typA	regulatory protein TypA
PA5118	**-1,31**	**-1,49**	-0,19	thiI	thiazole biosynthesis protein ThiI
PA5136	-0,88	**-1,34**	-0,45	NA	hypothetical protein
PA5139	**-1,38**	-1,12	0,26	NA	hypothetical protein
PA5152	-0,27	**-1,77**	**-1,50**	NA	probable ATP-binding component of ABC transporter
PA5153	0,26	-0,93	**-1,18**	NA	amino acid (lysine/arginine/ornithine/histidine/octopine) ABC transporter periplasmic binding protein
PA5154	-0,07	**-1,29**	-1,22	NA	probable permease of ABC transporter
PA5171	**-2,42**	**-2,38**	0,03	arcA	arginine deiminase
PA5172	**-2,59**	**-2,36**	0,23	arcB	ornithine carbamoyltransferase, catabolic
PA5173	**-2,74**	**-2,57**	0,18	arcC	carbamate kinase
PA5178	**1,23**	**1,51**	0,27	NA	conserved hypothetical protein
PA5180	**-1,66**	**-2,31**	-0,65	fdhD	conserved hypothetical protein
PA5181	**-1,63**	**-2,15**	-0,52	NA	probable oxidoreductase
PA5201	**-1,33**	**-1,36**	-0,02	yhgF; tex	conserved hypothetical protein
PA5203	**-1,02**	**-1,02**	0,00	gshA	glutamate--cysteine ligase
PA5212	1,05	**1,38**	0,33	NA	hypothetical protein
PA5219	**1,61**	0,89	-0,72	NA	hypothetical protein
PA5220	**1,96**	**1,27**	-0,69	NA	hypothetical protein
PA5239	**-1,01**	**-1,09**	-0,08	rho	transcription termination factor Rho
PA5261	0,84	**1,14**	0,30	algR	alginate biosynthesis regulatory protein AlgR
PA5298	**-1,17**	**-1,31**	-0,14	xpt	xanthine phosphoribosyltransferase
PA5303	**1,44**	1,17	-0,28	NA	conserved hypothetical protein
PA5304	0,81	**1,15**	0,34	dadA	D-amino acid dehydrogenase, small subunit
PA5316	**-1,38**	**-1,25**	0,14	rpmB	50S ribosomal protein L28
PA5340	**-1,10**	-0,91	0,19	NA	hypothetical protein
PA5348	**1,59**	**1,27**	-0,32	NA	probable DNA-binding protein
PA5359	**1,74**	**1,71**	-0,03	NA	hypothetical protein
PA5366	-0,65	**-1,19**	-0,54	pstB	ATP-binding component of ABC phosphate transporter
PA5380	**1,08**	0,62	-0,46	gbdR	GbdR
PA5396	**1,52**	0,88	-0,64	NA	hypothetical protein

PA5410	**1,23**	0,79	-0,44	gbcA	GbcA
PA5418	**1,15**	1,08	-0,07	soxA	sarcosine oxidase alpha subunit
PA5421	**1,98**	**1,74**	-0,24	fdhA	glutathione-independent formaldehyde dehydrogenase
PA5424	1,21	**1,94**	0,74	yeaQ	conserved hypothetical protein
PA5425	**-1,20**	**-1,28**	-0,08	purK	phosphoribosylaminoimidazole carboxylase
PA5426	**-1,29**	**-1,48**	-0,19	purE	phosphoribosylaminoimidazole carboxylase, catalytic subunit
PA5427	**-1,36**	-0,79	0,57	adhA	alcohol dehydrogenase
PA5435	**-1,58**	-0,81	0,77	oadA	probable transcarboxylase subunit
PA5436	**-1,53**	-0,56	0,97	NA	probable biotin carboxylase subunit of a transcarboxylase
PA5445	**-1,40**	**-1,30**	0,10	psecoA	probable coenzyme A transferase
PA5479	**-1,48**	**-1,76**	-0,28	gltP	proton-glutamate symporter
PA5481	**2,43**	**2,40**	-0,03	NA	hypothetical protein
PA5482	**2,20**	**1,78**	-0,42	NA	hypothetical protein
PA5490	**-1,09**	**-1,31**	-0,22	cc4	cytochrome c4 precursor
PA5502	-0,53	**-1,26**	-0,73	NA	hypothetical protein
PA5504	**-1,04**	**-1,05**	-0,01	NA	D-methionine ABC transporter membrane protein
PA5544	**1,26**	0,93	-0,33	NA	conserved hypothetical protein
PA5545	**1,39**	**1,11**	-0,28	NA	conserved hypothetical protein
PA5546	**1,24**	0,96	-0,29	NA	conserved hypothetical protein
PA5556	**-1,01**	**-1,08**	-0,07	atpA	ATP synthase alpha chain
PA5557	-1,00	**-1,22**	-0,23	atpH	ATP synthase delta chain
PA5559	-0,93	**-1,07**	-0,13	atpE	atp synthase C chain
PA5560	-0,81	**-1,05**	-0,24	atpB	ATP synthase A chain
PA5562	-0,98	**-1,15**	-0,16	spoOJ	chromosome partitioning protein Spo0J
PA5564	**-1,36**	**-1,30**	0,06	gidB	glucose inhibited division protein B
PA5568	**-1,74**	**-1,77**	-0,03	yidC	conserved hypothetical protein

[1]Red figures, significant difference (Padj<0.05)
[2]Boldface characters, deleted genes

	General sequencing statistics					
	Raw reads	**Mapped reads**	**HQ reads**	**HQ%**	**Strand Specific reads on known transcripts**	**SS%**
PAO1+GLU A	2858342	2774119	2665486	93,25%	2405388	84,15%
PAO1+GLU B	3612457	3499804	3263219	90,33%	2957221	81,86%
PAO1 A	3849630	3751918	3585149	93,13%	3167795	82,29%
PAO1 B	2965373	2917262	2793833	94,22%	2530642	85,34%
GUN+GLU A	3244245	3141297	2920182	90,01%	2528829	77,95%
GUN+GLU B	3116320	2976641	2795184	89,70%	2469372	79,24%

	rRNA removal evaluation			Strand specificity evaluation		
	mRNA%	**rRNA%**	**tRNA %**	**mRNA SS%**	**rRNA SS%**	**tRNA SS%**
PAO1+GLU A	68,26	0,23	0,54	94,94	83,77	98,47
PAO1+GLU B	72,16	0,56	0,77	93,94	78,33	98,47
PAO1 A	68,50	0,74	0,83	93,38	89,61	98,26
PAO1 B	75,71	0,24	0,44	95,12	88,25	98,18
GUN+GLU A	70,90	0,26	0,74	90,01	69,99	96,85
GUN+GLU B	58,64	2,30	0,68	91,04	97,13	96,30

*evaluation performed on mapped reads

	CDS strand specific coverage statitsics		
	Not expressed %	**Reads covering 90% of the transcripts**	**Transcripts covered for half of their length (%)**
PAO1+GLU A	2,6	4	76,2
PAO1+GLU B	1,3	8	86,0
PAO1 A	1,5	7	84,1
PAO1 B	2,1	4	77,3
GUN+GLU A	1,1	13	91,9
GUN+GLU B	1,4	8	84,1

Supplementary Table S3. Glucose responsive genes in PAO1

Locus	Log2 FC[a]			Name	Description	Regulator[b]
	PAO1+ *vs.* PAO1	GUN+ *vs.* PAO1+	GUN+ vs. PAO1			
PA0888	-1.31	-1.49	-2.80	*aotJ*	arginine/ornithine ABC transporter	ArgR[25]
PA2264	1.75	-1.13	0.62		hypothetical protein	PtxS[26]
PA2265	1.77	-0.84	0.93	*gad*	gluconate dehydrogenase	PtxS[26]
PA2290	1.68	-0.48	1.20	*gcd*	glucose dehydrogenase	nd
PA2291	1.88	-0.09	1.79		glucose-sensitive porin	nd
PA2320	1.88	-1.67	0.20	*gntR*	GntR transcriptional regulator	GntR[26]
PA2321	5.28	-5.62	-0.34	*gntK*	gluconokinase	nd
PA2322	5.15	-5.87	-0.72	*gntP*	gluconate permease	GntR[26]
PA2323	4.71	-1.62	3.09	*gapN*	glyceraldehyde-3-phosphate dehydrogenase	nd
PA3181	2.78	-3.77	-0.99	*edaA*	2-dehydro-3-deoxy-phosphogluconate aldolase	HexR[26]
PA3182	2.74	-3.77	-1.03	*pgl*	6-phosphogluconolactonase	HexR[26]
PA3183	2.92	-4.01	-1.09	*zwf*	glucose-6-phosphate 1-dehydrogenase	HexR[26]
PA3186	5.69	-0.15	5.55	*oprB*	porin B	GltR[26]
PA3187	5.70	-2.96	2.74	*gltK*	ABC transporter ATP-binding protein	GltR[26]
PA3188	4.98	-6.24	-1.26	*gltG*	sugar ABC transporter permease	GltR[26]
PA3190	5.60	0.23	5.83	*gltB*	sugar ABC transporter substrate-binding protein	GltR[26]
PA3192	1.78	-1.90	-0.12	*gltR*	response regulator GltR	nd
PA3193	1.79	-1.91	-0.12	*glk*	glucokinase	nd
PA3194	2.35	-3.07	-0.72	*edd*	phosphogluconate dehydratase	nd
PA3195	2.46	-3.04	-0.58	*gapA*	glyceraldehyde 3-phosphate dehydrogenase	nd
PA3560	2.40	-0.39	2.01	*fruA*	PTS system fructose-specific transporter subunit IIBC	FruR[27]
PA3561	2.38	0.16	2.55	*fruK*	1-phosphofructokinase	FruR[27]
PA3562	2.78	-0.25	2.53	*fruI*	PTS system fructose-specific transporter subunit FruI	FruR[27]
PA4496	-1.28	1.23	-0.05	*dppA1*	ABC transporter	nd
PA4588	1.74	0.36	2.09	*gdhA*	glutamate dehydrogenase	ArgR[25]
PA4710	1.31	-0.05	1.26	*phuR*	heme/hemoglobin uptake outer membrane receptor PhuR	Fur[28]
PA5152	-1.50	-0.27	-1.77		ABC transporter ATP-binding protein	ArgR[25]
PA5153	-1.18	0.26	-0.93		amino acid ABC transporter	ArgR[25]

[a]Red figures indicate statistically significant difference (Padj<0.05)
[b]Superscripts refer to bibliographic references. nd, not determined

Supplementary Table S4. DEGs encoding putative/known transcription regulators

Locus	Log2 FC[1]			Name	Description[2]
	PAO1+ *vs.* PAO1	GUN+ *vs.* PAO1+	GUN+ vs. PAO1		
PA0179	-0.34	1.44	1.10		TC response regulator
PA0527	0.82	-1.46	-0.64	*dnr*	transcriptional regulator Dnr
PA0547	-0.19	1.23	1.04		transcriptional regulator
PA0576	0.09	-1.21	-1.12	*rpoD*	sigma factor RpoD
PA0708	-0.25	1.90	1.65		transcriptional regulator
PA0893	-0.69	-0.69	-1.39	*argR*	transcriptional regulator ArgR
PA1196	0.86	-1.46	-0.61	*ddaR*	transcriptional regulator DdaR
PA2177	0.35	1.07	1.42		sensor/response regulator hybrid protein
PA2259[3]	1.55	-1.07	0.48	*ptxS*	PtxS transcriptional regulator
PA2320	1.88	-1.67	0.20	*gntR*	GntR transcriptional regulator
PA2572	-0.05	1.51	1.46		TC response regulator
PA3192	1.78	-1.90	-0.12	*gltR*	TC response regulator GltR
PA3308	-0.01	-0.99	-1.00	*hepA*	RNA polymerase-associated protein RapA
PA3477	-0.37	1.25	0.89	*rhlR*	transcriptional regulator RhlR
PA3622	-0.10	1.36	1.26	*rpoS*	sigma factor RpoS
PA4112	-0.19	1.56	1.37		sensor/response regulator hybrid protein
PA4296	-0.57	1.88	1.31	*pprB*	TC response regulator PprB
PA5105	-0.24	-2.55	-2.79	*hutC*	histidine utilization repressor HutC
PA5261	0.30	0.84	1.14	*algR*	TC response regulator AlgR
PA5380	-0.46	1.08	0.62	*gbdR*	protein GbdR

[1]Red figures indicate statistically significant difference (Padj<0.05)
[2]TC, Two-Component
[3]differential expression validated by qPCR

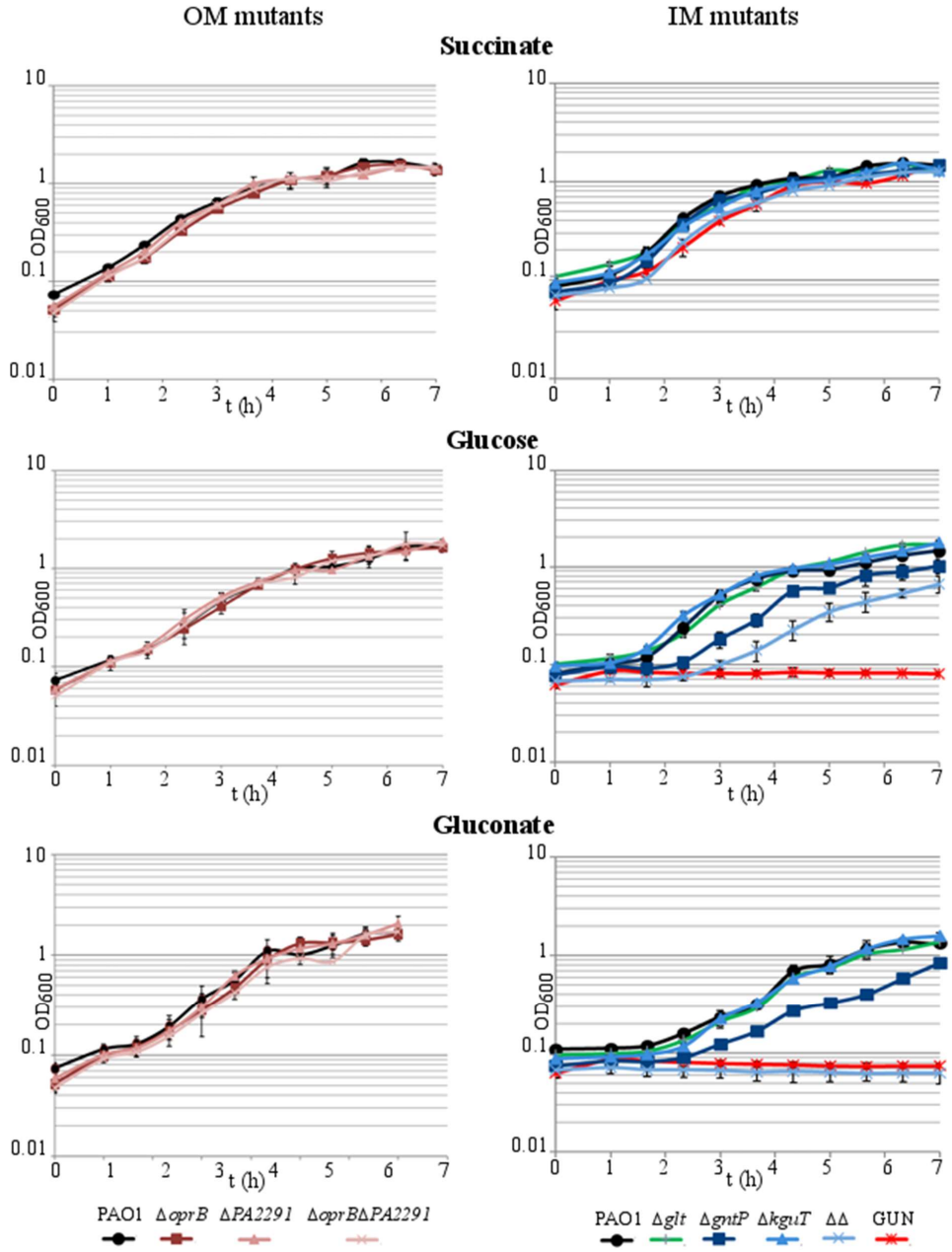

Fig. S1. Growth curves of glucose uptake mutants with different carbon source. Cultures of PAO1 and the indicated mutant strains were inoculated at the same OD_{600} in M9-Triton X-100 supplemented with 0.4% glucose, 0.4% gluconate or 0.5% succinate. The growth at 37°C was monitored every 40 min for 7 h. Symbols represent average (n=2) with SD of bacterial cell density (OD_{600}) at different time points. Generation time of PAO1 and IM mutants growing in the above media is reported in Table 1.

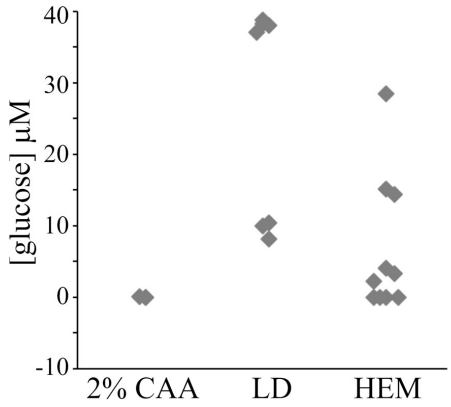

Fig. S2. Glucose concentration in bacterial media and *G. mellonella* hemolymph. Glucose concentration was estimated on 2% casamino acid stock solution (CAA; n=3); LD broth (LD; n=7) and *G. mellonella* hemolymph (HEM; n=10, each sample being a mix composed by 30 µl aliquots of hemolymph of 5 larvae). Diamonds indicate glucose concentration in individual samples.

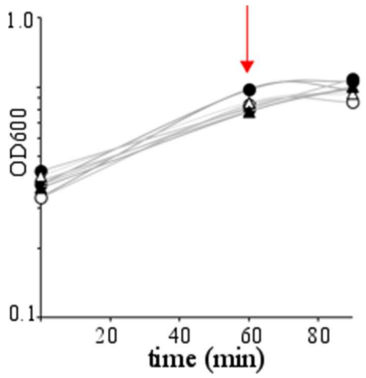

Fig. S3. Growth of cultures for RNA-Seq analysis. Independent cultures of PAO1 and GUN were grown in M9-CAA up to OD_{600}= 0.4. Glucose (0.4% (w/v) final concentration) was added and incubation at 37°C was protracted for 60 min before sampling the cultures for RNA extraction (red arrow). Triangle, PAO1; circle, GUN mutant. Empty symbols, no glucose added; black symbols, cultures supplemented with glucose.

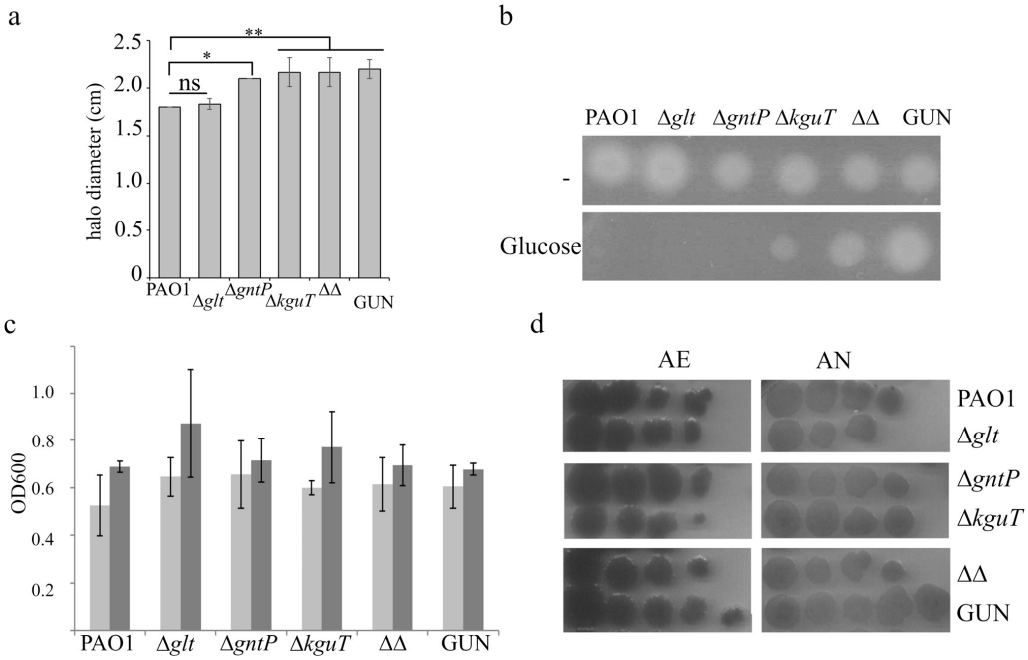

Fig. S4. *In vitro* phenotypic assays on glucose uptake mutants. In all panels, ΔΔ indicates PAO1 Δ*gntP* Δ*kguT* strain. Rhamnolipids (a) were measured as described in Supplementary Experimental procedures. Bars represent average (n=3) with SD. Significance was estimated with one-way Anova and Tukey post-hoc analysis, only the results of comparisons with PAO1 are reported (*, $P<0.05$; **, $P<0.01$; ns, not significant). Differences among Δ*kguT*, ΔΔ and GUN strains were not significant. b. Extracellular proteases from supernatants of cultures grown 17 h at 37°C in M9-CAA not supplemented (-) or supplemented with 0.4% glucose were detected by casein diffusion plate assay. The secretion of proteases is indicated by the formation of a white precipitate resulting from the hydrolysis of soluble casein to the insoluble *para*-casein derivative. The cultures were diluted to the same OD_{600} before the test. Three replicates gave comparable results. c. Growth in microaerophilic conditions. Light grey bars, cultures grown in M9-CAA; dark grey bars, cultures grown in LD. Bars represent average (n=3) with standard deviation. According to one-way Anova analysis, growth differences were not statistically significant at 0.05 level. d. Growth in anaerobiosis. Cultures were plated on LD-agar plates supplemented with 100 mM KNO_3 and incubated at 37 °C in aerobiosis (AE) for 16h or in anaerobiosis (AN) for 48h.

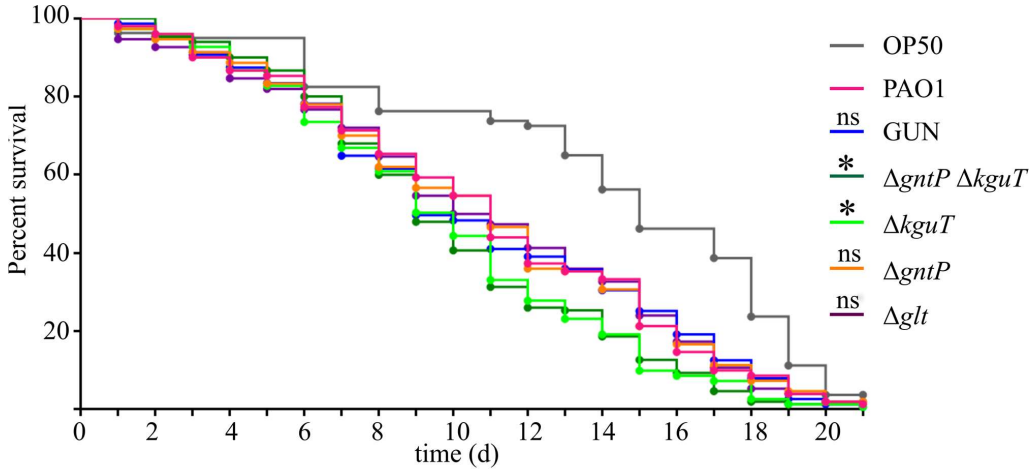

Fig. S5. *C. elegans* infection assay. Survival curves of *C. elegans* infected with glucose uptake mutants. Kaplan-Meyer curves represent results deriving from 3 independent experiments in which groups of 50 worms were fed on the indicated strains. OP50, *E. coli* strain. d, days post-infection. Significance was estimated with log-rank test; only the results relative to PAO1 are reported (*, P< 0.05; ns, not significant).

a

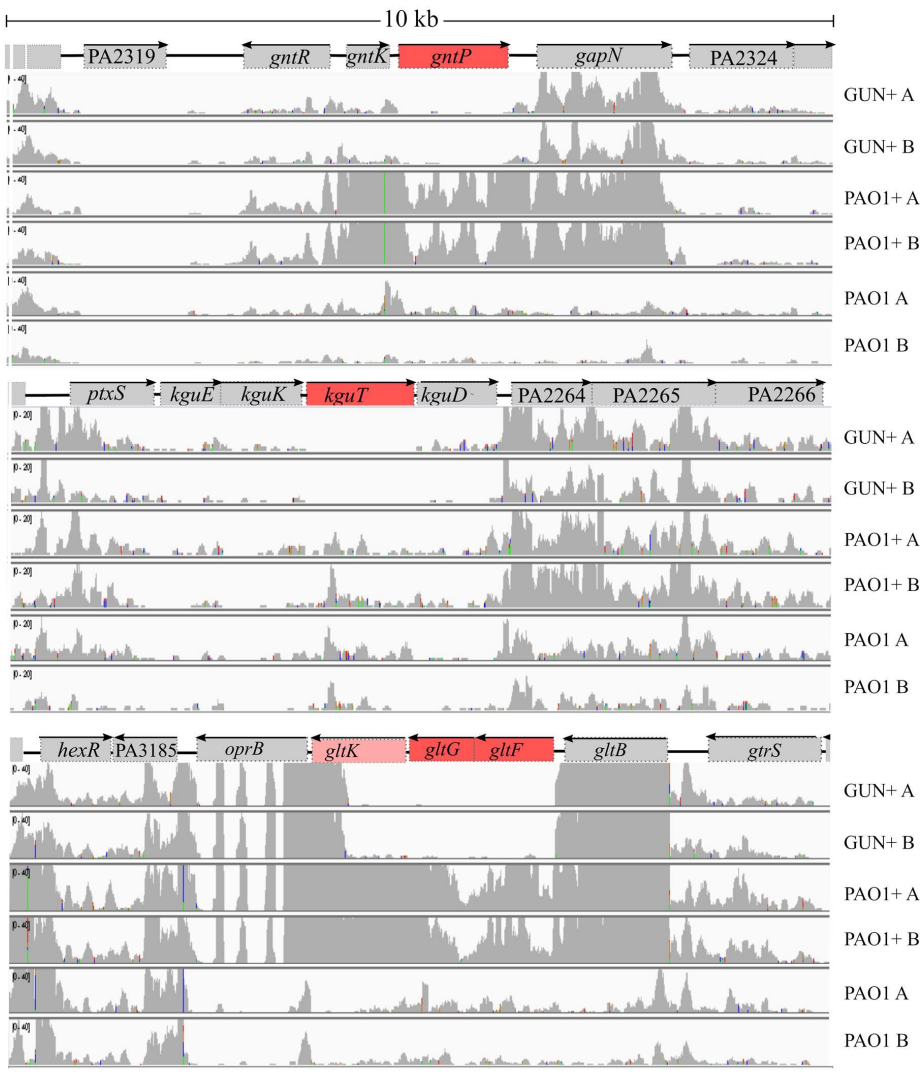
10 kb
PA2319
gntR
gntK
gntP
gapN
PA2324
GUN+ A
GUN+ B
PAO1+ A
PAO1+ B
PAO1 A
PAO1 B
ptxS
kguE
kguK
kguT
kguD
PA2264
PA2265
PA2266
GUN+ A
GUN+ B
PAO1+ A
PAO1+ B
PAO1 A
PAO1 B
hexR
PA3185
oprB
gltK
gltG
gltF
gltB
gtrS
GUN+ A
GUN+ B
PAO1+ A
PAO1+ B
PAO1 A
PAO1 B

b

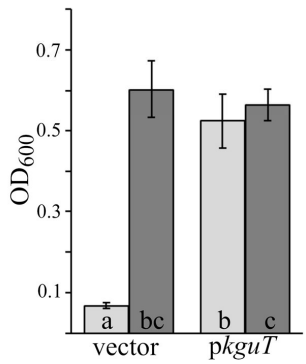
0.7
0.5
0.3
0.1
OD600
a
bc
b
c
vector
pkguT

Fig. S6. Polarity analysis of glucose uptake genes deletions. a. Transcriptional landscape of genomic regions encompassing the loci deleted in glucose uptake mutants. Illumina whole transcriptome reads per base in different strains/ conditions are reported below the map of the 10 kbp long genomic regions corresponding to deleted loci. Boxes, ORFs; lines, intergenic regions; arrows on top of boxes indicate the transcription direction. +, cultures supplemented with glucose; A and B, replicate samples analysed in the RNA-Seq experiment. b. Δ*kguT* mutation complementation assay. Cultures of PAO1 Δ*kguT* carrying either pGM931 (vector) or pGM2071 (p*kguT*) were inoculated in M9-Triton X-100-carbenicillin-arabinose supplemented with 0.1% 2-ketogluconate (light grey bars) or 0.5% succinate (dark grey bars). The cultures were incubated at 37°C and the OD_{600} was measured after 24 h. The bars represent average (n=3) with SD. Significance was evaluated with one-way Anova and Tukey post hoc test. Differences between means that share a letter (on the columns) are not statistically significant at 0.05 level.

Supplementary Table S5. Differentially expressed genes in GUN *vs* . PAO1 (10 min after glucose addition)

	Log$_2$ Fold Change[1]				
Locus[2]	**GUN+ *vs.* PAO1+**	**GUN+ *vs.* PAO1**	**PAO1+ *vs.* PAO1**	**Name**	**Description**
PA0023	-0,79	-1,28	-0,49	qor	oxygen-dependent quinone oxidoreductase
PA0038	-0,76	-1,09	-0,33	NA	hypothetical protein
PA0039	0,64	-0,63	-1,27	NA	hypothetical protein
PA0045	1,22	1,19	-0,03	NA	hypothetical protein
PA0046	1,24	1,06	-0,18	NA	hypothetical protein
PA0048	-0,99	-1,20	-0,21	NA	transcriptional regulator
PA0050	2,19	1,31	-0,88	NA	hypothetical protein
PA0059	-1,69	-1,45	0,24	osmC	osmotically inducible protein OsmC
PA0060	-0,53	-1,13	-0,60	NA	hypothetical protein
PA0085	0,21	-1,34	-1,55	hcp1	protein secretion apparatus assembly protein
PA0102	1,01	0,85	-0,16	NA	carbonic anhydrase
PA0103	1,54	2,19	0,65	NA	sulfate transporter
PA0115	-0,70	-1,23	-0,53	elaA	hypothetical protein
PA0118	-1,03	-0,86	0,17	NA	hypothetical protein
PA0119	-1,07	-1,69	-0,62	NA	C4-dicarboxylate transporter DctA
PA0120	-0,80	-1,01	-0,22	NA	transcriptional regulator
PA0121	-0,79	-1,36	-0,57	NA	hypothetical protein
PA0122	2,12	1,79	-0,33	rahU	hypothetical protein
PA0127	-0,97	-1,60	-0,63	NA	hypothetical protein
PA0130	-0,77	-1,18	-0,41	bauC	3-oxopropanoate dehydrogenase
PA0131	-0,85	-1,36	-0,51	bauB	beta-alanine degradation protein BauB
PA0132	-0,70	-1,42	-0,72	bauA	beta alanine--pyruvate transaminase
PA0147	-0,52	-1,02	-0,50	NA	oxidoreductase
PA0161	1,22	1,74	0,52	NA	NA
PA0162	1,89	2,41	0,52	opdC	histidine porin OpdC
PA0165	0,91	1,84	0,93	NA	hypothetical protein
PA0168	-0,90	-1,45	-0,55	yigZ	hypothetical protein
PA0169	1,09	1,53	0,44	siaD	hypothetical protein
PA0170	0,69	1,29	0,61	NA	hypothetical protein
PA0171	1,20	2,05	0,85	NA	hypothetical protein
PA0172	0,63	1,30	0,67	siaA	hypothetical protein
PA0192	0,77	1,69	0,93	NA	TonB-dependent receptor
PA0195	2,02	2,65	0,63	pntAA	NAD(P) transhydrogenase subunit alpha
PA0196	1,30	1,58	0,27	pntB	pyridine nucleotide transhydrogenase subunit beta
PA0200	0,90	1,10	0,20	NA	hypothetical protein
PA0208	2,44	2,83	0,39	mdcA	malonate decarboxylase subunit alpha
PA0209	1,73	2,14	0,41	mdcB	2-(5"-triphosphoribosyl)-3'-dephosphocoenzyme-A synthase
PA0211	2,11	2,00	-0,11	mdcD	malonate decarboxylase subunit beta
PA0213	2,06	1,69	-0,37	mdcG	phosphoribosyl-dephospho-CoA transferase
PA0214	2,49	2,06	-0,43	mdcH	acyl transferase
PA0226	-1,13	-1,61	-0,48	NA	CoA transferase subunit A
PA0227	-1,03	-1,30	-0,27	pcaJ	CoA transferase subunit B
PA0228	-0,82	-1,09	-0,27	pcaF	beta-ketoadipyl CoA thiolase
PA0229	-1,06	-1,35	-0,30	pcaT	dicarboxylic acid transporter PcaT
PA0231	-1,19	-1,47	-0,28	pcaD	3-oxoadipate enol-lactonase
PA0232	-1,10	-1,31	-0,21	pcaC	4-carboxymuconolactone decarboxylase
PA0248	-0,60	-1,56	-0,96	pobR	transcriptional regulator
PA0250	-0,60	-1,26	-0,66	NA	hypothetical protein
PA0252	0,50	1,64	1,14	NA	hypothetical protein
PA0258	-0,69	-1,07	-0,38	NA	hypothetical protein
PA0265	-1,81	-2,04	-0,23	davD	glutarate-semialdehyde dehydrogenase DavD
PA0266	-1,92	-2,19	-0,26	davT	5-aminovalerate aminotransferase DavT
PA0277	1,51	1,76	0,26	NA	hypothetical protein
PA0290	-0,56	-1,01	-0,45	NA	hypothetical protein
PA0296	-1,70	-2,07	-0,37	spuI	glutamine synthetase
PA0297	-2,34	-2,43	-0,09	spuA	glutamine amidotransferase
PA0298	-2,22	-2,60	-0,38	spuB	glutamine synthetase
PA0299	-2,11	-2,75	-0,64	spuC	aminotransferase
PA0300	-1,46	-1,96	-0,51	spuD	putrescine ABC transporter substrate-binding protein SpuD
PA0301	-1,32	-1,55	-0,23	spuE	spermidine ABC transporter substrate-binding protein SpuE
PA0302	-1,54	-1,82	-0,28	spuF	polyamine transporter PotG
PA0303	-1,77	-2,03	-0,26	spuG	polyamine transporter PotH
PA0304	-1,58	-2,05	-0,47	spuH	polyamine transporter PotI
PA0312	-0,67	-1,24	-0,57	NA	hypothetical protein
PA0321	-0,95	-1,45	-0,50	NA	acetylpolyamine aminohydrolase
PA0328	-1,31	-1,98	-0,67	aaaA	hypothetical protein
PA0329	-0,51	-1,76	-1,25	NA	hypothetical protein
PA0355	-2,29	-2,51	-0,22	pfpI	protease PfpI
PA0358	0,42	1,06	0,64	NA	hypothetical protein
PA0382	1,07	1,31	0,25	micA	tRNA (guanine-N(7)-)-methyltransferase
PA0425	0,62	1,64	1,02	mexA	multidrug resistance protein MexA
PA0426	0,72	1,59	0,86	mexB	multidrug resistance protein MexB
PA0427	0,92	1,97	1,05	oprM	outer membrane protein OprM
PA0430	0,87	1,20	0,34	metF	5,10-methylenetetrahydrofolate reductase
PA0431	1,24	1,63	0,39	NA	hypothetical protein
PA0432	0,96	1,21	0,25	sahH	adenosylhomocysteinase
PA0434	0,51	1,81	1,31	NA	hypothetical protein
PA0437	0,59	1,04	0,44	codA	cytosine deaminase
PA0438	0,82	1,36	0,54	codB	cytosine permease

PA0439	0,85	1,77	0,91	dypB	dihydropyrimidine dehydrogenase
PA0446	-0,38	0,93	1,31	NA	hypothetical protein
PA0447	-0,60	0,53	1,13	gcdH	glutaryl-CoA dehydrogenase
PA0456	-0,52	-1,29	-0,77	NA	cold-shock protein
PA0460	-0,95	-1,80	-0,85	NA	hypothetical protein
PA0461	-0,54	-1,02	-0,48	yihG	acyltransferase
PA0462	-0,60	-1,10	-0,50	NA	hypothetical protein
PA0465	0,57	1,53	0,97	creD	hypothetical protein
PA0466	0,56	1,91	1,35	NA	hypothetical protein
PA0470	0,32	1,70	1,39	fiuA	ferrichrome receptor FiuA
PA0475	-0,55	-1,50	-0,96	NA	transcriptional regulator
PA0484	-0,12	-1,26	-1,13	NA	hypothetical protein
PA0490	-0,51	-1,41	-0,90	NA	hypothetical protein
PA0505	-0,33	-1,19	-0,86	NA	hypothetical protein
PA0513	0,77	1,80	1,03	nirG	heme d1 biosynthesis protein NirG
PA0519	0,74	1,34	0,60	nirS	nitrite reductase
PA0527	1,04	1,86	0,82	dnr	transcriptional regulator Dnr
PA0546	1,54	1,58	0,04	metK	S-adenosylmethionine synthetase
PA0547	1,29	1,85	0,56	NA	transcriptional regulator
PA0567	-1,11	-1,38	-0,27	yqaE	hypothetical protein
PA0574	-1,00	-1,45	-0,46	NA	hypothetical protein
PA0578	0,60	1,20	0,60	NA	hypothetical protein
PA0579	0,68	1,23	0,55	rpsU	30S ribosomal protein S21
PA0580	0,82	1,55	0,73	gcp	tRNA N6-adenosine threonylcarbamoyltransferase
PA0599	-0,77	-1,05	-0,28	NA	hypothetical protein
PA0602	-0,86	-1,41	-0,54	NA	ABC transporter
PA0603	-2,38	-2,62	-0,24	agtA	ABC transporter ATP-binding protein
PA0604	-2,57	-2,69	-0,13	agtB	ABC transporter
PA0605	-1,90	-1,57	0,33	agtC	ABC transporter permease
PA0606	-1,08	-1,42	-0,34	agtD	ABC transporter permease
PA0639	0,68	1,08	0,41	NA	hypothetical protein
PA0648	-0,63	-1,15	-0,52	NA	hypothetical protein
PA0654	1,13	2,19	1,06	speD	S-adenosylmethionine decarboxylase
PA0656	-0,15	-1,20	-1,05	ycfF	HIT family protein
PA0708	-1,22	-2,56	-1,34	NA	transcriptional regulator
PA0709	1,24	1,65	0,41	NA	hypothetical protein
PA0710	1,12	2,02	0,90	gloA2	lactoylglutathione lyase
PA0713	1,02	2,25	1,23	NA	hypothetical protein
PA0714	1,51	1,74	0,23	NA	hypothetical protein
PA0715	-0,75	-1,03	-0,28	NA	hypothetical protein
PA0730	1,37	1,84	0,47	NA	(R)-3-hydroxydecanoyl-ACP:CoA transacylase
PA0732	-0,75	-1,45	-0,70	NA	hypothetical protein
PA0736	-0,53	-1,13	-0,60	NA	hypothetical protein
PA0744	-1,34	-1,47	-0,13	NA	enoyl-CoA hydratase
PA0745	-1,20	-1,52	-0,32	NA	enoyl-CoA hydratase
PA0746	-1,09	-0,99	0,10	NA	acyl-CoA dehydrogenase
PA0747	-1,14	-1,61	-0,46	NA	aldehyde dehydrogenase
PA0754	-0,97	-1,23	-0,27	NA	hypothetical protein
PA0755	-0,85	-1,16	-0,30	opdH	cis-aconitate porin OpdH
PA0765	-0,70	-1,16	-0,46	mucC	positive regulator for alginate biosynthesis MucC
PA0767	0,44	1,22	0,78	lepA	elongation factor 4
PA0768	0,51	1,08	0,57	lepB	signal peptidase I
PA0771	0,63	1,21	0,58	era	GTPase Era
PA0775	0,73	1,62	0,89	yecO	tRNA (cmo5U34)-methyltransferase
PA0779	-0,87	-2,13	-1,26	asrA	ATP-dependent protease
PA0781	0,76	2,41	1,65	NA	hypothetical protein
PA0788	0,78	1,34	0,56	NA	hypothetical protein
PA0789	-0,51	-1,34	-0,82	NA	amino acid permease
PA0792	-1,51	-1,68	-0,17	prpD	2-methylcitrate dehydratase
PA0793	-1,40	-1,86	-0,46	NA	hypothetical protein
PA0794	-1,79	-2,05	-0,26	NA	aconitate hydratase
PA0795	-1,67	-1,84	-0,16	prpC	methylcitrate synthase
PA0796	-1,58	-1,66	-0,08	prpB	2-methylisocitrate lyase
PA0797	-1,95	-1,77	0,18	NA	transcriptional regulator
PA0799	0,39	1,12	0,73	NA	helicase
PA0805	-0,49	-1,26	-0,76	NA	hypothetical protein
PA0815	-0,82	-1,42	-0,61	NA	transcriptional regulator
PA0820	-0,60	-1,13	-0,53	NA	hypothetical protein
PA0822	-0,73	-1,25	-0,52	NA	NA
PA0831	-1,01	-1,34	-0,33	oruR	ornithine utilization transcriptional regulator OruR
PA0833	-0,60	-1,18	-0,58	NA	hypothetical protein
PA0834	0,30	1,01	0,71	NA	acyltransferase
PA0839	-0,88	-1,09	-0,21	NA	transcriptional regulator
PA0840	-0,54	-1,20	-0,66	NA	oxidoreductase
PA0846	-0,79	-1,07	-0,28	cysZ	sulfate transporter CysZ
PA0852	1,59	1,70	0,12	cbpD	chitin-binding protein CbpD
PA0852.1	1,59	1,78	0,19	NA	NA
PA0857	-0,67	-1,15	-0,49	bolA	morphogene protein BolA
PA0862	-0,71	-1,15	-0,43	NA	hypothetical protein
PA0866	-1,28	-1,88	-0,60	aroP2	aromatic amino acid transporter AroP
PA0867	-0,73	-1,18	-0,45	mliC	lysozyme inhibitor
PA0886	-0,04	1,71	1,75	dctM	C4-dicarboxylate transporter
PA0887	-1,62	-4,00	-2,37	acsA	acetyl-CoA synthetase

PA0895	-1,38	-1,69	-0,31	aruC	acetylornithine aminotransferase
PA0896	-1,08	-1,27	-0,19	aruF	arginine N-succinyltransferase subunit alpha
PA0897	-1,27	-1,22	0,05	aruG	arginine N-succinyltransferase subunit beta
PA0898	-1,42	-1,60	-0,18	aruD	N-succinylglutamate 5-semialdehyde dehydrogenase
PA0899	-1,35	-1,65	-0,30	aruB	N-succinylarginine dihydrolase
PA0900	-0,98	-1,32	-0,33	NA	hypothetical protein
PA0901	-0,98	-1,30	-0,32	aruE	succinylglutamate desuccinylase
PA0906	-0,83	-1,24	-0,41	alpR	transcriptional regulator
PA0915	1,86	2,79	0,93	yehS	hypothetical protein
PA0916	1,59	2,55	0,96	yliG	ribosomal protein S12 methylthiotransferase RimO
PA0923	0,08	1,18	1,10	dinB	DNA polymerase IV
PA0945	0,60	1,04	0,44	purM	phosphoribosylformylglycinamidine cyclo-ligase
PA0947	0,17	1,02	0,85	NA	DNA replication initiation factor
PA0954	-0,84	-1,12	-0,27	NA	acylphosphatase
PA0958	-1,36	-1,85	-0,48	oprD	porin D
PA0968	0,63	1,18	0,55	ybgC	hypothetical protein
PA0975	1,06	1,52	0,46	NA	radical activating enzyme
PA0976	1,10	0,50	-0,61	NA	7-cyano-7-deazaguanine synthase
PA0982	-0,49	-1,10	-0,61	NA	hypothetical protein
PA0988	-0,88	-1,43	-0,55	NA	hypothetical protein
PA1001	0,94	1,32	0,38	phnA	anthranilate synthase component I
PA1002	1,08	0,91	-0,17	phnB	anthranilate synthase component II
PA1035	-0,81	-1,28	-0,47	NA	hypothetical protein
PA1048	-0,38	-1,04	-0,66	NA	hypothetical protein
PA1053	0,51	1,14	0,62	slyB	hypothetical protein
PA1070	-1,19	-1,65	-0,46	braG	ABC transporter ATP-binding protein
PA1071	-1,04	-1,01	0,04	braF	ABC transporter ATP-binding protein
PA1072	-1,14	-1,45	-0,32	braE	branched-chain amino acid ABC transporter permease BraE
PA1073	-0,85	-1,66	-0,81	braD	branched-chain amino acid ABC transporter permease BraD
PA1074	-1,03	-1,62	-0,60	braC	branched-chain amino acid ABC transporter substrate-binding protein BraC
PA1100	-0,59	-1,27	-0,68	fliE	flagellar hook-basal body complex protein FliE
PA1116	0,93	1,33	0,40	NA	hypothetical protein
PA1124	-0,61	-1,19	-0,58	dgt	deoxyguanosinetriphosphate triphosphohydrolase
PA1127	-0,63	-1,08	-0,45	gsp69	oxidoreductase
PA1140	-0,79	-1,21	-0,42	ylbA	hypothetical protein
PA1152	0,60	1,10	0,50	NA	NA
PA1159	-0,88	-2,16	-1,28	NA	cold-shock protein
PA1168	1,92	1,70	-0,22	NA	hypothetical protein
PA1169	1,47	1,28	-0,19	NA	arachidonate 15-lipoxygenase
PA1181	1,17	1,42	0,25	yegE	sensor protein
PA1189	0,70	1,43	0,73	NA	Zn-dependent metalloprotease
PA1190	-0,93	-1,39	-0,46	yohC	hypothetical protein
PA1203	-1,21	-1,54	-0,32	NA	hypothetical protein
PA1204	-0,94	-1,47	-0,52	yieF	NAD(P)H-dependent FMN reductase
PA1205	-1,11	-1,66	-0,55	NA	quercetin 2,3-dioxygenase
PA1213	1,43	2,12	0,69	NA	hypothetical protein
PA1214	1,38	2,00	0,61	NA	hypothetical protein
PA1215	1,62	2,38	0,76	NA	hypothetical protein
PA1216	2,23	2,54	0,32	NA	hypothetical protein
PA1217	2,08	2,44	0,36	NA	2-isopropylmalate synthase
PA1218	1,75	2,02	0,27	NA	hypothetical protein
PA1221	1,16	0,82	-0,34	NA	hypothetical protein
PA1228	1,17	1,78	0,61	NA	hypothetical protein
PA1249	0,64	1,04	0,40	aprA	alkaline metalloproteinase
PA1260	-0,87	-1,44	-0,57	lhpP	amino acid ABC transporter substrate-binding protein
PA1273	0,50	1,13	0,63	cobB	hydrogenobyrinate a,c-diamide synthase
PA1302	0,65	2,16	1,51	hxuC	heme utilization protein
PA1317	4,64	6,34	1,70	cyoA	cytochrome o ubiquinol oxidase subunit II
PA1318	4,55	5,97	1,42	cyoB	cytochrome o ubiquinol oxidase subunit I
PA1319	3,79	5,11	1,32	cyoC	cytochrome o ubiquinol oxidase subunit III
PA1320	3,29	4,12	0,83	cyoD	cytochrome o ubiquinol oxidase subunit IV
PA1321	3,18	3,74	0,56	cyoE	protoheme IX farnesyltransferase
PA1322	0,39	1,30	0,92	pfuA	TonB-dependent receptor
PA1323	-1,01	-0,69	0,31	NA	hypothetical protein
PA1324	-1,17	-1,07	0,10	NA	hypothetical protein
PA1337	-1,19	-2,16	-0,97	ansB	glutaminase-asparaginase
PA1338	-0,68	-2,37	-1,69	ggt	gamma-glutamyltranspeptidase
PA1339	-0,37	-1,52	-1,14	aatP	amino acid ABC transporter ATP binding protein
PA1340	-0,32	-1,57	-1,25	aatM	amino acid ABC transporter permease
PA1341	-0,07	-1,53	-1,47	aatQ	amino acid ABC transporter permease
PA1342	-0,95	-1,77	-0,82	aatJ	ABC transporter
PA1343	0,57	1,37	0,80	NA	hypothetical protein
PA1373	0,84	1,37	0,53	fabF2	3-oxoacyl-ACP synthase
PA1376	-0,88	-1,16	-0,27	aceK	bifunctional isocitrate dehydrogenase kinase/phosphatase
PA1377	-0,64	-1,28	-0,65	yhhY	hypothetical protein
PA1401	-1,03	-1,30	-0,27	NA	hypothetical protein
PA1414	1,27	1,50	0,23	NA	hypothetical protein
PA1418	-0,94	-1,51	-0,57	NA	sodium:solute symport protein
PA1419	-1,84	-2,07	-0,22	NA	transporter
PA1420	-1,83	-2,26	-0,43	NA	hypothetical protein
PA1421	-2,02	-2,20	-0,18	gbuA	guanidinobutyrase
PA1422	1,08	1,60	0,51	gbuR	protein GbuR
PA1425	1,86	1,52	-0,33	NA	ABC transporter ATP-binding protein

PA1427	1,00	1,98	0,98	NA	NA
PA1471	-0,54	-1,23	-0,69	NA	hypothetical protein
PA1476	0,67	1,34	0,67	ccmB	heme exporter protein CcmB
PA1478	0,91	1,17	0,27	helD	heme exporter protein CcmD
PA1479	0,86	1,30	0,44	ccmE	cytochrome c-type biogenesis protein CcmE
PA1481	0,96	1,27	0,31	ccmG	cytochrome c-type biogenesis protein CcmG
PA1483	0,98	1,36	0,38	cycH	cytochrome c-type biogenesis protein CycH
PA1499	0,52	1,94	1,42	NA	hypothetical protein
PA1535	-0,91	-1,69	-0,77	NA	acyl-CoA dehydrogenase
PA1546	1,55	2,00	0,44	hemN	oxygen-independent coproporphyrinogen-III oxidase
PA1549	1,49	1,24	-0,26	fixI	cation-transporting P-type ATPase
PA1550	1,48	1,65	0,17	NA	hypothetical protein
PA1551	1,45	2,04	0,59	fixG	ferredoxin
PA1552	1,56	2,35	0,79	ccoP1	cytochrome C oxidase cbb3-type subunit CcoP
PA1552.1	1,54	1,81	0,27	ccoQ1	cytochrome C oxidase cbb3-type subunit CcoQ
PA1553	1,52	1,91	0,39	ccoO1	cbb3-type cytochrome C oxidase subunit II
PA1554	1,64	2,34	0,70	ccoN1	cbb3-type cytochrome C oxidase subunit I
PA1555	2,48	1,86	-0,62	ccoP2	cytochrome C oxidase cbb3-type subunit CcoP
PA1555.1	1,77	1,87	0,10	ccoQ2	cytochrome C oxidase cbb3-type subunit CcoQ
PA1556	1,99	2,04	0,06	ccoO2	cbb3-type cytochrome C oxidase subunit II
PA1557	2,09	2,46	0,37	ccoN2	cbb3-type cytochrome C oxidase subunit I
PA1577	1,84	1,06	-0,78	NA	hypothetical protein
PA1578	1,29	1,64	0,35	NA	hypothetical protein
PA1579	-0,14	-1,02	-0,88	NA	hypothetical protein
PA1584	1,05	1,09	0,04	sdhB	succinate dehydrogenase iron-sulfur subunit
PA1591	1,36	1,96	0,60	NA	hypothetical protein
PA1592	-0,61	-1,31	-0,70	NA	hypothetical protein
PA1596	-0,45	-1,61	-1,15	htpG	chaperone protein HtpG
PA1597	-1,33	-2,27	-0,94	NA	hypothetical protein
PA1608	0,56	1,05	0,50	NA	chemotaxis transducer
PA1609	1,31	1,41	0,11	fabB	3-oxoacyl-ACP synthase
PA1610	1,38	1,32	-0,06	fabA	3-hydroxydecanoyl-ACP dehydratase
PA1617	-1,75	-3,31	-1,56	NA	AMP-binding protein
PA1618	-0,62	-1,22	-0,60	ybdB	esterase
PA1634	1,63	1,58	-0,05	kdpB	potassium-transporting ATPase subunit B
PA1641	-0,45	-1,10	-0,66	NA	hypothetical protein
PA1655	-0,75	-1,01	-0,26	NA	glutathione S-transferase
PA1656	1,01	0,82	-0,18	hsiA2	hypothetical protein
PA1657	1,35	1,28	-0,07	hsiB2	hypothetical protein
PA1658	1,21	1,07	-0,13	hsiC2	hypothetical protein
PA1660	0,88	1,21	0,33	hsiG2	hypothetical protein
PA1661	1,32	1,16	-0,16	hsiH2	hypothetical protein
PA1662	1,23	0,97	-0,26	clpV2	ClpA/B-type protease
PA1663	1,01	1,39	0,38	sfa2	transcriptional regulator
PA1666	1,29	1,10	-0,19	lip2	hypothetical protein
PA1667	1,16	0,85	-0,31	hsiJ2	hypothetical protein
PA1668	1,52	1,16	-0,36	dotU2	hypothetical protein
PA1669	1,18	1,04	-0,14	icmF2	hypothetical protein
PA1673	1,23	1,23	-0,01	NA	bacteriohemerythrin
PA1687	1,05	1,64	0,60	speE	polyamine aminopropyltransferase
PA1688	0,66	1,22	0,55	NA	hypothetical protein
PA1689	0,64	1,22	0,58	NA	hypothetical protein
PA1697	1,11	1,86	0,75	pscN	type III secretion system ATPase
PA1698	0,70	1,61	0,91	popN	type III secretion outer membrane protein PopN
PA1712	1,04	1,08	0,04	exsB	exoenzyme S synthesis protein ExsB
PA1717	1,01	1,63	0,63	pscD	type III export protein PscD
PA1718	1,01	1,55	0,54	pscE	type III export protein PscE
PA1719	0,77	1,02	0,26	pscF	type III export protein PscF
PA1721	0,22	1,45	1,23	pscH	type III export protein PscH
PA1727	0,62	1,25	0,64	mucR	signaling protein
PA1742	-2,07	-2,55	-0,48	pauD2	amidotransferase
PA1746	0,52	1,19	0,67	NA	hypothetical protein
PA1749	-0,65	-1,25	-0,60	NA	hypothetical protein
PA1751	-0,64	-1,15	-0,51	NA	hypothetical protein
PA1757	0,40	1,02	0,63	thrH	phosphoserine phosphatase
PA1759	-1,16	-1,91	-0,75	NA	transcriptional regulator
PA1760	-1,25	-1,39	-0,14	NA	transcriptional regulator
PA1761	-1,09	-1,97	-0,88	NA	hypothetical protein
PA1762	-1,15	-1,66	-0,51	NA	hypothetical protein
PA1763	-0,70	-1,29	-0,59	NA	hypothetical protein
PA1768	0,42	1,21	0,79	NA	hypothetical protein
PA1774	2,27	2,14	-0,14	crfX	hypothetical protein
PA1775	1,46	1,71	0,25	cmpX	hypothetical protein
PA1781	1,05	2,25	1,20	nirB	assimilatory nitrite reductase large subunit
PA1791	1,22	1,76	0,53	NA	hypothetical protein
PA1796	0,33	1,05	0,71	folD	bifunctional 5,10-methylene-tetrahydrofolate dehydrogenase/cyclohydrolase
PA1812	0,62	1,28	0,66	mltD	membrane-bound lytic murein transglycosylase D
PA1817	-0,95	-1,18	-0,23	NA	hypothetical protein
PA1818	-1,56	-2,00	-0,44	ldcA	lysine-specific pyridoxal 5'-phosphate-dependent carboxylase LdcA
PA1819	-1,11	-1,85	-0,74	yjdE	amino acid permease
PA1837	0,71	1,11	0,41	NA	hypothetical protein
PA1838	0,77	1,15	0,38	cysI	sulfite reductase
PA1839	1,08	1,75	0,67	NA	RNA methyltransferase

PA1852	2,84	2,96	0,12	NA	hypothetical protein
PA1854	0,24	1,72	1,48	NA	hypothetical protein
PA1856	0,78	1,97	1,19	NA	cbb3-type cytochrome C oxidase subunit I
PA1866	0,64	1,39	0,75	NA	hypothetical protein
PA1868	0,75	1,73	0,98	xqhA	secretion protein XqhA
PA1869	2,21	1,89	-0,32	NA	acyl carrier protein
PA1871	1,19	1,44	0,24	lasA	protease LasA
PA1874	0,93	1,44	0,52	NA	hypothetical protein
PA1885	-1,01	-1,47	-0,46	NA	hypothetical protein
PA1892	1,68	2,04	0,36	NA	hypothetical protein
PA1893	1,83	2,16	0,32	NA	hypothetical protein
PA1894	2,23	2,56	0,33	NA	hypothetical protein
PA1895	2,20	2,85	0,65	NA	hypothetical protein
PA1896	1,95	2,42	0,46	NA	hypothetical protein
PA1897	2,00	2,07	0,07	NA	hypothetical protein
PA1899	3,38	3,49	0,11	phzA2	phenazine biosynthesis protein PhzA
PA1900	4,22	4,58	0,36	phzB2	phenazine biosynthesis protein PhzB
PA1909	1,14	1,72	0,58	NA	hypothetical protein
PA1910	0,88	1,91	1,03	femA	ferric-mycobactin receptor FemA
PA1914	1,25	1,53	0,29	hvn	hypothetical protein
PA1920	0,90	2,14	1,24	nrdD	anaerobic ribonucleoside triphosphate reductase
PA1923	0,81	1,68	0,88	NA	cobaltochelatase subunit CobN
PA1926	1,02	1,33	0,31	ycaO	hypothetical protein
PA1941	-0,46	-1,02	-0,56	NA	hypothetical protein
PA1946	-0,92	-1,77	-0,85	rbsB	ribose ABC transporter substrate-binding protein
PA1947	-0,80	-1,37	-0,57	rbsA	ribose transporter RbsA
PA1950	-0,68	-1,19	-0,51	rbsK	ribokinase
PA1952	0,10	1,71	1,61	fapE	hypothetical protein
PA1954	0,78	1,66	0,87	fapC	hypothetical protein
PA1959	0,92	1,32	0,40	bacA	undecaprenyl-diphosphatase
PA1963	-0,69	-1,47	-0,78	NA	hypothetical protein
PA1964	1,04	1,73	0,69	ybiT	ABC-F family ATPase
PA1970	0,02	-1,59	-1,61	NA	hypothetical protein
PA1972	1,08	2,21	1,13	NA	hypothetical protein
PA1974	0,47	2,62	2,15	NA	hypothetical protein
PA1982	0,64	1,35	0,71	exaA	quinoprotein ethanol dehydrogenase
PA1991	-0,83	-1,58	-0,75	NA	iron-containing alcohol dehydrogenase
PA1992	-1,05	-1,55	-0,49	ercS	sensor histidine kinase
PA1996	0,49	1,47	0,98	ppiC1	peptidyl-prolyl cis-trans isomerase C1
PA1999	-1,39	-2,00	-0,61	dhcA	dehydrocarnitine CoA transferase subunit A
PA2000	-1,38	-1,94	-0,57	dhcB	dehydrocarnitine CoA transferase subunit B
PA2001	-1,07	-1,15	-0,08	atoB	acetyl-CoA acetyltransferase
PA2002	-1,20	-1,58	-0,37	atoE	hypothetical protein
PA2006	-1,00	-1,29	-0,29	NA	major facilitator superfamily transporter
PA2011	-1,25	-1,52	-0,27	liuE	3-hydroxy-3-isohexenylglutaryl-CoA/hydroxy-methylglutaryl-CoA lyase
PA2012	-1,55	-1,79	-0,24	liuD	methylcrotonyl-CoA carboxylase subunit alpha
PA2013	-1,64	-1,74	-0,10	liuC	gamma-carboxygeranoyl-CoA hydratase
PA2014	-1,62	-1,85	-0,23	liuB	methylcrotonyl-CoA carboxylase subunit beta
PA2015	-1,56	-1,76	-0,20	liuA	isovaleryl-CoA dehydrogenase
PA2016	-1,61	-1,89	-0,28	liuR	liu genes regulator
PA2018	2,54	2,34	-0,20	mexY	multidrug efflux protein
PA2019	2,47	3,00	0,52	mexX	multidrug efflux lipoprotein
PA2031	0,95	1,16	0,21	NA	hypothetical protein
PA2040	-2,85	-3,20	-0,35	pauA4	glutamine synthetase
PA2041	-3,12	-3,63	-0,51	NA	amino acid permease
PA2057	0,45	1,54	1,09	sppR	hypothetical protein
PA2069	2,74	2,58	-0,16	NA	carbamoyl transferase
PA2070	0,91	2,12	1,21	NA	hypothetical protein
PA2076	0,71	1,36	0,65	NA	transcriptional regulator
PA2079	-1,57	-2,03	-0,47	NA	amino acid permease
PA2080	-1,17	-1,14	0,03	kynU	kynureninase KynU
PA2081	-1,11	-1,13	-0,02	kynB	kynurenine formamidase KynB
PA2082	-0,84	-1,38	-0,54	kynR	transcriptional regulator
PA2089	0,47	1,82	1,35	NA	hypothetical protein
PA2119	1,58	1,70	0,12	adh	alcohol dehydrogenase
PA2130	0,37	2,31	1,94	cupA3	usher CupA3
PA2131	1,00	2,24	1,23	cupA4	fimbrial subunit CupA4
PA2152	0,29	1,76	1,47	NA	trehalose synthase
PA2160	0,78	1,53	0,75	glgX	glycosyl hydrolase
PA2179	0,60	1,75	1,16	NA	hypothetical protein
PA2189	0,72	2,63	1,91	NA	hypothetical protein
PA2193	3,77	3,96	0,18	hcnA	hydrogen cyanide synthase subunit HcnA
PA2194	3,34	3,62	0,28	hcnB	hydrogen cyanide synthase subunit HcnB
PA2195	3,36	3,71	0,34	hcnC	hydrogen cyanide synthase subunit HcnC
PA2196	1,10	1,39	0,29	NA	transcriptional regulator
PA2198	1,09	0,88	-0,21	NA	hypothetical protein
PA2231	0,90	1,03	0,13	pslA	biofilm formation protein PslA
PA2234	1,22	1,35	0,13	pslD	biofilm formation protein PslD
PA2235	1,34	1,34	0,00	pslE	biofilm formation protein PslE
PA2236	1,33	1,97	0,64	pslF	biofilm formation protein PslF
PA2237	1,30	0,87	-0,44	pslG	biofilm formation protein PslG
PA2242	0,85	1,25	0,41	pslL	hypothetical protein
PA2246	-1,43	-1,37	0,06	bkdR	Bkd operon transcriptional regulator BkdR

PA2247	-1,02	-1,00	0,02	bkdA1	2-oxoisovalerate dehydrogenase subunit alpha
PA2248	-0,95	-1,24	-0,28	bkdA2	2-oxoisovalerate dehydrogenase subunit beta
PA2250	-0,73	-1,08	-0,35	lpdV	branched-chain alpha-keto acid dehydrogenase complex dihydrolipoyl dehydrogenase
PA2252	1,81	2,30	0,49	NA	AGCS sodium/alanine/glycine symporter
PA2254	0,90	1,62	0,72	pvcA	paerucumarin biosynthesis protein PvcA
PA2259	-2,31	-1,34	0,97	ptxS	transcriptional regulator PtxS
PA2261	-2,91	-1,07	1,84	kguK	2-ketogluconate kinase
PA2262	-3,25	-1,27	1,98	kguT	2-ketogluconate transporter
PA2263	-2,24	-0,56	1,68	kguD	2-hydroxyacid dehydrogenase
PA2264	-0,12	1,53	1,65	NA	hypothetical protein
PA2265	0,04	1,64	1,60	gad	gluconate dehydrogenase
PA2266	-0,20	1,42	1,62	NA	cytochrome C
PA2289	1,39	3,80	2,41	NA	hypothetical protein
PA2290	1,27	2,80	1,52	gcd	glucose dehydrogenase
PA2291	0,98	2,52	1,53	oprB2	glucose-sensitive porin
PA2300	1,44	2,08	0,65	chiC	chitinase
PA2307	0,60	1,60	1,00	NA	ABC transporter permease
PA2320	-3,17	-0,81	2,35	gntR	GntR family transcriptional regulator
PA2321	-8,47	-1,37	7,11	gntK	gluconokinase
PA2322	-7,69	-1,73	5,96	gntP	gluconate permease
PA2323	-2,94	2,73	5,68	gapN	glyceraldehyde-3-phosphate dehydrogenase
PA2335	0,72	1,55	0,84	optO	TonB-dependent receptor
PA2349	0,68	1,57	0,89	NA	hypothetical protein
PA2352	0,97	1,51	0,54	NA	glycerophosphoryl diester phosphodiesterase
PA2366	1,18	1,14	-0,04	hsiC3	uricase
PA2371	1,05	1,08	0,02	clpV3	ClpA/B-type protease
PA2389	1,19	1,49	0,31	pvdR	pyoverdine biosynthesis protein PvdR
PA2419	1,01	1,38	0,37	slsA	hydrolase
PA2424	0,83	1,28	0,45	pvdL	peptide synthase
PA2433	-0,83	-1,00	-0,18	NA	hypothetical protein
PA2439	0,51	1,49	0,99	NA	hypothetical protein
PA2466	0,82	1,21	0,39	foxA	ferrioxamine receptor FoxA
PA2486	-0,55	-1,23	-0,68	NA	hypothetical protein
PA2507	-1,82	-1,98	-0,16	catA	catechol 1,2-dioxygenase
PA2508	-1,41	-2,04	-0,63	catC	muconolactone delta-isomerase
PA2509	-1,51	-1,97	-0,46	catB	muconate cycloisomerase I
PA2512	0,89	1,12	0,24	antA	anthranilate dioxygenase large subunit
PA2513	1,06	1,65	0,59	antB	anthranilate dioxygenase small subunit
PA2520	0,46	1,62	1,16	czcA	resistance-nodulation-cell division (RND) divalent metal cation efflux transporter CzcA
PA2533	-0,65	-1,09	-0,44	NA	sodium:alanine symporter
PA2550	-0,78	-1,00	-0,22	NA	acyl-CoA dehydrogenase
PA2552	-1,64	-1,66	-0,02	acdB	acyl-CoA dehydrogenase
PA2553	-1,65	-1,67	-0,02	NA	acyl-CoA thiolase
PA2554	-1,73	-1,78	-0,05	NA	short-chain dehydrogenase
PA2555	-1,89	-2,27	-0,38	NA	AMP-binding protein
PA2556	-1,79	-2,46	-0,67	NA	transcriptional regulator
PA2557	-2,29	-2,79	-0,50	NA	AMP-binding protein
PA2561	0,95	1,37	0,42	ctpH	methyl-accepting chemotaxis protein CtpH
PA2563	1,42	1,90	0,48	NA	sulfate transporter
PA2570	1,44	1,59	0,15	lecA	PA-I galactophilic lectin
PA2592	1,36	1,41	0,05	potF5	spermidine/putrescine-binding protein
PA2629	1,32	2,49	1,17	purB	adenylosuccinate lyase
PA2630	1,05	1,70	0,65	ycfD	hypothetical protein
PA2653	1,19	1,78	0,59	yuiF	transporter
PA2664	1,17	1,53	0,35	fhp	flavohemoprotein
PA2666	0,42	1,15	0,73	ptpS	6-carboxytetrahydropterin synthase QueD
PA2667	-0,87	-1,45	-0,58	mvaU	hypothetical protein
PA2686	0,94	1,62	0,69	pfeR	two-component response regulator PfeR
PA2688	0,68	1,88	1,20	pfeA	ferric enterobactin receptor
PA2747	-0,96	-1,95	-0,99	NA	hypothetical protein
PA2754	-1,24	-1,61	-0,37	NA	hypothetical protein
PA2756	-0,45	-1,13	-0,69	NA	hypothetical protein
PA2759	-1,07	-1,65	-0,58	NA	hypothetical protein
PA2761	0,38	1,45	1,07	NA	hypothetical protein
PA2769	0,98	1,05	0,07	NA	hypothetical protein
PA2770	0,73	1,52	0,79	NA	isomerase
PA2774	0,27	-1,00	-1,27	tse4	hypothetical protein
PA2776	-2,31	-2,95	-0,64	pauB3	hypothetical protein
PA2805	-0,58	-1,14	-0,56	NA	hypothetical protein
PA2815	-0,67	-1,07	-0,39	yafH	acyl-CoA dehydrogenase
PA2817	1,07	1,67	0,60	NA	hypothetical protein
PA2825	-0,97	-1,93	-0,97	ospR	transcriptional regulator
PA2826	-0,84	-1,67	-0,83	NA	glutathione peroxidase
PA2830	-0,67	-1,23	-0,55	htpX	protease HtpX
PA2832	-0,79	-1,60	-0,82	tpm	thiopurine S-methyltransferase
PA2835	0,70	2,21	1,51	NA	major facilitator superfamily transporter
PA2840	2,00	3,23	1,23	deaD	ATP-dependent RNA helicase
PA2851	0,55	1,14	0,59	efp	elongation factor P
PA2853	-0,14	-1,87	-1,73	oprI	outer membrane lipoprotein OprI
PA2862	-1,83	-2,83	-1,00	lipA	lactonizing lipase
PA2863	-1,46	-1,84	-0,38	lipH	lipase chaperone
PA2870	0,37	1,41	1,04	NA	hypothetical protein
PA2883	-1,18	-1,48	-0,30	NA	hypothetical protein

PA2885	-0,57	-1,13	-0,55	atuR	atu genes repressor
PA2886	-1,36	-1,90	-0,53	atuA	hypothetical protein
PA2887	-1,29	-1,94	-0,65	atuB	citronellol catabolism dehydrogenase
PA2888	-1,75	-2,03	-0,28	atuC	geranyl-CoA carboxylase subunit beta
PA2889	-1,34	-2,13	-0,80	atuD	citronellyl-CoA dehydrogenase
PA2890	-1,75	-1,91	-0,15	atuE	isohexenylglutaconyl-CoA hydratase
PA2891	-1,33	-1,45	-0,12	atuF	geranyl-CoA carboxylase subunit alpha
PA2892	-1,21	-1,42	-0,21	atuG	short-chain dehydrogenase
PA2897	-0,65	-1,03	-0,39	NA	transcriptional regulator
PA2905	0,77	1,44	0,67	cobH	precorrin-8X methylmutase
PA2912	0,42	1,19	0,77	NA	ABC transporter ATP-binding protein
PA2937	0,88	1,37	0,49	NA	hypothetical protein
PA2939	1,67	1,62	-0,05	pepB	aminopeptidase
PA2950	1,43	1,56	0,12	pfm	proton motive force protein
PA2957	0,92	1,55	0,63	NA	transcriptional regulator
PA2967	2,21	2,53	0,32	fabG	3-oxoacyl-[acyl-carrier-protein] reductase FabG
PA2968	2,16	2,28	0,11	fabD	malonyl CoA-ACP transacylase
PA2971	1,14	1,79	0,66	yceD	hypothetical protein
PA2976	0,51	1,30	0,79	rne	ribonuclease E
PA3000	1,13	1,00	-0,13	aroP1	aromatic amino acid transporter AroP
PA3006	-0,57	-1,11	-0,55	psrA	transcriptional regulator PsrA
PA3015	-0,90	-1,32	-0,42	NA	hypothetical protein
PA3017	-0,49	-1,40	-0,90	NA	hypothetical protein
PA3023	-0,76	-1,26	-0,50	yegS	lipid kinase
PA3031	-0,75	-1,05	-0,30	NA	hypothetical protein
PA3032	0,89	1,49	0,61	snr1	cytochrome C Snr1
PA3038	-2,82	-4,34	-1,52	opdQ	porin
PA3043	-0,99	-1,24	-0,25	NA	deoxyguanosinetriphosphate triphosphohydrolase
PA3048	1,04	0,91	-0,13	ycbY	ribosomal RNA large subunit methyltransferase K/L
PA3058	0,69	1,54	0,85	pelG	pellicle/biofilm biosynthesis Wzx-like polysaccharide transporter PelG
PA3059	0,67	1,16	0,49	pelF	pellicle/biofilm biosynthesis glycosyltransferase PelF
PA3067	-0,13	0,88	1,00	NA	transcriptional regulator
PA3068	-1,26	-0,92	0,35	gdhB	NAD-specific glutamate dehydrogenase
PA3079	-1,79	-2,53	-0,74	NA	hypothetical protein
PA3080	-1,35	-2,09	-0,74	NA	hypothetical protein
PA3112	1,26	1,66	0,41	accD	acetyl-CoA carboxylase carboxyltransferase subunit beta
PA3124	-0,61	-1,10	-0,49	NA	transcriptional regulator
PA3126	-0,18	-1,62	-1,45	ibpA	heat-shock protein IbpA
PA3161	-0,70	-1,26	-0,56	himD	integration host factor subunit beta
PA3162	1,02	1,65	0,63	rpsA	30S ribosomal protein S1
PA3171	0,50	1,05	0,55	ubiG	ubiquinone biosynthesis O-methyltransferase
PA3179	1,90	2,61	0,71	yciL	ribosomal large subunit pseudouridine synthase B
PA3181	-4,57	-3,14	1,43	edaA	2-dehydro-3-deoxy-phosphogluconate aldolase
PA3182	-4,85	-2,99	1,86	pgl	6-phosphogluconolactonase
PA3183	-5,07	-3,48	1,59	zwf	glucose-6-phosphate 1-dehydrogenase
PA3186	-1,82	4,17	5,99	oprB	porin B
PA3187	-3,66	2,18	5,83	gltK	ABC transporter ATP-binding protein
PA3188	-7,23	-1,47	5,76	gltG	sugar ABC transporter permease
PA3189	-6,82	-1,80	5,02	gltF	sugar ABC transporter permease
PA3190	-0,73	4,38	5,10	gltB	sugar ABC transporter substrate-binding protein
PA3191	-2,16	-1,40	0,76	gtrS	two-component sensor
PA3192	-2,47	-1,71	0,76	gltR	two-component response regulator GltR
PA3193	-2,66	-2,03	0,63	glk	glucokinase
PA3194	-3,69	-2,80	0,89	edd	phosphogluconate dehydratase
PA3195	-4,67	-3,04	1,62	gapA	glyceraldehyde 3-phosphate dehydrogenase
PA3229	-0,97	-1,96	-0,99	NA	hypothetical protein
PA3232	0,21	-1,33	-1,54	NA	DNA polymerase III subunit epsilon
PA3233	-0,71	-2,48	-1,77	NA	hypothetical protein
PA3234	-1,30	-3,89	-2,58	yjcG	acetate permease
PA3235	-1,36	-4,23	-2,87	yjcH	hypothetical protein
PA3263	-0,13	1,19	1,32	yaiD	recombination associated protein RdgC
PA3266	-0,36	-1,62	-1,26	capB	major cold shock protein CspA
PA3268	1,75	2,32	0,57	NA	TonB-dependent receptor
PA3272	-0,76	-1,33	-0,57	lhr	ATP-dependent DNA helicase
PA3286	0,94	1,26	0,31	NA	3-oxoacyl-ACP synthase
PA3296	1,55	2,05	0,51	phoA	alkaline phosphatase
PA3300	-1,38	-1,83	-0,45	fadD2	long-chain-fatty-acid--CoA ligase
PA3308	0,53	1,31	0,78	hepA	RNA polymerase-associated protein RapA
PA3309	1,45	0,98	-0,47	uspK	hypothetical protein
PA3321	-1,57	-1,54	0,03	NA	transcriptional regulator
PA3326	1,68	1,51	-0,16	clpP2	ATP-dependent Clp protease proteolytic subunit
PA3327	1,99	2,09	0,10	NA	non-ribosomal peptide synthetase
PA3328	2,53	2,62	0,09	NA	FAD-dependent monooxygenase
PA3329	2,22	2,52	0,29	NA	hypothetical protein
PA3330	3,00	3,33	0,34	NA	short-chain dehydrogenase
PA3331	3,07	3,18	0,11	NA	cytochrome P450
PA3332	3,01	3,10	0,09	NA	hypothetical protein
PA3333	3,18	3,39	0,21	fabH2	3-oxoacyl-ACP synthase III
PA3334	2,92	3,26	0,34	NA	acyl carrier protein
PA3335	2,48	2,81	0,33	NA	hypothetical protein
PA3336	2,28	2,00	-0,28	NA	major facilitator superfamily transporter
PA3342	-1,19	-1,83	-0,64	NA	hypothetical protein
PA3343	-0,53	-1,00	-0,47	hsbD	hypothetical protein

PA3354	-0,65	-1,37	-0,72	NA	hypothetical protein
PA3355	-1,35	-1,56	-0,21	NA	hypothetical protein
PA3356	-1,97	-1,95	0,02	pauA5	hypothetical protein
PA3359	1,12	1,52	0,40	NA	hypothetical protein
PA3360	1,11	1,79	0,67	NA	secretion protein
PA3361	1,75	1,64	-0,11	lecB	fucose-binding lectin PA-IIL
PA3369	-1,68	-2,44	-0,76	NA	hypothetical protein
PA3370	-0,80	-1,83	-1,03	NA	hypothetical protein
PA3383	0,26	1,68	1,42	phnD	phosphonate ABC transporter substrate-binding protein
PA3391	0,35	1,71	1,36	nosR	regulatory protein NosR
PA3397	1,59	2,19	0,61	fprA	ferredoxin-NADP reductase
PA3399	-0,96	-1,77	-0,82	NA	hypothetical protein
PA3408	0,52	1,53	1,01	hasR	heme uptake outer membrane receptor HasR
PA3410	0,96	1,36	0,40	hasI	ECF subfamily sigma-70 factor
PA3424	0,55	1,47	0,91	NA	hypothetical protein
PA3425	0,45	1,63	1,18	NA	hypothetical protein
PA3427	-0,63	-1,09	-0,46	NA	short-chain dehydrogenase
PA3452	0,17	1,82	1,65	mqoA	malate:quinone oxidoreductase
PA3455	-0,70	-1,06	-0,36	NA	hypothetical protein
PA3459	-1,56	-1,51	0,05	asnB	glutamine amidotransferase
PA3460	-1,45	-1,27	0,18	NA	acetyltransferase
PA3461	-1,10	-0,90	0,20	yhfE	hypothetical protein
PA3471	-0,95	-1,04	-0,09	sfcA	NAD-dependent malic enzyme
PA3478	2,12	3,02	0,90	rhlB	rhamnosyltransferase subunit B
PA3479	2,50	3,06	0,56	rhlA	rhamnosyltransferase subunit A
PA3491	0,79	1,10	0,30	rnfC	electron transport complex subunit C
PA3495	0,58	1,11	0,52	nth	endonuclease III
PA3496	-0,98	-2,58	-1,60	NA	hypothetical protein
PA3499	-1,39	-1,29	0,09	NA	hypothetical protein
PA3500	-1,63	-1,47	0,16	NA	hypothetical protein
PA3503	-1,49	-1,47	0,02	NA	NA
PA3504	-1,52	-1,53	0,00	NA	aldehyde dehydrogenase
PA3506	-1,38	-1,49	-0,11	NA	hypothetical protein
PA3508	-1,16	-2,04	-0,88	NA	transcriptional regulator
PA3509	-1,62	-1,95	-0,33	NA	hydrolase
PA3510	-1,94	-2,40	-0,46	NA	hypothetical protein
PA3511	-1,71	-1,52	0,19	NA	short-chain dehydrogenase
PA3514	-1,64	-2,62	-0,98	NA	ABC transporter ATP-binding protein
PA3531	-0,87	0,29	1,16	bfrB	bacterioferritin
PA3560	-0,04	4,09	4,13	fruA	PTS system fructose-specific transporter subunit IIBC
PA3561	-0,34	3,07	3,41	fruK	1-phosphofructokinase
PA3562	-0,17	3,95	4,12	fruI	PTS system fructose-specific transporter subunit FruI
PA3567	-1,07	-1,11	-0,04	NA	oxidoreductase
PA3568	-1,14	-1,55	-0,41	ymmS	propionyl-CoA synthetase
PA3581	-2,59	-2,66	-0,08	glpF	glycerol uptake facilitator protein
PA3582	-2,62	-3,25	-0,64	glpK	glycerol kinase
PA3601	0,72	1,31	0,59	ykgM	50S ribosomal protein L31 type B
PA3607	1,73	1,67	-0,06	potA	polyamine transporter ATP-binding protein PotA
PA3608	1,25	2,24	0,99	potB	polyamine ABC transporter permease PotB
PA3609	0,96	2,41	1,45	potC	polyamine ABC transporter permease PotC
PA3610	0,61	1,93	1,31	potD	polyamine ABC transporter substrate-binding protein PotD
PA3613	0,99	1,16	0,17	NA	hypothetical protein
PA3615	-0,69	-1,41	-0,72	NA	hypothetical protein
PA3621	0,51	1,35	0,84	fdxA	ferredoxin I
PA3622	-0,81	-1,44	-0,63	rpoS	RNA polymerase sigma factor RpoS
PA3623	-0,81	-1,76	-0,95	NA	hypothetical protein
PA3629	-1,06	-1,07	-0,01	adhC	alcohol dehydrogenase
PA3633	0,57	1,15	0,58	ygbP	2-C-methyl-D-erythritol 4-phosphate cytidylyltransferase
PA3639	0,79	1,07	0,29	accA	acetyl-CoA carboxylase carboxyltransferase subunit alpha
PA3641	1,28	1,81	0,53	NA	amino acid permease
PA3645	0,84	1,48	0,64	fabZ	3-hydroxyacyl-[acyl-carrier-protein] dehydratase FabZ
PA3652	1,02	1,11	0,09	uppS	ditrans,polycis-undecaprenyl-diphosphate synthase
PA3653	1,11	1,43	0,32	frr	ribosome recycling factor
PA3654	0,96	1,18	0,22	pyrH	uridylate kinase
PA3655	1,15	1,54	0,38	tsf	elongation factor Ts
PA3656	1,16	1,95	0,79	rpsB	30S ribosomal protein S2
PA3659	0,38	1,23	0,85	dapC	succinyldiaminopimelate transaminase
PA3662	-0,71	-1,63	-0,92	NA	hypothetical protein
PA3687	-0,74	-1,09	-0,35	ppc	phosphoenolpyruvate carboxylase
PA3689	-0,76	-1,65	-0,89	yhdM	transcriptional regulator
PA3691	-1,50	-1,63	-0,13	NA	hypothetical protein
PA3692	-1,16	-0,62	0,54	lptF	outer membrane porin F
PA3698	-0,67	-1,03	-0,35	NA	hypothetical protein
PA3700	0,69	1,46	0,77	lysS	lysine--tRNA ligase
PA3709	-1,46	-2,65	-1,19	NA	major facilitator superfamily transporter
PA3710	-1,08	-1,53	-0,45	NA	GMC-type oxidoreductase
PA3712	-1,05	-1,54	-0,49	NA	hypothetical protein
PA3713	0,44	1,28	0,84	spdH	spermidine dehydrogenase SpdH
PA3721	0,69	1,13	0,44	nalC	transcriptional regulator
PA3724	1,70	1,74	0,05	lasB	elastase LasB
PA3741	1,03	1,83	0,80	NA	acyl-CoA thioesterase
PA3743	1,26	2,23	0,97	trmD	tRNA (guanine-N(1)-)-methyltransferase
PA3744	1,03	1,60	0,56	rimM	ribosome maturation factor RimM

PA3745	0,99	1,80	0,81	rpsP	30S ribosomal protein S16
PA3754	-0,74	-1,50	-0,76	yeaB	hypothetical protein
PA3757	-0,98	-1,22	-0,24	nagR	transcriptional regulator
PA3758	-1,09	-1,17	-0,08	nagA	N-acetylglucosamine-6-phosphate deacetylase
PA3760	-1,35	-1,42	-0,08	nagF	N-acetyl-D-glucosamine phosphotransferase system transporter
PA3761	-0,56	-1,38	-0,82	nagE	N-acetyl-D-glucosamine phosphotransferase system transporter
PA3766	-0,20	-1,71	-1,50	NA	aromatic amino acid transporter
PA3769	0,98	1,46	0,47	guaA	GMP synthase
PA3770	0,83	1,40	0,58	guaB	inosine 5'-monophosphate dehydrogenase
PA3795	-0,87	-1,16	-0,28	NA	oxidoreductase
PA3807	0,80	1,05	0,25	ndk	nucleoside diphosphate kinase
PA3809	0,80	1,23	0,42	fdx2	(2Fe-2S) ferredoxin
PA3810	0,77	1,30	0,53	hscA	chaperone protein HscA
PA3814	0,50	1,03	0,53	iscS	cysteine desulfurase
PA3815	0,61	1,34	0,73	iscR	HTH-type transcriptional regulator
PA3818	1,64	2,88	1,24	suhB	type III secretion system regulator SuhB
PA3819	-0,61	-1,62	-1,02	ycfJ	hypothetical protein
PA3823	0,39	1,01	0,62	tgt	queuine tRNA-ribosyltransferase
PA3824	0,76	1,20	0,44	queA	S-adenosylmethionine--tRNA ribosyltransferase-isomerase
PA3836	-1,25	-1,76	-0,51	NA	hypothetical protein
PA3837	-1,02	-1,10	-0,08	NA	ABC transporter permease
PA3838	-0,73	-1,08	-0,35	NA	ABC transporter ATP-binding protein
PA3844	-0,76	-1,22	-0,46	NA	hypothetical protein
PA3846	-0,89	-1,28	-0,39	NA	hypothetical protein
PA3851	-0,42	-1,22	-0,79	NA	hypothetical protein
PA3852	-0,51	-1,30	-0,79	NA	hypothetical protein
PA3860	-1,55	-2,36	-0,81	NA	acyl-CoA synthetase
PA3865	-1,14	-1,57	-0,43	NA	amino acid binding protein
PA3875	0,85	1,37	0,52	narG	respiratory nitrate reductase subunit alpha
PA3888	-1,71	-1,10	0,61	opuCD	ABC transporter permease
PA3890	-1,19	-0,18	1,01	opuCB	ABC transporter permease
PA3891	-1,44	-0,95	0,49	opuCA	ABC transporter ATP-binding protein
PA3892	1,88	2,70	0,82	NA	hypothetical protein
PA3893	1,71	2,95	1,24	NA	hypothetical protein
PA3894	1,67	2,74	1,07	opmI	hypothetical protein
PA3901	0,60	1,77	1,17	fecA	Fe(III) dicitrate transporter FecA
PA3909	0,40	1,47	1,08	eddB	extracelullar DNA degradation protein EddB
PA3919	-1,14	-1,74	-0,60	ylaK	hypothetical protein
PA3921	-0,93	-1,01	-0,08	NA	transcriptional regulator
PA3922	-2,66	-3,72	-1,06	NA	hypothetical protein
PA3923	-2,43	-3,51	-1,08	NA	hypothetical protein
PA3924	-1,17	-2,16	-0,99	NA	long-chain-fatty-acid--CoA ligase
PA3927	-1,40	-1,43	-0,03	NA	transcriptional regulator
PA3934	-1,01	-1,42	-0,42	NA	hypothetical protein
PA3952	-0,68	-1,88	-1,21	NA	hypothetical protein
PA3959	-1,18	-0,84	0,34	NA	hypothetical protein
PA3962	-0,61	-1,40	-0,79	NA	hypothetical protein
PA3967	1,18	1,34	0,16	NA	hypothetical protein
PA3972	-0,55	-1,50	-0,95	aidB	acyl-CoA dehydrogenase
PA3973	-0,69	-1,73	-1,04	NA	transcriptional regulator
PA3979	0,71	1,42	0,72	NA	hypothetical protein
PA3980	0,55	1,30	0,75	miaB	(dimethylallyl)adenosine tRNA methylthiotransferase
PA3986	-0,38	-1,43	-1,06	NA	hypothetical protein
PA4021	-1,23	-1,38	-0,15	NA	transcriptional regulator
PA4022	-2,02	-1,92	0,11	hdhA	aldehyde dehydrogenase
PA4023	-2,43	-2,62	-0,19	eutP	transporter
PA4024	-2,35	-2,33	0,02	eutB	ethanolamine ammonia-lyase large subunit
PA4025	-2,35	-2,58	-0,23	eutC	ethanolamine ammonia-lyase small subunit
PA4026	-0,98	-1,39	-0,41	NA	acetyltransferase
PA4061	-0,56	-1,10	-0,54	ybbN	thioredoxin
PA4067	2,26	2,55	0,28	oprG	outer membrane protein OprG
PA4082	0,15	1,08	0,93	cupB5	adhesive protein CupB5
PA4094	-0,86	-1,47	-0,61	NA	transcriptional regulator
PA4099	0,64	2,34	1,70	NA	hypothetical protein
PA4103	0,92	1,65	0,73	NA	hypothetical protein
PA4113	1,27	1,50	0,23	ydeA	sugar efflux transporter
PA4115	-0,79	-1,09	-0,30	NA	hypothetical protein
PA4131	2,27	2,54	0,27	NA	iron-sulfur protein
PA4132	1,94	1,80	-0,13	NA	hypothetical protein
PA4133	2,10	2,68	0,59	ccoN	cbb3-type cytochrome C oxidase subunit I
PA4139	1,78	1,46	-0,32	NA	hypothetical protein
PA4140	1,47	1,58	0,11	NA	hypothetical protein
PA4141	1,93	1,14	-0,79	NA	hypothetical protein
PA4142	1,66	1,92	0,26	NA	secretion protein
PA4143	1,17	1,39	0,22	cyaB	toxin transporter
PA4147	-1,22	-2,03	-0,81	acoR	transcriptional regulator AcoR
PA4156	0,08	1,25	1,16	fvbA	TonB-dependent receptor
PA4164	-0,31	-1,02	-0,71	NA	hypothetical protein
PA4178	0,46	1,97	1,51	eftM	hypothetical protein
PA4180	-0,76	-1,22	-0,46	NA	acetolactate synthase
PA4198	-1,15	-1,81	-0,66	NA	acyl-CoA synthetase
PA4199	-0,75	-1,35	-0,60	NA	acyl-CoA dehydrogenase
PA4201	-0,85	-1,22	-0,36	ddlA	D-alanine--D-alanine ligase

PA4204	-0,83	-1,03	-0,20	ppgL	gluconolactonase PpgL
PA4206	0,69	1,10	0,41	mexH	resistance-nodulation-cell division (RND) efflux membrane fusion protein
PA4209	3,31	3,00	-0,31	phzM	phenazine-specific methyltransferase
PA4210	4,07	4,11	0,04	phzA1	phenazine biosynthesis protein
PA4211	4,71	4,77	0,06	phzB1	phenazine biosynthesis protein
PA4212	2,46	3,03	0,57	phzC1	phenazine biosynthesis protein PhzC
PA4217	4,42	5,22	0,80	phzS	hypothetical protein
PA4221	1,01	0,98	-0,03	fptA	Fe(III)-pyochelin outer membrane receptor
PA4238	0,74	1,20	0,46	rpoA	DNA-directed RNA polymerase subunit alpha
PA4239	0,91	1,33	0,42	rpsD	30S ribosomal protein S4
PA4240	0,96	1,44	0,48	rpsK	30S ribosomal protein S11
PA4241	0,94	1,33	0,39	rpsM	30S ribosomal protein S13
PA4242	1,21	1,73	0,52	rpmJ	50S ribosomal protein L36
PA4243	1,09	1,55	0,45	secY	preprotein translocase subunit SecY
PA4244	0,90	1,16	0,26	rplO	50S ribosomal protein L15
PA4245	0,90	1,43	0,53	rpmD	50S ribosomal protein L30
PA4247	1,03	1,58	0,55	rplR	50S ribosomal protein L18
PA4248	0,83	1,53	0,70	rplF	50S ribosomal protein L6
PA4249	0,91	1,43	0,52	rpsH	30S ribosomal protein S8
PA4251	1,07	1,14	0,07	rplE	50S ribosomal protein L5
PA4252	1,37	1,75	0,38	rplX	50S ribosomal protein L24
PA4253	1,03	1,35	0,32	rplN	50S ribosomal protein L14
PA4254	1,26	1,77	0,51	rpsQ	30S ribosomal protein S17
PA4255	1,06	1,23	0,18	rpmC	50S ribosomal protein L29
PA4256	1,12	1,26	0,14	rplP	50S ribosomal protein L16
PA4257	1,09	1,49	0,39	rpsC	30S ribosomal protein S3
PA4258	1,26	1,62	0,37	rplV	50S ribosomal protein L22
PA4259	1,13	1,97	0,83	rpsS	30S ribosomal protein S19
PA4260	1,05	1,76	0,71	rplB	50S ribosomal protein L2
PA4261	1,14	1,96	0,82	rplW	50S ribosomal protein L23
PA4262	1,09	1,83	0,74	rplD	50S ribosomal protein L4
PA4263	1,01	1,82	0,82	rplC	50S ribosomal protein L3
PA4264	0,96	1,65	0,69	rpsJ	30S ribosomal protein S10
PA4266	0,76	1,21	0,45	fusA1	elongation factor G
PA4268	0,81	1,45	0,65	rpsL	30S ribosomal protein S12
PA4269	1,07	1,28	0,21	rpoC	DNA-directed RNA polymerase subunit beta'
PA4270	0,94	1,29	0,35	rpoB	DNA-directed RNA polymerase subunit beta
PA4271	0,98	1,05	0,06	rplL	50S ribosomal protein L7/L12
PA4272	1,25	1,56	0,31	rplJ	50S ribosomal protein L10
PA4273	1,30	1,74	0,44	rplA	50S ribosomal protein L1
PA4274	1,24	1,78	0,54	rplK	50S ribosomal protein L11
PA4275	0,79	1,08	0,29	nusG	transcription antitermination protein NusG
PA4276	0,70	1,41	0,71	secE	preprotein translocase subunit SecE
PA4277	0,76	1,31	0,55	tufB	elongation factor Tu
PA4280	0,29	1,12	0,83	birA	biotin--protein ligase
PA4290	-0,13	-1,97	-1,84	NA	chemotaxis transducer
PA4292	0,86	1,53	0,67	NA	phosphate transporter
PA4296	-0,31	-1,02	-0,72	pprB	two-component response regulator PprB
PA4311	-0,92	-1,29	-0,37	NA	hypothetical protein
PA4317	-0,15	-1,00	-0,85	NA	hypothetical protein
PA4326	-0,31	-1,22	-0,90	NA	hypothetical protein
PA4328	1,06	1,21	0,15	NA	hypothetical protein
PA4333	0,49	1,00	0,51	fumA	fumarase
PA4341	-1,36	-1,55	-0,19	NA	transcriptional regulator
PA4345	-1,08	-1,45	-0,38	NA	hypothetical protein
PA4346	-1,25	-1,12	0,13	NA	hypothetical protein
PA4348	0,96	1,17	0,21	NA	hypothetical protein
PA4352	1,63	1,65	0,02	NA	hypothetical protein
PA4363	-0,72	-1,47	-0,75	iciA	chromosome replication initiation inhibitor protein
PA4385	-1,02	-1,65	-0,64	groEL	molecular chaperone GroEL
PA4386	-0,80	-1,68	-0,88	groES	co-chaperonin GroES
PA4428	1,03	1,02	-0,01	sspA	stringent starvation protein A
PA4433	0,90	1,26	0,36	rplM	50S ribosomal protein L13
PA4435	-0,64	-1,69	-1,05	NA	acyl-CoA dehydrogenase
PA4438	0,88	2,22	1,34	yhcM	hypothetical protein
PA4440	-0,97	-1,18	-0,21	NA	hypothetical protein
PA4472	-0,59	-1,49	-0,90	pmbA	PmbA protein
PA4474	-0,46	-1,17	-0,72	tldD	hypothetical protein
PA4481	0,59	1,21	0,62	mreB	rod shape-determining protein MreB
PA4494	0,88	1,37	0,49	roxS	sensor histidine kinase RoxS
PA4496	-2,14	-2,73	-0,59	dppA1	ABC transporter
PA4497	-1,48	-1,71	-0,23	dppA2	ABC transporter
PA4500	-1,15	-1,46	-0,31	dppA3	ABC transporter
PA4501	-1,79	-2,27	-0,48	opdD,opdP	glycine-glutamate dipeptide porin OpdP
PA4502	-1,64	-1,98	-0,33	dppA4	ABC transporter
PA4503	-1,57	-1,83	-0,26	dppB	ABC transporter permease
PA4504	-1,49	-1,23	0,26	dppC	ABC transporter permease
PA4505	-1,65	-1,61	0,04	dppD	ABC transporter ATP-binding protein
PA4506	-1,53	-1,74	-0,20	dppF	peptide ABC transporter ATP-binding protein
PA4514	1,36	1,97	0,61	piuA	iron transport outer membrane receptor
PA4519	1,43	1,76	0,32	speC	ornithine decarboxylase
PA4520	-1,00	-1,43	-0,42	NA	chemotaxis transducer
PA4522	-0,55	-1,27	-0,71	ampD	N-acetyl-anhydromuranmyl-L-alanine amidase

PA4530	-0,71	-1,33	-0,62	NA	zinc-binding protein
PA4536	-0,61	-1,13	-0,51	NA	hypothetical protein
PA4540	0,41	1,44	1,03	lepB	hypothetical protein
PA4542	-0,61	-1,85	-1,25	clpB	chaperone protein ClpB
PA4556	-0,77	-1,15	-0,38	pilE	type 4 fimbrial biogenesis protein PilE
PA4563	0,86	1,75	0,88	rpsT	30S ribosomal protein S20
PA4568	1,09	1,55	0,46	rplU	50S ribosomal protein L21
PA4571	1,10	1,79	0,69	NA	cytochrome C
PA4572	0,49	1,35	0,86	fklB	peptidyl-prolyl cis-trans isomerase FklB
PA4579	-1,44	-1,52	-0,08	NA	hypothetical protein
PA4587	1,69	1,88	0,19	ccpR	cytochrome C551 peroxidase
PA4598	0,56	1,24	0,68	mexD	resistance-nodulation-cell division (RND) multidrug efflux transporter MexD
PA4602	0,51	1,13	0,63	glyA3	serine hydroxymethyltransferase
PA4605	-0,83	-1,59	-0,77	ybdD	hypothetical protein
PA4606	-0,80	-1,84	-1,03	cstA	hypothetical protein
PA4613	0,36	1,13	0,77	katB	catalase
PA4615	-0,86	-1,18	-0,32	fprB	oxidoreductase
PA4616	0,84	1,81	0,97	NA	C4-dicarboxylate-binding protein
PA4624	1,02	0,53	-0,48	cdrB	hypothetical protein
PA4627	0,60	1,41	0,81	yjjT	16S rRNA methyltransferase
PA4628	0,80	1,07	0,27	lysP	lysine-specific permease
PA4644	1,38	1,76	0,38	NA	hypothetical protein
PA4645	1,16	1,80	0,64	hprT	hypoxanthine-guanine phosphoribosyltransferase
PA4646	0,72	1,28	0,56	upp	uracil phosphoribosyltransferase
PA4647	0,57	1,12	0,56	uraA	uracil permease
PA4661	-0,49	-1,31	-0,83	pagL	lipid A 3-O-deacylase
PA4665	0,41	1,08	0,66	prfA	peptide chain release factor 1
PA4670	0,89	1,51	0,62	prs	ribose-phosphate pyrophosphokinase
PA4671	0,97	1,20	0,23	rplY	50S ribosomal protein L25/general stress protein Ctc
PA4672	1,11	1,63	0,52	pth	peptidyl-tRNA hydrolase
PA4673	1,41	2,15	0,74	ychF	GTP-dependent nucleic acid-binding protein EngD
PA4684	0,50	1,21	0,71	NA	hypothetical protein
PA4710	0,56	1,76	1,20	phuR	heme/hemoglobin uptake outer membrane receptor PhuR
PA4714	-0,74	-1,46	-0,73	NA	hypothetical protein
PA4719	1,01	1,95	0,94	NA	transporter
PA4720	0,99	1,65	0,66	trmA	tRNA (uracil-5-)-methyltransferase
PA4724.1	-0,87	-1,28	-0,41	NA	hypothetical protein
PA4726	-0,75	-1,09	-0,34	cbrB	two-component response regulator CbrB
PA4733	-1,27	-1,79	-0,52	acsB	acetyl-CoA synthetase
PA4736	-0,54	-1,16	-0,63	NA	hypothetical protein
PA4738	-1,09	-1,54	-0,45	yjbJ	hypothetical protein
PA4739	-1,11	-0,84	0,27	NA	hypothetical protein
PA4740	0,61	1,08	0,47	pnp	polynucleotide phosphorylase
PA4742	0,57	1,53	0,96	truB	tRNA pseudouridine synthase B
PA4743	0,74	1,08	0,34	rbfA	ribosome-binding factor A
PA4744	0,84	1,27	0,43	infB	translation initiation factor IF-2
PA4745	0,78	1,25	0,47	nusA	transcription elongation factor NusA
PA4746	0,70	1,64	0,94	yhbC	hypothetical protein
PA4748	0,52	1,03	0,51	tpiA	triosephosphate isomerase
PA4751	-0,57	-1,23	-0,66	ftsH	cell division protein FtsH
PA4757	1,04	1,83	0,79	yeaS	leucine export protein LeuE
PA4758	0,94	1,03	0,09	carA	carbamoyl phosphate synthase small subunit
PA4759	-0,22	-1,48	-1,26	dapB	4-hydroxy-tetrahydrodipicolinate reductase
PA4761	-0,56	-1,65	-1,08	dnaK	molecular chaperone DnaK
PA4762	-0,37	-1,53	-1,16	grpE	heat shock protein GrpE
PA4765	0,13	1,03	0,90	omlA	outer membrane lipoprotein OmlA
PA4782	-0,48	-1,45	-0,96	NA	hypothetical protein
PA4786	-0,74	-1,58	-0,84	NA	3-ketoacyl-ACP reductase
PA4787	-1,09	-1,39	-0,30	NA	transcriptional regulator
PA4811	-0,39	-1,35	-0,96	fdnH	nitrate-inducible formate dehydrogenase subunit beta
PA4812	-0,55	-1,31	-0,76	fdnG	formate dehydrogenase-O major subunit
PA4817	1,39	1,64	0,25	NA	hypothetical protein
PA4825	0,13	1,30	1,16	mgtA	Mg(2+) transport ATPase
PA4833	-0,52	-1,60	-1,08	NA	hypothetical protein
PA4837	0,27	1,75	1,49	NA	hypothetical protein
PA4842	-0,65	-1,44	-0,79	NA	hypothetical protein
PA4846	0,40	1,16	0,76	aroQ1	3-dehydroquinate dehydratase
PA4847	0,86	1,07	0,20	accB	acetyl-CoA carboxylase biotin carboxyl carrier protein subunit
PA4852	0,85	1,31	0,46	yhdG	hypothetical protein
PA4853	0,80	1,30	0,50	fis	Fis family transcriptional regulator
PA4854	0,70	1,41	0,71	purH	bifunctional phosphoribosylaminoimidazolecarboxamide formyltransferase/IMP cyclohy
PA4855	0,90	1,52	0,62	purD	phosphoribosylamine--glycine ligase
PA4861	0,69	1,49	0,80	NA	ABC transporter ATP-binding protein
PA4873	0,82	1,48	0,66	NA	heat-shock protein
PA4876	-1,38	-2,00	-0,62	osmE	OsmE family transcriptional regulator
PA4877	-1,08	-1,28	-0,20	NA	hypothetical protein
PA4880	-2,20	-1,86	0,34	NA	bacterioferritin
PA4888	0,19	1,66	1,48	desB	acyl-CoA desaturase
PA4909	-0,91	-1,57	-0,66	NA	ABC transporter ATP-binding protein
PA4910	-0,86	-1,49	-0,63	NA	ABC transporter ATP-binding protein
PA4912	-0,71	-1,37	-0,66	NA	branched-chain amino acid ABC transporter
PA4913	-1,50	-2,70	-1,20	NA	ABC transporter
PA4914	-0,90	-1,40	-0,50	amaR	transcriptional regulator

PA4918	-1,21	-1,09	0,12	pcnA	hypothetical protein
PA4919	-0,96	-1,09	-0,13	pncB1	nicotinate phosphoribosyltransferase
PA4920	-1,12	-0,91	0,22	nadE	NAD synthetase
PA4921	-1,01	-1,16	-0,15	choE	hypothetical protein
PA4928	0,94	1,87	0,93	ygiR	hypothetical protein
PA4933	1,16	1,78	0,62	NA	hypothetical protein
PA4934	1,26	2,18	0,92	rpsR	30S ribosomal protein S18
PA4935	1,12	2,06	0,94	rpsF	30S ribosomal protein S6
PA4936	-0,89	-1,50	-0,61	spoU	23S rRNA (guanosine(2251)-2'-O)-methyltransferase RlmB
PA4971	-0,80	-1,10	-0,31	aspP	adenosine diphosphate sugar pyrophosphatase
PA4976	-1,20	-1,27	-0,07	aruH	arginine:pyruvate transaminase AruH
PA4977	-0,93	-1,65	-0,72	aruI	hypothetical protein
PA4978	-1,30	-2,15	-0,85	NA	hypothetical protein
PA4979	-1,19	-1,55	-0,36	NA	acyl-CoA dehydrogenase
PA4980	-0,77	-1,59	-0,82	NA	enoyl-CoA hydratase
PA4982	-1,71	-2,05	-0,34	NA	two-component sensor
PA4983	-1,28	-1,89	-0,60	dmsR	two-component response regulator
PA4985	-1,11	-1,39	-0,28	NA	hypothetical protein
PA4986	-1,32	-1,73	-0,41	NA	oxidoreductase
PA5016	-1,08	-1,08	0,00	aceF	dihydrolipoamide acetyltransferase
PA5027	1,87	1,68	-0,19	NA	hypothetical protein
PA5029	-0,54	-1,15	-0,61	ynfL	transcriptional regulator
PA5030	1,43	2,64	1,20	ynfM	major facilitator superfamily transporter
PA5034	0,72	1,17	0,45	hemE	uroporphyrinogen decarboxylase
PA5052	0,50	1,50	1,00	NA	hypothetical protein
PA5053	-0,34	-1,54	-1,20	hslV	ATP-dependent protease peptidase subunit
PA5054	-0,44	-1,80	-1,36	hslU	ATP-dependent protease ATP-binding subunit HslU
PA5055	-0,27	-1,57	-1,30	NA	hypothetical protein
PA5056	-0,75	-1,10	-0,34	phaC1	poly(3-hydroxyalkanoic acid) synthase
PA5060	-0,62	-1,06	-0,44	phaF	polyhydroxyalkanoate synthesis protein PhaF
PA5061	-0,95	-1,22	-0,27	phaI	hypothetical protein
PA5062	-0,40	0,73	1,13	NA	hypothetical protein
PA5072	1,25	1,78	0,53	NA	chemotaxis transducer
PA5112	-0,75	-1,25	-0,49	estA	esterase
PA5117	1,14	1,77	0,63	typA	regulatory protein TypA
PA5118	1,32	2,22	0,90	thiI	thiamine biosynthesis protein ThiI
PA5129	0,43	1,42	1,00	grxC	glutaredoxin
PA5137	-0,82	-1,09	-0,27	NA	hypothetical protein
PA5139	0,65	1,98	1,33	NA	hypothetical protein
PA5150	-1,06	-1,51	-0,45	NA	short-chain dehydrogenase
PA5152	-1,46	-1,82	-0,36	NA	ABC transporter ATP-binding protein
PA5153	-1,97	-3,04	-1,06	NA	amino acid ABC transporter substrate-binding protein
PA5154	-1,84	-2,11	-0,26	NA	ABC transporter permease
PA5155	-1,65	-2,14	-0,48	NA	amino acid ABC transporter permease
PA5158	0,40	1,30	0,90	opmG	hypothetical protein
PA5160	0,60	1,24	0,65	emrB; pmrB	drug efflux transporter
PA5167	-1,69	-2,68	-0,99	dctP	C4-dicarboxylate-binding protein
PA5168	-1,26	-2,02	-0,77	dctQ	dicarboxylate transporter
PA5169	-1,37	-2,18	-0,81	dctM	C4-dicarboxylate transporter
PA5170	1,50	1,68	0,18	arcD	arginine/ornithine antiporter
PA5171	1,75	1,71	-0,05	arcA	arginine deiminase
PA5172	2,03	2,07	0,04	arcB	ornithine carbamoyltransferase
PA5173	1,60	1,45	-0,15	arcC	carbamate kinase
PA5174	1,61	1,70	0,09	NA	beta-ketoacyl synthase
PA5178	-0,36	-1,08	-0,72	NA	hypothetical protein
PA5180	1,53	1,23	-0,30	fdhD	hypothetical protein
PA5181	1,44	1,09	-0,34	NA	oxidoreductase
PA5183.1	-0,29	-1,71	-1,43	rsmN	hypothetical protein
PA5184	-0,97	-1,32	-0,35	NA	chorismate mutase
PA5191	-0,69	-1,65	-0,96	NA	hypothetical protein
PA5201	0,47	1,10	0,63	yhgF	hypothetical protein
PA5212	-1,56	-2,11	-0,55	NA	hypothetical protein
PA5219	1,51	2,22	0,71	NA	hypothetical protein
PA5220	1,64	1,45	-0,20	NA	hypothetical protein
PA5227	-0,87	-1,16	-0,29	ygfE	hypothetical protein
PA5239	0,51	1,05	0,55	rho	transcription termination factor Rho
PA5240	-0,35	-1,31	-0,96	trxA	thioredoxin
PA5253	-0,83	-1,38	-0,54	algP	alginate regulatory protein AlgP
PA5254	-0,83	-1,26	-0,42	fkbZ	FkbP-type peptidyl-prolyl cis-trans isomerase
PA5255	-1,11	-1,47	-0,36	algQ	anti-RNA polymerase sigma 70 factor
PA5258	-0,49	-1,02	-0,54	hemX	hypothetical protein
PA5261	-1,03	-1,66	-0,63	algR	alginate biosynthesis regulatory protein AlgR
PA5262	-0,75	-1,40	-0,65	fimS	alginate biosynthesis protein AlgZ/FimS
PA5268	-0,90	-1,23	-0,33	corA	magnesium/cobalt transporter
PA5269	-0,61	-1,41	-0,80	NA	hypothetical protein
PA5284	0,29	1,63	1,34	NA	hypothetical protein
PA5286	0,65	1,21	0,56	yjbQ	hypothetical protein
PA5298	0,70	1,16	0,46	xpt	xanthine phosphoribosyltransferase
PA5301	-1,19	-1,46	-0,28	pauR	transcriptional regulator
PA5302	-0,47	-1,88	-1,41	dadX	alanine racemase
PA5303	-0,36	-1,89	-1,53	NA	hypothetical protein
PA5304	-0,93	-2,14	-1,21	dadA	D-amino acid dehydrogenase small subunit
PA5309	-1,38	-1,70	-0,31	pauB4	oxidoreductase

PA5312	-3,10	-3,72	-0,63	pauC	aldehyde dehydrogenase
PA5313	-3,00	-3,58	-0,58	gabT2	omega amino acid--pyruvate transaminase
PA5314	-3,30	-4,04	-0,74	NA	hypothetical protein
PA5316	1,17	1,89	0,72	rpmB	50S ribosomal protein L28
PA5324	-0,95	-1,35	-0,40	sphR	transcriptional regulator
PA5348	-2,21	-3,42	-1,21	NA	DNA-binding protein
PA5364	-0,61	-1,07	-0,46	NA	two-component response regulator
PA5371	-0,72	-1,48	-0,76	yciA	acyl-CoA thioesterase
PA5376	-0,63	-1,16	-0,53	cbcV	ABC transporter ATP-binding protein
PA5377	-0,53	-1,12	-0,59	cbcW	ABC transporter permease
PA5378	-0,76	-1,10	-0,34	cbcX	hypothetical protein
PA5380	-0,76	-1,44	-0,68	gbdR	protein GbdR
PA5383	1,77	1,25	-0,53	yeiH	hypothetical protein
PA5387	0,68	1,96	1,28	cdhC	carnitine dehydrogenase
PA5388	0,49	1,37	0,88	caiX	hypothetical protein
PA5394	-0,38	-1,29	-0,91	cls	cardiolipin synthetase
PA5396	-0,59	-1,18	-0,60	NA	hypothetical protein
PA5398	-0,64	-1,34	-0,70	dgcA	dimethylglycine catabolism protein DgcA
PA5404	0,74	2,04	1,29	NA	hypothetical protein
PA5409	-0,79	-1,62	-0,83	NA	hypothetical protein
PA5411	-0,84	-1,17	-0,33	gbcB	protein GbcB
PA5415	-0,27	-2,15	-1,87	glyA1	serine hydroxymethyltransferase
PA5424	-0,85	-1,48	-0,63	yeaQ	hypothetical protein
PA5427	1,80	1,81	0,01	adhA	alcohol dehydrogenase
PA5428	1,34	1,02	-0,33	NA	transcriptional regulator
PA5429	3,77	3,82	0,05	aspA	aspartate ammonia-lyase
PA5435	-1,24	-1,15	0,09	oadA	pyruvate carboxylase subunit B
PA5436	-1,22	-0,96	0,26	NA	acetyl-CoA carboxylase subunit alpha
PA5440	1,27	1,76	0,49	yegQ	peptidase
PA5442	-1,14	-1,86	-0,72	NA	hypothetical protein
PA5445	-0,19	-1,57	-1,37	psecoA	coenzyme A transferase
PA5446	1,48	1,58	0,09	NA	hypothetical protein
PA5447	-0,82	-1,30	-0,48	wbpZ	glycosyltransferase WbpZ
PA5448	-1,07	-1,74	-0,67	wbpY	glycosyltransferase WbpY
PA5449	-1,13	-1,37	-0,24	wbpX	glycosyltransferase WbpX
PA5450	-0,98	-1,40	-0,42	wzt	ABC transporter
PA5451	-1,01	-1,28	-0,27	wzm	LPS efflux transporter membrane protein
PA5452	-1,18	-1,53	-0,35	wbpW	phosphomannose isomerase/mannose-1-phosphate guanylyl transferase
PA5453	-1,14	-1,75	-0,61	gmd	GDP-mannose 4,6-dehydratase
PA5454	-1,05	-1,74	-0,69	rmd	oxidoreductase Rmd
PA5455	-0,98	-1,31	-0,32	NA	hypothetical protein
PA5470	1,56	1,23	-0,33	prfH	peptide chain release factor-like protein
PA5471	1,53	1,56	0,04	armZ	hypothetical protein
PA5471.1	1,49	1,51	0,02	NA	NA
PA5473	-0,55	-1,06	-0,52	yjbB	hypothetical protein
PA5475	1,84	2,31	0,47	NA	hypothetical protein
PA5479	1,89	2,72	0,83	gltP	glutamate/aspartate:proton symporter
PA5481	-1,86	-2,40	-0,54	NA	hypothetical protein
PA5482	-1,95	-2,48	-0,52	NA	hypothetical protein
PA5484	-1,05	-1,10	-0,05	kinB	two-component sensor
PA5487	-1,05	-1,39	-0,34	NA	hypothetical protein
PA5490	0,81	1,24	0,43	cc4	cytochrome C4
PA5502	0,76	1,52	0,76	NA	hypothetical protein
PA5503	0,99	1,71	0,72	NA	ABC transporter ATP-binding protein
PA5504	1,14	2,25	1,11	NA	D-methionine ABC transporter
PA5507	-1,04	-1,04	0,00	NA	hypothetical protein
PA5508	-1,06	-1,32	-0,26	pauA7	glutamine synthetase
PA5521	-1,67	-2,36	-0,69	NA	short-chain dehydrogenase
PA5522	-1,25	-1,59	-0,34	pauA6	glutamine synthetase
PA5523	-1,36	-2,23	-0,87	NA	aminotransferase
PA5526	-0,56	-1,90	-1,34	NA	hypothetical protein
PA5530	-0,21	-1,01	-0,80	NA	MFS dicarboxylate transporter
PA5541	0,65	1,74	1,10	pyrQ	dihydroorotase
PA5542	-0,73	-1,16	-0,43	NA	hypothetical protein
PA5544	-1,07	-1,67	-0,60	NA	hypothetical protein
PA5545	-0,93	-1,49	-0,57	NA	hypothetical protein
PA5547	-0,51	-1,37	-0,86	NA	hypothetical protein
PA5553	1,66	1,28	-0,38	atpC	ATP synthase subunit epsilon
PA5554	1,89	1,97	0,07	atpD	ATP synthase subunit beta
PA5555	1,99	2,19	0,20	atpG	ATP synthase subunit gamma
PA5556	1,80	2,19	0,38	atpA	ATP synthase subunit alpha
PA5557	1,92	2,33	0,41	atpH	ATP synthase subunit delta
PA5558	1,84	2,09	0,24	atpF	ATP synthase subunit B
PA5559	1,85	1,91	0,06	atpE	ATP synthase subunit C
PA5560	1,52	1,67	0,15	atpB	ATP synthase subunit A
PA5561	1,09	0,97	-0,12	atpI	ATP synthase subunit I

1. Red figures, significant difference (Padj < 0.05)
2. Boldface characters, deleted genes

Table S6. Glucose responsive genes in PAO1 (10 min after glucose addition)

Locus	Log2 FC[1]			Name	Description
	PAO1+ *vs.* PAO1	GUN+ *vs.* PAO1+	GUN+ vs. PAO1		
PA0039	-1.27	0.64	-0.63		hypothetical protein
PA0085	-1.55	0.21	-1.34	*hcpI*	protein secretion apparatus assembly protein
PA0329	-1.25	-0.51	-1.76		hypothetical protein
PA0425	1.02	0.62	1.64	*mexA*	multidrug resistance protein
PA0427	1.05	0.92	1.97	*oprM*	outer membrane protein
PA0446	1.31	-0.38	0.93		hypothetical protein
PA0447	1.13	-0.60	0.53	*gcdH*	glutaryl-CoA dehydrogenase
PA0654	1.06	1.13	2.19	*speD*	S-adenosylmethionine decarboxylase
PA0779	-1.26	-0.87	-2.13	*asrA*	ATP-dependent protease
PA0887	-2.37	-1.62	-4.00	*acsA*	acetyl-CoA synthetase
PA1159	-1.28	-0.88	-2.16		cold-shock protein
PA1302	1.55	0.65	2.16	*hxuC*	heme utilization protein
PA1317	1.70	4.64	6.34	*cyoA*	cytochrome o ubiquinol oxidase subunit II
PA1318	1.42	4.55	5.97	*cyoB*	cytochrome o ubiquinol oxidase subunit I
PA1338	-1.69	-0.68	-2.37	*ggt*	γ-glutamyltranspeptidase
PA1339	-1.14	-0.37	-1.52	*aatP*	amino acids ABC transporter ATP binding protein
PA1340	-1.25	-0.32	-1.57	*aatM*	amino acids ABC transporter permease
PA1341	-1.47	-0.07	-1.53	*aatQ*	amino acids ABC transporter permease
PA1596	-1.15	-0.45	-1.61	*htpG*	chaperone protein
PA1617	-1.56	-1.75	-3.31		AMP-binding protein

PA1974	2.15	0.47	2.62		hypothetical protein
PA2262	1.98	-3.25	-1.27	*kguT* [2]	2-ketogluconate transporter
PA2264	1.65	-0.12	1.53		hypothetical protein
PA2265	1.60	0.04	1.64	*gad*	gluconate dehydrogenase
PA2266	1.62	-0.20	1.42		cytochrome C precursor
PA2289	2.41	1.39	3.80		hypothetical protein
PA2290	1.52	1.27	2.80	*gcd*	glucose dehydrogenase
PA2291	1.53	0.98	2.52	*oprB2*	glucose-sensitive porin
PA2320	2.35	-3.17	-0.81	*gntR*	transcriptional regulator
PA2321	7.11	-8.47	-1.37	*gntK*	gluconokinase
PA2322	5.96	-7.69	-1.73	*gntP* [2]	gluconate permease
PA2323	5.68	-2.94	2.73	*gapN*	glyceraldehyde-3-phosphate dehydrogenase
PA2629	1.17	1.32	2.49	*purB*	adenylosuccinate lyase
PA2774	-1.27	0.27	-1.00	*tse4*	hypothetical protein
PA2853	-1.73	0.14	-1.87	*oprI*	outer membrane lipoprotein
PA2862	-1.00	-1.83	-2.83	*lipA*	lactonizing lipase
PA3038	-1.52	-2.82	-4.34	*opdQ*	porin
PA3067	1.00	-0.13	0.88		transcriptional regulator
PA3126	-1.45	-0.18	-1.62	*ibpA*	heat-shock protein
PA3181	1.43	-4.57	-3.14	*edaA*	2-dehydro-3-deoxy-phosphogluconate aldolase
PA3182	1.86	-4.85	-2.99	*pgl*	6-phospho-gluconolactonase
PA3183	1.59	-5.07	-3.48	*zwf*	glucose-6-phosphate 1-dehydrogenase
PA3186	5.99	-1.82	4.17	*oprB*	porin B
PA3187	5.83	-3.66	2.18	*gltK* [2]	sugar ABC transporter ATP-binding protein
PA3188	5.76	-7.23	-1.47	*gltG* [2]	sugar ABC transporter permease

PA3189	5.02	-6.82	-1.80	*gltF* [2]	sugar ABC transporter permease
PA3190	5.10	-0.73	4.38	*gltB*	sugar ABC transporter substrate-binding protein
PA3195	1.62	-4.67	-3.04	*gapA*	glyceraldehyde 3-phosphate dehydrogenase
PA3234	-2.58	-1.30	-3.89	*yjcG*	acetate permease
PA3235	-2.87	-1.36	-4.23	*yjcH*	hypothetical protein
PA3263	1.32	-0.13	1.19	*yaiD*	recombination associated protein
PA3452	1.65	0.17	1.82	*mqoA*	malate:quinone oxidoreductase
PA3496	-1.60	-0.98	-2.58		hypothetical protein
PA3531	1.16	-0.87	0.29	*bfrB*	bacterioferritin
PA3560	4.13	-0.04	4.09	*fruA*	PTS system fructose-specific transporter subunit
PA3561	3.41	-0.34	3.07	*fruK*	1-phosphofructokinase
PA3562	4.12	-0.17	3.95	*fruI*	PTS system fructose-specific transporter subunit
PA3766	-1.50	-0.20	-1.71		aromatic amino acids transporter
PA3818	1.24	1.64	2.88	*suhB*	type III secretion system regulator SuhB
PA3819	-1.02	-0.61	-1.62	*ycfJ*	hypothetical protein
PA3890	1.01	-1.19	-0.18	*opuCB*	ABC transporter permease
PA3922	-1.06	-2.66	-3.72		hypothetical protein
PA3923	-1.08	-2.43	-3.51		hypothetical protein
PA4290	-1.84	-0.13	-1.97		chemotaxis transducer
PA4435	-1.05	-0.64	-1.69		acyl-CoA dehydrogenase
PA4438	1.34	0.88	2.22	*yhcM*	hypothetical protein
PA4542	-1.25	-0.61	-1.85	*clpB*	chaperone protein
PA4606	-1.03	-0.80	-1.84	*cstA*	hypothetical protein
PA4759	-1.26	-0.22	-1.48	*dapB*	tetrahydrodipicolinate reductase
PA4761	-1.08	-0.56	-1.65	*dnaK*	molecular chaperone

PA4762	-1.16	-0.37	-1.53	*grpE*	heat shock protein
PA4888	1.48	0.19	1.66	*desB*	acyl-CoA desaturase
PA4913	-1.20	-1.50	-2.70		ABC transporter
PA5052	1.00	0.50	1.50		hypothetical protein
PA5053	-1.20	-0.34	-1.54	*hslV*	heat-shock protein
PA5054	-1.36	-0.44	-1.80	*hslU*	heat-shock protein
PA5062	1.13	-0.40	0.73		hypothetical protein
PA5153	-1.06	-1.97	-3.04		amino acids ABC transporter substrate-binding protein
PA5183.1	-1.43	-0.29	-1.71	*rsmN*	hypothetical protein
PA5302	-1.41	-0.47	-1.88	*dadX*	alanine racemase
PA5303	-1.53	-0.36	-1.89		hypothetical protein
PA5304	-1.21	-0.93	-2.14	*dadA*	D-amino acids dehydrogenase small subunit
PA5348	-1.21	-2.21	-3.42		DNA-binding protein
PA5415	-1.87	-0.27	-2.15	*glyA1*	serine hydroxymethyltransferase
PA5445	-1.37	-0.19	-1.57	*psecoA*	coenzyme A transferase
PA5504	1.11	1.14	2.25		D-methionine ABC transporter
PA5526	-1.34	-0.56	-1.90		hypothetical protein

[1]Red figures indicate statistically significant difference (Padj < 0.05).
[2]Genes deleted in GUN.

Table S7. DEGs encoding putative/known transcription factors (10 min after glucose addition)

Locus	Log2 FC[1]			Name	Description[2]
	PAO1+ *vs.* PAO1	GUN+ *vs.* PAO1+	GUN+ vs. PAO1		
PA0048	-0.21	-0.99	-1.20		transcriptional regulator
PA0120	-0.22	-0.80	-1.01		transcriptional regulator
PA0248	-0.96	-0.60	-1.56	*pobR*	PHBA metabolism regulator
PA0475	-0.96	-0.55	-1.50		transcriptional regulator
PA0527	0.82	1.04	1.86	*dnr*	denitrifaction regulator
PA0547	0.56	1.29	1.85		transcriptional regulator
PA0708	-1.34	-1.22	-2.56		transcriptional regulator
PA0797	0.18	-1.95	-1.77		transcriptional regulator
PA0815	-0.61	-0.82	-1.42		transcriptional regulator
PA0831	-0.33	-1.01	-1.34	*oruR*	ornithine metabolism regulator
PA0839	-0.21	-0.88	-1.09		transcriptional regulator
PA0906	-0.41	-0.83	-1.24	*alpR*	lysis phenotype repressor
PA1663	0.38	1.01	1.39	*sfa2*	RpoN sigma factor activator
PA1759	-0.75	-1.16	-1.91		transcriptional regulator
PA1760	-0.14	-1.25	-1.39		transcriptional regulator
PA2016	-0.28	-1.61	-1.89	*liuR*	leucine metabolism regulator
PA2076	0.65	0.71	1.36		transcriptional regulator
PA2082	-0.54	-0.84	-1.38	*kynR*	tryptophan metabolism regulator
PA2196	0.29	1.10	1.39		transcriptional regulator
PA2246	0.06	-1.43	-1.37	*bkdR*	branched-chain amino acids metabolism regulator

PA2259	0.97	-2.31	-1.34	*ptxS*	2-ketogluconate metabolism regulator
PA2320	2.35	-3.17	-0.81	*gntR*	gluconate metabolism regulator
PA2556	-0.67	-1.79	-2.46		transcriptional regulator
PA2686	0.69	0.94	1.62	*pfeR*	enterobactin receptor regulator
PA2825	-0.97	-0.97	-1.93	*ospR*	oxidative stress response regulator
PA2897	-0.39	-0.65	-1.03		transcriptional regulator
PA2957	0.63	0.92	1.55		transcriptional regulator
PA3006	-0.55	-0.57	-1.11	*psrA*	fatty acid β-oxidation regulator
PA3067	1.00	-0.13	0.88		transcriptional regulator
PA3124	-0.49	-0.61	-1.10		transcriptional regulator
PA3192	0.76	-2.47	-1.71	*gltR*	TC response regulator
PA3321	0.03	-1.57	-1.54		transcriptional regulator
PA3410	0.40	0.96	1.36	*hasI*	ECF sigma factor HasI
PA3508	-0.88	-1.16	-2.04		transcriptional regulator
PA3622	-0.63	-0.81	-1.44	*rpoS*	sigma factor RpoS
PA3689	-0.89	-0.76	-1.65	*yhdM*	transcriptional regulator
PA3721	0.44	0.69	1.13	*nalC*	TetR family repressor
PA3757	-0.24	-0.98	-1.22	*nagR*	GlcNAc metabolism regulator
PA3815	0.73	0.61	1.34	*iscR*	iron-sulphur cluster biosynthesis regulator
PA3921	-0.08	-0.93	-1.01		transcriptional regulator
PA3927	-0.03	-1.40	-1.43		transcriptional regulator
PA3973	-1.04	-0.69	-1.73		transcriptional regulator
PA4021	-0.15	-1.23	-1.38		transcriptional regulator
PA4094	-0.61	-0.86	-1.47		transcriptional regulator
PA4147	-0.81	-1.22	-2.03	*acoR*	2.3-butanediol metabolism regulator

PA4296	-0.72	-0.31	-1.02	*pprB*	TC response regulator
PA4341	-0.19	-1.36	-1.55		transcriptional regulator
PA4726	-0.34	-0.75	-1.09	*cbrB*	TC response regulator
PA4787	-0.30	-1.09	-1.39		transcriptional regulator
PA4853	0.50	0.80	1.30	*fis*	Fis family regulator
PA4914	-0.50	-0.90	-1.40	*amaR*	lysine metabolism regulator
PA4983	-0.60	-1.28	-1.89	*dsmR*	TC response regulator
PA5029	-0.61	-0.54	-1.15	*ynfL*	transcriptional regulator
PA5261	-0.63	-1.03	-1.66	*algR*	transcriptional regulator
PA5301	-0.28	-1.19	-1.46	*pauR*	polyamine metabolism regulator
PA5324	-0.40	-0.95	-1.35	*sphR*	sphingosine-responsive regulator
PA5364	-0.46	-0.61	-1.07		TC response regulator
PA5380	-0.68	-0.76	-1.44	*gbdR*	protein GbdR
PA5428	-0.33	1.34	1.02		transcriptional regulator

[1]Red figures indicate statistically significant difference (Padj < 0.05).
[2]PHBA, p-hydroxybenzoic acid; TC, Two-Component; GlcNAc, N-acetylglucosamine.